Estimation Methodology for the Electricity Usage of Daylight and Occupancy Controlled Artificial Lighting

Therese Antonsen & Ida Strømberg

8th of june 2015

Master Thesis

Aalborg University

Department of Civil Engineering

M.Sc. Indoor Environmental and Energy Engineering

AALBORG UNIVERSITET

M.Sc. Indoor Environmental and Energy Engineering
Sofiendalsvej 9-11
9200 Aalborg SV
Denmark
Phone No. 99 40 84 84

Title:
Estimation Methodology for the Electricity Usage of Daylight and Occupancy Controlled Artificial Lighting

Project period:
Master Thesis
September 2014 - June 2015

Authors:
Therese Antonsen
Ida Strømberg

Supervisors:
Rasmus Lund Jensen
Olena Kalyanova Larsen

Editions: 5
Number of pages: 177
Number of appendix pages: 152
Appendix-DVD
Completed: 08-06-2015

Synopsis:

This report is the product of the completion of the two year master programme in Master of Science, with concentration in Indoor Environmental and Energy Engineering, at Aalborg University, Department of Civil Engineering.

Buildings accounts for about 40 % of the energy usage in the word today, and artificial lighting stands for about 15-30 % of the total electricity usage in buildings in Scandinavia. This shows that there is potential for reducing the electricity usage of buildings with more efficient artificial lighting. Prior to obtaining more efficient artificial lighting, the electricity usage for artificial lighting should be accurately determined.

The existing estimation methodology for calculating the electricity usage of daylight and occupancy controlled artificial lighting in Norway is based on a very rough estimate. The objective of this thesis is to develop a new estimation methodology which is both rapid and accurate.

In order to obtain the estimation methodology of daylight and occupancy controlled artificial lighting, occupancy profiles and the interior illuminance due to external sky conditions must be established. The occupancy profiles were retrieved from gathered data of the occupant time in an office building. The interior illuminance was determined with measurements and simulation. The exterior sky conditions were established with pictures, solar irradiance measurements and simulation.

Two estimation methodologies are established; the *CIE Sky Method* and the *Hourly Average Method*. The calculated electricity usage by the methodologies were validated with measurements of the electricity usage. The *Hourly Average Method* proved to be the most rapid and accurate methodology.

Abstract

The estimation of the electricity usage for daylight and occupancy controlled artificial lighting in Norway today, is based on a very rough estimate in *NS 3031:2014*. The objective of this thesis is to develop a new estimation methodology for the electricity usage of daylight and occupancy controlled artificial lighting in an office, which is both accurate and rapid. The methodology is developed with the idea that it can be applied by consultant engineers who wish to accurately and rapidly determine the electricity usage of the artificial lighting in an office. The methodology should not require the user to be dependent on parameters that require measurements.

As the artificial lighting is controlled by daylight and the presence of occupants, these two parameters needs to be established prior to developing the estimation methodologies. In order to do so, a cell office in an office building was applied as a case where measurements were conducted.

Occupancy profiles were obtained by analysing data gathered for several cell offices and open landscape offices in the case building for 2013 and 2014. An occupancy profile that specifies hours per day, days per week and weeks per year, was developed for a cell office and an open landscape office. The developed occupancy profiles were different from the existing occupancy profiles from Danish and Norwegian regulations. When calculating the electricity usage for daylight and occupancy controlled artificial lighting, the result obtained with the developed occupancy profile were closer to the measured electricity usage compared to the existing occupancy profiles from the regulations.

The electricity usage of the armature is also controlled by the available daylight, which is then dependent on the outdoor conditions. Comission Internationale de l'Eclairage (CIE) has defined a set of standardized sky models. Daylight simulation software require a specified CIE sky condition when determining the interior illuminance. The solar irradiance was measured in order to specify which CIE sky conditions that were present simultaneously as the interior illuminance level in the office was measured. However, specifying the real sky conditions as different CIE skies proved to be problematic as the variations in the real sky condition is highly complex. Therefore solar light factors and the external illuminance on the façade obtained with *NS 3031:2014* weather file in BSim was applied in order to determine the interior illuminance level. Two different estimation methodologies to calculate the electricity usage of daylight and occupancy controlled artificial lighting were established. The methods apply the obtained occupancy profile. Both estimation methodologies determine the available daylight due to the external illuminance level obtained with BSim and solar light factors. However, how the interior illuminance is obtained is what deviates the two methods.

Initially a method that sorts the sky conditions over a year into different CIE sky intervals, and thereby determines the available daylight within this CIE sky interval, was established. This method is called the *CIE Sky Method*. The available daylight is stated to be the same for all hours within every CIE sky interval. The amount of occupancy hours within every CIE sky interval was applied in order to establish the hours of needed artificial lighting, which then leads to the electricity usage of daylight and occupancy controlled artificial lighting.

The second method is called the *Hourly Average Method*, and as the name indicates, this methodology applies the average of every hour of a year. The hourly average of available daylight due to external sky conditions is calculated, and the hours where the occupant is present and there is not sufficient daylight, sums up to the electricity usage of the daylight and occupancy controlled artificial lighting.

The two established methodologies together with the estimation methodology from *NS 3031:2014* were compared to the measured electricity usage for the occupancy and daylight controlled artificial lighting in the cell office in the case building. The method from *NS 3031:2014* proved to over estimate the electricity usage, while the results from the two obtained estimation methodologies were closer to the actual value. The solar irradiance and occupancy profile was inserted in the electricity usage calculation in the *CIE Sky Method* and *Hourly Average Method* for further validation of the two methods, the *Hourly Average Method* proved to be the most accurate and rapid method.

Preface

This thesis is a result of a two year master programme in Master of Science, with concentration in Indoor Environmental and Energy Engineering, at Aalborg University, Department of Civil Engineering.

The thesis is developed over a period of ten months from September 1^{st} 2014 to June 8^{th} 2015. The report consist of a main report and an appendix. The main report is subdivided into five parts, and the appendices assist the material in the main report. Attached is a DVD with the report in pdf-format, as well as all simulation models, calculations and files which construct the basis of this thesis. The two developed estimation methodologies for the electricity usage of occupancy and daylight controlled artificial lighting, the *CIE Sky Method* and the *Hourly Average Method*, are attached as Excel spreadsheets. All references can be found in the bibliography in the end of the report, the references are in accordance to the Harvard method.

The thesis addresses consultant engineers as well as people who are interested in artificial lighting which is controlled by available daylight and occupancy. However, it is expected that the reader have an academic level of a Master of Science student. Throughout this project we have gained knowledge on how to establish occupancy profiles for calculation of electricity usage in office buildings, as well as calculation methods for available daylight and calculation engines in simulation software.

This thesis could not have been accomplished without the help and guidance from our supervisors at Aalborg University, Olena Kalyanova Larsen and Rasmus Lund Jensen.

We take this opportunity to express gratitude to Ida Bryn and Arnkell J. Petersen from Erichsen & Horgen AS for showing interest in the thesis and sharing inspirational information, as well helping as us get in touch with Norges Vassdrag og Energidirektorat (NVE).

The generosity of Truls Erik Bønsnes from NVE for letting us fill his office with lux meters and connecting a SparOmeter to his armature is greatly appreciated. We could not have done the measurements without you, Truls.

We wish to acknowledge the help from Glenn Thomas Gustavsen from Entra, and Espen Treider and Hans Petter Arvesen from NVE with information about the NVE-building, as well as giving us access to the building at all times and always helping us out with a smile.

Interesting information and thoughts about how the Danish building industry cope with estimating electricity usage for daylight controlled artificial lighting from Allan Hesselholt from Cowi Denmark is greatly appreciated.

We are grateful for Helle Wøhlk Jæger Sørensen from Erichsen & Horgen AS splendid help with different simulation software programs.

A special thanks goes to Line Røseth Karlsen from Høgskolen i Oslo og Akershus for always answering our never ending questions and for always responding so quickly to our emails. Her PhD thesis about integrating daylight in commercial buildings in Nordic climate due to comfort and electricity use, is the inspiration for this master thesis.

Last but not least, we would like to thank family and friends for the support, and for illuminating our lives through the dark times.

Therese N. Antonsen   Ida Strømberg

Table of Contents

Introduction 1

The global climate change going on today demands for sustainable solutions. As buildings accounts for about 40% of the energy use in the world today (Programme, March 2015), sustainable buildings can help decrease the impact on the global climate change.

The electricity for artificial lighting stands for about 15-30 % of the total electricity usage in buildings in Scandinavia (Karlsen, 2014), this means that the electricity usage can be reduced, by a significant amount, with efficient artificial lighting. Daylight control systems for artificial lighting can reduce 30-60 % of the total electricity usage in buildings (Dubois og Blomsterberg, 2011).

It is possible to reduce the electricity usage for artificial lighting with reasonable cost in new and rehabilitated buildings (Dubois og Blomsterberg, 2011), which means that achieving lower electricity usage for the artificial lighting is realizable and should be an easy goal to choose.

Prior to reducing the electricity usage for artificial lighting, a more accurate calculation method to estimate the electricity usage for artificial lighting with daylight and occupancy control is required, than the rough estimate in *NS 3031:2014*.

The goal of this thesis is to develop an accurate and rapid estimation methodology for the electricity usage for artificial lighting which is daylight and occupancy controlled.

Our hope is that this thesis will be a step in the right direction of achieving a sustainable building industry.

1.1 Research Question

On the basis of the previous mentioned goal of obtaining an accurate and rapid estimation methodology for the electricity usage of daylight and occupancy controlled artificial lighting, the following research question will be investigated throughout this project:

How can the electricity usage be rapidly and accurately determined for daylight and occupancy controlled artificial lighting?

As the artificial lighting is controlled by available daylight and the presence of the occupants, the electricity usage is dependent on these parameters. Therefore a set of new questions arise:

- How is the interior daylight availability?
  - How can the interior illuminance level be established due to exterior illuminance?
  - How can the real life sky conditions be implemented in the calculation of interior illuminance level?

- How is the occupancy profile of an office?
  - When is an office occupied and how is the distribution?
  - How is the actual occupancy in an office compared to existing occupancy profiles from regulations?

By answering these questions a developed estimation methodology for the electricity usage for daylight and occupancy controlled artificial lighting will be established.

1.2 Reading Guide

The report is divided into five parts:

- Background Theory and the Case Building
- Natural and Artificial Light
- Occupancy Profile
- Established Estimation Methodology
- Conclusion

Throughout the report the focus is to obtain an estimation methodology for the electricity usage for daylight and occupancy controlled artificial lighting. However, prior to obtaining this methodology, some steps must be taken to establish parameters regarding available daylight, the electricity use and the occupancy.

In part I background theory needed for a better understanding of the parameters applied when determining available daylight is presented. The calculation engines in the simulation programs applied later in part II are also presented. The case building, and the cell office, which is applied for validation of the obtained method, is also presented. The data used when establishing the occupancy profiles in part III are gathered from the case building.

Different approaches to categorize real sky conditions as different CIE sky conditions is presented in part II. Simulated interior illuminance level due to different CIE sky conditions is presented and compared to the actual interior illuminance. The electricity usage of the armature in the cell office is presented, together with specifications about the control of the artificial lighting due to available daylight. Knowledge gained in this part will be applied in part IV when the estimation methodology is utilized.

How the occupancy profiles are developed is presented in part III. The data applied is gained from the central operating system of the case building. The importance of the occupancy profile when determining the electricity usage of occupancy controlled artificial lighting is shown.

The existing estimation methodology for calculating the electricity usage of daylight and occupancy controlled artificial lighting from *NS 3031:2014* is presented in part IV. Afterwards the two obtained estimation methodologies, the *CIE Sky Method* and the *Hourly Average Method*, are presented. Lastly, all three methods are validated against the measured electricity usage of the daylight and occupancy controlled artificial lighting in the cell office.

The conclusion can be found in part V, the conclusion sums up all significant findings throughout this thesis.

The report can be read independent of the appendices. However, additional information, results and description of the conduction of the measurements are found in the appendices in part VI.

Part I

Background Theory and the Case Building

In this part light transportation theory is presented for a better understanding of the parameters applied when determining available daylight.

The case building, where the cell office for validation of the obtained estimation methodologies is located, is presented. All measurements are performed on this case building. The data applied for obtaining the occupancy profiles in part III is gathered from the central operating system of the case building.

The calculation engines in Relux and VELUX Daylight Visualizer is presented, as well as simulation of the cell office in the case building is performed. These simulation programs will be applied later in part II.

The Case 2

In this chapter a description of the building which is applied as a case will be described. The cell office where the electricity usage for the daylight and occupancy controlled artificial lighting is measured is facing South-East in the office building. In this thesis, all measurements and simulations are performed for the cell office in this office building. The obtained occupancy profile in part III is gathered form the central operating system in this building.

A brief description of the cell office is included in this chapter, for a detailed description, please refer to appendix A.

As a tool for this thesis, the office building for Norges vassdrags- og energidirektorat (NVE) is applied. The building can be seen in picture 2.1.

Figure 2.1. The NVE-building (Norges vassdrags- og energidirektorat (NVE), September 2011)

The office building was constructed in 1964 for the tenant, NVE. Entra ASA is the building owner. The building was renovated by Skanska Norge AS. And in April 2011 NVE moved back into the building.

The NVE-building, from now on referred to as the case building, is situated in Oslo, Norway as seen on figure 2.2 on the following page. The address is Middelthunsgate 29 in the district of the city called Majorstua. The latitude is 59.929563° and the longitude 10.707524°.

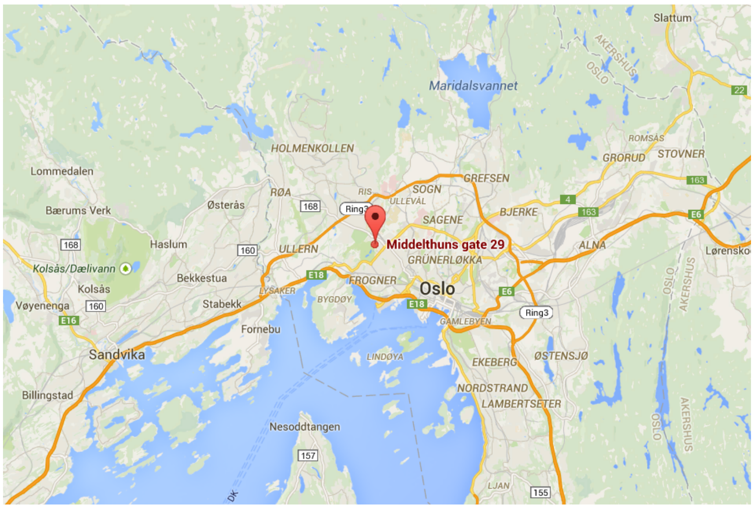

Figure 2.2. The building is situated in Oslo

The East façade can be seen on figure 2.3. The cell office is facing East on the third floor, approximately were it is situated is marked with yellow. The solar irradiance was measured on the roof of the case building, this will be explained in section 3.1.1.

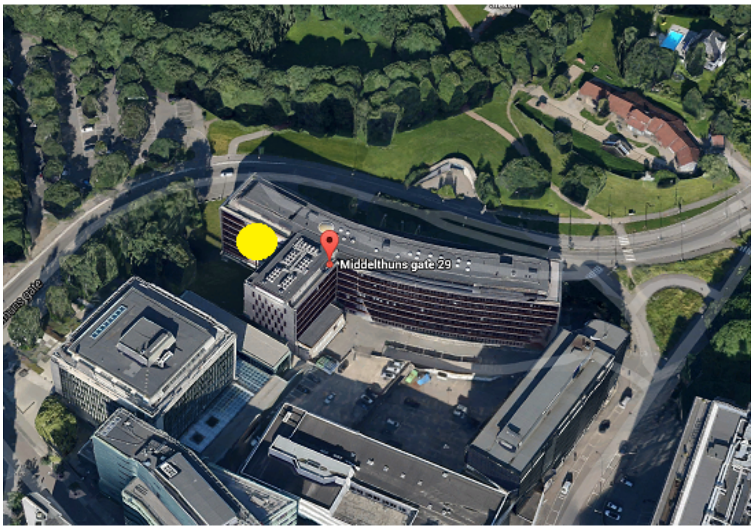

Figure 2.3. 3D view of the East façade from Google Maps were the cell office is situated is marked with yellow.

Figure 2.4 is an elevation view of the East façade, the two windows for the cell office is marked with yellow.

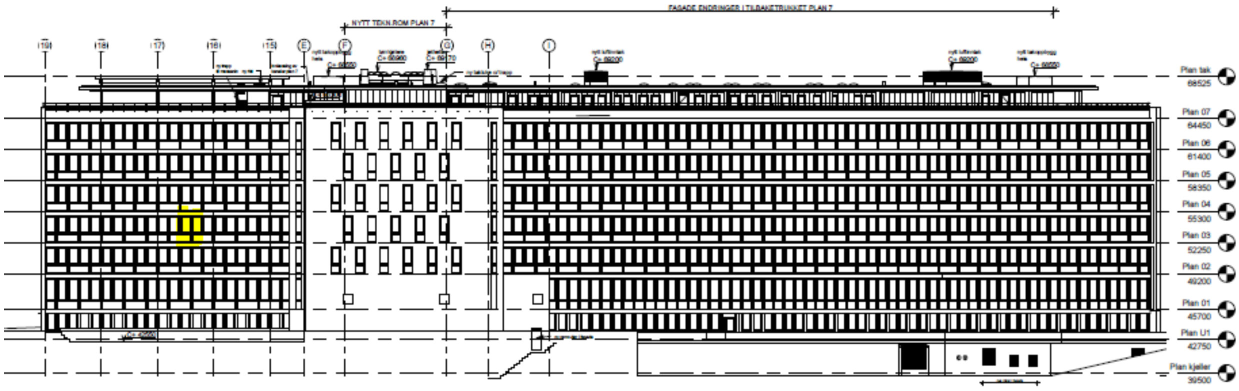

Figure 2.4. Elevation view of the East façade.

Figure 2.5 is a plan view of the third floor where the cell office is located, the cell office is marked in yellow.

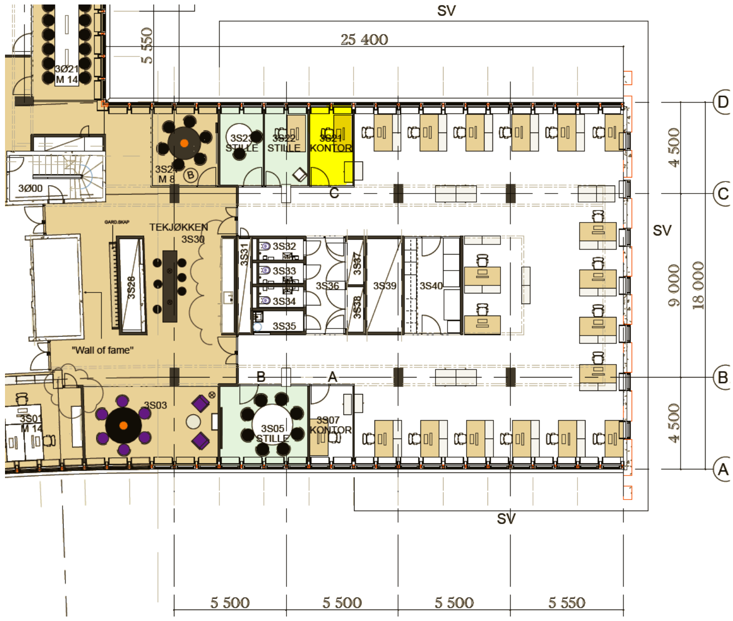

Figure 2.5. Elevation view of the East façade.

The cell office in the case building can be seen in figures 2.6 and 2.7. Interior illuminance and the electricity usage of the armature was measured in this office.

The cell office can be seen in figures 2.6 and 2.7.

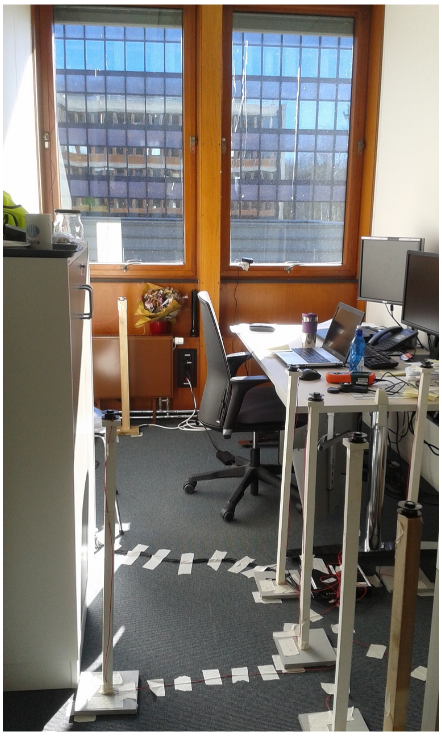

Figure 2.6. Cell office, towards the façade

Figure 2.7. Cell office, towards the corridor

As seen on figure 2.6 the cell office has two windows with a glazed area of $0.8m^2$ each. The parameters of the cell office are listed in table 2.1. These parameters will be inserted in simulation programs when simulation of the cell office is conducted. The reflectance of the surfaces was measured and will be explained in section 3.4.

Picture 2.8 show the windows in the cell office, and picture 2.9 show the façade where the cell office is located on the third floor. There is a web cam placed in the window taking snap shots of the sky, this will be explained in section 5.1.

Figure 2.8. The windows in the cell office and the office building opposite the case building seen through the window

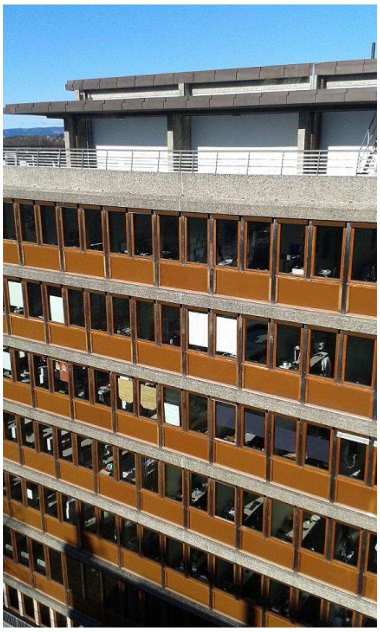

Figure 2.9. The South-East façade where the cell office is

The building seen through the window of the cell office on figure 2.8 is a glazed building which is 40 m from the case building and the roof of this building is approximately 12 m above the ceiling of the cell office. Simulation with and without obstructions will be conducted in section 4.6.

Component	Value
Transmittance of glazing	70%
Reflectance of the three white walls	0.4 (Statens Byggeforskningsinstitut, 2008) refer to section 3.4
Reflectance of the wooden wall	0.30 (RELUX Informatik AG, 2007) refer to section 3.4
Reflectance of the ceiling	0.9 (Statens Byggeforskningsinstitut, 2008) refer to section 3.4
Reflectance of the floor	0.1 (Statens Byggeforskningsinstitut, 2008) refer to section 3.4
Orientation	128°
Size of glazed area	0.8 m^2 (1.6 m^2 for both)
Area of the cell office	8.26 m^2
Height of room	2.85 m
Depth of room	3.931 m
Width of room	2.102 m

Table 2.1. Parameters of the materials and the geometry for the cell office.

The solar light factor for the cell office will be calculated in section 14.7.6 with regard to the geometry of the cell office and the parameters of the materials.

The orientation of the East, South and West façades are illustrated in figure 2.10.

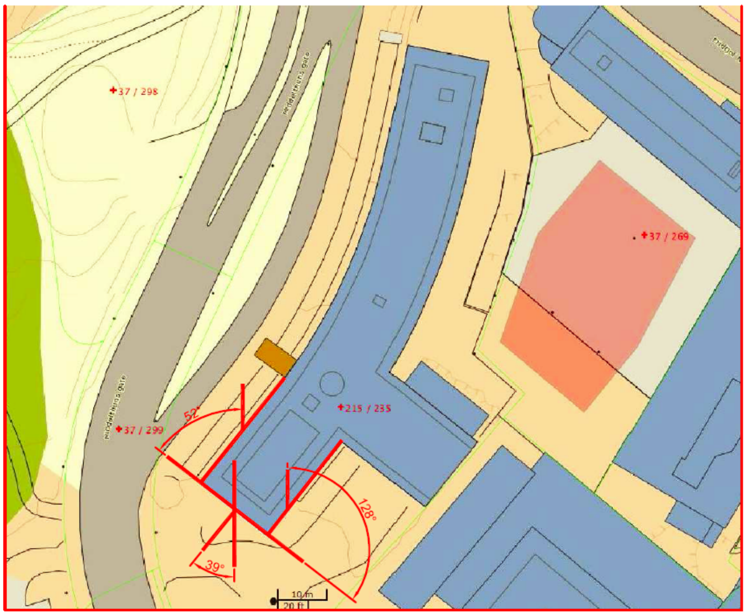

Figure 2.10. The orientation of the façades measured with AutoCAD on the map obtained from Kartverket

The façade for the cell office is facing South-East with an orientation of 128 ° as seen in figure 2.10.

The dimensions of the cell office can be seen in figures 2.11 and 2.12.

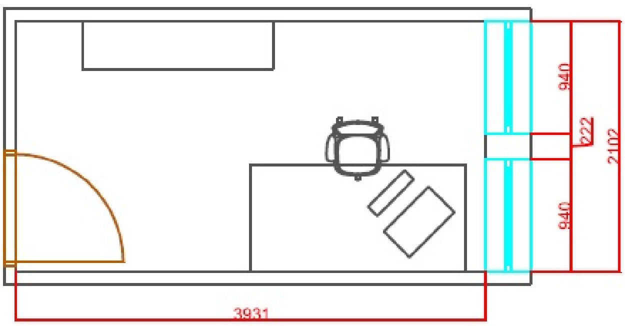

Figure 2.11. Plan view of the cell office with dimensions

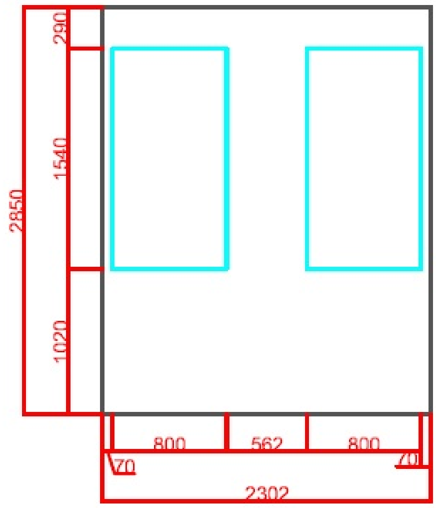

Figure 2.12. Façade of the cell office with dimensions

Illustrative pictures of the the cell office from Relux, including interior obstructions, can be seen in figures 2.13 and 5.14.

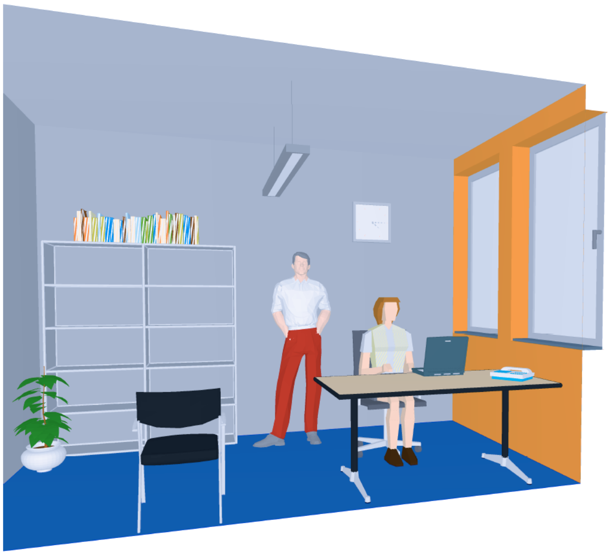

Figure 2.13. Illustration of the cell office with interior obstructions in Relux.

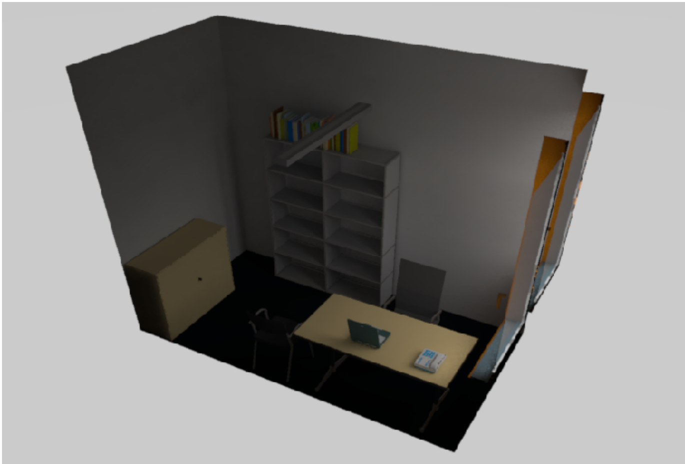

Figure 2.14. Illustration of the cell office with interior obstructions in Relux.

The armature in the cell office is shown in figures 2.15 and 2.16. The electricity usage of this armature is measured and explained in section 6.1.

Figure 2.15. The armature in the cell office

Figure 2.16. The electricity usage and power of the armature measured with a SparOmeter

The power of the armature and how it is controlled due to available daylight is explained in section 6.1.

As mentioned in the beginning of this chapter, this is only a brief description of the case building and the cell office. For a detailed description, please refer to appendix A.

The Physics of Light 3

Light is electromagnetic energy. The color of a surface observed by our eyes is the color of the light reflected of it, all other colors are observed.

The electricity usage for daylight and occupancy controlled artificial lighting is dependent on the available daylight in the room. A number of different parameters such as the room geometry, the sky conditions, the reflectance of the surfaces in the room and for the surroundings of the building affect the daylight availability in a room. These parameters can usually be found in standards, which can be utilized to give a fairly good approximation of the electricity usage. However, for a more accurate estimation, these parameters should be measured.

The solar irradiance, interior and exterior illuminance, the reflectance of the surfaces in the room and the transmittance dependency on the cleanliness of the window was measured for the case building.

In this chapter, these parameters and the conduction of the measurements will be described.

3.1 Irradiance

Irradiance is the total specific radiant power, or radiant flux, per area incident on a surface (Quaschning, May 2003), the unit is $\frac{\mathrm{W}}{\mathrm{m}^2}$. Solar irradiation is irradiance integrated over a time period, and the unit is $\frac{\mathrm{Wh}}{\mathrm{m}^2}$ or $\frac{\mathrm{J}}{\mathrm{m}^2}$. When considering daylight only the visible part of the sunlight will be considered (Quaschning, May 2003). The annual mean solar irradiance is known as the solar constant and is $1367 \pm 2\ \frac{\mathrm{W}}{\mathrm{m}^2}$ (Quaschning, May 2003).As seen in figure 3.1 solar irradiance can be either direct, diffuse or reflected, or a combination of these.

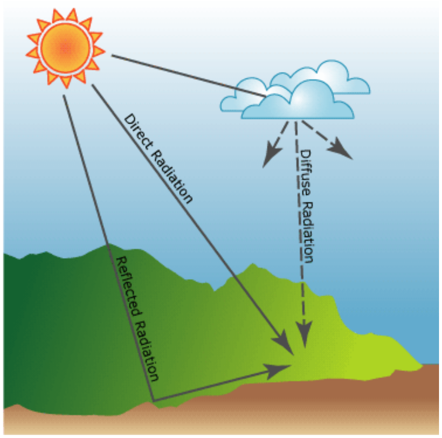

Figure 3.1. Direct, diffuse and reflected solar irradiance through the atmosphere (Moon, 2010).

Only a part of the irradiance beam will reach the point at consideration directly, the rest will be either reflected of another surface or scattered from particles in the atmosphere (Quaschning, May 2003). The global irradiance on a horizontal surface consists of direct and diffuse irradiance as seen in equation 3.1.

$$E_g = E_{dir} + E_{dif} \tag{3.1}$$

Where:

E_g	The global irradiance $[\frac{\mathrm{W}}{\mathrm{m}^2}]$
E_{dir}	The direct irradiance $[\frac{\mathrm{W}}{\mathrm{m}^2}]$
E_{dif}	The diffuse irradiance $[\frac{\mathrm{W}}{\mathrm{m}^2}]$

On a tilted plane the component consisting of reflected irradiance must be included as seen in equation 3.2.

$$E_{tilt} = E_{dir} + E_{dif} + E_{ref} \tag{3.2}$$

Where:

E_{tilt}	The tilted irradiance $[\frac{\mathrm{W}}{\mathrm{m}^2}]$
E_{ref}	The reflected irradiance $[\frac{\mathrm{W}}{\mathrm{m}^2}]$

The average ground reflection is about 20% of the global irradiance (Quaschning, May 2003). A surface perpendicular to the incoming direct sunlight will usually receive the highest irradiance. The irradiance will normally be below 1000 $\frac{\mathrm{W}}{\mathrm{m}^2}$, but in cases with snow or clouds which reflects irradiance onto the receiving surface the irradiance may be above 1000 $\frac{\mathrm{W}}{\mathrm{m}^2}$ (Quaschning, May 2003).

3.1.1 Measured Solar Irradiance

As weather data is usually obtained from weather stations, and not the specific location of the building at interest, they do not give completely accurate results especially when the sky conditions are in the range between clear sky and overcast. Nearby obstacles and reflectance from other buildings are also naturally not taken into account in these data. Therefore, for better accuracy, the solar irradiance should be measured for the building.

The global solar irradiance was measured by a pyranometer located on the roof of the case building. A detailed description of the measurements can be found in appendix D on page 229.

Figure 3.2 is an example of the result obtained from the solar irradiance measurements. The blue line displays the diffuse irradiance, the red line represents the direct component and the green dotted line shows the total solar irradiance.

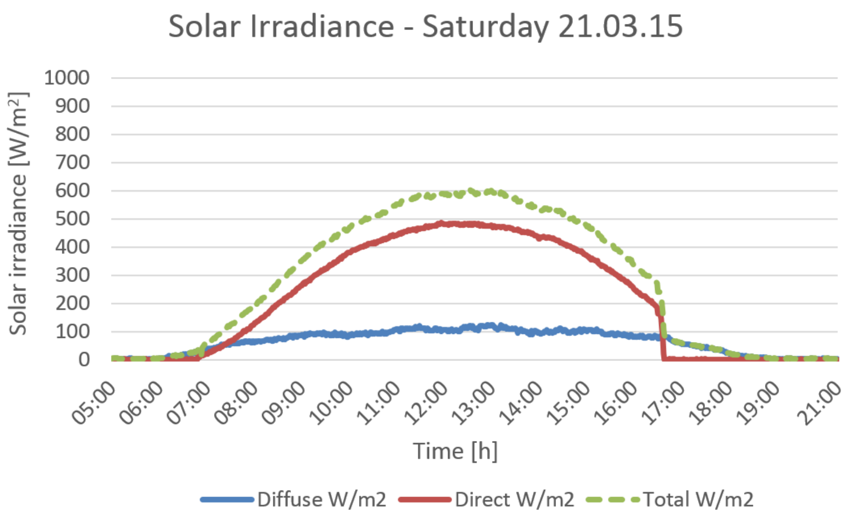

Figure 3.2. The diffuse, direct and total irradiation for Saturday 21.03.2015

The solar irradiance was measured to classify the sky conditions present during the measurement period according to CIE sky conditions. The CIE sky conditions are sky models defined by the luminance distribution on the sky dome. An analysis of the sky conditions present during the measurement period can be found in chapter 5 on page 43.

3.2 Luminance and Illuminance

There exist different definitions describing how the lumens of light interact in different ways (Lighting Ever, February 2015). Luminance is the light leaving a surface at a specific density in a specific direction, while illuminance is the quantity of light falling onto a surface (Lighting Ever, February 2015).

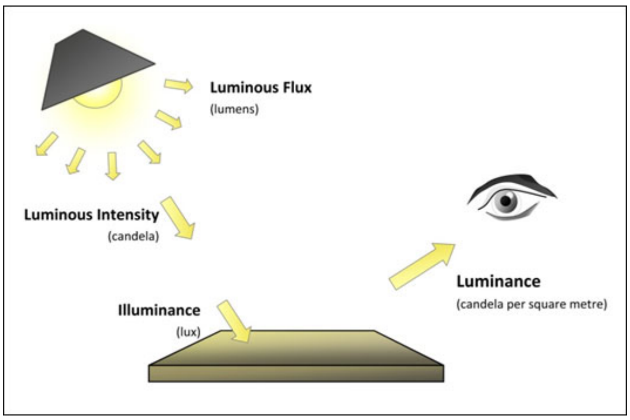

Figure 3.3. Lumination and illumination (Dementia Enabling Environments, January 2011)

Luminance is defined as the luminous intensity per unit area projected in a given direction (Halsted, February 2015), the unit is candela per square meter. The projected area is the in-focus spot on the receiving surface. The luminance phenomena can be seen in figure 3.4.

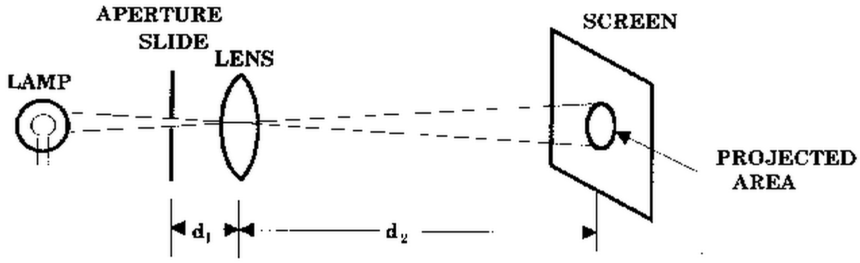

Figure 3.4. Luminous intensity per unit area projected in a specific direction depends on the projected area (Halsted, February 2015).

Illuminance is the luminous flux incident on a surface per unit area (Halsted, February 2015), a surface being illuminated by light. The unit is either lux or lumen per square meter.

Figure 3.5 illustrates how luminance and illuminance should be measured.

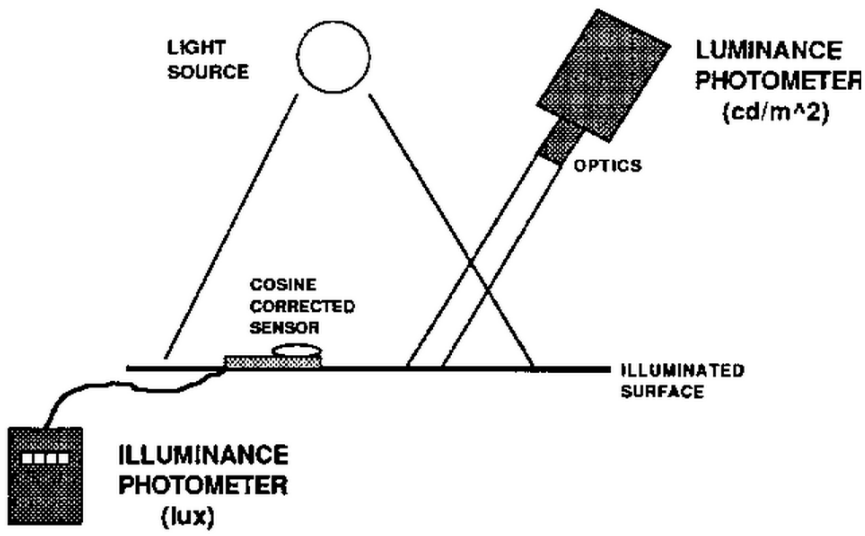

Figure 3.5. Measurement of luminance and illuminance (Halsted, February 2015).

3.2.1 Measured Exterior and Interior Illuminance

Exterior Illuminance

The exterior illuminance was measured as point measurements, vertically as well as horizontally with a hand-held illuminance meter. The measurements were conducted on the roof of the case building, and in an open space close to the case building. The results from the exterior illuminance measurements can be seen in the following table 3.6.

Date	Time	Location	Recieved Horizontal Illuminance [lux]	Receieved Vertical Illuminance [lux]			
				North	South	East	West
16.mar	16:00	Case building	3539	1457	1902	Not measured	Not measured
17.mar	11:00	Open space	12474	Not measured	Not measured	Not measured	6991
17.mar	11:15	Open space	13804	Not measured	Not measured	Not measured	7411
17.mar	13:30	Open space	54607	11339	47652	27091	14305
17.mar	15:30	Open space	22642	7503	27388	7810	21926
18.mar	07:50	Case building	1822	1821	1831	1728	1890
19.mar	08:00	Case building	5938	2531	3053	2685	2409
21.mar	09:55	Case building	47140	7452	80282	7554	74452
21.mar	14:30	Case building	26682	8168	77009	7145	75884
21.mar	16:20	Case building	13896	6020	10827	6531	80998
23.mar	08:00	Case building	3155	1519	1519	1621	1519
23.mar	13:00	Open space	24974	7063	20616	9508	19062
24.mar	11:50	Case building	66984	8168	98899	23716	9191
26.mar	15:30	Case building	12177	10305	9477	9774	9549

Figure 3.6. Results from the exterior illuminance measurements

It was of interest to compare the luminance distribution from the measurements to the luminance distribution for different sky conditions defined by CIE. This proved to be difficult due to inadequate measurement results and inaccuracies in connection to the conduction of the measurements. A more detailed description of the measurements can be found in appendix F on page 239.

Interior illuminance

The interior illuminance was measured in the cell office simultaneously with the solar irradiance. 11 luxmeters were placed in the cell office to obtain the interior illuminance level in different locations of the room during different sky conditions. A detailed description of the interior illuminance measurements can be found in appendix E on page 235. In figure I.13 and I.32 the measured interior illuminance throughout two days of the measurement period are shown. As seen on the figures, the illuminance levels varies a lot between the days for the individual sensor.

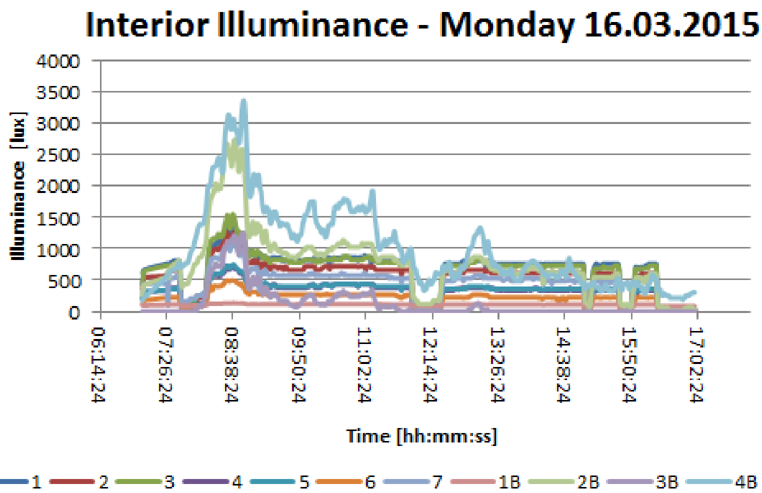

Figure 3.7. Interior illuminance in the cell office during Monday the 16^{th}.

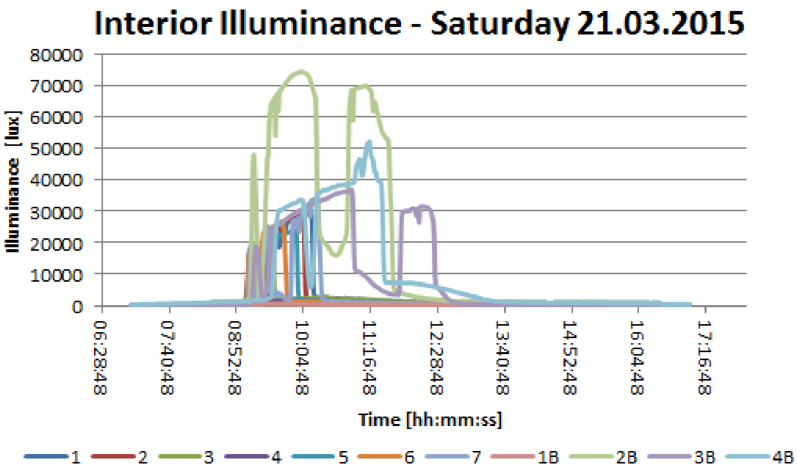

Figure 3.8. Interior illuminance in the cell office during Saturday the 21^{st}.

The interior illuminance should be seen in correspondence with the solar irradiance measurements for the certain days. An overview of the interior illuminance measurements and the corresponding solar irradiance measurements from each day of the measurement period can be found in appendix I on page 257

3.3 Light Transmittance

If an electromagnetic wave with a frequency that do not match the natural vibrating frequency of the object hits the object, the electrons will start to vibrate only for a short period of time and with small amplitudes (Tom Henderson, January 2015). After this short vibration time the energy will be re-emitted as an electromagnetic wave.

The light wave will be transmitted if the object is transparent. In a transparent object the vibration of the electrons are transported to the neighbouring electrons through the objects and re-emitted on the opposite side (Tom Henderson, January 2015).

3.3.1 Measured Cleanliness of the Glazing

According to *SBi anvisning 219 Dagslys i rum og bygninger* the effect of the cleanliness of vertical glazings is insignificantly small compared to other parameters for the available daylight, and can therefore be neglected (Statens Byggeforskningsinstitut, 2008). *SBi anvisning 203 Beregning af dagslys i bygninger*, on the other hand, states that the correction factor due to dirt on the glazing is 0.9 for a normal office building. This factor is dependent on how often the glazings are cleaned, but for a office building with normal use it is 0.9 (Statens Byggeforskningsinstitut, 2003).

Because of the split opinion in these two manuals, it was of interest to measure the significance of the cleanliness of the glazing. The light transmittance of the glazing was measured before and after the glazing was cleaned. It was expected that the light transmittance of the glazing would improve when the glazing was clean compared to a glazing with filth on it.

The results for the light transmittance from the cleanliness measurements are displayed in graph 3.9.

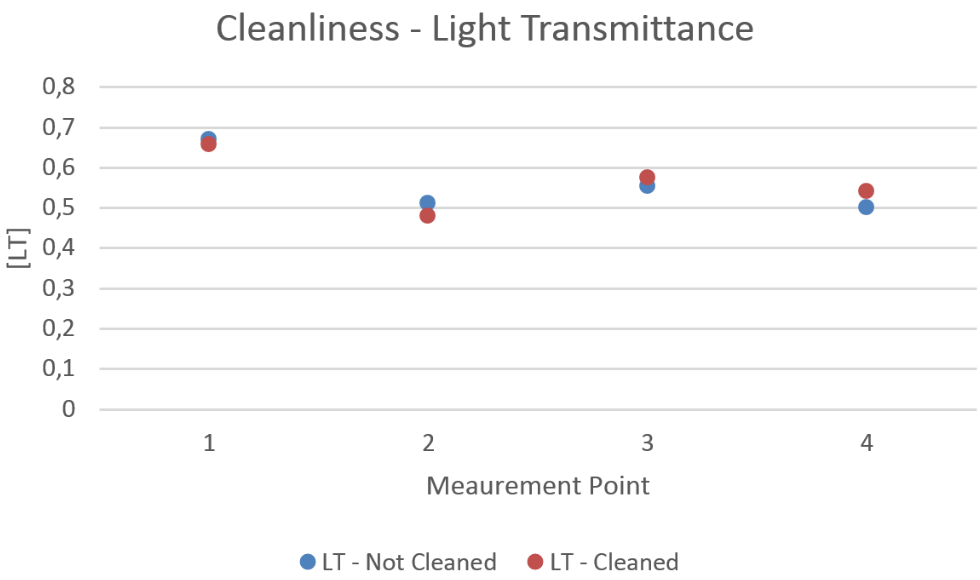

Figure 3.9. Light transmittance before and after the glazing was cleaned

As graph 3.9 clearly illustrates, there is not much difference for the light transmittance before and after the glazing was cleaned. When studying each light transmittance obtained for each measurement point in table 3.1 it can easily be seen that the light transmittance is fairly similar before and after the glazing was cleaned.

Point Measurements	**Light Transmittance - Not Cleaned**	**Light Transmittance - Cleaned**	**Δ Light Transmittance**	**Percentage difference [%]**
1	0.669	0.657	0.012	1.807
2	0.511	0.480	0.031	6.074
3	0.553	0.573	0.021	3.715
4	0.500	0.540	0.040	8.045

Table 3.1. The light transmittance before and after the glazing was cleaned.

As mentioned earlier it was expected that the light transmittance would increase after the glazing was cleaned, but when studying the results in graph 3.9 and table 3.1 the light transmittance only increase in two of the cases; point measurement 1 and 2. While it actually decreases in point measurements 3 and 4. The average light transmittance before and after the glazing was cleaned:

- Average light transmittance before the glazing was cleaned: 0.562
- Average light transmittance after the glazing was cleaned: 0.570

The deviation between the two values are only 0.009, which is undoubtedly small. The percentage difference is 1.552 % and it is therefore concluded that the effect of the cleanliness of the glazing can be neglected in further analysis.

3.4 Light Reflectance

In an opaque object the electrons on the surface of the objects will vibrate for a short period of time, then re-emit the energy as a reflected electromagnetic wave (Tom Henderson, January 2015). As seen in figure 3.10, there are two types of reflectance depending on the material of the surface it reflects from.

Specular reflectance is created when light hits a smooth surface, for example a mirror. The angle of the beam hitting the surface is equal to the angle of the reflection. Therefore specular materials will generate mirror images on their surface.

Diffuse reflectance is the one created from a rough surface. The angle of the ray hitting the surface will in this case create multiple reflection angles, and a mirror image is not produced. Most of the objects in the world are diffuse reflectors (Taylor, 2009).

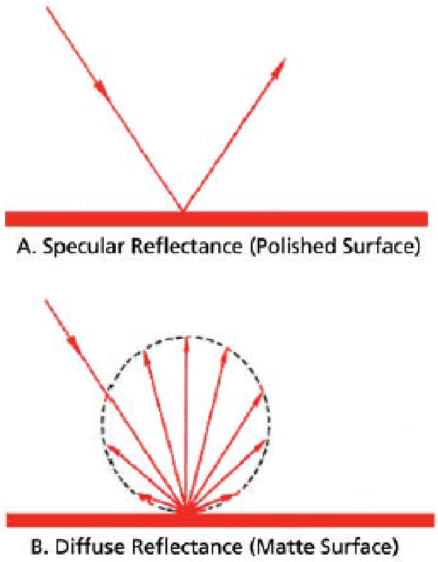

Figure 3.10. Types of reflectance (Taylor, 2009)

3.4.1 Reflectance - According to Different Sources

The exact reflectance of the materials in the cell office was difficult to obtain from the manufacturer. In many cases standard values for the different surfaces will be applied. Figure 3.2 shows the reflectance for different construction elements.

Byggforsk 421.621: Metoder for distribusjon av dagslys i bygninger		**LEED - U.S. Green Building Council**	
Walls	50 %	Walls	60 %
Ceiling	70 %	Ceiling	85 %
Floor	20-30 %	Floor	25 %

Table 3.2. The reflectance (rho) of different construction elements according to different regulations.

In table 3.3 the reflectance of different materials or colours according to *SBi* are shown. Only the materials and colors corresponding to the case office surfaces are presented. The full table of reflectance for different materials and colors can be seen in table O.12 on page 320 found in appendix O.3 on page 318.

Sbi anvisning 219 Dagslys i Rum og Bygninger	
Limfarve, snavset, hvid	0.40
Oliefarve, ny, hvid	0.80-0.90
Mørkegrå	0.10-0.35
Lysebrun	0.30-0.45

Table 3.3. The reflectance based on material or colours of the surfaces (Statens Byggeforskningsinstitut, 2008)

3.4.2 Surface Reflectance - Measured Value

The reflectance of the surfaces in the room was measured with a hand-held illuminance meter. Point measurements were conducted on the four walls of the room, the ceiling and the floor, as well as on the furniture in the room. The measurements were conducted at a point of the day when there was no direct sunlight entering the room. A description of the measurement procedure can be found in J on page 285.

The following table 3.4 shows the measured surface reflectance of the cell office in the case building.

Surface	**Measured luminance of the surface [lux]**	**Measured illuminance recieved by the surface [lux]**	**Reflectance [-]**
Wall	105.6	139.1	0.76
Desk	245.3	580.8	0.42
Teak wall by window	92.9	199.2	0.47
Ceiling	199.2	142.0	1.40 - N/A
Floor	22.3	349.6	0.06 - N/A
Door	104.1	133.8	0.78

Table 3.4. The measured surface reflectance of different building elements in the cell office of the case building.

As seen in the table, the measured reflectance of the ceiling is 1.40. This is clearly an error as the reflectance can only go from 0 to 1. The reflectance of the floor is measured to 0.06, which is extremely low and therefore unlikely to be accurate. This may be due to inaccuracies of the hand-held illuminance, or in the conduction of the measurements. Because of these inaccuracies, the measurement results are not to be trusted.

A set of surface reflectance values were chosen from *SBi* table O.12 on page 320. The table contains values for different colors and materials, and it was not certain which one corresponded the most with the walls in the cell office. Two different sets of reflectance values were therefore chosen to investigate. The results are presented in the following section.

3.4.3 Comparison of Measured and Simulated Interior illuminance Using different Surface Reflectance Values

To investigate how much the reflectance of the surfaces affects the interior illuminance level in the room, the interior illuminance level in the cell office was simulated in Relux with different values for surface reflectance. The initial set of reflectance values have very high values for the walls and ceiling. The second set of reflectance value are extracted from the *SBi* table O.12 on page 320. The resulting interior illuminance from the simulations were compared to the measured interior illuminance. Graph 3.11 and 3.12 show the results from the two simulations with the two different set of reflectance values.

First set of reflectance values is presented in the following table 3.5.

Surface	Reflectance [-]
Walls	0.9
Ceiling	0.9
Floor	0.1
Teak wall	0.45

Table 3.5. First set of reflectance values for the different surfaces in the room

The second set of reflectance values are presented in table 3.6

Surface	Reflectance [-]
Walls	0.4
Ceiling	0.9
Floor	0.1
Teak wall	0.3

Table 3.6. The second set of reflectance values for the different surfaces in the room

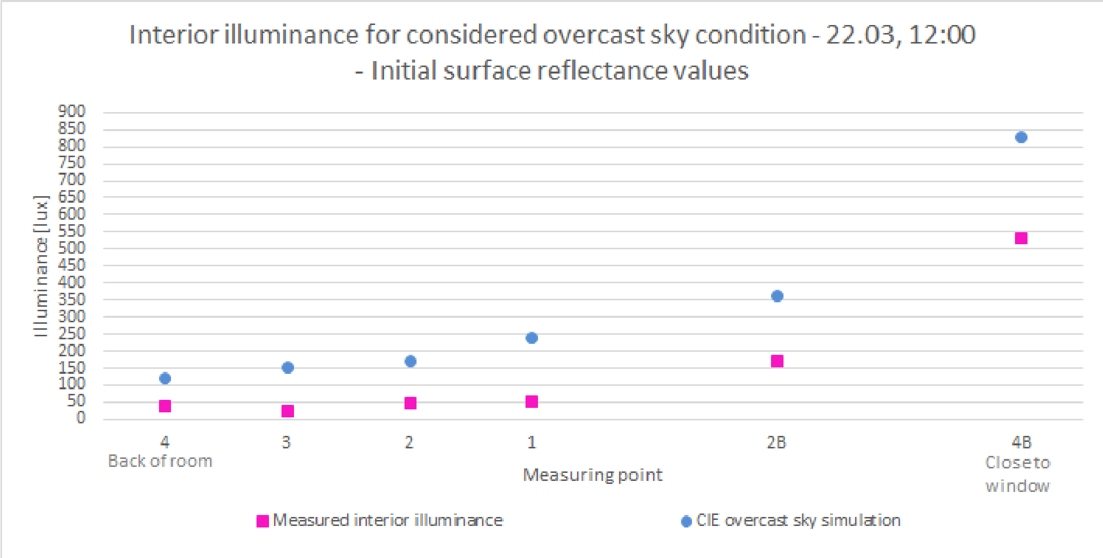

Figure 3.11. Measured interior illuminance compared to simulated interior illuminance when the first set of reflectance values are applied

Graph 3.12 for

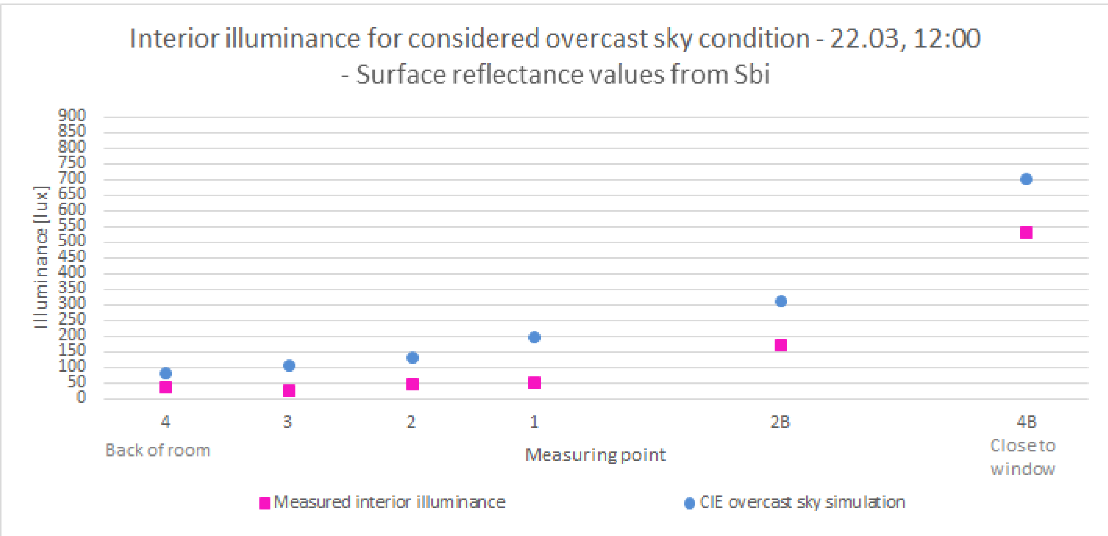

Figure 3.12. Measured interior illuminance compared to simulated interior illuminance with surface reflectance values extracted from *SBi*

The simulations were conducted for the 22^{nd} of March with CIE overcast sky conditions. Both of the graphs show that the measured interior illuminance has lower values than the simulated interior illuminance. It can be seen that the simulated values follows the same trend as the measured values where the illuminance increases closer to the window. There is not a large variation between the two simulation results. However, it is clear that the initial reflectance values results in higher values for the interior illuminance. The results from the simulation where the second set of reflectance values from *SBi* are applied are much closer to the measured illuminance, especially in the back of the room. It can be concluded that the reflectance does have an effect on the interior illuminance.

Since the measured surface reflectance values contained large inaccuracies, it was chosen not to further proceed with these values. The values from *SINTEF Byggforsk* does not take different materials and colors into account, but only displays a value for different construction elements in the room. It was therefore decided that it would be more accurate to apply the reflectance values from *SBi* for the materials and colors that corresponded to the colors and materials of the surfaces in the case office room. The following table 3.7 shows the values that was chosen for the case.

Surface	**Reflectance [-]**
Façade wall, Teak	0.30
Walls, matte white	0.4
Ceiling, white	0.9
Floor, carpet, dark grey	0.1

Table 3.7. The chosen surface reflectance values for further use in simulations. The values are extracted from corresponding materials and colors from table O.12 on page 320 found in O.3 on page 318.

3.5 Waves and Photons

Photons are quantum, extremely small particles, of electromagnetic energy. Photons are always in motion and move at the speed of light in vacuum, c=2.988 $*10^8 m/s$ (Jones, January 2015). An electromagnetic wave is a stream of photons which are capable of travelling through vacuum. They are produced by a vibrating electric charge, and consist of both an electric and a magnetic component (Henderson, January 2015). The electromagnetic waves have a wide range of frequencies from radio waves with long wavelength and low frequency, to gamma waves with short wavelength and high frequency as seen in figure 3.13. The visible light region is between infra-red and ultra violet.

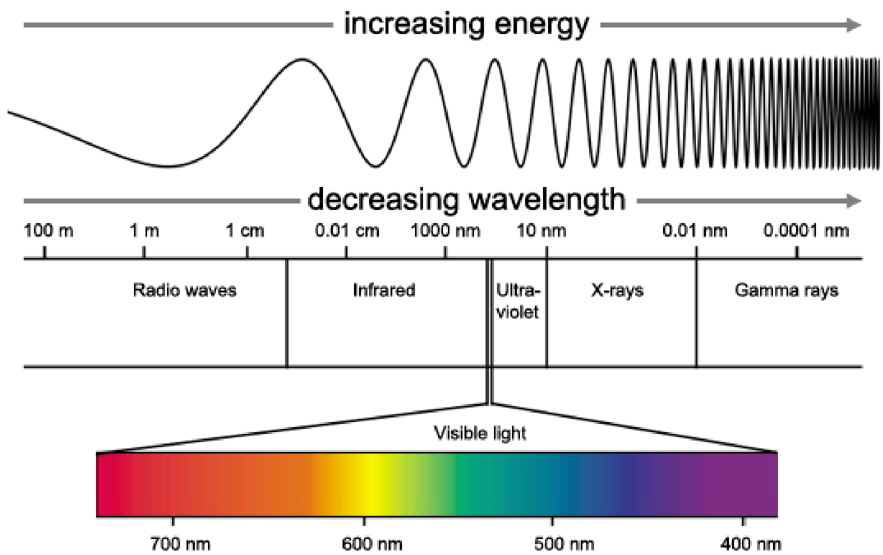

Figure 3.13. Different wavelengths and the visible light spectrum (Piatt, January 2015)

Photons do not have any mass, but they carry energy and momentum, the amount is related to the frequency and wavelength of the electromagnetic wave. When radiation is absorbed photons are destroyed, and when radiation is emitted photons are created.

3.6 Visible Light Spectrum

The visible light spectrum ranges from red light at 780 nm to violet light at 390 nm, which can be seen in figure 3.14. It is this narrow region of wavelengths our eyes are sensitive to.

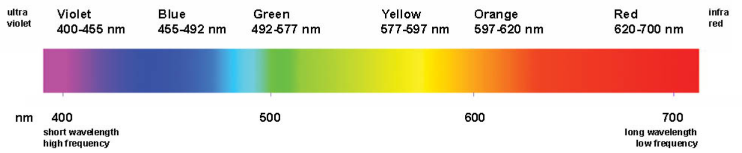

Figure 3.14. The visible light spectrum (Piatt, January 2015)

In the visible light region the different wavelengths represent different colours, so when a specific wavelength hit the retina in our eyes we perceive that specific color. Our eyes are sensitive to visible light, and it is the retina of our eyes which is responsible for this sensitivity. In the retina the cones receive the visible light. The retina of the eye is a part of the central nervous system, the retina is a light sensitive tissue at the inner surface of the eye (Kolb, October 2011).

Black will be perceived by the eye when there is an absence of all the colors in the visible light spectrum. The eye will perceive white light when a combination of all the colors in the visible light spectrum hit the eye at the same time (Henderson, January 2015). It was Sir Isaac Newton who first discovered this phenomenon by passing white light through two prisms (Indiana University Bloomington, January 2015). The first prism made the with light into a spectrum of colors, while the second prism recomposed the light back to white as seen in figure 3.15.

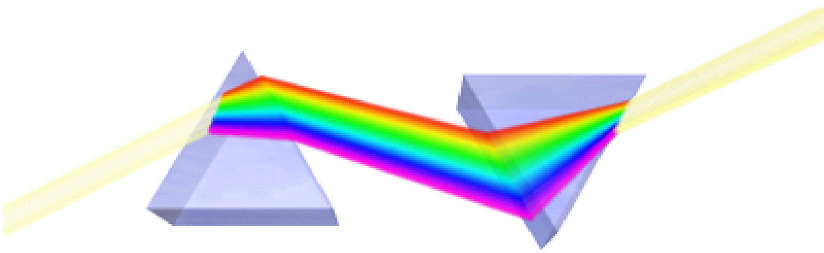

Figure 3.15. Sir Isaac Newton's prism experiment (Indiana University Bloomington, January 2015)

Calculation Methods 4

In this chapter different simulation programs for daylight analysis and their calculation engine will be presented. These programs will be applied later in chapter 5.

4.1 Daylight Factor

The daylight factor is defined as the ratio of internal light level to the external light level (Statens Byggeforskningsinstitut, 2013), and the value is normally in percent [%]. The daylight factor describes the amount of daylight in a specific point inside a room.

$$DF = \frac{E_i}{E_o} \cdot 100\% \tag{4.1}$$

Where:

E_i	The illuminance due to daylight at a point on the indoor working plane [lux]
E_o	Simultaneous outdoor illuminance on a horizontal plane from an unobstructed hemisphere of overcast sky [lux]

The daylight factor is calculated for a standard overcast sky, thus the daylight factor is independent of the orientation of the windows (Statens Byggeforskningsinstitut, 2013).

4.2 Radiosity

The radiosity method calculates the energy exchange between each surface in a scene, these surfaces are divided into patches in order to obtain exact light visualization distributions (Witzel, 2012). The method was initially developed to study thermal heat transfer, radiosity is an algorithm solving rendering equations for scenes applying the finite element method (Statens Byggeforskningsinstitut, 2013).

A high resolution visualization is achieved as the software programs will ensure a fine grid where the difference in the illuminance is high (Witzel, 2012). In addition to the calculation of the surfaces the calculation points must be determined, or the results at the calculation points must be interpolated from the results on the surfaces (Witzel, 2012). One of the weaknesses of the radiosity method is that the calculation time for large scenes or complex geometries can be significantly long, another weakness of the method is that it only considers diffusely reflecting materials. The radiosity method can consider transmittance and mirroring, highly reflecting surfaces, if some refining have been applied.

Between every pair of mesh patches view factors are computer, hereafter the illumination of each mesh patch is calculated by adding the contribution if all visible surrounding mesh patches and light sources (Witzel, 2012). However, the calculation of the view factors between the patches is on of the most troublesome parts of this method (Tsangrassoulis og Bourdakis, 2002). The required amount of data storage increases with the number of mesh patches, this indicates that the radiosity method cannot effectively model the reflectivity.

The radiosity method should only be applied to estimate simple scenes, the method also has constraints for the daylight simulations for diffuse surfaces and complex descriptions of the sky (Statens Byggeforskningsinstitut, 2013).

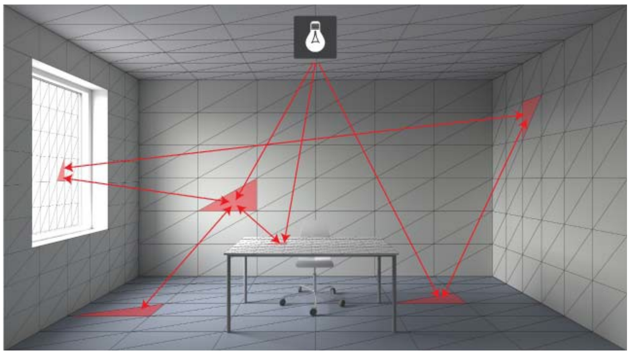

Figure 4.1. The radiosity calculation method (Statens Byggeforskningsinstitut, 2013)

In Relux the default calculation engine is radiosity, but Relux can also apply the ray tracing method (Statens Byggeforskningsinstitut, 2013). The simulation software SimLight, which is an addition to BSim, applies the radiosity calculation engine.

4.2.1 The Radiosity Method in Relux

The cell office in the case building is simulated for CIE overcast sky conditions and CIE clear sky conditions for a room with similar geometry and orientation as the cell office in the case building. The clear day simulated was Saturday 14^{th} of March and the overcast day simulated was Sunday 22^{nd} of March, both at 12:00. No external obstructions was inserted in the scene as of now.

Component	Value
Transmittance of glazing	70%
Reflectance of the three white walls	0.4 (Statens Byggeforskningsinstitut, 2008)
Reflectance of the wooden wall	0.30 (RELUX Informatik AG, 2007)
Reflectance of the ceiling	0.9 (Statens Byggeforskningsinstitut, 2008)
Reflectance of the floor	0.1 (Statens Byggeforskningsinstitut, 2008)
Orientation	128°
Size of glazed area	0.8 m^2 (1.6 m^2 for both)
Area of the cell office	8.26 m^2
Height of room	2.85 m
Depth of room	3.931 m
Width of room	2.102 m

Table 4.1. Inputs in Relux.

The interreflections are set to 2 as this is sufficient for our situation as the cell office receives both direct and indirect illumination (RELUX Informatik AG, 2011), for scenes with only indirect illumination interreflections of at least 4 is recommended.

Only daylight is simulated in 4.3 and 4.2.

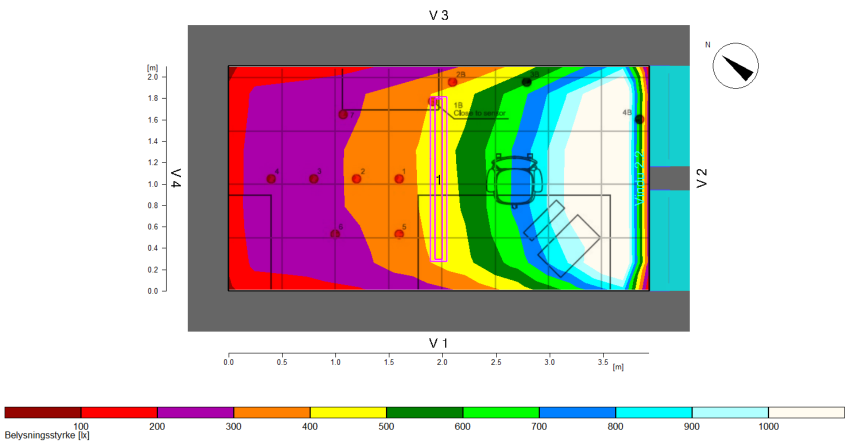

Figure 4.2. The radiosity calculation method in Relux for CIE overcast sky showing illuminance distribution in the cell office without external obstruction

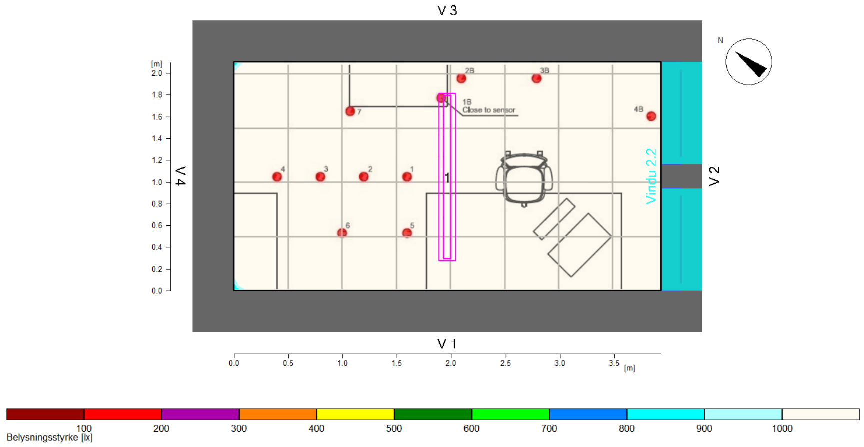

Figure 4.3. The radiosity calculation method in Relux for CIE clear sky showing illuminance distribution in the cell office without external obstruction

The illuminance scale is customized to easily see the steps of 100 lux from the minimum of below 100 lux to the maximum of above 1000 lux.

The result for the overcast day shown in figure 4.2 show an illuminance distribution ranging from 100 lux to above 1000 lux. Closest to the window the illuminance level is above 1000 lux and then the level is decreasing towards the back of the cell office which seams reasonable. For the clear day shown in figure 4.3 has an illuminance distribution above 1000 lux for almost the whole cell office except in the back corners where it is 900 lux. This does not seam reasonable and will be looked further into in section 4.5.

4.3 Ray Tracing

The ray tracing method is a rendering technique, the distribution of a high number of rays emitted in a scene are calculated (Statens Byggeforskningsinstitut, 2013). The method can be subdivided into two methods, namely the forward and backward ray tracing methods. The forward ray tracing method applies rays emitted from the light source, while the backward ray tracing applied rays emitted from a view point.

The ray tracing algorithm is capable of calculating reflection, transmission and refraction properties of surfaces which allows the user to apply complex materials in the simulations (Statens Byggeforskningsinstitut, 2013). The ray tracing method can also easily deal with complex building forms (Tsangrassoulis og Bourdakis, 2002).

(Tsangrassoulis og Bourdakis, 2002): In more detail, for the forward ray tracing rays are emitted from the light source and striking the surfaces in the space which contribute to the luminances of these surfaces. For the backward ray tracing the rays are emitted from a point in the scene trying to trace the light sources (Tsangrassoulis og Bourdakis, 2002). The backward ray tracing is faster compared to the forward method as the backward method only calculated the rays reaching the view point (Statens Byggeforskningsinstitut, 2013).

Every ray carries a ”weight” which corresponds to the intensity of that ray, after a ray strikes the surface a new ray will be generated and the ”weight” of the new ray depends on the reflection of the surface. When the ”weight” is below a certain value it is absorbed and then the process is repeated with a new emission (Tsangrassoulis og Bourdakis, 2002).

An illustrative figure of the ray tracing method can be seen in figure 4.4.

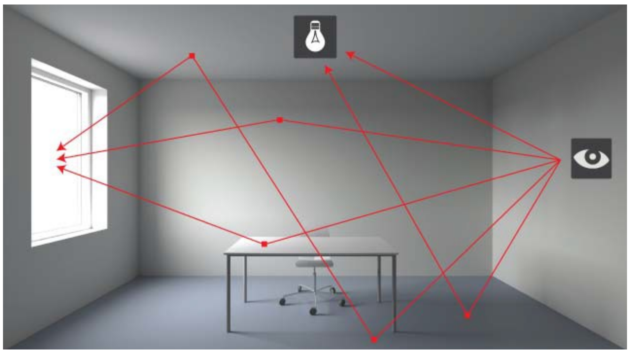

Figure 4.4. The backward ray tracing calculation method (Statens Byggeforskningsinstitut, 2013)

Relux can apply this calculation engine if desired, the raytracing module in ReluxPro is based on backward raytracing (RELUX Informatik AG, 2011).

4.3.1 The Ray Tracing Method in Relux

The same model and values were applied for the ray tracing method, the values can be found in table 4.1.

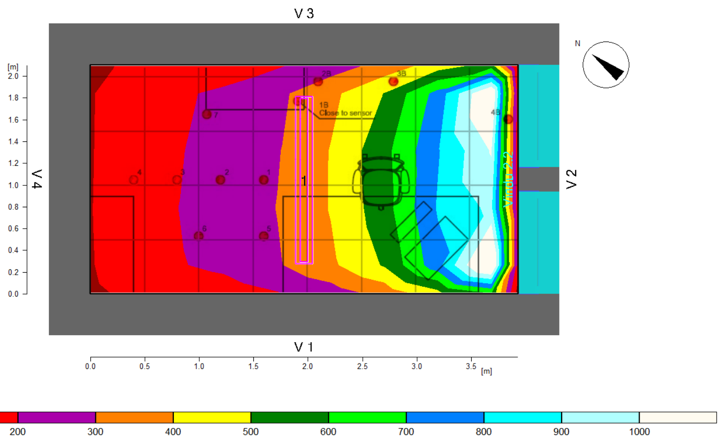

Figure 4.5. The ray tracing calculation method in Relux for CIE overcast sky showing illuminance distribution in the cell office without external obstruction

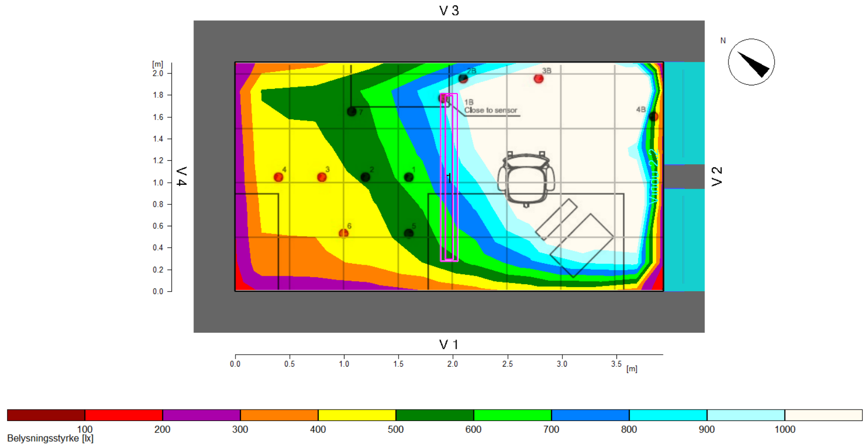

Figure 4.6. The ray tracing calculation method in Relux for CIE clear sky showing illuminance distribution in the cell office without external obstruction

As seen in figure 4.5 closest to the window the illuminance level is between 800 lux to above 1000 lux for two small patches. In figure 4.6 the illuminance level is considerable higher and covering quite a significant part of the cell office. The results in Relux will be studied further in section 4.5.

4.4 Photon Mapping

Bi-directional ray tracing is applied in the photon mapping rendering technique. First forward ray tracing and photon mapping is applied to distribute the light in the scene, then backward ray tracing is applied from the view point to compute the final image (Statens Byggeforskningsinstitut, 2013).

In more detail, in photon mapping the photon maps are made by emitting a large number of photons from the light source. Then each photon is traced through the scene applying a method which is similar to the forward ray tracing method (Jensen, 1996). When a photon hits the surface it is stored within the photon map and it is chosen if the photon is absorbed, transmitted or reflected dependent on the property of the material (Witzel, 2012). If the photon is reflected then the direction is computed by applying the bidirectional reflectance distribution function of the surface. The rendering of the final image is done by applying Monte Carlo backward ray tracing (Jensen, 1996). The accuracy of the method can be increased by increasing the number of photons (Statens Byggeforskningsinstitut, 2013).

The photon mapping method is illustrated in figure 4.7.

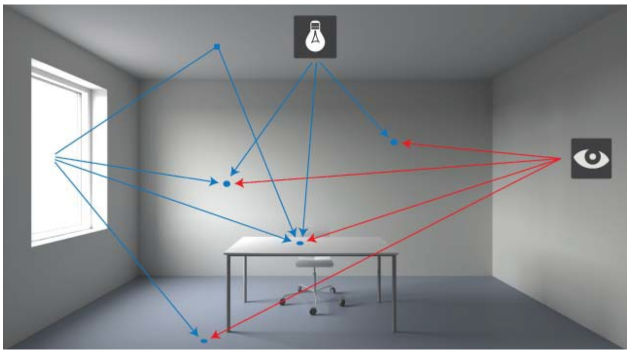

Figure 4.7. The photon mapping calculation method (Statens Byggeforskningsinstitut, 2013)

Photon mapping is applied as the calculation engine in VELUX Daylight Visualizer.

4.4.1 The Photon Mapping Method in VELUX Daylight Visualizer

The cell office in the case building is simulated for CIE overcast sky conditions and CIE clear sky conditions for a room with similar geometry and orientation as the cell office in the case building. The clear and overcast days were simulated at the 21^{st} of March, both at 12:00. It is only possible to select the 21^{st} of every month in VELUX Daylight Visualizer. No external obstructions was inserted in the scene for now. All walls must have the same material, therefore the wooden wall on the façade is said to have the same reflectance as the three other walls. The input in VELUX Daylight Visualizer is shown in table 4.2.

Component	Value
Transmittance of glazing	70%
Reflectance of the three white walls	0.4 (Statens Byggeforskningsinstitut, 2008)
Reflectance of the ceiling	White paint (matte) 0.9
Reflectance of the floor	Black tiles 0.21
Orientation	128°
Size of glazed area	0.8 m^2 (1.6 m^2 for both)
Area of the cell office	8.26 m^2
Height of room	2.85 m
Depth of room	3.931 m
Width of room	2.102 m

Table 4.2. Input in VELUX Daylight Visualizer.

It is not possible to change the reflectance of the floor material. It is not possible to customize the illuminance scale in VELUX Daylight Visualizer. The overcast and clear CIE sky conditions are simulated and the results are shown in figure 4.8 and figure 4.9.

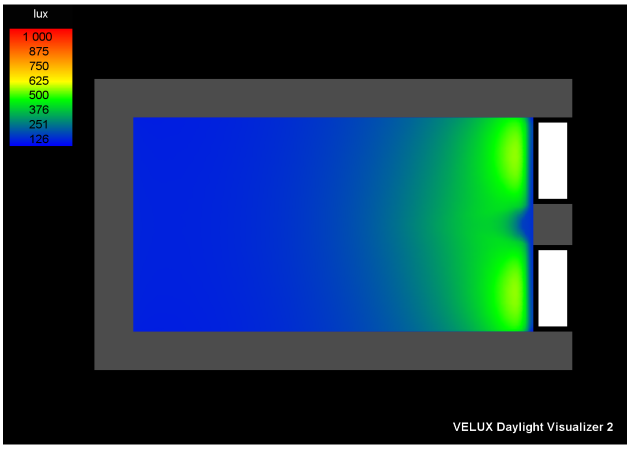

Figure 4.8. Photon mapping in VELUX Daylight Visualizer CIE overcast sky showing illuminance distribution in the cell office

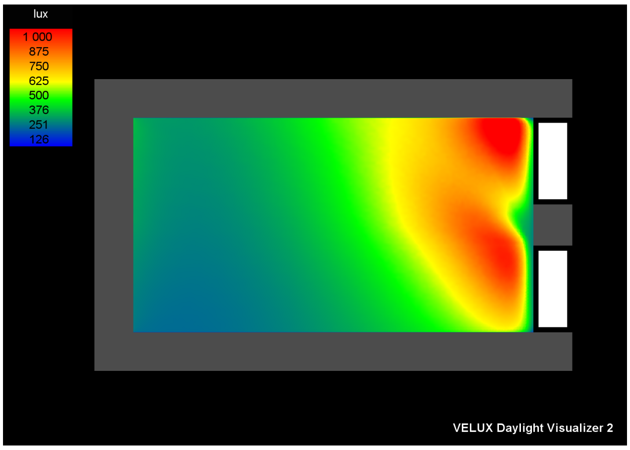

Figure 4.9. Photon mapping in VELUX Daylight Visualizer CIE clear sky showing illuminance distribution in the cell office

For the overcast sky condition the illuminance level is rather low for the cell office as seen in figure 4.8. The illuminance maximum reaches 500 lux close to the window. For the clear sky on the other hand the illuminance level reaches 1000 lux for a larger part of the cell office close to the window, and the illuminance level is about 500 lux further in to the depth of the cell office.

4.5 Comparing Radiosity, Ray Tracing and Photon Mapping

When studying the result for the clear day simulated with the photon mapping 4.9 and ray tracing 4.6 methods it is noticed that the results are very similar for the two methods. The illuminance distribution within the cell office has the same trends in the two results, epicyclically close to the window. The radiosity method on the other hand is completely different with above 1000 lux for the whole cell office.

When comparing the overcast CIE sky conditions the radiosity method 4.2 show higher illuminance for a larger part of the cell office close to the window compared to the ray tracing method 4.5 and photon mapping 4.8. Again, the result for the photon mapping and ray tracing have similar trends.

4.6 Simulation of the Cell Office in the Case Building

It is desired to find a simulation software which can most accurately simulate the situation for the case building. A software which can be customized as much as possible to fit as exactly as possible to the geometry of the cell office and the properties of the materials.

As the exact reflectance of the surfaces cannot be inserted in VELUX Daylight Visualizer, as well as the software holds limitations in the window parameters and the geometry of the window this make the model inaccurate.

It is possible to insert interior obstacles such as furniture and people in Relux and VELUX Daylight Visualizer as seen for Relux in figure 4.10, interior obstacles has not been inserted in this chapter.

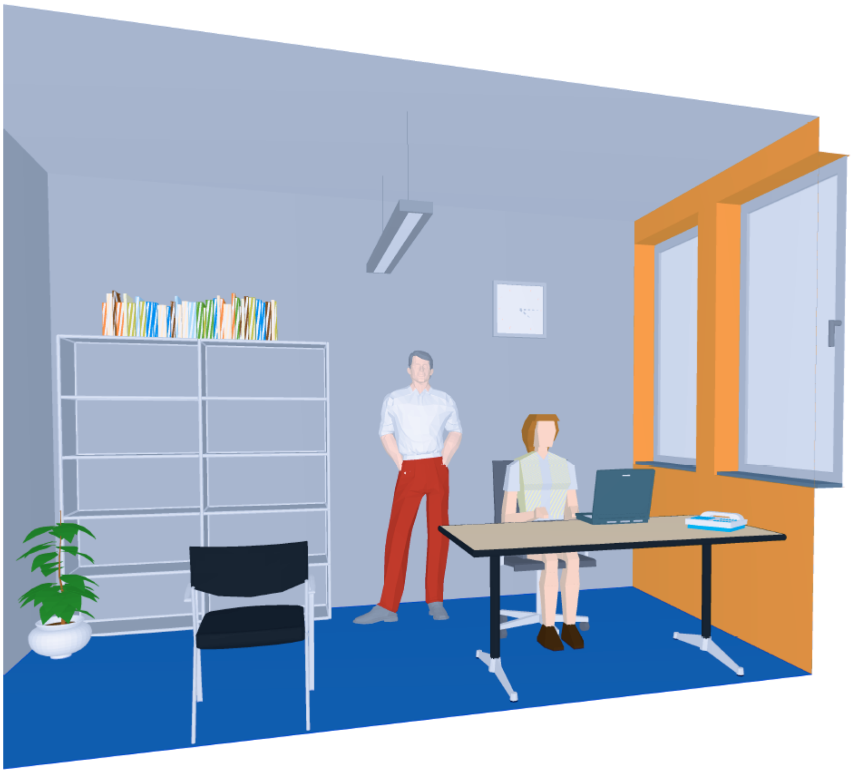

Figure 4.10. The cell office with interior obstacles in Relux

In order to simulate the exact same situation as the case building it is important to include the exterior obstacles. There is an office building opposite the cell office towards the East. The reflectance of the building opposite the façade where the cell office is placed is not know, the reflectance of this building as well as the distance between the case building and this building is important in order to simulate a scene which is as similar to the actual scene as possible. As it is a glazing building the value for reflectance of windows is set to 0.15 (Statens Byggeforskningsinstitut, 2008). The distance between the two buildings is 40 m, the height is not known, but it is about the same height as the case building as the building regulation in the area is the same for the two buildings. The cell office is on the third floor, therefore it is assumed that the roof of the building across the cell office is 12 m above the ceiling of the cell office.

Relux allows us to insert external obstacles, as well as the geometry of the model and the properties of the materials can be customized to be as close to reality as possible. Simulation of the cell office with the office building opposite the case building inserted in the model as external obstruction with reflectance of 0.15 is performed. In VELUX Daylight Visualizer external obstruction is inserted as well with the same reflectance.

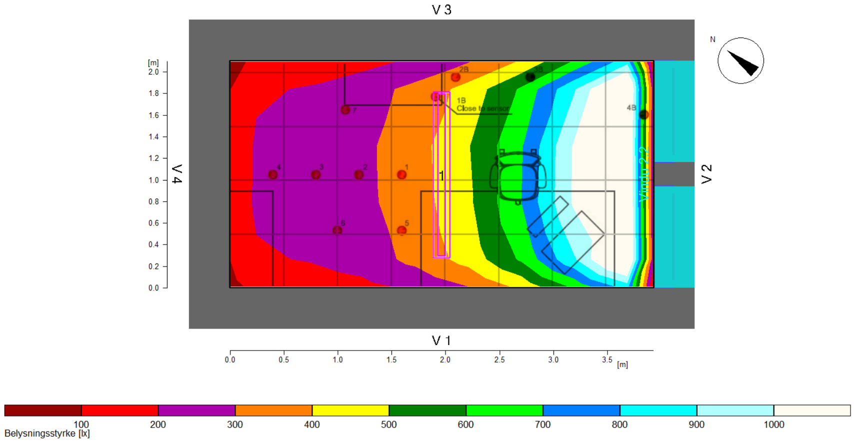

Figure 4.11. The radiosity calculation method in Relux for CIE overcast sky showing illuminance distribution in the cell office with external obstruction

As seen in the simulation result from Relux with the radiosity method for CIE overcast sky with external obstruction in figure 4.11 the illuminance level is slightly lower compared to the result for the radiosity method without external obstruction seen in figure 4.2.

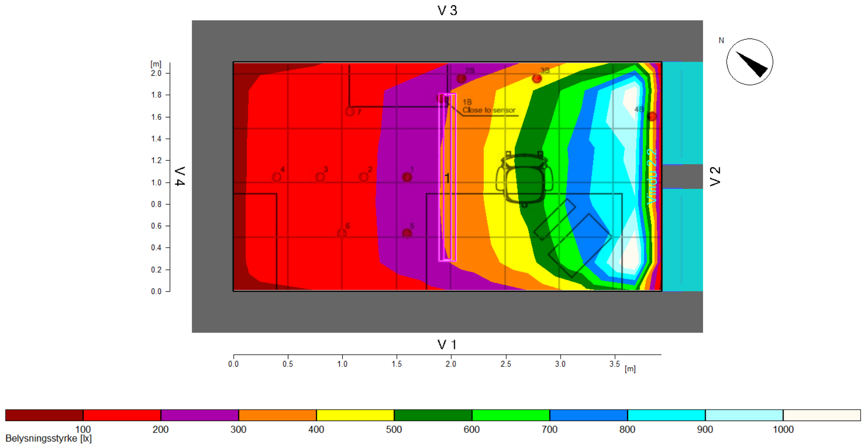

Figure 4.12. The ray tracing calculation method in Relux for CIE overcast sky showing illuminance distribution in the cell office with external obstruction

The simulation result from Relux with the ray tracing method for the CIE overcast sky with external obstruction seen in figure 4.12 has slightly lower illuminance level compared to the result without external obstruction seen in figure 4.5. Especially can it be noticed that the illuminance level decreases faster close to the side walls in the model with external obstruction meaning the illuminance level steps of 100 lux are more "flatter" in the middle of the room, compared to the model without external obstruction.

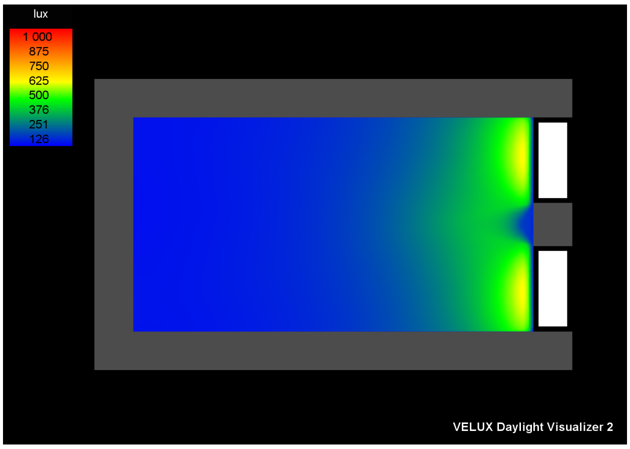

Figure 4.13. Photon mapping in VELUX Daylight Visualizer for CIE overcast sky showing illuminance distribution in the cell office with external obstruction

As seen in figure 4.13 the illuminance is slightly higher for the situation with obstruction compared with the situation without obstruction in figure 4.8. This is probably due to the reflected component from the building opposite the cell office is increased, and as the sky is overcast there is no shading of the direct component as it is only the diffuse component which contributes to the lighting level inside.

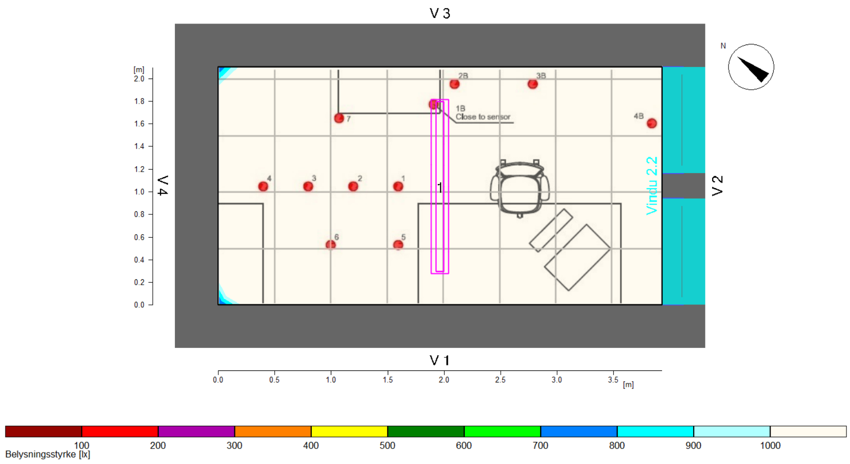

Figure 4.14. The radiosity calculation method in Relux for CIE clear sky showing illuminance distribution in the cell office with external obstruction

The simulation result of the CIE clear sky for the radiosity method in Relux with external obstruction seen in figure 4.14 is very similar to the simulation without external obstruction seen in figure 4.3. Both situations have an illuminance level above 100 lux for most of the cell office. This does not seam reasonable. The direct fraction, low indirect fraction, middle indirect fraction and high indirect fraction can be chosen for the precision of the radiosity method in Relux. All have been tested but the result is the same for all variations of the fractions. Therefore it can be concluded that the radiosity method cannot calculate the situation for the cell office.

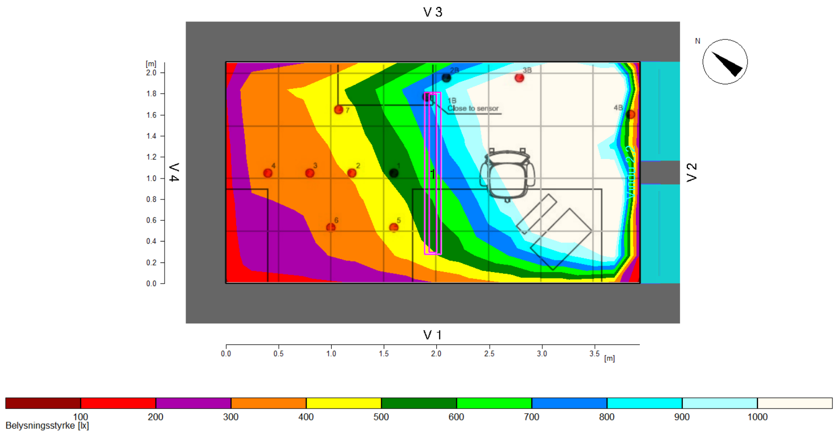

Figure 4.15. The ray tracing calculation method in Relux for CIE clear sky showing illuminance distribution in the cell office with external obstruction

The simulation result for CIE clear sky with external obstruction applying the ray tracing method seen in figure 4.15 has similar illuminance distribution as the simulation result without external obstruction seen in figure 4.6. The difference is a slightly lower illuminance level for the simulation with external obstruction compared to the model without.

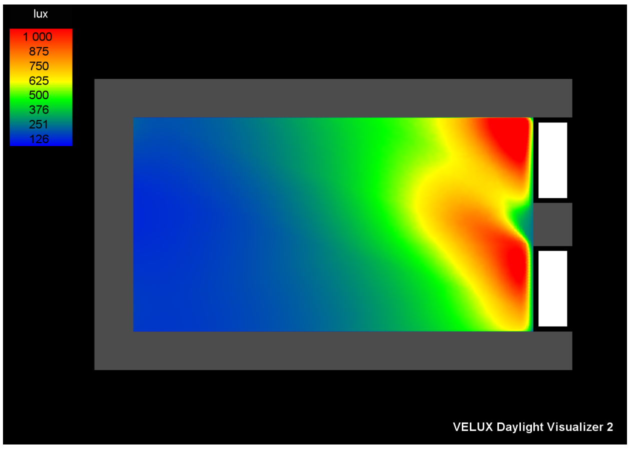

Figure 4.16. Photon mapping in VELUX Daylight Visualizer for CIE clear sky showing illuminance distribution in the cell office with external obstruction

A decrease in the illuminance level can be seen for the result with external obstruction in figure 4.16 compared to the simulation result without external obstruction 4.9. This is due to shading caused by the external obstruction reducing the direct illumination entering the cell office.

As expected for most of the simulation results with external obstruction the illuminance level was slightly lower compared to the simulation results without the external obstructions, except for the photon mapping with overcast sky condition. The office building across the case building will shade and allow less direct and diffuse daylight entering the cell office, at the same time as it will increase the reflected component from the outside. The increased reflected component is for the case building smaller compared to the diffuse and direct components of contribution to daylight and therefore the decrease in illuminance level when external obstruction is included in the scene, except as mentioned for photon mapping for overcast sky condition. Relux nor VELUX Daylight

Visualizer allow the user to see the size of the three different components of daylight, the direct, diffuse and reflected, only the sum is shown by the illuminance level.

It is concluded to apply the ray tracing method for most of the simulations of the cell office as Relux allows more customization of the model compared to VELUX Daylight Visualizer which applies the photon mapping. The radiosity method does not seam to be able to calculate the situation for the cell office. Therefore, the raytracing method in Relux and the photon mapping in VELUX Daylight Visualizer will both be applied for simulations of the cell office, but they will be applied for different purposes as they have different qualities and the most suited for a certain case will be applied. A comparison between simulated interior illuminance level and measured interior illuminance level will be conducted in section 5.2.4 on page 51.

Part II

Natural and Artificial Light

In this part of the report different approaches to categorize real sky conditions as different CIE sky conditions is utilized.

The results for the interior illuminance level due to different CIE sky conditions is presented and compared to the actual interior illuminance.

The electricity usage of the armature in the cell office is presented, together with specifications about the control of the artificial lighting due to available daylight.

Knowledge gained in this part will be applied in part IV when the estimation methodology is utilized.

Sky Conditions 5

To be able to determine daylight availability in a building, the sky must be modelled. The luminance distribution of the sky changes due to the cloud thickness and distribution. Together with the altitude and azimuth angle of the sun, the atmosphere affects the amount of illumination reaching the earth's surface. The cloud cover holds an infinite number of combinations between thickness and the scattering of the clouds.

By observing the sky, it can simply be said to be clear or overcast. If the sky is cloudless it is said to be clear, and if it is covered by clouds it is said to be overcast. When determining daylight availability in a building, however, a more detailed analysis of the sky conditions is needed. CIE (Comission Internationale de l'Eclairage) has defined a set of standardized sky conditions for daylight design purposes, according to the luminance distribution of the sky dome during different conditions.

In this chapter, the solar irradiance during the days when the sky was determined to be clear or overcast, simply according to observations, will be presented. This is done to see if there is a typical pattern in the relation between diffuse and direct solar irradiance for the two different conditions. This simple study is followed by an analysis of the interior illuminance measured on the clear and overcast days, compared to the interior illuminance simulated with CIE sky conditions in Relux.

5.1 Classifying Sky Conditions According to Measured Solar Irradiance and Observations

The global irradiance was measured by a pyranometer located on the roof of the case building. This includes measurements of both direct and diffuse irradiance. The irradiance was measured for 13 days from Friday the 13^{th} of March to Wednesday the 25^{th} of March with a time interval of one minute. A detailed description of the irradiance measurements can be found in appendix D on page 229.

A web camera was installed in the window of the cell office. The web camera was facing the sky outside the cell office. Snapshots were taken of the sky at 08:00, 10:00, 12:00, 14:00, 16:00 and 18:00. Pictures of the sky as well as notes about observations of the changes in sky condition from each day of the measurement period is located in appendix I on page 257.

5.1.1 Observed Clear Sky and the Corresponding Solar Irradiance

Two days during the measurement period, 14.03.15 and 21.03.15 are according to the observations defined as days with clear sky conditions. The sky during these days were cloudless. Pictures of the sky at different times of the day can be seen in figure 5.1, and the solar irradiance measurements for the same day can be seen in figure 5.2.

Figure 5.1. Change in sky condition throughout Saturday 14.03.2015

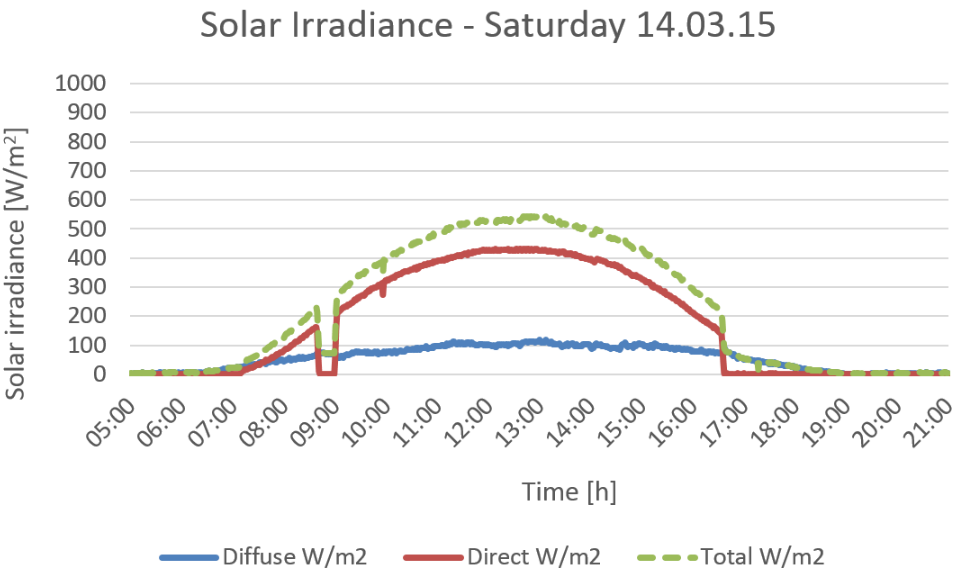

Figure 5.2. The diffuse, direct and total irradiation for Saturday 14.03.2015

As seen in 5.1, the sky was clear and cloudless throughout the entire day. This also shows on the graph 5.2 where it can be seen that the direct component of the irradiation is high compared to the diffuse component. The diffuse irradiance is low and stable throughout the day, while the direct irradiance has a smooth curve rising until noon and decreasing towards the evening. The rapid decrease at 16:40 is due to shadow from the crane on the construction site next to the case building.

Figure 5.3. Change in sky condition throughout Saturday 21.03.2015

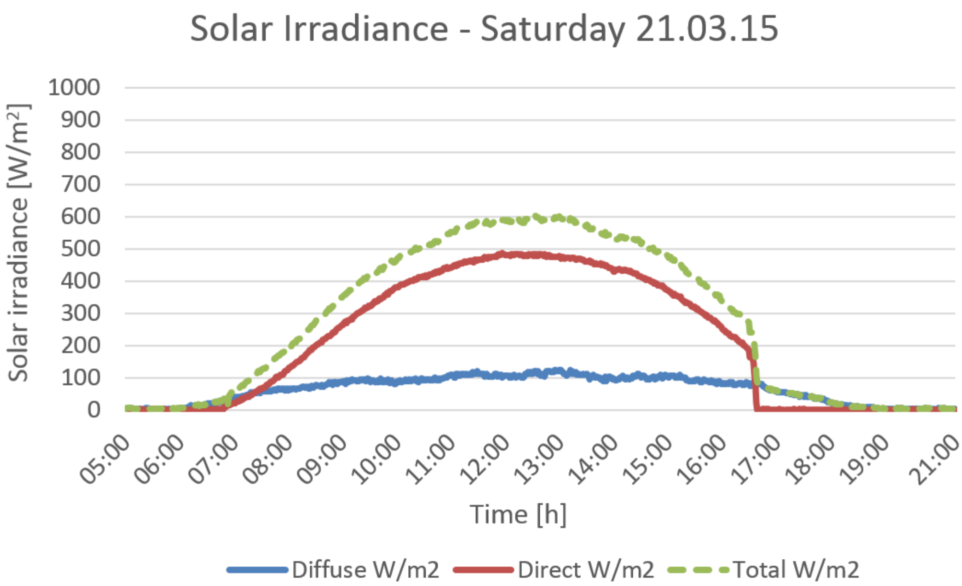

Figure 5.4. The diffuse, direct and total irradiation for Saturday 21.03.2015

As seen in 5.3 there were little to no clouds during this day as well. The irradiance graph 5.4 has similar characteristics as the graph from the 14.03.15, with the high smooth direct component, and low stable diffuse component.

To compare the two days, the relative magnitude of the direct and the diffuse component to the total irradiance is determined. On the 14.03.15 the total irradiance reached its maximum value of 545 W/m^2 at 12:45. The corresponding direct and diffuse irradiance at the same time is 431 W/m^2 and 114 W/m^2 respectively. This means that the direct irradiance provides 79.08% of the total irradiance, while the diffuse irradiance provides 20.91% of the total irradiance.

On the 21.03.15 the total irradiance reached its maximum value of 605 W/m^2 at 12:33. The corresponding direct irradiance at the same time is 483 W/m^2 and the diffuse irradiance is 122 W/m^2. The direct irradiance then provides 79.83% of the total irradiance, while the diffuse component provides 20.16% of the total irradiance.

From these results it can be concluded that a certain pattern do occur in the relation between the diffuse and direct solar irradiance on days that are, by observations, stated to be clear. The direct irradiance has a smooth curve throughout the day and provides approximately 80% of the total irradiance, while the diffuse irradiance provides only approximately 20% of the total irradiance in both of the days.

5.1.2 Observed Overcast Sky and the Corresponding Solar Irradiance

When looking at the snapshots taken by the web camera, Monday 16.03.15 5.5, Wednesday 18.03.15 5.7 and Sunday 22.03.15 5.9 are the days where the sky can be said to be stably overcast throughout the entire day.

As seen in 5.6, 5.8 and 5.10, the irradiance on an overcast day is characterized by the low diffuse component, and the non-existing direct component of the solar irradiance. On the graphs, the total irradiance is below 300 W/m^2 for the three days. On Sunday 22.03.15 the total irradiance is even below 200 W/m^2.

Figure 5.5. Change in sky condition throughout Monday 16.03.2015

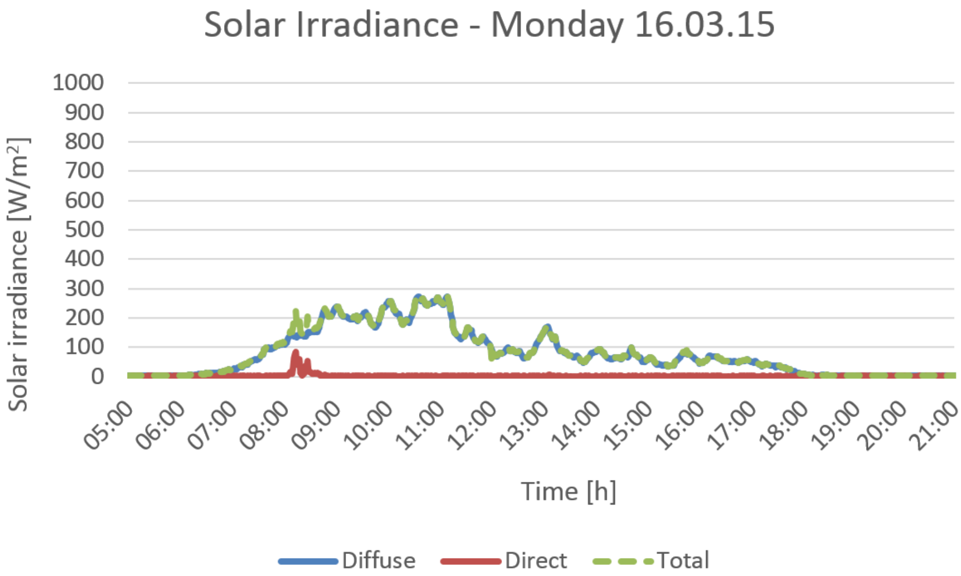

Figure 5.6. The diffuse, direct and total irradiation for Monday 16.03.2015

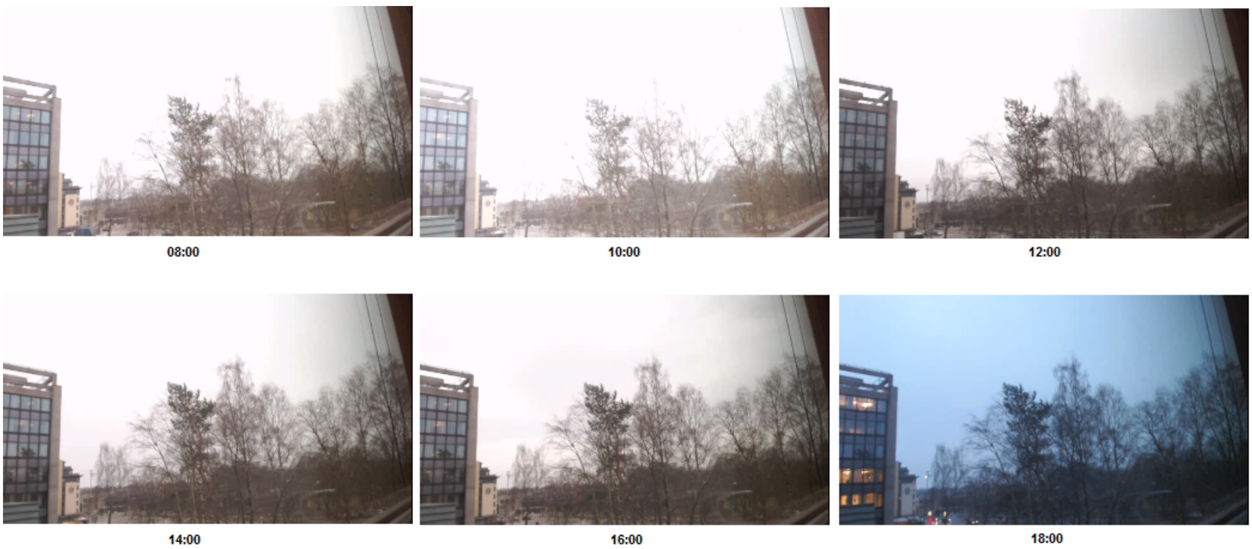

Figure 5.7. Change in sky condition throughout Wednesday 18.03.2015

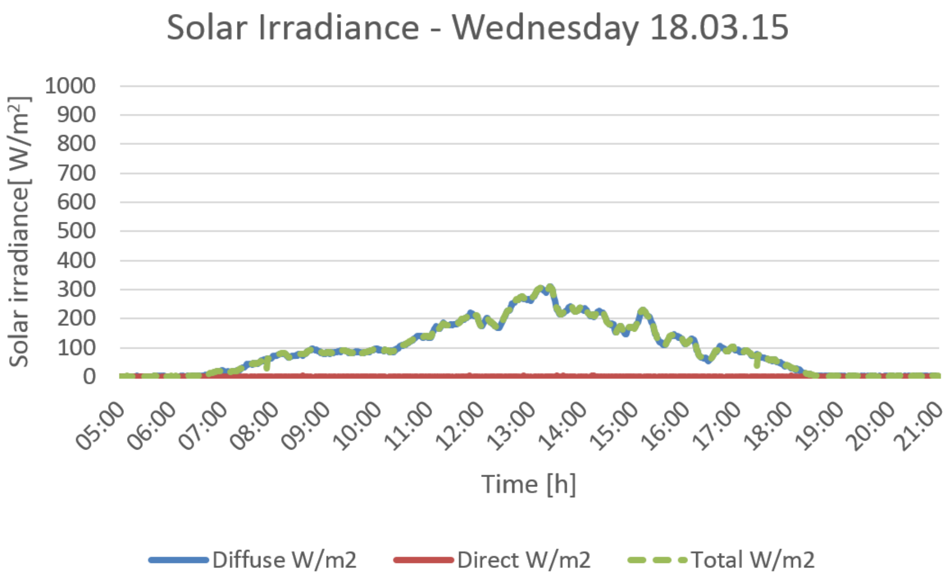

Figure 5.8. The diffuse, direct and total irradiation for Wednesday 18.03.2015

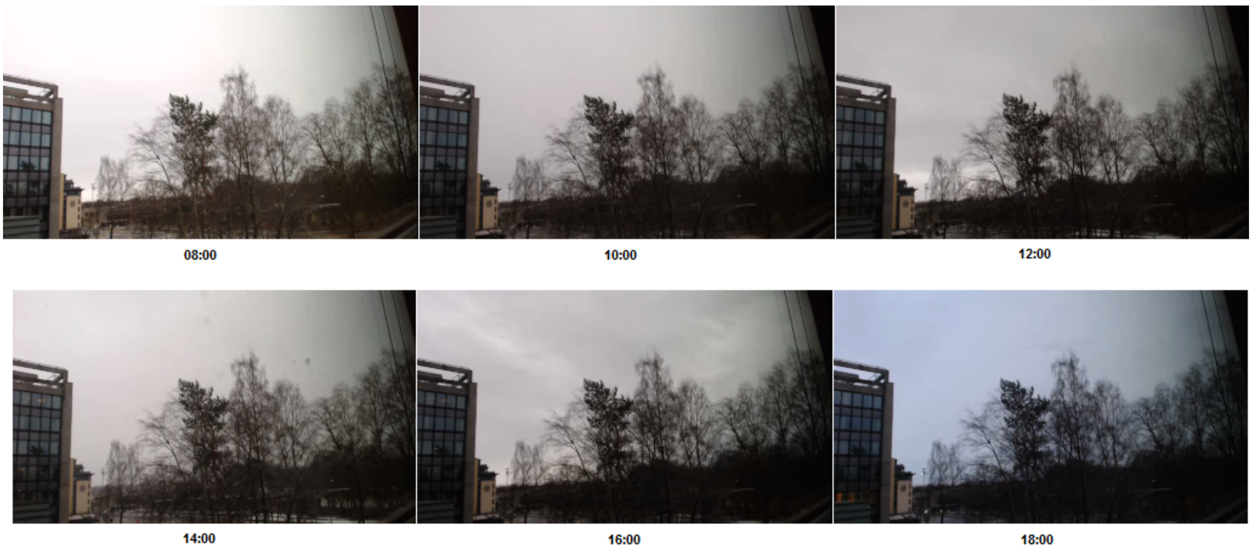

Figure 5.9. Change in sky condition throughout Sunday 22.03.2015

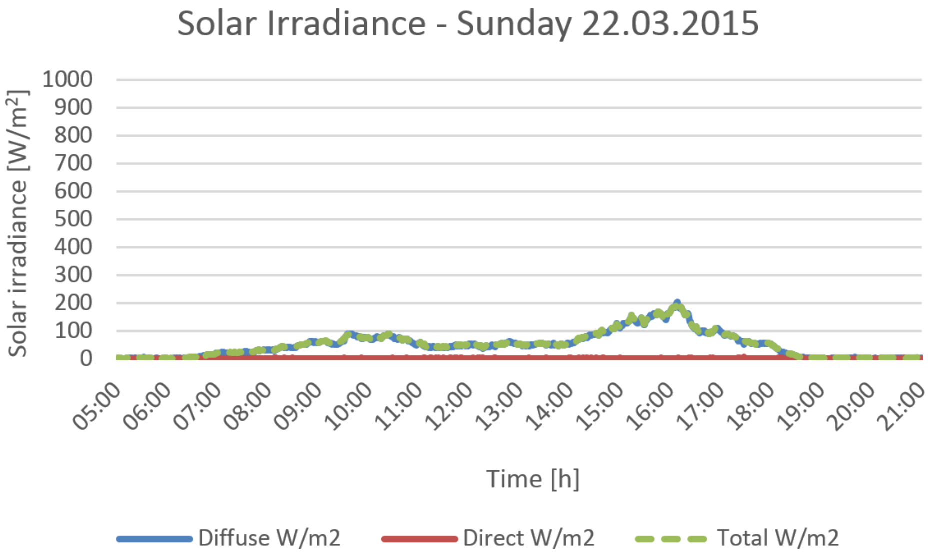

Figure 5.10. The diffuse, direct and total irradiation for Sunday 22.03.2015

Graph 5.10 show that the total solar irradiance is only due to the diffuse solar irradiance.

5.1.3 Correspondance Between Observed Sky Conditions and Measured Solar Irradiance

Two days from the measurement period, 14.03.15 and 21.03.15, are days when the sky conditions are stated to be clear, simply by observation. For the corresponding solar irradiance, the direct component provides approximately 80% of the total irradiance, while the diffuse component provides for only 20% of the total irradiance.

Three days during the measuring period, 16.03.15, 18.03.15 and 22.03.15, are days when the sky conditions are assumed to be overcast by observation. The corresponding solar irradiance for these dayys is characterized by the diffuse component having values below 200 $\mathrm{W/m^2}$, while there is no direct irradiance throughout the day.

The remaining days in the measuring period have varying sky conditions throughout the day with a combination of cloudy and clear conditions. For example does Monday the 23^{rd} have overcast conditions in the morning until approximately 13:00, and in the afternoon it has intermediate sky conditions. These days are considered as days with intermediate sky conditions. Out of all the days in the measuring period, the majority of the days have intermediate sky conditions. Pictures as well as solar irradiance measurement results from all the days of the measurement period can be found in appendix I on page 257.

The most widely used sky conditions in simulation software are CIE clear- and overcast sky. The interior illuminance measurement results from the days defined as clear and overcast are further utilized for matching the simulation results to the measurement results.

5.2 Comparison of Measured Interior Illuminance and Simulated Interior Illuminance During Different CIE Sky Conditions

CIE (Comission Internationale de l'Eclairage) has defined a set of standardized sky models for different sky conditions with the intention to give a method for calculating sky luminance and classify measured sky luminance in daylight design procedures. (de l'Eclairage, May 2015).

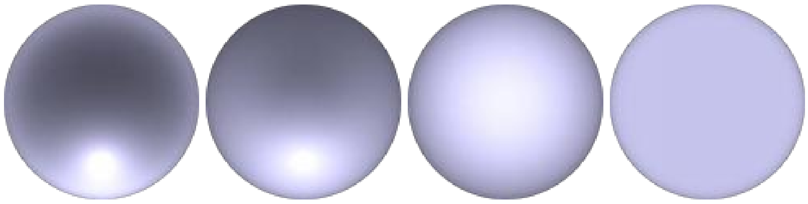

Figure 5.11. The luminance distribution [$\frac{\text{kcd}}{\text{m}^2}$]for four different CIE sky types (Satel-Light, April 2015).

5.2.1 CIE Clear Sky

The luminance in the standard CIE clear sky is dependent on both altitude and azimuth. It is brightest around the sun and dimmest opposite of the sun. In the horizon, the luminance value lays between the two extreme values (Satel-Light, April 2015).

5.2.2 CIE Intermediate Sky

The luminance of the standard CIE intermediate sky has a similar distribution to the clear sky. The difference is that the sun is not as bright, and the bright and dim values are not so extreme compared to each other as in the clear sky model (Satel-Light, April 2015).

5.2.3 CIE Overcast Sky

In the standard CIE overcast sky, the luminance in the zenith is three times as high as the luminance in the horizon. The overcast sky model is used when the daylight factor is calculated (Satel-Light, April 2015).

In the previous sections the solar irradiance during the overcast and clear days for the measurement period has been stated, but it is of interest to study their correspondence to the CIE sky types. This have been done by first studying the interior illuminance for the different sky conditions, and then in further detail investigate the exterior illuminance on a vertical plane.

It should be noted that the exterior illuminance was measured by a hand-held illuminance meter at certain times during the measurement period, but due to large inaccuracies these measurements are not included in this analysis. The exterior illuminance measurements are presented in appendix .

5.2.4 Interior Illuminance Due to Measured Exterior Illuminance and Different CIE Sky Conditions

As mentioned in 5.1.2 on page 46 the sky condition for the 22^{nd} of March is stated to be overcast, therefore the results for the measured interior illuminance in the cell office for this day is compared with simulated interior illuminance for CIE overcast sky. In order to investigate the interior illuminance and its dependency on the exterior illuminance, the measured interior illuminance is compared to simulated interior illuminance for different CIE skies. It is of interest to investigate how close the simulation result for interior illuminance is to the actual measured illuminance during an overcast sky. Interior obstacles has not been inserted in the simulation model as the desk can be elevated and the used elevates it up and down and it was uncertain at what level it was on for the different times, the user is not inserted as he moves about in the office.

The illuminance meters are placed as seen in figure 5.12. The results for the illuminance meters in point 1 - 4 in the center of the room as well as 2B and 4B close to the window is included for comparison. The results from illuminance meter in point 3B is excluded as there was an error to this illuminance meter. The occupant is not in office this day and only daylight is available.

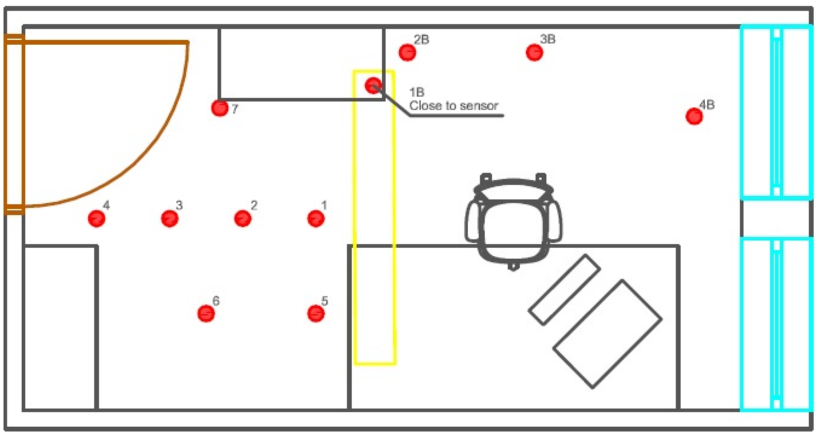

Figure 5.12. The placement of the illuminance meters in the cell office.

Relux is applied as simulation software and the inputs are shown in table 5.2.

Parameter	Value
Transmittance of glazing	70%
Reflectance of the three white walls	0.4 (Statens Byggeforskningsinstitut, 2008)
Reflectance of the wooden wall	0.30 (RELUX Informatik AG, 2007)
Reflectance of the ceiling	0.9 (Statens Byggeforskningsinstitut, 2008)
Reflectance of the floor	0.1 (Statens Byggeforskningsinstitut, 2008)
Orientation	308°
Reflectance of office opposite	0.15

Table 5.1. Input in Relux.

Graph 5.13 show the measured illuminance at 12:00 for each measurement point compared to CIE overcast sky. The location of the measurement point is shown in figure E.2. For the simulation the CIE overcast sky is set, and it is of interest to investigate how close the simulation is to the measure illuminance.

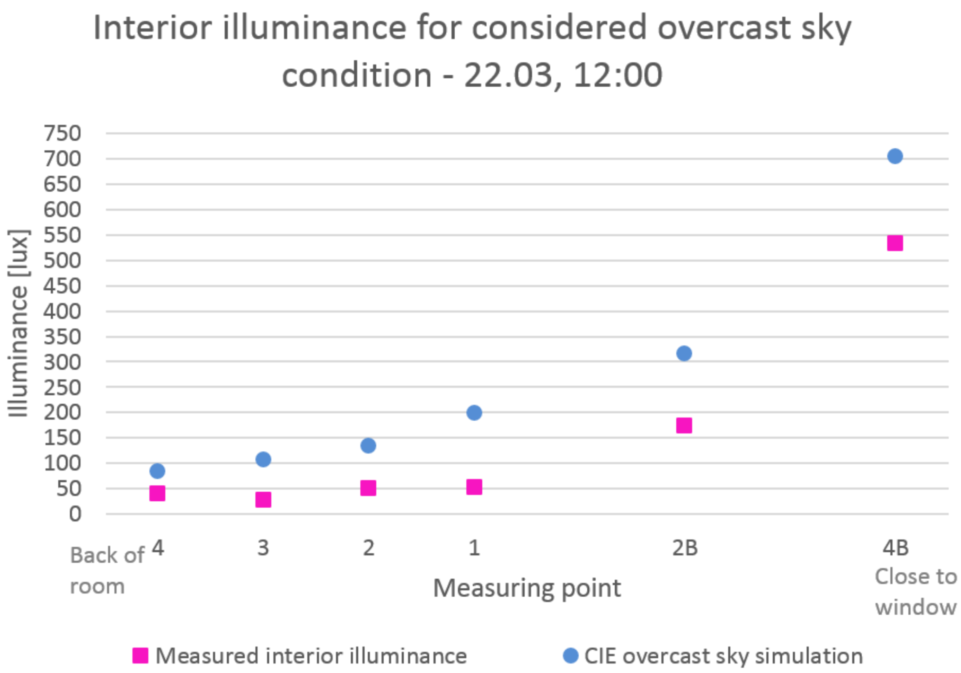

Figure 5.13. The interior illuminance for believed overcast sky condition the 22^{nd} of March compared with simulated interior illuminance for overcast CIE sky condition at 12:00.

As seen in graph 5.13 the measured illuminance is considerably lower compared to the simulated illuminance. The simulated illuminance for the point furthest in the back of the room is approximately twice as large as the measured illuminance, while the measured illuminance closest to the window is 25 % lower than the simulated illuminance. In graph 5.13 it is seen that the measured interior illuminance decreases fast with the depth of the cell office, this is due to the geometry of the room interfering with the diffuse illuminance from the sky and the diffuse illuminance from the sky is not able to reach in the depth of the cell office. Further in the back of the office the illuminance level is strongly affected by the properties of the room, such as the reflectance of the surfaces. The illuminance level close to the window is not as effected by the properties of the room as the illuminance level in the depth of the room.

As the CIE overcast sky is the darkest CIE sky possible, it is surprising that the measured interior illuminance is actually lower compared to the CIE overcast sky. It would have been expected that the measured interior illuminance was higher compared to the simulated interior illuminance as the sky during the measurements might not be completely similar to the CIE overcast sky. When studying the exterior illuminance in section 5.2.5 it is seen that the actual exterior illuminance on a south oriented vertical façade at 12:00 on the 22^{nd} of March is lower than the simulated illuminance for a CIE overcast sky. This might also be the reason the measured interior illuminance is lower compared to the simulated interior illuminance seen in graph 5.13.

Interior obstacles may also influence the result. Therefore the same scene was simulated with interior obstacles for comparison, an illustrative scene is shown in figure 5.14.

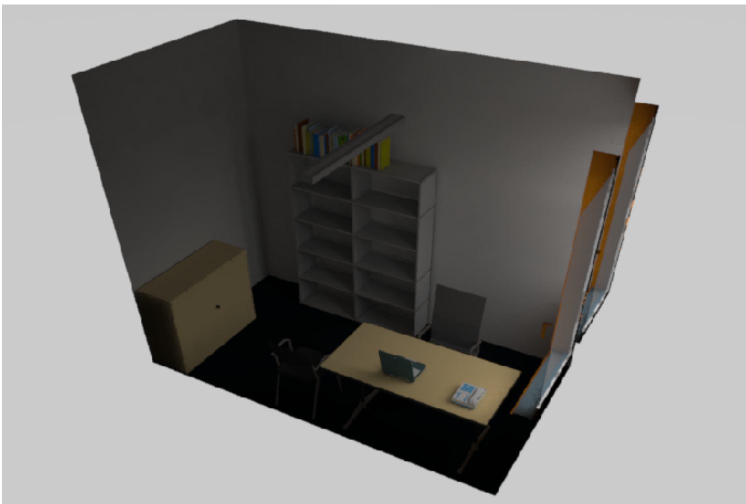

Figure 5.14. Illustrative picture of the scene in Relux for the interior luminance obtained with ray tracing for CIE overcast sky condition the 22^{nd} of March at 12:00.

Graph 5.15 shows the simulated result with internal obstructions compared with the measured interior illuminance.

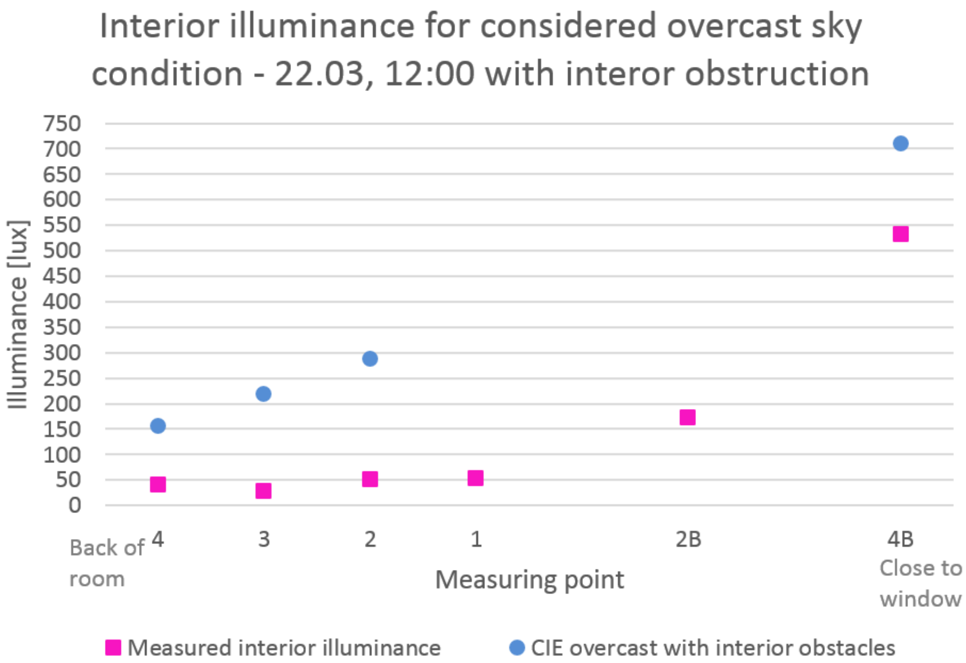

Figure 5.15. The interior illuminance for believed overcast sky condition the 22^{nd} of March compared with simulated interior illuminance with internal obstructions for overcast CIE sky condition at 12:00.

The ray tracing calculation engine in Relux was not capable of obtaining a result for measurement point 1 and 2B. This is due to the furniture interfering with the reference plane at 0.85. For the measurement points Relux has been able to obtain a result the illuminance level is higher for all the measurement points compared to the measured illuminance. The illuminance level obtained with the simulation model without internal obstructions was closer to the measured illuminance level and it has been concluded to apply a simulation model without internal obstructions for the rest of the simulations.

In order to further investigate the interior illuminance and its dependency on the exterior illuminance, the measured interior illuminance for the believed clear sky during March the 14^{th} is compared to simulated interior illuminance for the clear CIE sky. Initially the measured interior illuminance were only compared to the CIE clear sky, but the result deviated significantly between the measured and CIE clear sky as seen in graph 5.16. Therefore the interior illuminance was simulated for the CIE intermediate and CIE overcast skies as well for comparison.

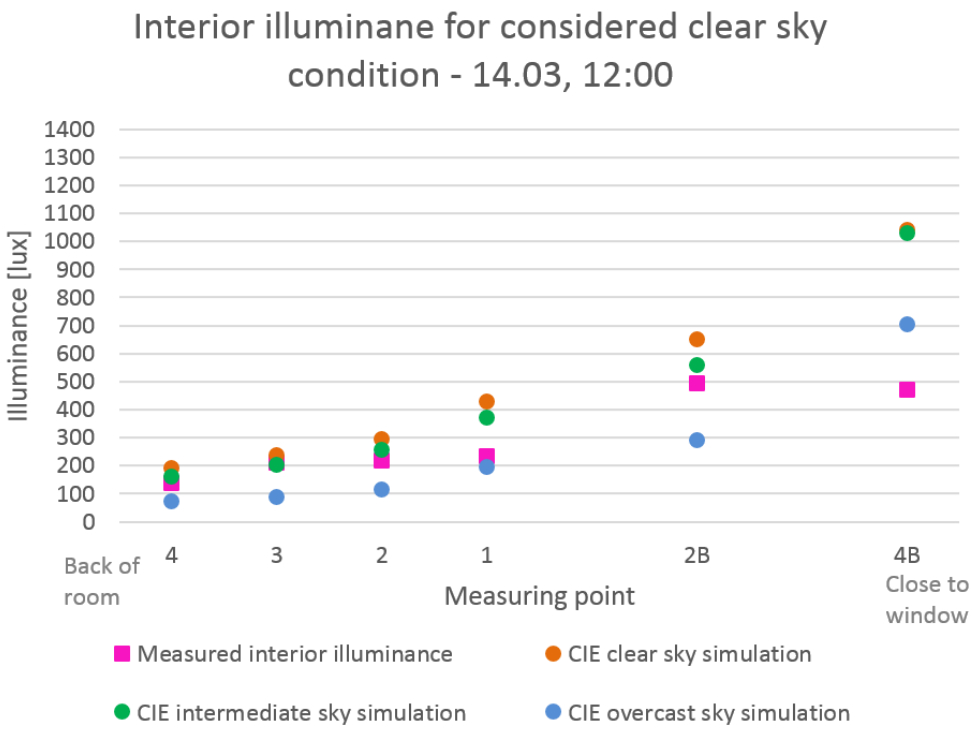

Figure 5.16. The interior illuminance for believed overcast sky condition for 14^{th} of March compared with simulated interior illuminance for overcast, intermediate and clear CIE sky conditions.

The interior illuminance for the clear and intermediate CIE skies are fairly similar. The interior illuminance for the CIE overcast sky condition has very similar results for the 14^{th} as it had for the 22^{nd}, the difference of only eight days is very small. The measured interior illuminance is higher than the interior illuminance for the CIE overcast sky for all the measurement points, only the illuminance meter closest to the window has a lower illuminance level than the simulated illuminance for the CIE overcast sky. When studying the data closer it was noticed that right before 12:00 and for about 30 minutes the illuminance level for the measurement point closest to the window decreased slightly to 470,90 lux from 507,60 lux. The value of 470,90 lux at 12:00 might be due to shading from obstruction in the cell office or external shading. The same tendency happens for every day from right before 12:00 and for about 30 minutes.

According to graph 5.16 the measured illuminance level indicates that the sky condition at 12:00 for the 14^{th} of March lay between CIE overcast and CIE intermediate sky conditions. It should be noted that even though the sky condition this day is considered as clear, the measured interior illuminance has a closer correlation with the interior simulated illuminance for the CIE intermediate or overcast sky conditions. For the three measurement points in the back of the room, as well as measurement point 2B close to the middle of the room, the illuminance level for the CIE intermediate sky condition is closer to the measured illuminance level. While for measurement point 1 and 4B, which is the closest to the window, the interior measured illuminance has a closer correspondence to the simulated interior illuminance for the CIE overcast sky condition. The measured interior illuminance is 232 lux lower than the interior simulated illuminance for the CIE overcast sky condition.

However, as mentioned in section 5.1.1, the sky condition for the 14^{th} is believed to be clear due to the solar irradiation graph I.6 and the pictures in figure 5.1. Therefore it is decided to investigate the measured vertical exterior illuminance compared to simulated exterior illuminance for different CIE skies.

5.2.5 Actual Exterior Illuminance and Different CIE Sky Conditions

In order to determine which CIE sky the actual sky was during the measurements applying a different method than studying pictures of the sky and the distribution of direct and diffuse solar irradiance, simulation is applied. The simulation software Relux is applied as it has the possibility to insert a vertical reference plane on the surface of a façade.

The measured solar irradiance from the pyranometer on the roof of the case building, explained in detail in appendix D, is inserted as a weather file in BSim. The solar irradiance is converted into illuminance applying the luminous efficacy. The luminous efficacy is known for Copenhagen and the following equations are applied in BSim.

$$\begin{aligned} K_D &= 103\frac{lm}{W} \\ K_{oc} &= 121\frac{lm}{W} \\ K_{cl} &= 146\frac{lm}{W} \end{aligned} \tag{5.1}$$

Where:

K_D	Direct sunlight
K_{oc}	Overcast sky
K_{cl}	Clear sky

For both BSim and Relux the illuminance on a vertical south oriented plane is studied.

The reference plane outside the window façade in Relux is the same width and height of the cell office, 2.102 m and 2.8 m. The mean of the illuminance on the vertical reference plane is applied for comparison with the results from BSim. The ray tracing calculation method, as explained in section 4.3 on page 30, is applied in Relux with an inter-reflection of 2, as explained in section 4.2.1 on page 28. The office opposite the building is neglected as it is not possible to insert external obstructions in Bsim and it is desired that the results from Relux and Bsim are based on as similar model as possible, as well as the solar irradiance was measured on the roof of the case building where there was no external obstructions.

The day with stated overcast sky in section 5.1.2, March the 22^{nd}, and the day with stated clear sky in section 5.1.1, March the 14^{th}.

Measured Sky Conditions for the Measurement Period

The measured solar irradiance inserted as a weather file in BSim and shown as illuminance on a South oriented vertical plane is compared to simulated illuminance on a south oriented vertical plane for different CIE sky conditions in Relux. A clear sky without sun is not realistic as it will not happen in real life, but it is included for comparison. The result for all the days in the measurement period is shown in graph 5.26. The graph show the actual illuminance obtained from the solar irradiance measurement into BSim. The solar irradiance is included for comparison, the measured horizontal illuminance is converted into vertical illuminance on the south oriented reference plane by applying BSim.

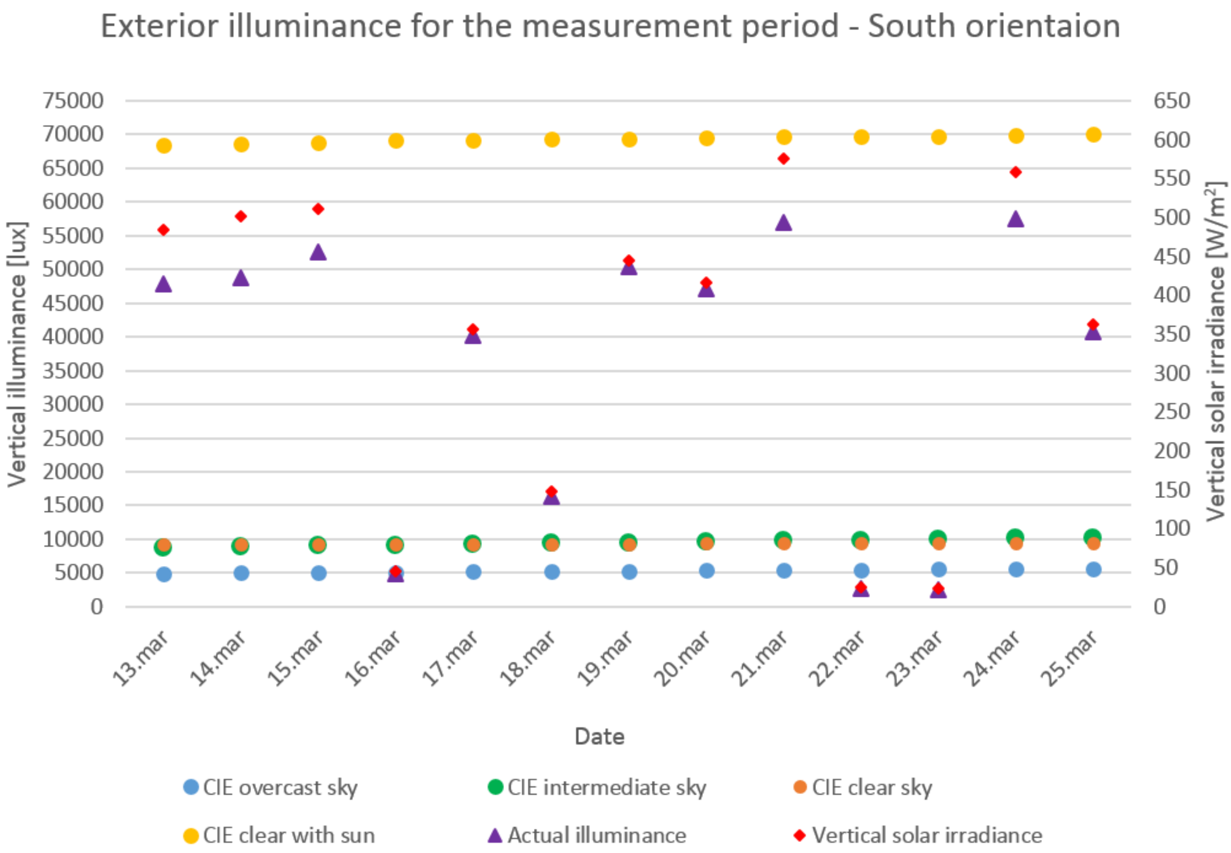

Figure 5.17. The exterior illuminance on a vertical reference plane on the south façade at 12:00 for the measurement period comparing vertical solar irradiance and actual illuminance to simulated overcast, intermediate, clear and clear with sun CIE sky conditions.

According to the results in graph 5.17 the measured sky condition for the measurement days are overcast for only three of the days. The days stated to be overcast in section 5.1.3 was the 16^{th}, 18^{th} and 22^{nd} of March. The overcast days here are the 16^{th}, 22^{nd} and 23^{rd}. The 18^{th} is close to intermediate and clear CIE sky conditions. The clear and intermediate CIE sky conditions simulate in Relux have very similar illuminance values at 12:00 throughout the whole measurement period. This is due to the diffuse component being larger for the intermediate sky compared to the clear sky, and even thought the direct sky component is higher for the clear sky, the increased diffuse component for the intermediate sky evens out the difference between the two CIE sky conditions. At some points do the CIE intermediate actually have a higher illuminance level on the vertical south oriented reference plane than the CIE clear sky.

The sky condition was changing rapidly throughout the day for many of the days during the measurement period. For example the sky conditions for March the 15^{th} was shifting throughout the day as explained in detail in appendix I.0.1 on page 261. At exactly 12:00 the condition for the actual sky might be close to a CIE clear sky with sun.

March the 18^{th} is stated to be overcast in 5.1.3, and even though it seams to not be overcast according to graph 5.17, the day can still be overcast as graph 5.17 only display results at exactly 12:00.

The 24^{th} is the day with the highest illuminance level at 12:00 for all the days in the measurement period. The sky condition for the 24^{th} was mostly clear sky with some scattered clouds in the distance which corresponds well with the result shown in graph fig:exverticalillumeasurementperiod, the sky conditions for the 24^{th} is explained in detail in appendix I.0.1 on page 277.

The sky condition for the 19^{th} is said to be even cloud layer throughout the day as explained and shown with pictures and solar irradiance graph in appendix I.0.1 on page 268. It is therefore surprising that the illuminance almost correspond to a CIE clear sky with sun. Therefore the illuminance throughout the day is compared to different CIE sky conditions as seen in graph 5.18.

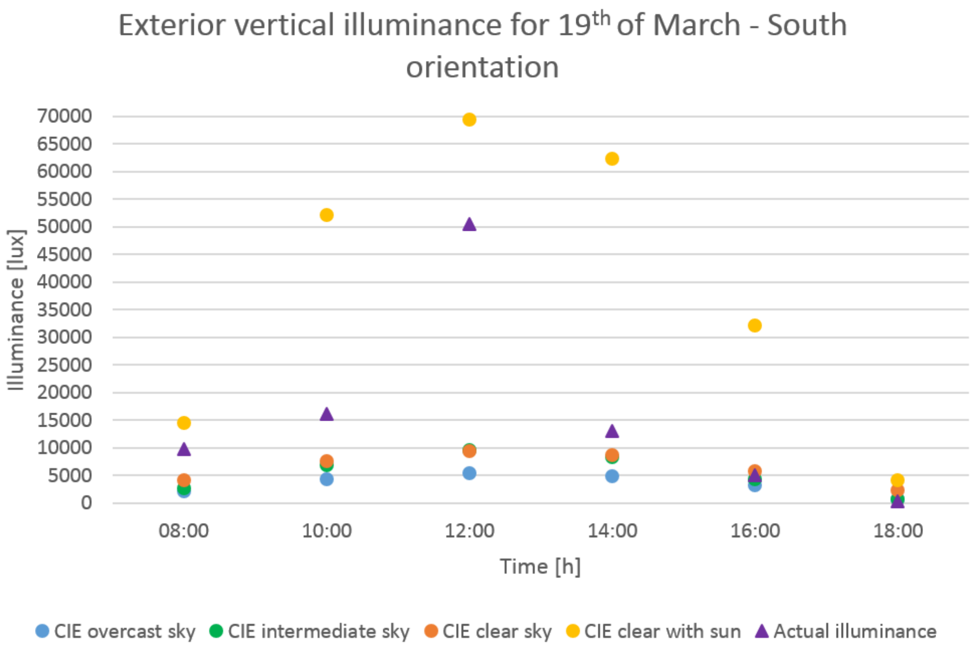

Figure 5.18. The exterior illuminance on a vertical reference plane on the south façade at 12:00 for 19^{th} of March comparing measured sky to simulated overcast, intermediate and clear CIE sky conditions.

As seen in graph 5.18 the measured illuminance level only almost reaches the illuminance level for CIE clear sky with sun at 12:00. At other times during the day the measured illuminance is lower and closer to the values for CIE intermediate and CIE clear sky. It is believed that the the other days follow the same tendency. The overcast day of the 22^{nd} and the clear day of the 14^{th} are studied in more detail in the following sections.

Measured Overcast Sky

The exterior illuminance which is measured and simulated for different CIE skies on a south oriented vertical plane at 12:00 for March the 22^{nd} is shown in graph 5.19.

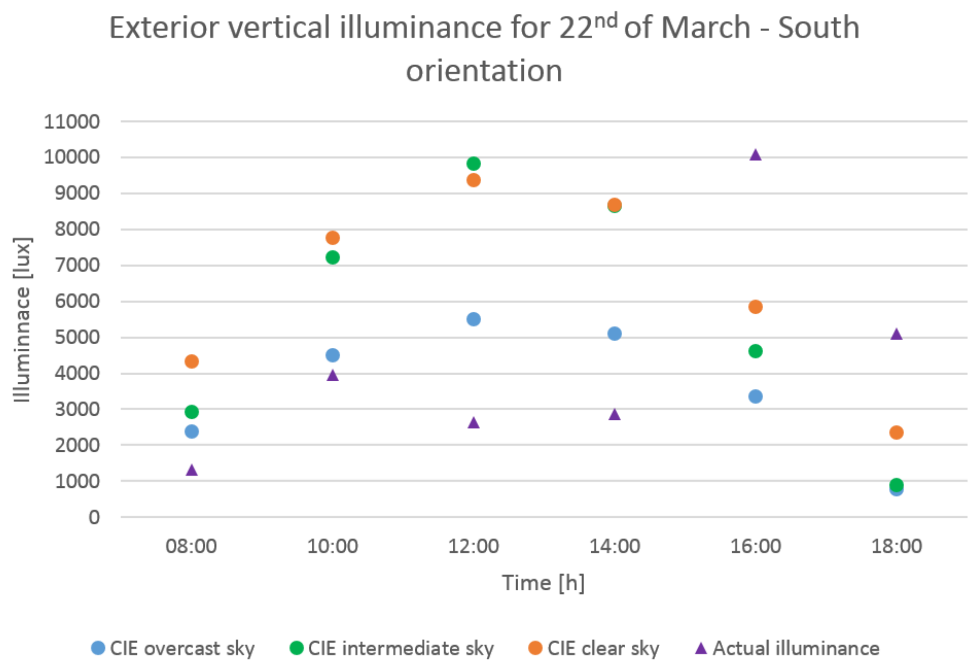

Figure 5.19. The exterior illuminance on a vertical reference plane on the south façade at 12:00 for 22^{nd} of March comparing measured sky to simulated overcast, intermediate and clear CIE sky conditions.

As shown in graph 5.19 the measured illuminance is below the CIE overcast illuminance for most of the day until 16:00. This corresponds to the solar irradiance for the 22^{nd} of March seen in graph I.35. March the 22^{nd} is the day which is most overcast as the total solar irradiance only has one peak reaching 200 W/m^2 at 16:00 before decreasing again. For the 18^{th} and 16^{th} the total solar irradiance is almost reaches and slightly above 300 W/m^2, respectively, for a short period of the day. Nevertheless, from graph 5.19 it can be concluded that the sky condition for March the 22^{nd} is CIE overcast until 16:00 when it becomes CIE clear.

Measured Clear Sky

The exterior illuminance which is measured and simulated for different CIE skies on a south oriented vertical plane at 12:00 for March the 14^{th} is shown in graph 5.20.

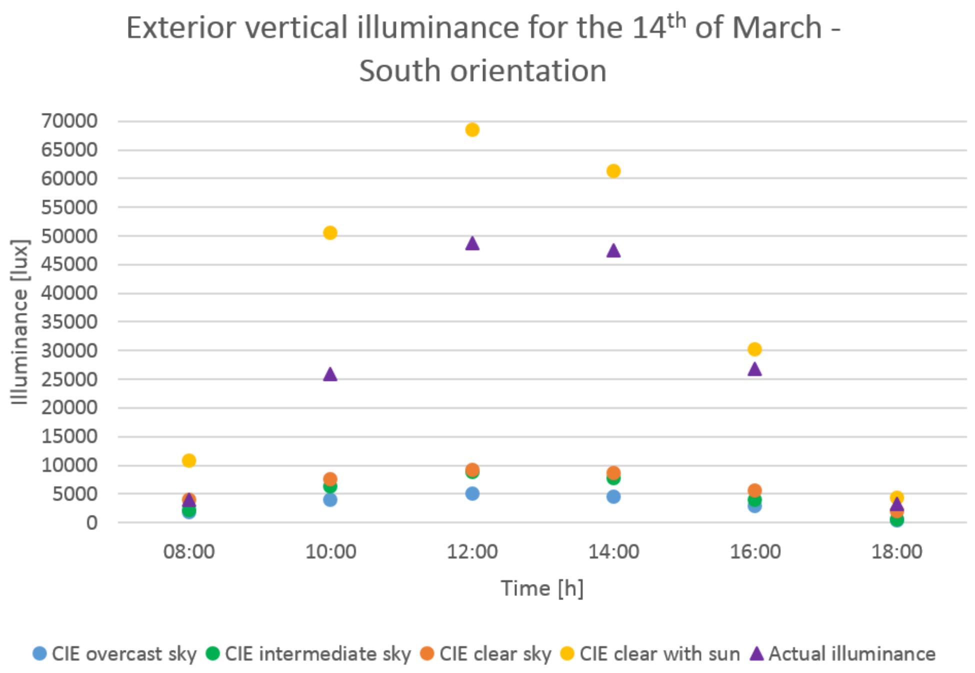

Figure 5.20. The exterior illuminance on a vertical reference plane on the south façade at 12:00 for 14^{th} of March comparing measured sky to simulated overcast, intermediate, clear and clear with sun CIE sky conditions.

Graph 5.20 show a correlation in the tendency for the illuminance throughout the day for the CIE clear sky with sun and the measured sky for March the 14^{th}. The measured illuminance level does not quite reach the illuminance level for the CIE clear sky with sun, but the trend is similar. The actual illuminance is considerably higher than the CIE clear sky at all times except at 08:00 in the morning is the illuminance level for the CIE clear sky slightly higher than the actual illuminance. The sky condition for March the 14^{th} is stated to be clear as mentioned in 5.1.1 and the pictures in figure 5.1 and the solar irradiance in graph I.6 supports this statement. The day does have direct sunlight and it is therefore concluded that the sky condition for March the 14^{th} is between CIE clear sky and CIE clear sky with sun.

5.2.6 Completion of the Measured Skies to CIE Skies

When studying the previous graphs comparing measured overcast sky to different CIE sky types it was noted that the measured illuminance level often was below the illuminance level of the CIE overcast sky. On the other hand, if the measured sky was believed to be clear then the illuminance level was often close to the illuminance level of a clear sky with sun. When the sky was believed to be intermediate then the illuminance level often was somewhere between the CIE clear sky and CIE clear sky with sun. It seams that the illuminance for the CIE sky conditions are quite sensitive, a small variation in the measured illuminance will result in very different CIE sky conditions. The measured illuminance fluctuates in the extreme from below overcast CIE sky to almost CIE clear sky with sun.

One of the uncertainties in this approach to determine the sky conditions for the measured sky can be in the different simulation software. For example can the reflection of the sky and the sunlight be very affected by the external surface for some scenes. The default ground plane reflection in Relux for the ray tracing method is the mirrored sky concept (RELUX Informatik AG, 2011), as seen in figure 5.21. While the ground reflectance in BSim *ReflLight* was set to 0.1 which corresponds to grass.

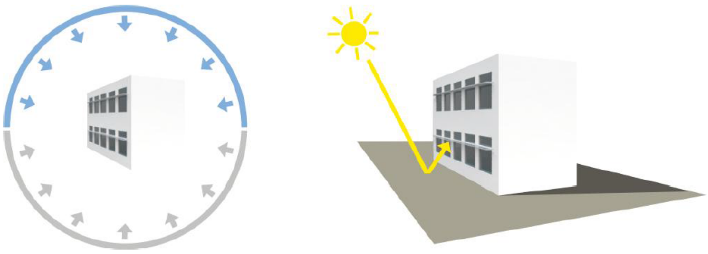

Figure 5.21. Mirrored sky concept for ground plane reflection for the ray tracing method in Relux (RELUX Informatik AG, 2011).

5.3 Comparison of the Norwegian Reference Year to CIE Skies

A reference year weather file consists of hourly data for a single year, extracted from a multi-year data set. 12 typical months are selected from the multi-year data set where the parameters from each month are given mean values and variances corresponding to the multi-year period where the months are selected from. The hourly values are selected from average days representing typical weather conditions for the certain location (Pernigotto et al., 2014).

BSim was applied to get solar irradiance from the Norwegian reference year from *NS 3031* at a vertical surface for all the cardinal orientations, the results are seen in graph 5.22.

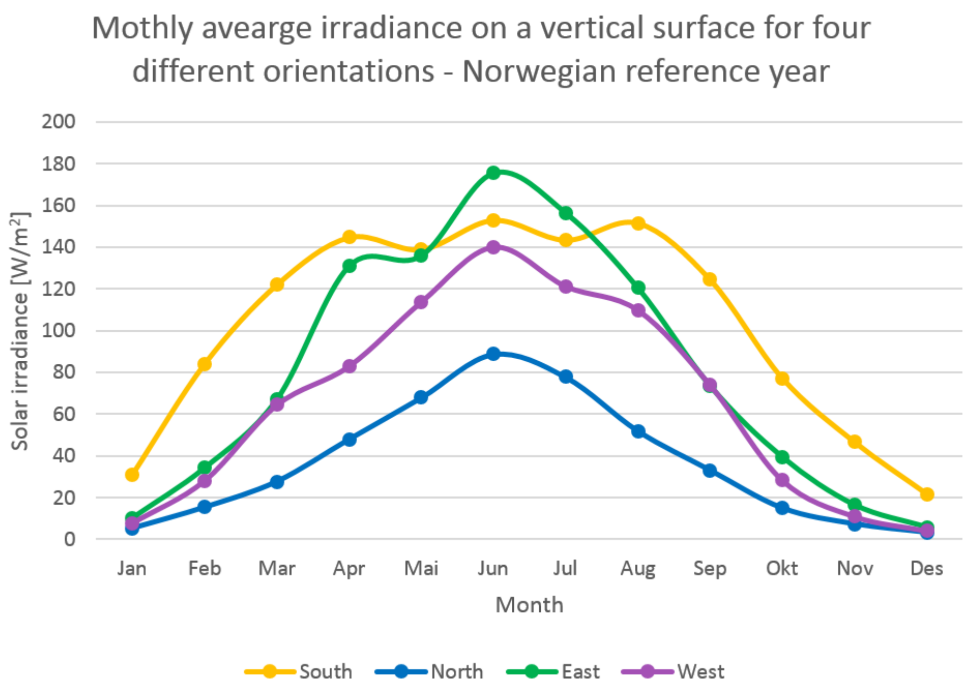

Figure 5.22. The monthly average solar irradiance on a vertical surface for the four cardinal orientations for the Norwegian reference year

The variation of the different CIE sky types throughout a year for Oslo is investigated in VELUX Daylight Visualizer and Relux. As it is not possible to have a vertical reference plane in Velux, it is also not possible to have an external reference plane. Therefore a horizontal reference plane was inserted inside the cell office, the transmittance of the glazing was set to 1.0 and oriented towards the South. The reflectance of all the interior surfaces was set to 0.0 to ensure that the inter-reflected component did not add to the illuminance. The ground reflectance was set to 0.1 as this is the reflectance of grass and it is the same reflectance as applied in BSim. However, the ground reflectance will not contribute to the illuminance result from VELUX Daylight Visualizer as the reflected light from the ground will not hit the interior reference plane directly and the reflectance of the interior surfaces are set to 0.0. The office opposite is not included in the model to ensure that the model in VELUX Daylight Visualizer is as similar as possible to the models in Relux and Bsim.

Parameter	**Value**
Transmittance of glazing	100%
Reflectance of the three white walls	0.0
Reflectance of the wooden wall	0.0
Reflectance of the ceiling	0.0
Reflectance of the floor	0.0
Orientation	180°
Reflectance the ground	0.1

Table 5.2. Input in VELUX Daylight Visualizer.

In VELUX Daylight Visualizer it is only possible to calculate the illuminance for the 21^{st} of every month because:

- Equinox in 2014: 20^{th} of March and 23^{rd} of September
- Solstice in 2014: 21^{st} of June and 21^{st} of December

The result for the horizontal illuminance simulated for overcast, intermediate and clear CIE skies for the 21^{st} of every month at 12:00 is shown in graph 5.23.

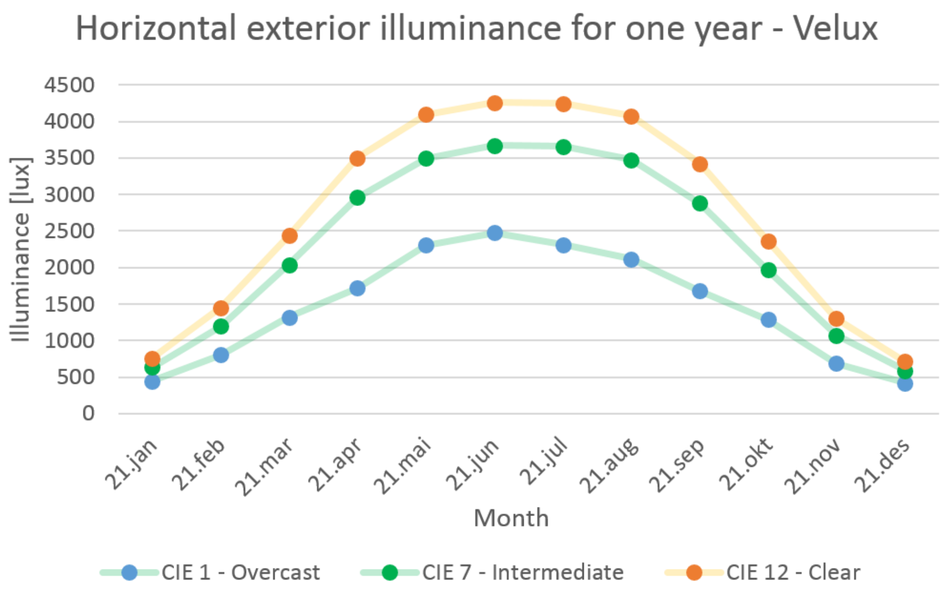

Figure 5.23. The exterior horizontal illuminance at 12:00 for the 21^{st} of every month of a year comparing the overcast, intermediate and clear CIE sky conditions.

Throughout the year the CIE clear sky has a higher illuminance level than the intermediate and overcast CIE skies. This distribution has similar trends as the solar irradiation on a horizontal plane from the Norwegian reference year seen in graph 5.24. It is not possible to simulate a clear CIE sky with sunlight in VELUX Daylight Visualizer.

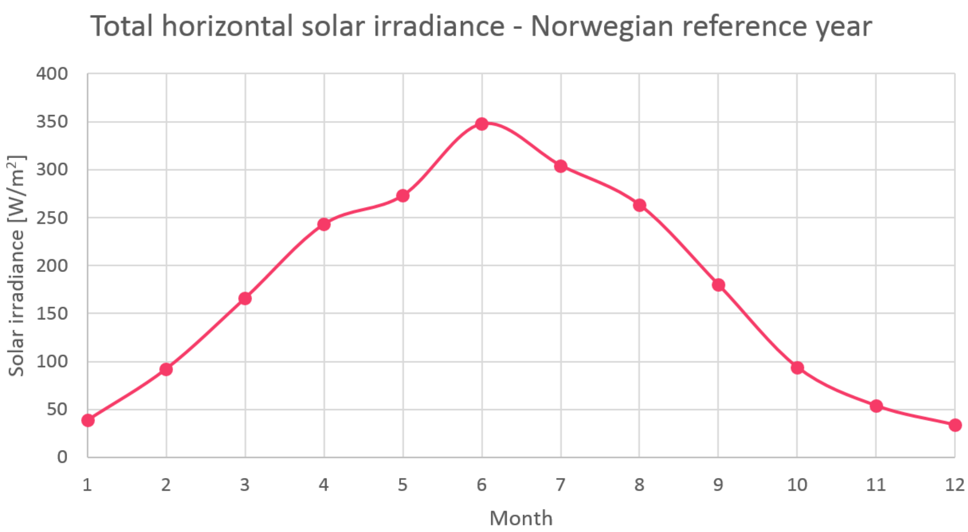

Figure 5.24. The monthly average for horizontal solar irradiance for the Norwegian reference year.

The trend throughout of the horizontal illuminance obtained with VELUX Daylight Visualizer is similar as the trend throughout the year for the solar irradiance from the Norwegian reference year.

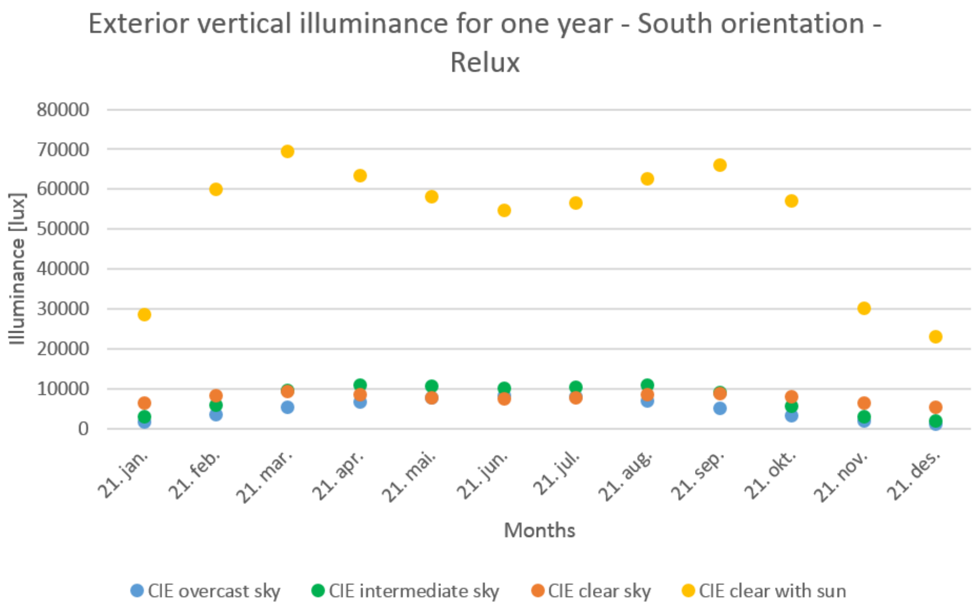

Figure 5.25. The exterior illuminance on a vertical reference plane at 12:00 for the 21^{st} of every month of a year comparing the overcast, intermediate, clear and clear with sun CIE sky conditions.

The distribution holds the same trend as the distribution of solar irradiance for the South surface for the Norwegian reference year as seen in graph 5.22.

The solar irradiance data from the Norwegian reference year (Standard Norge, 2007) is inserted into BSim. The illuminance on a vertical south oriented façade for the 21^{st} of every month throughout a year at 12:00 is compared to simulated overcast, intermediate, clear and clear with sun CIE skies. The result is shown in graph 5.17.

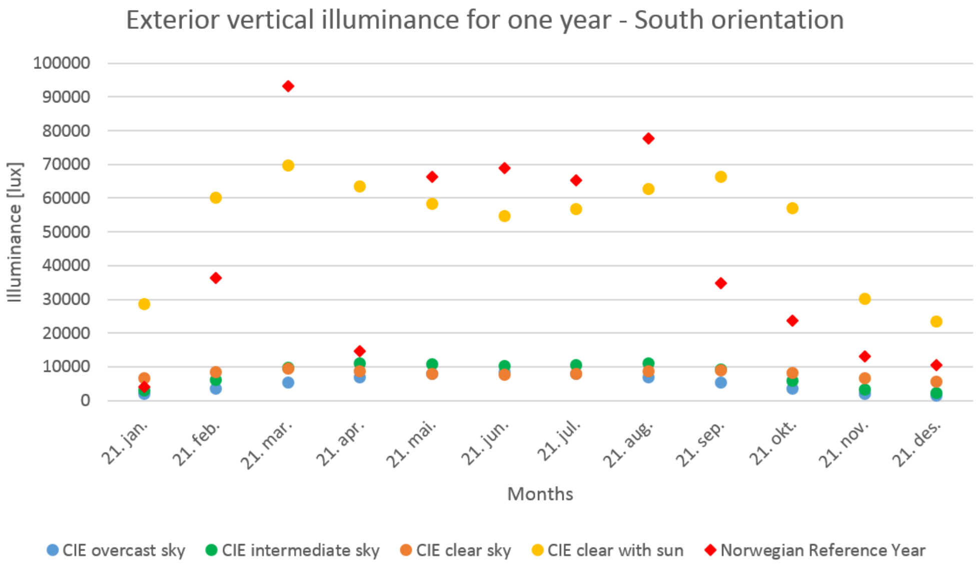

Figure 5.26. The exterior illuminance on a vertical reference plane on the south façade at 12:00 for the 21^{st} of every month of a year comparing the Norwegian reference year to simulated overcast, intermediate, clear and clear with sun CIE sky conditions.

The simulated result for the Norwegian reference year on the vertical south oriented reference plane is varying rapidly throughout the year. When studying the illuminance for every hour throughout the whole year it was seen that it was large variation for the direct solar irradiance between different days. As graph 5.26 only show values at 12:00 for the 21^{st} of every month the result for the illuminance for the Norwegian reference year is varying quite a lot. For example in April the illuminance decreases rapidly, this is due to the direct component being extremely low at 12:00 for the 21^{st} of April. For the summer months the Norwegian reference year has illuminance values above the CIE clear sky with sun, while for the winter and autumn months it lays between CIE clear sky and CIE clear with sun. Only in January is the Norwegian reference year below the CIE clear sky. It must be kept in mind that the values for the Norwegian reference year is obtained with BSim, while the CIE skies are obtained with Relux. The differences in the calculation engines and the structure of the scenes may affect the result.

5.3.1 Dividing Norwegian Reference Year into CIE Sky Condition Intervals

Simulation software for daylight analysis, such as Relux and VELUX, only provides results from a chosen CIE sky condition rather than for real weather data. Classifying the real sky conditions, for each day, as different CIE sky conditions was in the previous sections proved to be difficult as the real sky is more complex than the CIE sky and has more variations throughout the day.

In this section a new approach is tested where hours, rather than days, in the Norwegian reference year weather file is divided into intervals of illuminance values from different CIE sky conditions.

A South oriented cell office is simulated in Relux for the 21^{st} of each month at different times of the day for overcast, intermediate and clear sky. This results in different levels of exterior illuminance values for the CIE sky conditions on the South façade. These levels of the exterior illuminance are used to obtain CIE sky intervals which the hourly average of the Norwegian reference year is sorted by.

The Norwegian reference year is simulated in BSim to obtain the hourly exterior illuminance on the South façade throughout a year. These hourly exterior illuminance values are sorted from highest to lowest value and divided into the CIE illuminance intervals obtained with Relux.

The following graph 5.27 shows the exterior illuminance on the South façade throughout the year from the Norwegian reference year obtained with BSim, and the different ranges of exterior illuminance levels for different CIE sky conditions obtained with Relux. The upper five lines represents different illuminance values for CIE clear sky with sunlight, while the lower green line represents CIE overcast sky.

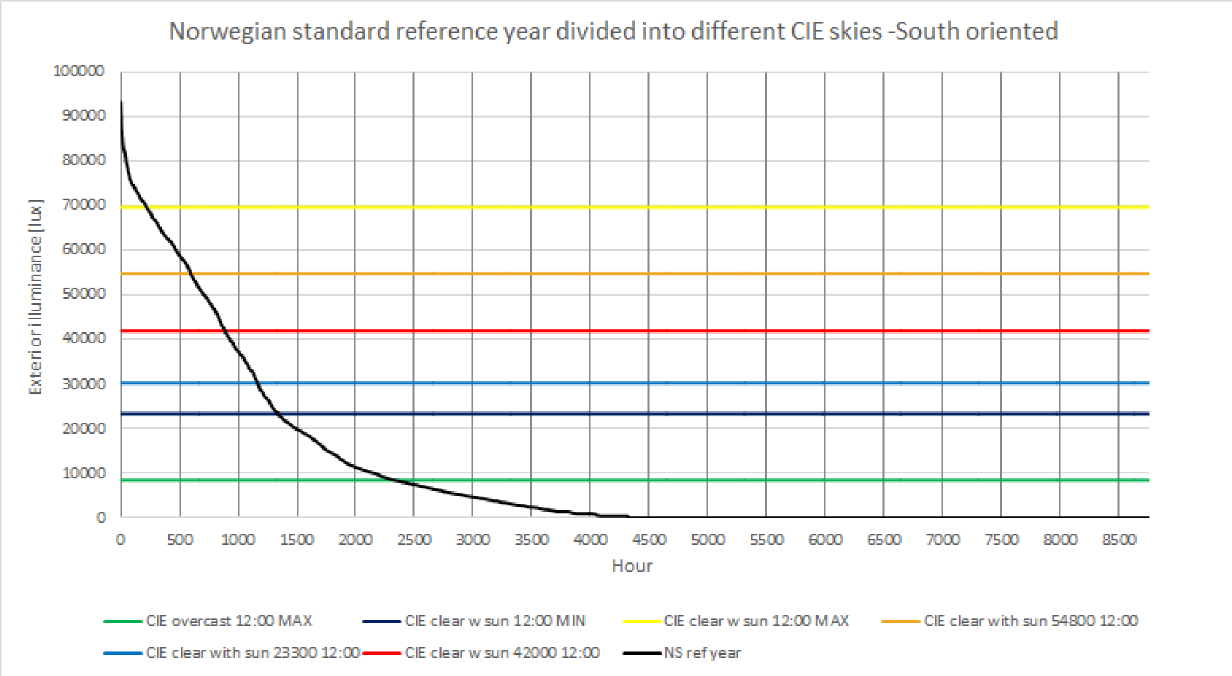

Figure 5.27. The exterior illuminance on a South oriented façade from the Norwegian reference year and the different levels of illuminance from the CIE sky conditions, extracted from simulations in Relux

As seen on the graph, the exterior illuminance from the Norwegian reference year contains all of the illuminance levels from the CIE sky conditions. According to this graph, CIE clear sky with sunlight have a range from 23000 lux to 70000 lux on the South facade. CIE overcast sky have a range from 0 lux to 9000 lux.

In graph 5.28 hours from the Norwegian reference year is divided into intervals where different CIE illuminance values occur. The remaining hours after the last interval are assumed to have an exterior illuminance of zero.

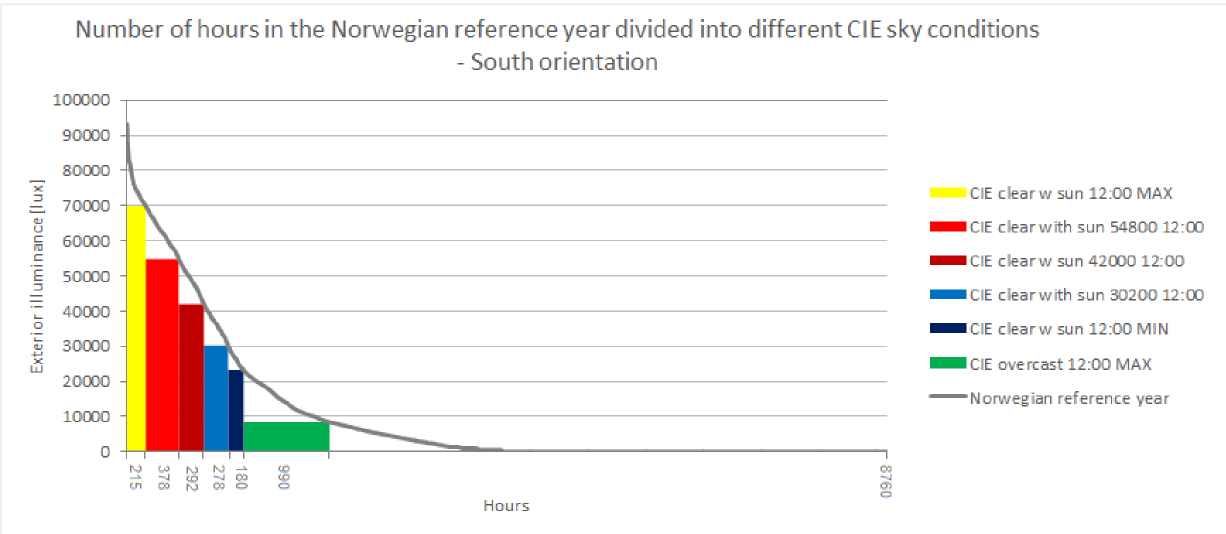

Figure 5.28. Number of hours in the Norwegian reference year where the different illuminance levels from the CIE sky conditions occur

When dividing the reference year into intervals of different CIE illuminance levels it can be seen the amount of hours during the year where different sky conditions occur according to the CIE definition.

As seen on the graph 5.28 the Norwegian reference year contains 1149 hours of clear sky and 7611 hours with overcast sky conditions.

It is clearly preferable to divide the year into hours where different CIE sky conditions occur rather than whole days, as the sky conditions usually changes a lot during the day as mentioned in 5.1.3 on page 49.

When the exterior illuminance from the reference year is determined, it can be further applied to calculate the interior illuminance value. This approach for establishing the interior illuminance will be further investigated in 15 on page 147.

Artificial Light 6

In this chapter the electricity usage for the daylight and occupancy controlled artificial lighting is presented, as well as the correlation between the generated illuminance on the working plane and the corresponding power of the armature.

6.1 Electricity Usage for the Armature in the Cell Office

During this measuring period of two weeks from Friday the 13^{th} to Thursday the 26^{th} of March one occupant used the cell office. He used the office as he normally would do. Due to the occupant being absent for some of the days days, only seven days out of the fourteen days in the measurement period are included in the analysis.

The results are displayed in graphs showing the increase of the electricity usage throughout the day and the power the armature is using as seen in appendix H on page 253. The power is varying from 0 when the armature is off to 8.956 W/m^2, which is maximum. The varying maximum power displayed in table 6.1 is probably not due to varying effect of the armature, rather inaccuracies of the SparOmeter as described in appendix H.2 on page 255. A power of zero is not realistic as the presence detector and the illuminance sensor of the armature will have a parasite load.

Some key values are displayed in table 6.1, for graphs and detailed explanation for every day see appendix H on page 253.

Day	Day number	Hours in Office	Total energy $[kWh/m^2]$	Average power $[W/m^2]$	Maximum power $[W/m^2]$	Energy use per Hour $[\frac{\mathrm{kWh}}{\mathrm{hm}^2}]$
Monday 16.03.2015	1	06:52	0.0605	8.557	8.907	0.00881
Tuesday 17.03.2015	2	04:52	0.0.0400	7.589	8.956	0.00823
Friday 20.03.2015	3	04:45	0.0380	6.642	8.895	0.00800
Saturday 21.03.2015	4	07:13	0.0439	5.703	8.944	0.00609
Tuesday 24.03.2015	5	04:38	0.0384	7.933	8.944	0.00828
Wednesday 25.03.2015	6	07:03	0.0612	8.201	8.944	0.00869
Thursday 26.03.2015	7	06:43	0.0595	8.688	8.919	0.00886

Table 6.1. The hours in office as well as power and energy used by the armature for the different days.

The values seen in table 6.1 are displayed in graph 6.1.

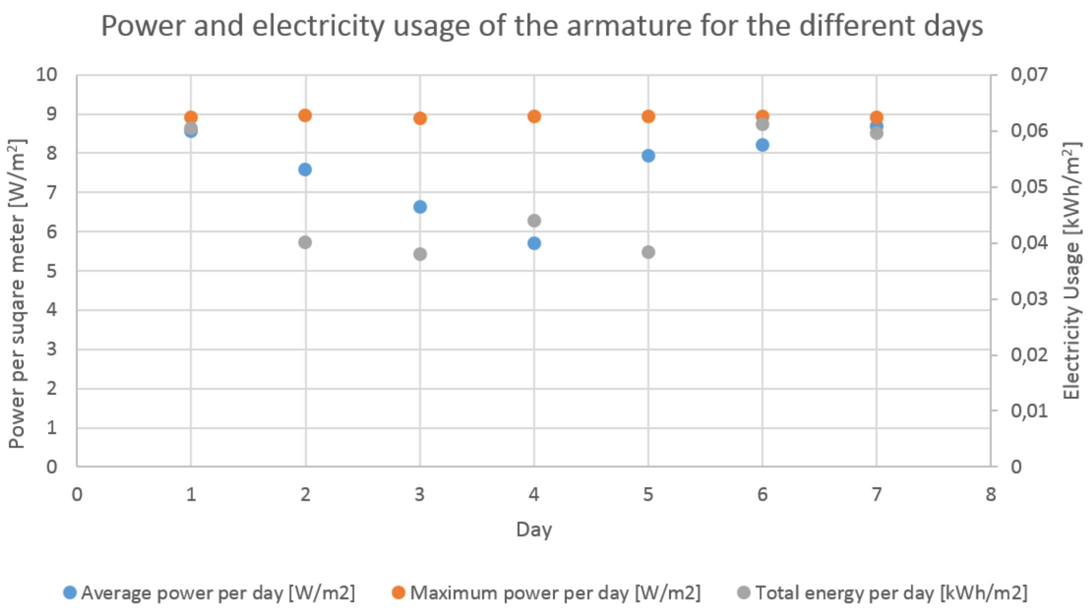

Figure 6.1. The effect, power and hours of use of the armature for the different days.

In graph 6.1 it is shown that the maximum power does not vary significantly, but the average power varies quite a bit during the different days. This is due to the different sky conditions during the measurement period. For example the sky was clear during day 4, Saturday the 21^{st}, where the average effect is low, compared to day 1, Monday the 16^{th}, when the sky condition was cloudy, as seen later in graphs 6.2 and 6.3.

The average values for the measuring period is calculated and shown in table 6.2.

Average Hours in Office	**Average Total energy** $[kWh/m^2]$	**Average power** $[W/m^2]$	**Average Maximum power** $[W/m^2]$	**Average energy use per hour** $[\frac{\text{kWh}}{\text{hm}^2}]$
06:00	0.0489	7.617	8.930	0.00814

Table 6.2. Average values for hours in office, and power and energy use of the armature.

The average time from the user arrived at the office to he left was 7 hours and 17 minutes, while the average time the cell office was occupied during a day was 6 hours 0 minutes as seen in table 6.2. The average time the occupant spent in his cell office corresponds well with the occupancy profile for cell offices which will be explained in detail in chapter 8 on page 83. The average lunch lasted for 33 minutes and the average time the user was in meetings through the day was 42 minutes.

The electricity usage and power of the armature during Monday the 16^{th} with overcast sky condition as explained in section 5.1.2 on page 46 is shown in graph 6.2, and the electricity usage and power of the armature during Saturday the 21^{st} with clear sky condition as explained in section 5.1.1 on page 43 is shown in graph 6.3.

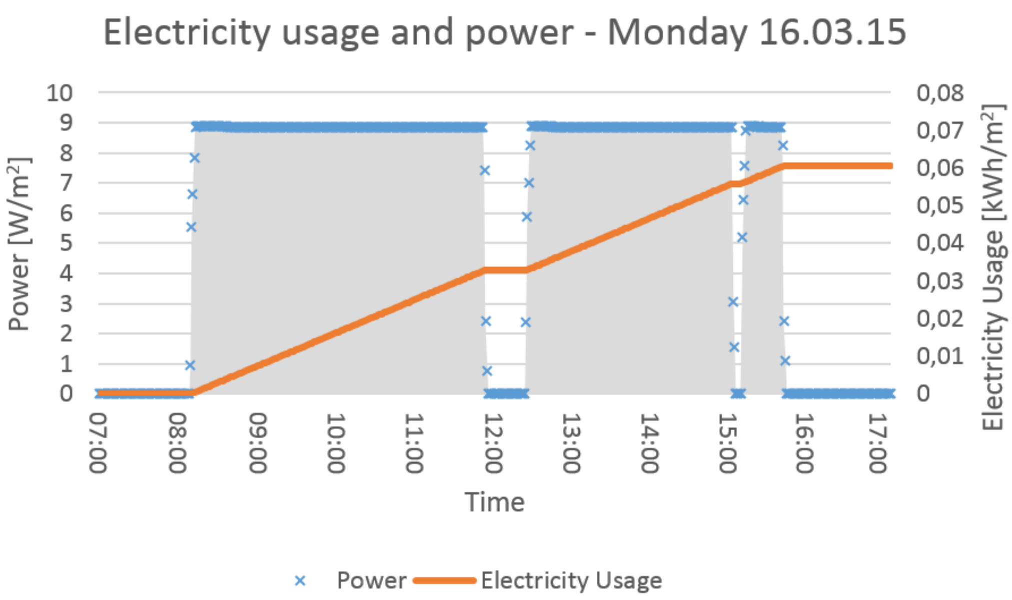

Figure 6.2. The power and electricity usage of the armature in the cell office during Monday the 16^{th}.

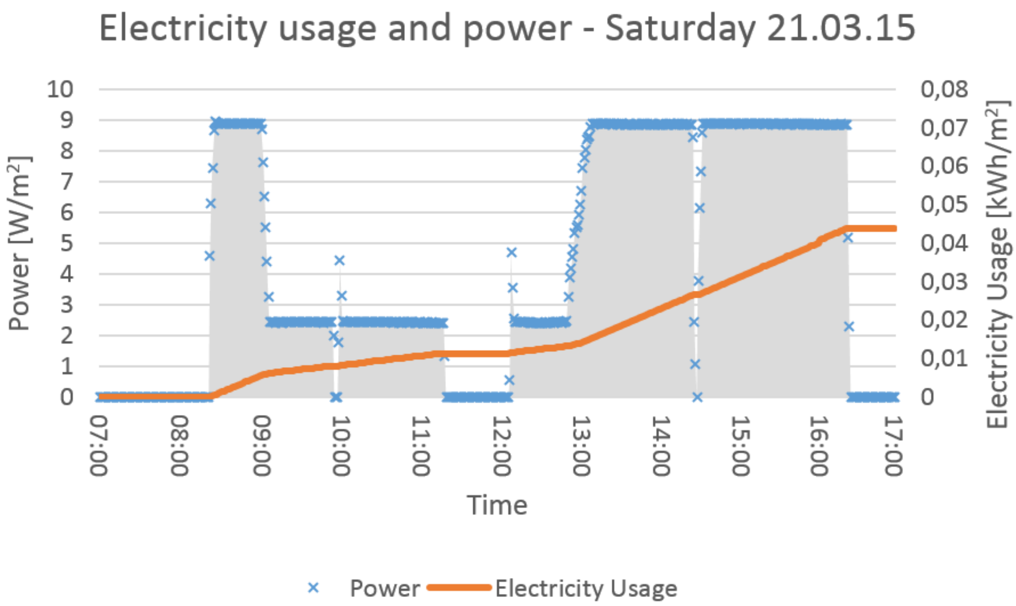

Figure 6.3. The power and electricity usage of the armature in the cell office during Saturday the 21^{st}.

Graph 6.2 and 6.3 clearly show a difference in the power of the armature due to the sky condition. The armature has a lower electricity usage for Saturday the 21^{st} compared to Monday the 16^{th}, as well as the power of the armature is on the minimum value of 21.1 W for almost three hours. The difference of the electricity usage for the two days is displayed in graph 6.4.

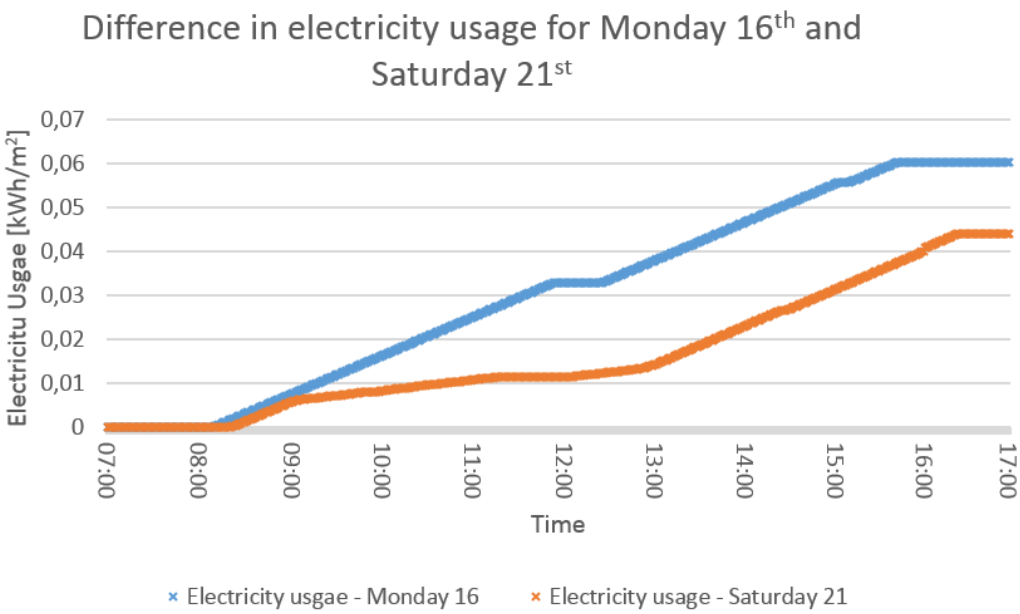

Figure 6.4. The difference in kWh/m^2 between Monday the 16^{th} and Saturday the 21^{st}.

The total electricity usage of the armature for the total of seven days the occupant was present during the fourteen day measurement period was 0.342 kWh/m^2. The average per day was 0.049 kWh/m^2. These values are displayed in table 6.3 and will be applied for validation of the obtained methodologies in part IV on page 121.

Average electricity usage [kWh/m^2]	Total electricity usage [kWh/m^2]
0.342	0.049

Table 6.3. Total and average electricity usage of the armature during the measurement period.

Later in chapter 9 on page 97 the amount of days per week in the occupancy profile will be explained in detail, the amount of days per week for a cell office is five days. It is desired to obtain the electricity usage of the armature for ten days to correspond to the obtained occupancy profile. Therefore the average of the electricity usage is added for three days to the measured seven days and the total electricity usage for a ten day period is 0.488 kWh/m^2.

6.2 Correlation Between Power and Illuminance for the Armature

The correlation between the power of the armature and the generated illuminance level on the working plane shown in graph 6.5.

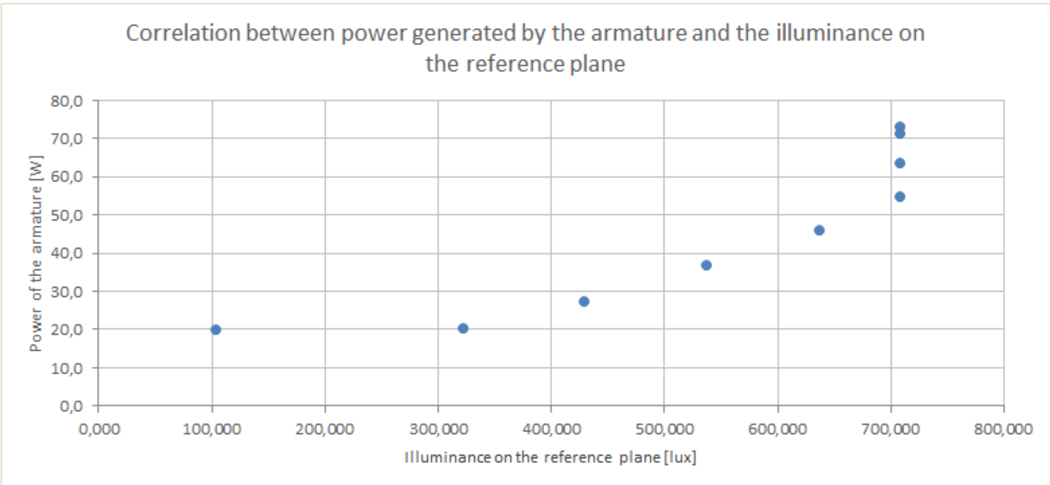

Figure 6.5. The correlation between the power of the armature and generated illuminance

Graph 6.5 shows that the minimum power of the armature is 20.1 W, while the maximum power is 74.4 W. When the armature uses maximum power it generates an illuminance level of 707.66 lux on the working plane, while when the armature uses minimum power it generates an illuminance level of 103,35 lux. The measurement when finding the correlation between the power and generated illuminance of the armature is explained in detail in appendix G on page 245.

As explained in appendix G.4 on page 246, the armature i the case building does not have dimming due to daylight, it does only have two steps; maximum at 100 % and minimum at 27 %. At maximum the armature uses a power of 74.4 W, while at minimum it uses 20.1 W.

Part III

Occupancy Profile

In this part of the report the approach for determining occupancy profiles is presented together with existing occupancy profiles from Danish and Norwegian regulations. The importance of the occupancy profile when determining the electricity usage of occupancy controlled artificial lighting is also shown.

Statistical data analysis is applied on the data gained from the central operating system in order to establish occupancy profiles for cell offices and open landscape offices.

The resulting occupancy profiles which will be applied in the estimation methodology in part IV are presented.

Occupancy Profiles 7

For artificial light which is controlled by the presence of occupants it is important to apply an occupancy profile for the energy calculations in the design phase which represents the actual occupancy profile of the office at hand. For occupancy controlled artificial lighting the electricity usage for artificial lighting is highly dependent on the hours of occupancy. The different building regulations provide occupancy profiles, but as the variation between them is rather high it is interesting to investigate and determine new occupancy profiles for cell offices and open landscape offices for the case building. The case building is an office building with "normal" usage, it is assumed that the use of this office building will represent other office buildings.

In this chapter it is investigated how often people are actually present at their working stations in the office building. The case building has presence detectors for the artificial lighting, which means the armature switches on when people arrive, and turns off 10 minutes after people have left. Occupancy profiles are developed including how many hours per day the occupants are present, the arrival time and leaving time, the days per week, weeks per year and hours per year.

When calculating the electricity usage using a simulation software, an occupancy profile needs to be inserted. The inputs needed vary with the simulation software, some require the total hours per year the office is occupied, while other software require more specified inputs of which weeks and hours per day the office is occupied. For example in Relux the occupancy profile, called operation time, inserted is the annual day hours and annual night hours. A relative absence factor and a reduction factor for building operation time must also be specified. While for BSim it is different. In BSim the input for occupancy, called time schedule, require the user to specify which months, weeks, days and hours during the day occupants will be in the office.

Nevertheless, the obtained occupancy profiles should be applicable for all types of simulation software. The parameter needed for one specific simulation software can be selected from the obtained occupancy profiles and inserted into the simulation software.

7.1 The Importance of the Occupancy Profile

When presence detectors for the artificial lighting system is installed, it is important that the occupancy profile applied when estimating the electricity usage represents the actual occupancy profile in the building in order to accurately determining the electricity usage.

Some people leave late, some arrive early. Some work part time from home, other spend a significant amount of time at meetings, while other do field work. Therefore it is of interest to establish how often during one year an office actually is occupied.

7.2 Hours of Occupancy in Different Regulations

Prior establishing a new occupancy profile existing occupancy profiles in different regulations were investigated. The occupancy profiles are defined differently in different regulations, such as in *SBi 184 Bygningers Energibehov* and *NS 3031 Beregning av bygningers energiytelse Metode og data* as seen in table 7.1.

Regulation	**Note**	**Hours**	**Days per week**	**Weeks per year**	**Hours of use every year**
SBi 184	"Enkeltpersoner", table 14 page 93	8	5	45	1800
NS 3031	"Kontorbygning, driftstid for oppvarming og belysning", table A.43 page 40	12	5	52	3120

Table 7.1. Occupancy profiles from *SBi 184 Bygningers Energibehov* and *NS 3031 Beregning av bygningers energiytelse Metode og data.*

As seen in table 7.1, there is a significant difference between the hours of occupancy between *NS 3031* and *SBi 184*. In order to analyse the different occupancy profiles the two occupancy profiles were simulated in BSim.

7.2.1 Investigation of Existing Occupancy Profiles

As the different regulations define the occupancy profiles differently, it was of interest to investigate the influence of the different occupancy profiles on the electricity usage. This has been done by simulations in BSim. The parameters inserted in BSim can be seen in table 7.2. The Norwegian reference year from *NS 3031* has been applied.

Component	Value
Transmittance of glazing	70%
Reflectance of the three white walls	0.4 (Statens Byggeforskningsinstitut, 2008)
Reflectance of the wooden wall	0.30 (RELUX Informatik AG, 2007)
Reflectance of the ceiling	0.9 (Statens Byggeforskningsinstitut, 2008)
Reflectance of the floor	0.1 (Statens Byggeforskningsinstitut, 2008)
Orientation	128°
Size of glazed area	0.8 m^2 (1.6 m^2 for both)
Area of the cell office	8.26 m^2
Height of room	2.85 m
Depth of room	3.931 m
Width of room	2.102 m

Table 7.2. Inputs in Bsim.

The electricity usage due to the different occupancy profiles calculated by applying BSim is shown in graph 7.1. The calculated electricity usage is for the exact same cell office, and every parameter in BSim is the same for the simulation, except the occupancy profile.

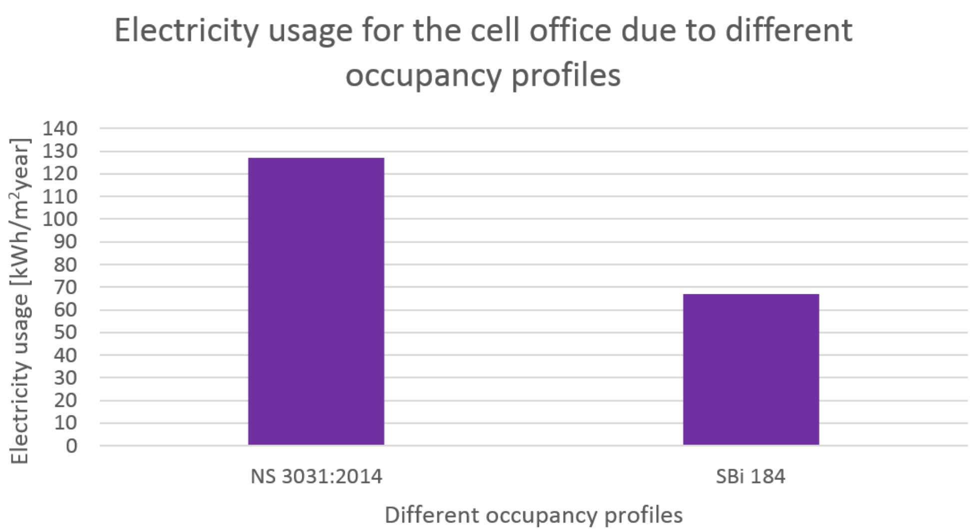

Figure 7.1. Yearly electricity usage for the cell office due to different occupancy profiles from NS3031:2014 and SBi 184

It is remarkable that the electricity usage obtained with the occupancy profile from *NS 3031* gives a yearly electricity usage of 126.89 $\mathrm{kWh/m^2 \cdot year}$, while the electricity usage obtained with *SBi*

184 gives a result almost half of that of 66.80 kWh/m^2 · year. This clearly shows that the electricity usage is highly dependent on the occupancy profile.

7.3 Investigation of the Time of Occupancy in the Case Building

In order to investigate the hours of occupancy in the case building, six cell offices and eight open landscape offices with varying size from two to eight people were investigated. Data from the central operating system for the offices were investigates for a period of two years, 2013 and 2014. The data shows when someone was present by the number 1 as the armature then switches on, and when the offices was empty with 0. The data showed when the exact time the armature switched on and off down to the second.

It was of interest to establish how many hours per year the offices were actually in use. This was done by developing an occupancy profile that included how many weeks per year the offices were in use, how many days per week and how many hours per day. It was also of interest to gain knowledge of when the offices were used, at what time during the day the armature was on.

For every office one occupancy profile was established. The occupancy profile was developed from data for a whole year.

The occupancy profile include:

- How many hours per day the office is occupied
- At what time the user arrived and left
- How many days per week the office is occupied
- How many weeks per year the armature was on
- Which weeks during the year the office is occupied
- How many hours per year the office is occupied

The following chapter establishes an occupancy profile for the cell offices and the open landscape offices including the previous list of points. How many hours per year the office is occupied is described in appendix M.0.6 on page 301.

7.4 Developed Occupancy Profile

A selection of offices on the third floor are included in the investigation of the occupancy profile. These offices are randomly chosen, and include a variety of placement within the third floor as well as the open landscape offices vary in size and layout. The cell offices are all the same size and have the same layout.

Data gained from the central operating system contains data from six different cell offices for 2013 and 2014. These six cell offices are evaluated per year, which means that every cell office is treated as two different cell offices in 2013 and 2014 expect cell office *303* which is only treated for 2013. There is a variation from 2013 to 2014 within the same cell offices, the cell offices are therefore treated as eleven different cell offices. The same goes for the open landscape offices. Eight different open landscape offices for 2013 and 2014. Every open landscape office is treated for the two years except one, *307 - open landscape office north 4 people 2013*, which means data from seventeen different open landscape offices are treated.

- 11 cell offices

- 17 open landscape offices of varying size
- A total of 28 different offices

An abbreviation is made for the different offices, the different offices will be explained with this abbreviation from now on. The abbreviations can be found in the following table 7.3.

Type of office	**Abbreviation**
Cell office	CO
Open landscape office - 2 people	OLO2
Open landscape office - 4 people	OLO4
Open landscape office - 5 people	OLO5
Open landscape office - 6 people	OLO5
Open landscape office - 8 people	OLO5

Table 7.3. The abbreviation for the different types of offices

7.5 Inaccuracies and Errors

As the control strategy of ON-OFF for the occupancy of the armature is a rather simple control strategy it was expected that the uncertainty of the data is small. Nevertheless, is was noticed that the central operating system was registering some mistakes for a few days. This error was the armature being on for several days in a row. The error only occurred once for every office throughout the year, it varied at what time during the year the error occurred.

The errors:

- 3 of the cell offices had errors varying from 3-6 days
- 7 of the open landscape offices had errors varying from 4 days to 1 week and 3 days

Another error was that in 2013 weeks 3 and 22 were constantly off for all the offices, and in week 13 the armature was said to be constantly off in 2014. These weeks are assumed to be an error as it is the same weeks for all the offices in the whole case building, and there is not a holiday during these weeks.

The errors were treated by first excluding these days, and a few times even weeks, then estimate an average of hours per day, days per week and weeks per year for all the cell offices and another average for all the open landscape offices. Then this average replaced the error. This method will not give as accurate result as if there was no errors, but it was concluded that when an error of up to maximum one week and three days is substituted with the average values for all similar offices this will give a more realistic view of the occupancy profile than if these errors where only neglected.

Hours per Day 8

When calculating the electricity usage for the artificial lighting, it is interesting to know how many hours, and especially which hours, of the day the occupant is present in the office. The daylight availability in a room varies a lot throughout the day and the need for artificial lighting will vary correspondingly. If the occupant is present mostly early in the day, the need for artificial lighting will be lower than if they are present mostly in the afternoon.

BSim requires the user to specify the number of hours per day when the occupant is present in the office, and how these hours are distributed throughout the day.

SBi 184 Bygningers Energibehov and *NS 3031 Beregning av bygningers energiytelse Metode og data* have stated hours per day of 8 and 12 respectively. It was of interest to investigate if these numbers correspond to the hours of occupancy for the case building.

The hours of occupancy for every day was investigate for all the offices, the offices are for now divided into two: Cell offices and open landscape offices. The open landscape offices vary in size from two to eight people. The offices in the case building all represent the same work field, nevertheless a small deviation was expected for the hours of occupancy per day between the different offices as people have different habits, working hours and working tasks. It was expected that the cell offices would have a small deviation in hours of occupancy, while the deviation for the open landscape offices would be larger.

8.1 Average of Hours Per day

Initially an average of the hours the offices were occupied for the days the occupant was present throughout one year were investigated for every offices, i.e. hours the occupant was in the office divided by the number of days the occupant was there. The hours are only the hours the occupants were actually present in the offices during the day, which means that these hours do not correspond to the hours the occupants were at work. Lunch, meetings and similar activities are not a part of these hours. The results are displayed in graph 8.1 for all the cell offices and 8.2 for all the open landscape offices.

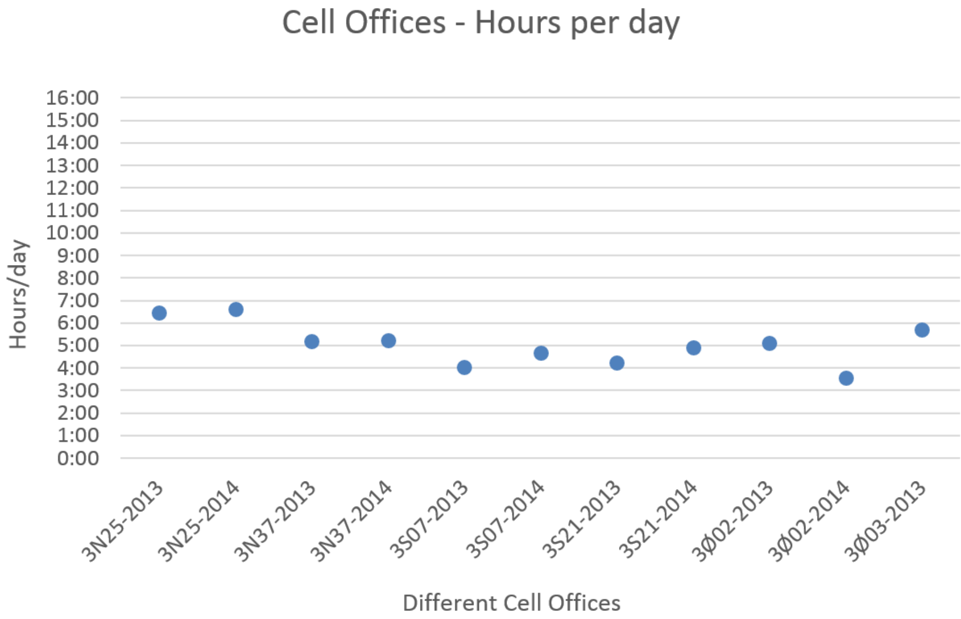

Figure 8.1. Hours per day on average over a year for the cell offices

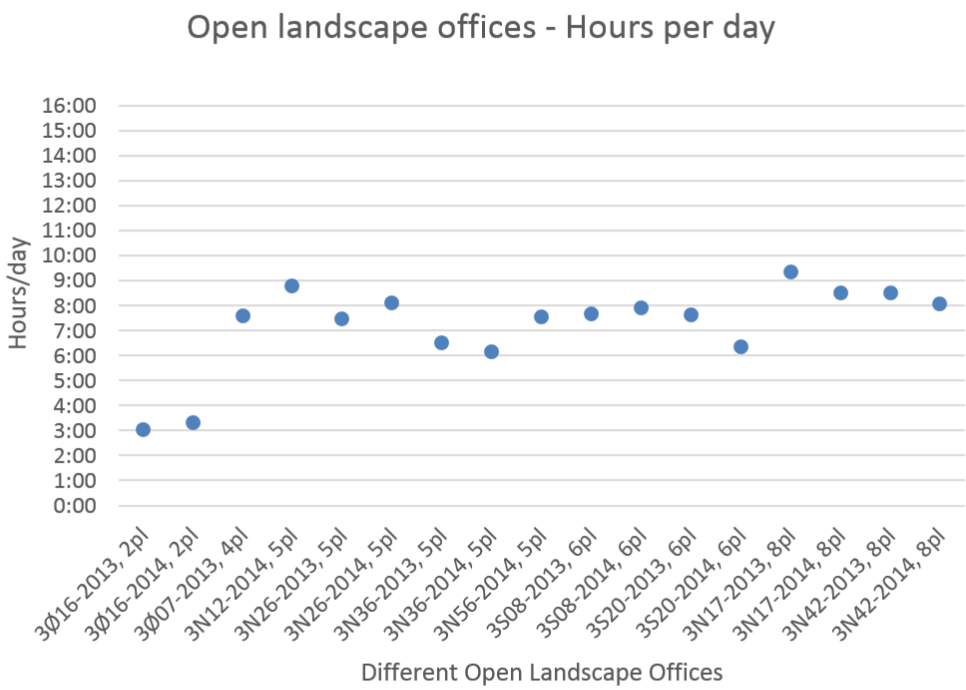

Figure 8.2. Hours per day on average over a year for the open landscape offices

The graphs 8.1 and 8.2 show a variation in the average hours per day. Graph 8.1 show a variation of maximum hours per day on average from 6 hours and 36 minutes for *CO 3N25-2014*, to minimum of 3 hours and 33 minutes for *CO 3ø02-2014*. In graph 8.2 *OLO2 3ø16-2013* was occupied on an average of 3 hours and 1 minute, while *OLO8 3N17-2013* 9 hours and 20 minutes.

The variation in average hours per day for the cell offices and open landscape offices:

- Cell offices: 3:33-6:36 gives a deviation of 3:03

- Open landscape offices: 3:01-9:20 gives a deviation of 6:19

The deviation for the open landscape offices was expected as a variation of the size from two to eight people will cause differences in the hours of use per day. Nevertheless, a deviation of 6 hours and 19 minutes is quite large. It is therefore concluded that the open landscape offices need to be divided between the different sizes. How they should be divided will be established later in 11 on page 111.

A deviation of 3 hours and 3 minutes for the average hours per day for the cell offices is quite large. The cell offices should have fairly similar occupancy profiles as they all are only occupied by one person.

8.2 Variation of Hours per Day

To better show the variation of the hours per day for the different cell offices a box plot diagram was made. The box plot show the variation from maximum to minimum hours per day for all the offices, as well as the median and the first quartile of 25 % and the third quartile of 75%. The data included to form the box plot diagram is the hours the armature is on for every day for every single cell office.

8.2.1 Variation of Hours per Day for the Cell Offices

Graph 8.3 is a box plot diagram for all the cell offices showing the variation in hours per day from minimum to maximum as well as the median and first and third quantiles.

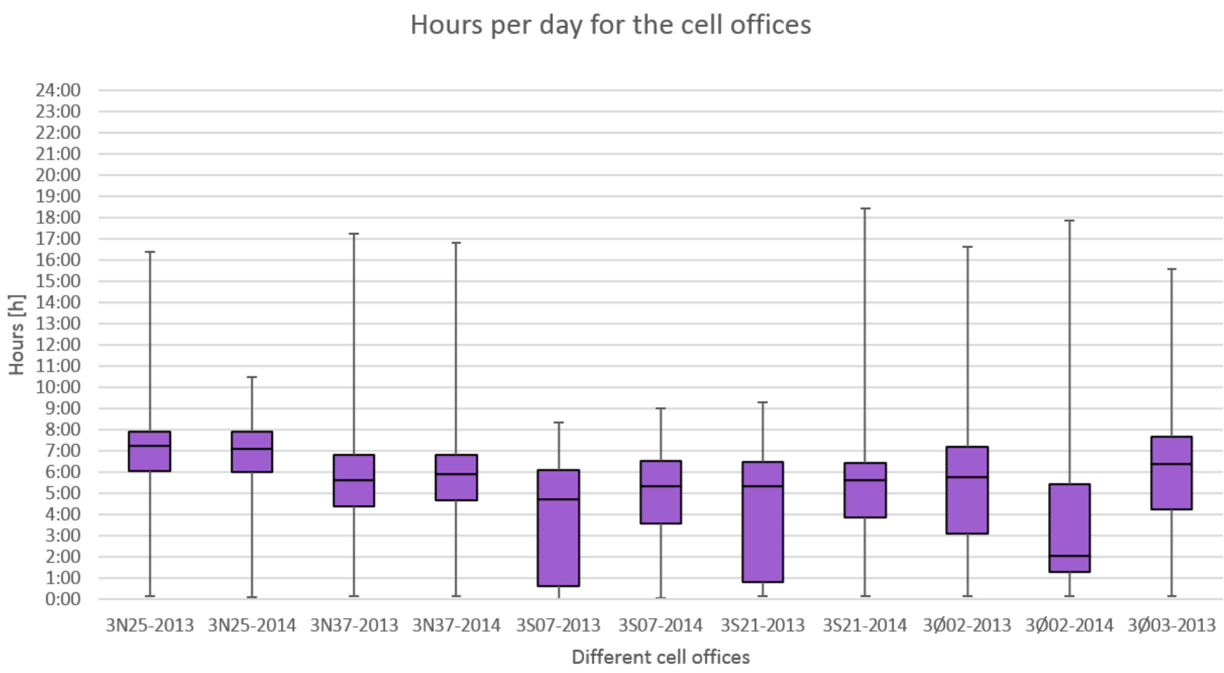

Figure 8.3. Box plot diagram of hours per day for different sizes of open landscape offices

The box plot diagram shows the variation of maximum hours per day of 18 hours and 26 minutes, to minimum of 10 minutes. The minimum of 10 minutes is probably someone just swinging by the office or the cleaning staff. As the armature turns off after 10 minutes, 10 minutes is the minimum for all the cell office as sometime during a year someone will just drop by the office and this becomes the minimum of that year.

The average median of all the cell offices is 5 hours and 34 minutes, while the maximum median is 7 hours and 14 minutes and the minimum median is 2 hours and 4 minutes. The variation between the cell offices seen in graph 8.3 is extensive and combining the result for all the cell offices stating one certain amount of hours per day representing all the cell offices will include a large inaccuracy.

8.2.2 Variation of Hours per Day for Open Landscape Offices

To investigate the difference in hours per day for the different sizes of open landscape offices a box plot diagram of different sized open landscape offices was made. The sizes vary from two people to eight people. As for the cell offices, the data included is the hours of occupancy for all the days someone is present in the office. Graph 8.4 is a box plot diagram for all the cell offices showing the variation in hours per day from minimum to maximum as well as the median and first and third quantiles.

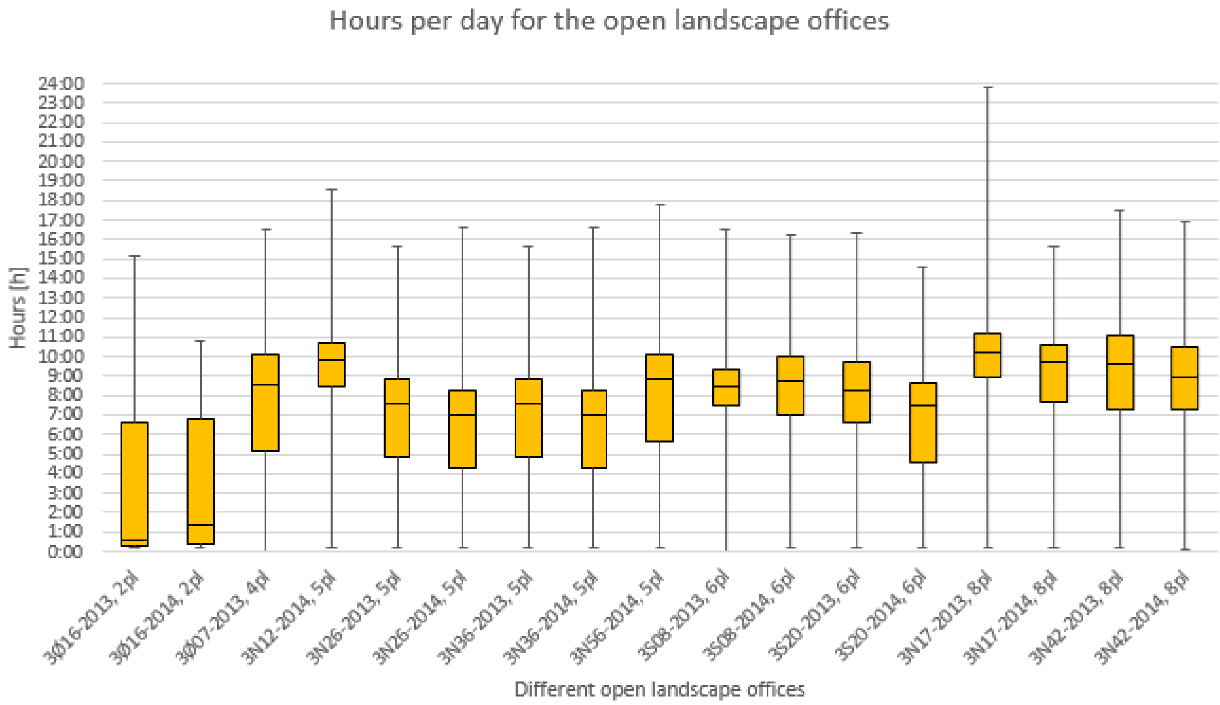

Figure 8.4. Box plot diagram of hours per day for all the cell offices

The maximum hours per day in graph 8.4 is shown by the whisker plot and is 23 hours and 49 minutes for *OLO8 3N17-2013*. This is an open landscape office for eight people and it is reasonable that at some point thorough the year the armature is on for 23 hours and 49 minutes as eight people may arrive and leave very differently at the office and if they are very busy at the office they might stay for quite long. Similar to the cell offices, the minimum for all the open landscape offices is 10 minutes.

Special attention should be given to the open landscape office for two people for 2013 and 2014, the median in 2013 is 37 minutes which is extremely low. The third quartile has a wide range reaching 6 hours and 37 minutes. The extremely low median values of 37 minutes in 2013 and 1 hour and

20 minutes in 2014 give reason to believe this open landscape office is not regularly occupied. The results from these offices will therefore be excluded in the further determination of hours per day. The two people open landscape offices is not representative for the open landscape offices, when studying the data in detail it was notices that the occupants in the two people open landscape offices spend a considerably lower amount of time in their office throughout the year compared to the other occupants. It is believed that the occupants in the open landscape offices for two people has a different position in the firm, compared to the other occupants, which either require more field work or meeting activities. As the occupancy profiles for these offices shows a significant variation from the other offices, they are not considered representative for for the open landscape offices. Due to this they will be excluded in the analysis of the occupancy profile for open landscape offices except from 11 on page 111 where the occupancy profiles dependency on number of people is investigated. The results including these offices can, however, be found in appendix M.0.1 on page 295.

The average median for the open landscape offices, excluding the ones for two people, is 8 hours and 31 minutes, while the minimum is 7 hours and 2 minutes and the maximum 19 hours and 13 minutes. Combining all the open landscape offices stating a specific amount of hours per day will include a large inaccuracy.

Graphs 8.3 and 8.4 clearly show the variation in the hours per day for all the offices. The data is not symmetric, it is for most of the offices skewed down meaning the first quartile has a larger range.

8.3 Establishing Hours per Day for the Offices

As it is hard to conclude on hours per day for the different offices using the box plot graphs with large variations between the offices, frequency histograms with distribution curves were made. The frequency histogram shows the frequency of the days with the same hours per day and the distribution curve illustrate the density of the frequency of the days for different hours per day.

8.3.1 Frequency of Hours per Day for the Cell Offices

The frequency histogram and distribution curve shown in graph 8.5 shows the frequency of the hours per day for all the cell offices.

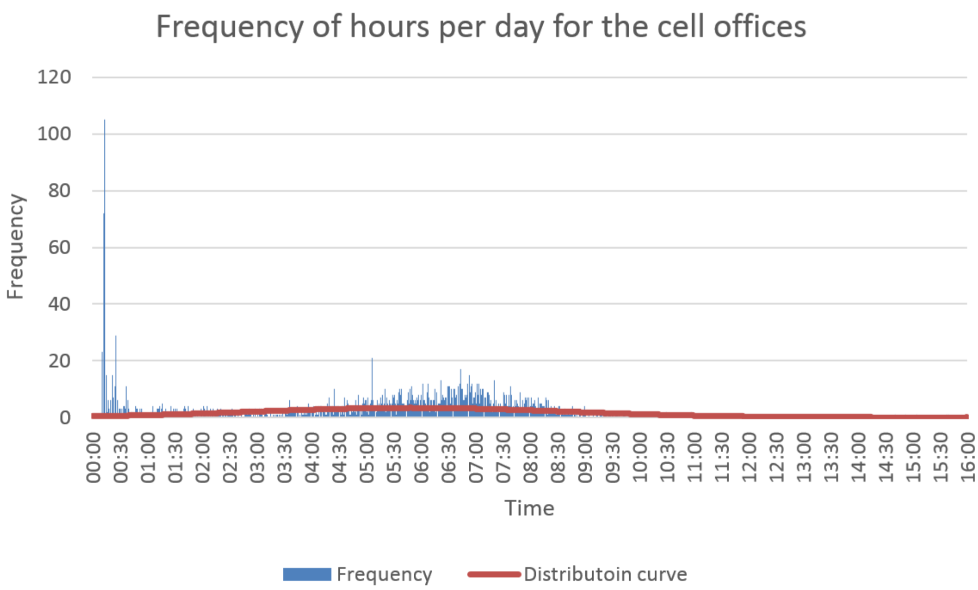

Figure 8.5. Frequency histogram and normal distribution of hours per day for cell offices

As seen in graph 8.5 the frequency between 10 minutes to 25 minutes is quite high. With modes at 72 for 12 minutes and 105 for 13 minutes.

The distribution can be said to be double peaked with one peak between 10 to 29 minutes and the second between 6:00 to 7:30. It is believed that the first peak is due to the cleaning staff or people just dropping by the office

- The mean is 5 hours and 6 minutes
- The median is 5 hours and 49 minutes
- The mode is 0:13 and occurs for 105 of the days
- The standard deviation is 2 hours and 51 minutes

The mean, median and mode will be equal in a perfectly normal distributed data set. The mean, median and mode are not the same in this data set, the distribution is skewed. When the data set is skewed it i recommend to use the median for the central tendency as the mean can be distorted by the outliers and it is not common to apply the mode (Lund og Lund, May 2015).

The sum of the frequency for the peak from 10 to 29 minutes is 304, while the peak from 6:00 to 7:30 is 669. The first peak is not of interest when investigating regular hours of occupancy per day. The first peak is more interesting when it comes to the days per week the occupants are present. If many of these days are only 10-29 minutes long, they might be neglected as they should not be treated as a full or regular working day.

These short days also causes some of the weeks to consist of six days per weeks as will be discussed in section 9.3.1 on page 101.

For now it is interesting to establish an estimate for hours of occupancy per day for the cell office for a regular working day. Therefore, days consisting of time per day less than 30 minutes are excluded. The new frequency histogram and distribution curve is seen in graph M.2.

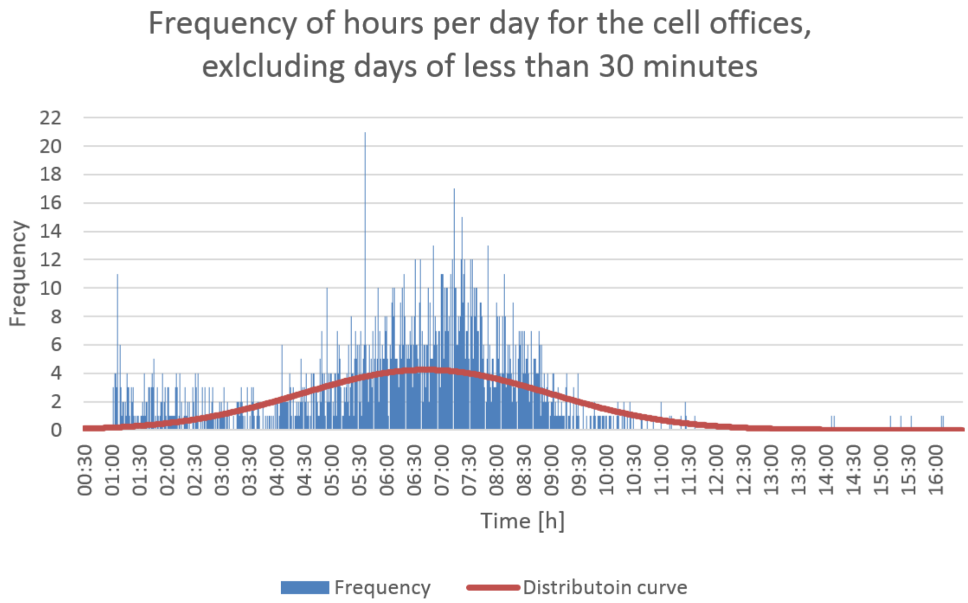

Figure 8.6. Frequency histogram and normal distribution of hours per day for cell offices, excluding the days shorter than 30 minutes

- The mean is 5 hours and 52 minutes
- The median is 6 hours and 13 minutes
- The mode is 5:07 and occurs for 21 of the days
- The standard deviation is 2 hours and 15 minutes

The standard deviation is a measure of the deviation for the data to the mean value. The standard deviation is here 2 hours and 15 minutes which is quite significant when the mean is 5 hours and 52 minutes. This means that the distribution curve, the density curve, is wide. The narrower the bell curve the more confident result, and as this bell curve is the opposite, the confidence in the result is quite low.

8.3.2 Frequency of Hours per Day for the Open Landscape Offices

The frequency histogram and distribution curve shown in graph 8.7 shows the frequency of the hours per day for the open landscape offices. Days of less than 30 minutes are excluded as for the cell offices in section 8.3.1, the graph including days of less than 30 minutes can be found in appendix M.0.1 on page 295.

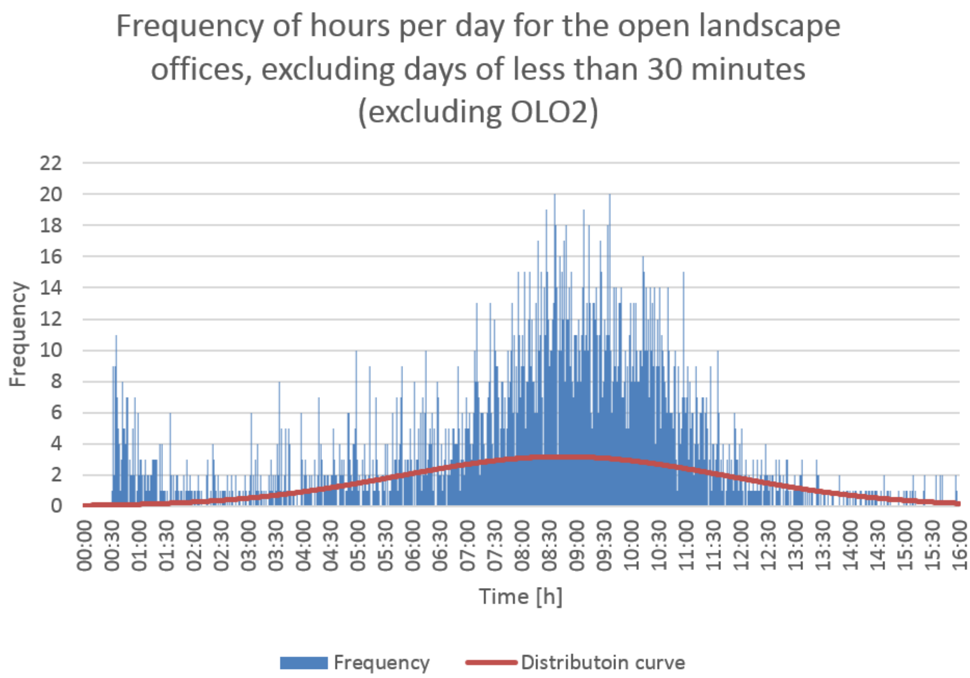

Figure 8.7. Frequency and distribution curve of hours per day for open landscape offices excluding the ones for 2 people, and excluding days shorter than 30 minutes

- The mean is 8 hours and 17 minutes
- The median is 8 hours and 45 minutes
- There are two modes at 8:36 and 9:37, each occur for 20 of the days
- The standard deviation is 3 hours and 1 minute

As seen on the graph and from the parameters listed above, the days most frequently last from approximately 8 hours and 30 minutes to 9 hours and 30 minutes. As expected, the open landscape offices has longer working days than the cell offices, as there is more people that might have different arriving and leaving time which may stretch out the occupancy hours. The arriving and leaving time for the offices is examined in section 8.5.

8.4 Developed Profile for Hours per Day

As the data for both the cell offices and open landscape offices were skewed, it was chosen to apply the median for the number of hours per day rather than the mean as this value may be affected by outlying values of the data. As a result, the following values are chosen for the occupancy profiles for the two different office types:

- Cell offices: 6 hours per day
- Open landscape offices: 8 hours and 30 minutes per day

The open landscape offices are of size four to eight people.

8.5 Distribution of Hours per Day

As mentioned earlier, it is not only interesting to know the number of hours when the occupant is present in the office, but also which hours during the day the office is in use.

In *NS 3031 Beregning av bygningers energiytelse Metode og data* the 12 hours of occupancy per day is stated to be symmetrical around 13:00 o'clock. It is of interest to see if this corresponds to the distribution of occupancy hours for the case building.

In this section, the arrival and leaving time for the offices is investigated followed by an analysis of the distribution of the hours throughout the day.

8.5.1 Distribution of Hours per Day for the Cell Offices

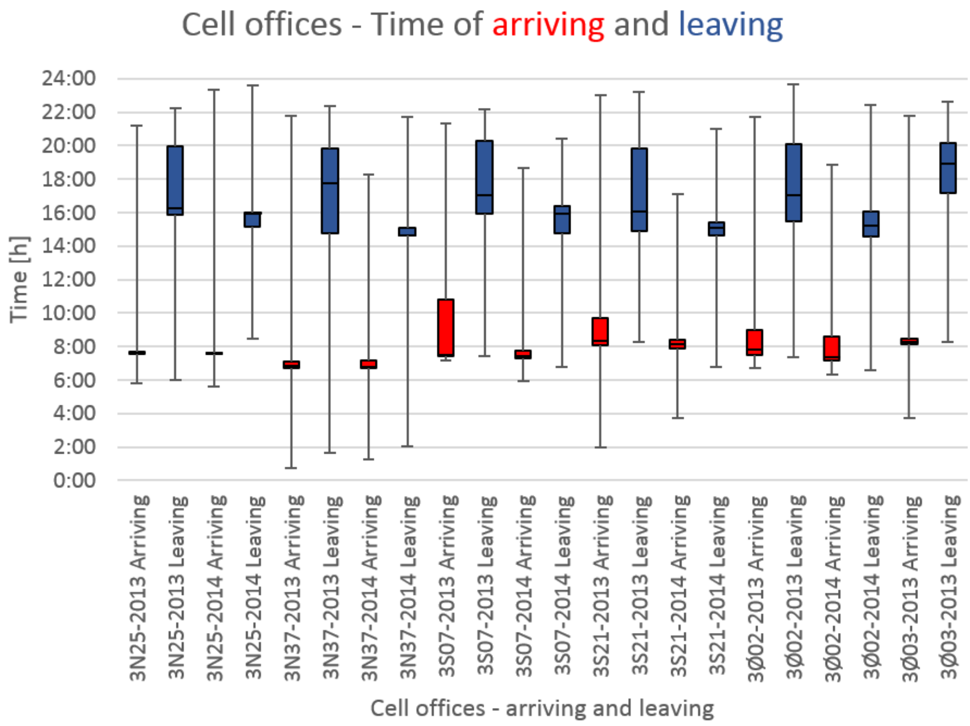

Figure 8.8. Box plot diagram of the leaving and arriving time for the cell offices

Box plot diagram 8.8 show that for most of the cell offices the occupants arrive sometime between 6:30 and 8:15 most of the time. Some cell offices vary in the arrival time, especially *CE 3S07-2013*. The arrival time of the cell offices are more or less consistent in the arrival time, but the leaving time, on the other hand, hold more variation. The leaving time vary from about 14:30 to 18:00.

Nevertheless, in order to conclude on an arrival and leaving time for the cell offices the median for every cell office is applied, rather than the mean value, as the data is skewed.

- The average median for arriving is 7:37
- The average median for leaving is 16:21

As the average median time for arriving and leaving for a cell office is 7:37 and 16:21 respectively, this results in a 8:44 hour long working day. However, as determined in 8.4, the average working day is 6 hours, which means that there must be approximately 3 hours during the day where the occupant is not present in the office. These hours most likely includes a lunch break and meetings.

To determine where these 3 hours occur, the distribution of the hours per day was investigated. Four weeks of a year, consisting of five days each, were analysed for two of the cell offices. The four weeks represents one week for each season of the year. The offices of interest, *3N37-2014* and *3S21-2014*, were chosen due to the median values for the time of arriving and leaving for these offices in year 2014 were closest to the overall median for all of the cell offices combined. The distribution was made by looking at the hours where the artificial light in the office was on and off. The distribution of hours per day for the two offices can be seen in the following graphs 8.9 and 8.10.

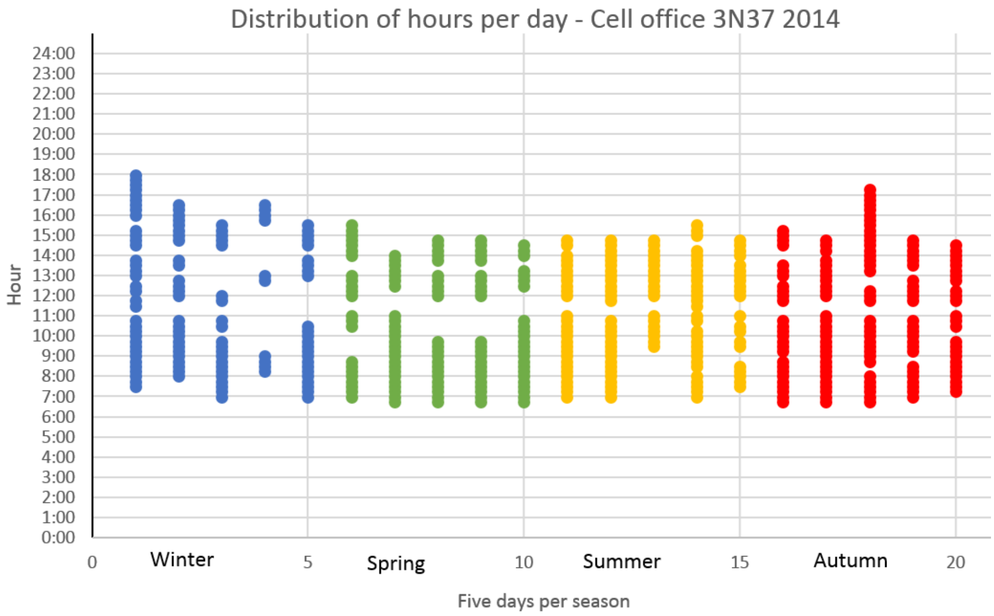

Figure 8.9. Distribution of hours per day for *3N37-2014* for five days per season

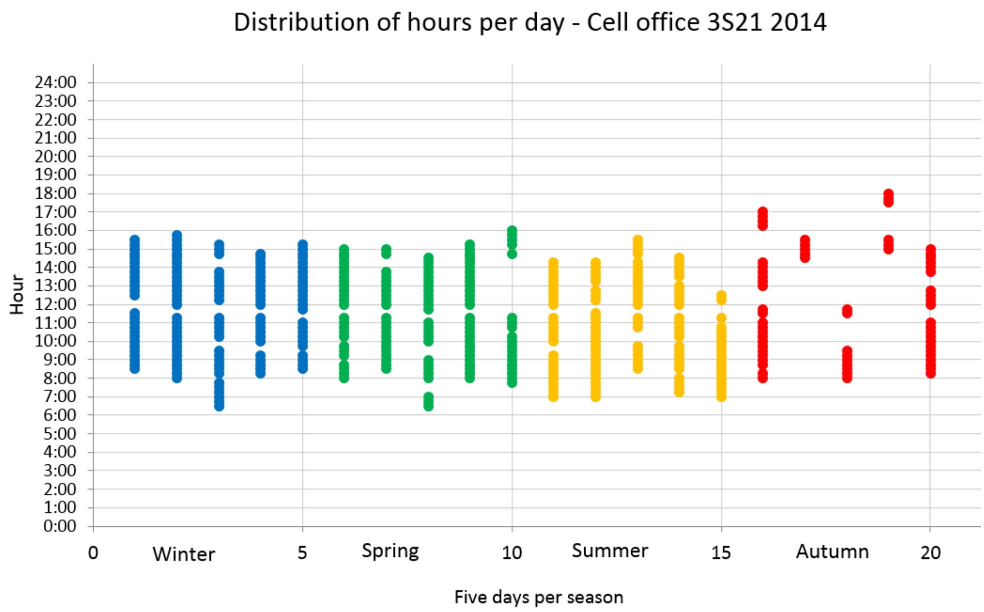

Figure 8.10. Distribution of hours per day for *3N21-2014* for five days per season

As seen in the graphs, both offices have a more or less consistent break between 11 and 12 o'clock every day. This is most likely the lunch break. It can also be seen that there is often one break during the morning between 9 and 10 o'clock. This is especially visible for *3S21-2014*. For *3N37-*

2014, a break during the afternoon between 13 and 14 o'clock occur for most of the days. This is also, to some extend, the case for *3S21-2014*.

According to this distribution, these three hours during the day can be excluded from the occupancy profile for the cell offices:

- In the morning: 09:00-10:00
- Lunch: 11:00-12:00
- Afternoon: 13:00-14:00

8.5.2 Distribution of Hours per Day for the Open Landscape Offices

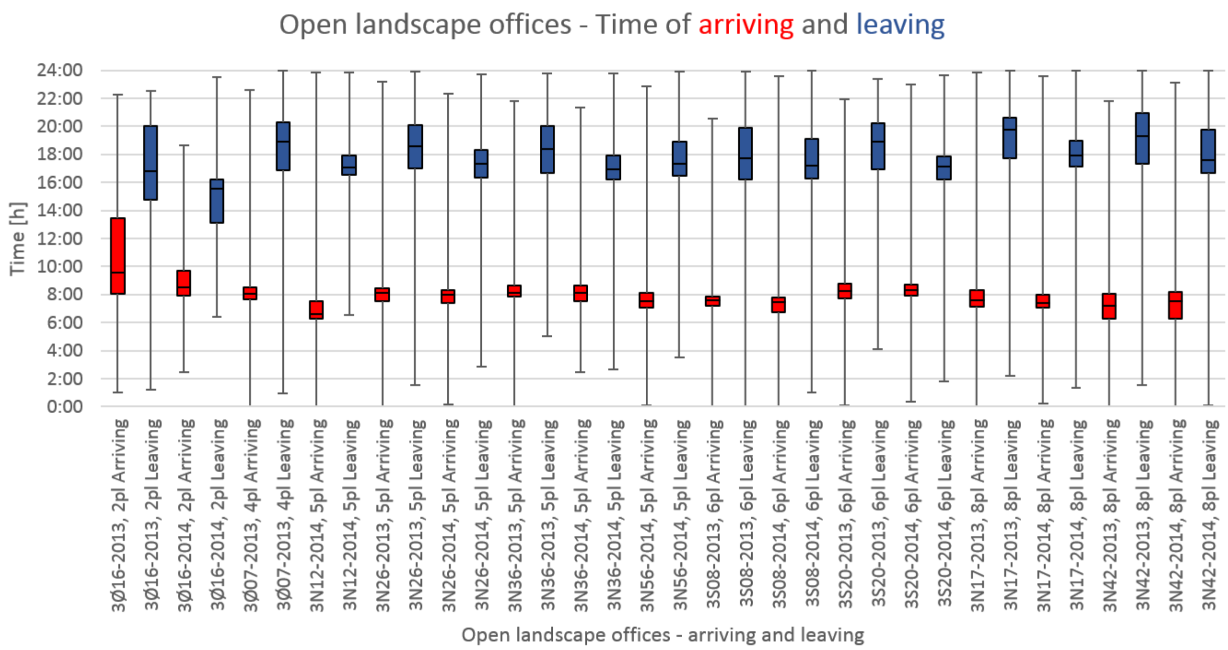

Figure 8.11. Box plot diagram of the leaving and arriving time for the open landscape offices

As for the cell offices, the arriving time in the open landscape offices are also more consistent than the time of departure. As earlier discovered, the offices with only two people have a very different profile than the rest of the offices. This can also be seen in this graph. Due to this, it is chosen to exclude the results from these offices also for this analysis.

The median values are utilized to determine the average time of arrival and departure and the results are as following:

- Time of arrival: 8:00 o'clock
- Time of departure: 18:00 o'clock

This results in a 10 hour long working day. However, as determined in 8.4 the average working day for open landscape offices was 8 hours and 30 minutes which means that there is 1 hour and 30 minutes during the day where the occupants are not present in the office.

When investigating the number of days per week in 9.3.2 on page 102, it was discovered that the occupants were often present in the open landscape offices for 6 and even 7 days per week. This indicates that the occupants are frequently present in the office for some time during the weekends.

Such as for the cell offices, these two offices was chosen because of their median of hours per day was closest to the overall median for all the open landscape offices combined.

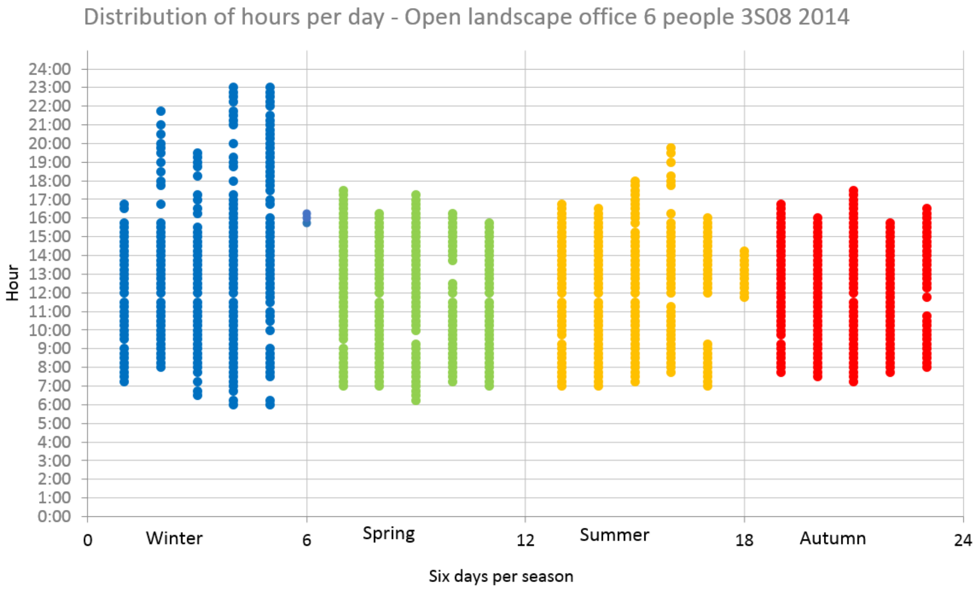

Figure 8.12. Distribution of hours per day for *OLO6 3S08-2014* for seven days per season

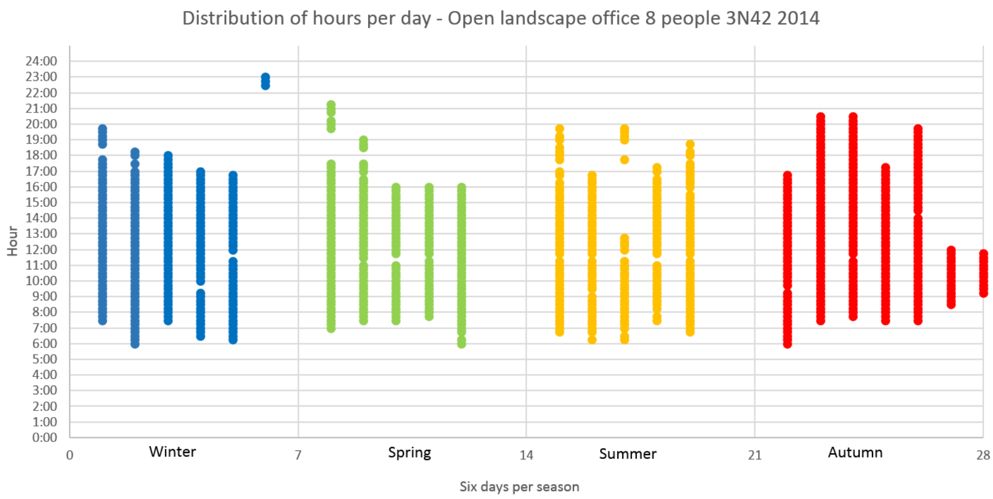

Figure 8.13. Distribution of hours per day for *OLO8 3N42-2014* for seven days per season

In graph 8.12 there is a clear trend of absence in the office between 11:30 and 12:00. This is most likely the lunch break. The same trend can also be seen for most of the days in the other office 8.13. Both of the graphs show that there is often a short break in the morning and in the afternoon. Half an hour is therefore excluded in the morning, in the afternoon and at lunchtime. The time for the breaks are:

One and a half hours throughout the day which are excluded:

- In the morning: 09:30-10:00
- Lunch: 11:00-11:30
- Afternoon: 16:15-16:45

When studying the raw data it was discovered that that the occupancy time for the sixth and seventh day normally was from one to four hours. Some of the days were just above 30 minutes long. This is significantly shorter than the other days of the weeks.

8.6 Completion of Hours per Day

It was determined that the occupants in the cell offices were present on an average of 6 hours per day. They were normally arriving at 7:37 in the morning and leaving at 16:21 in the afternoon. The breaks during the day was found to be from 09:00 to 10:00, from 11:00 to 12:00 and from 13:00 to 14:00.

In some cases, such as in BSim, it is not possible to divide the occupancy profile into half hours. If it is necessary to have the occupancy profile in whole hours, the arriving time of 07:30 and the departure time of 16:21 could be set to 08:00 and 17:00 respectively.

The occupants in the open landscape offices were present on an average of 8 hours and 30 minutes per day. The average time of arrival was 08:00, and they were normally leaving at 18:00. The breaks throughout the day was found to be from 09:30 to 10:00, from 11:00 to 11:30, and from 16:15 to 16:45. If a profile containing whole hours is desired, the break in the morning could be added to the lunch break. The 30 minute break in the afternoon could be neglected, as an overestimation of the hours of presence in the office is better than an underestimation. The open landscape offices would then have a working day of 10 hours with a one hour break from 11:00 to 12:00.

In 8.14 the final profile of hours per day for a cell office and an open landscape office is shown.

Hour	Cell office	Open landscape office
1:00	0	0
2:00	0	0
3:00	0	0
4:00	0	0
5:00	0	0
6:00	0	0
7:00	0	0
8:00	1	1
9:00	0	1
10:00	1	1
11:00	0	0
12:00	1	1
13:00	0	1
14:00	1	1
15:00	1	1
16:00	1	1
17:00	0	1
18:00	0	0
19:00	0	0
20:00	0	0
21:00	0	0
22:00	0	0
23:00	0	0
24:00	0	0

Figure 8.14. Occupancy profile for hours per day on hourly average for cell office and open landscape office

Days per Week 9

The amount of days per week the occupants are present in the office will influence the electricity usage of an occupancy controlled artificial lighting system. According to both *Norsk Standard NS 3031:2014 Beregning av bygningers energiytelse* and *By og Byg Anvisning 203 Beregning af dagslys i bygninger* the amount of days per week is five days. The amount of days per week for the offices in the case building is studied. Simulation software such as BSim requires the user to specify the amount of days per week in the occupancy profile.

9.1 Average Amount Days per Week

The average days per week for the cell offices and open landscape offices are illustrated in graphs 9.1 and 9.2.

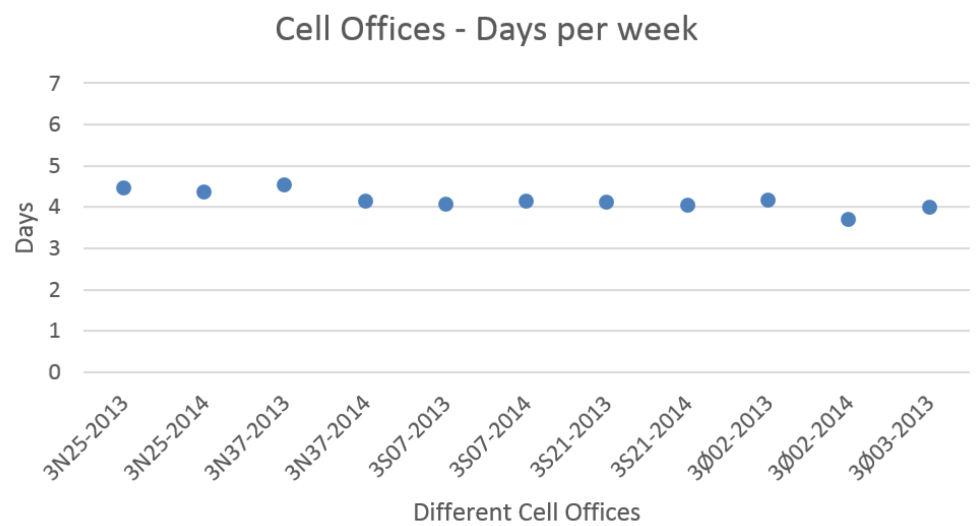

Figure 9.1. Days per week on average over a year for the cell offices

The average days per week for the cell offices are for most of the cell offices varying between four and five days. This variation will be investigated further in section 9.2.1.

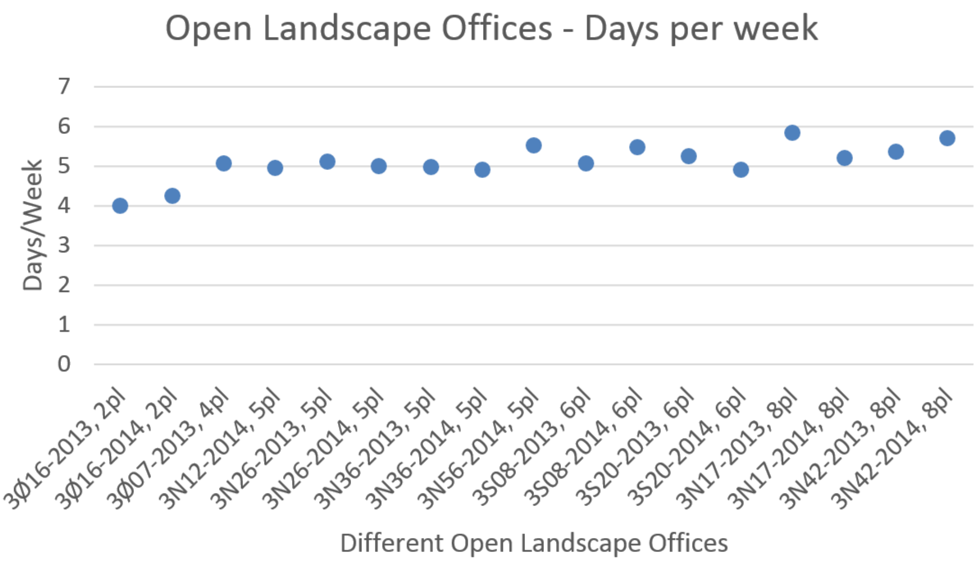

Figure 9.2. Days per week on average over a year for the open landscape offices

The mean of the days per week for most of the open landscape offices are close to five days, but for some of the open landscape offices the mean is actually close to six days per week. Open landscape office *3N17-2013, 8pl* has the highest average of days per week with a value of 5.85 days per week, this will be discussed in section 9.3.2.

The average of the days per week for the two people open landscape is lower than all the other offices with a value of four. Even though the two people open landscape offices are neglected from the analysis of the hours per day due to significantly lower amount of hours per day as mentioned in section 8.2.2, the data from the two people open landscape offices are included in further analysis of the days per week in order to obtain a profile which includes a open landscape offices from the size of two to eight people.

9.2 Variation of Days per Week

As seen in graphs 9.1 and 9.2 there is a variation in the average amount of days per week over a year for the offices. This is further studied by investigating box plot diagrams for a better picture of the variation.

9.2.1 Variation of Days per Week for the Cell Offices

The variation of the amount of days per week for the 11 cell offices can be seen in graph 9.3.

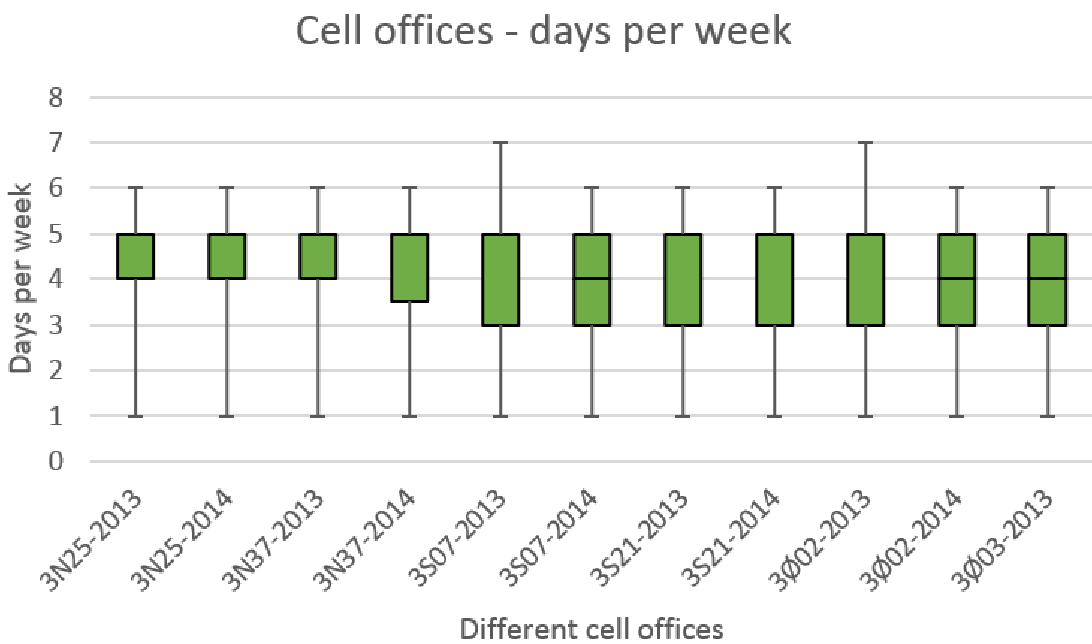

Figure 9.3. Box plot diagram of days per week for the different cell offices

As seen in the graph, all the offices have an upper quartile of 5 days per week. Three of the offices have a lower quartile of four days per week, one office has a lower quartile of three and a half days per week, and the remaining seven offices have a lower quartile of three days per week. For three of the offices, the median is 4 days per week. For the remaining offices there is no clear median showing in the box. This is due to the median and the upper quartile overlapping each other. This overlap occurs when the majority of the numbers in the dataset has the same value. This overlap can be illustrated by looking at the distribution of the data for these offices. Figure 9.4 shows the distribution of the data for CO *3N25-2013*.

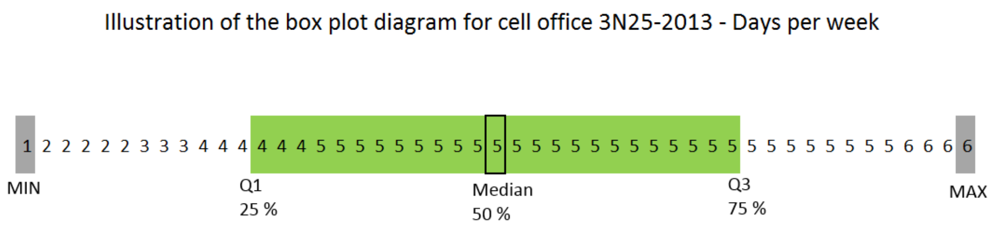

Figure 9.4. Illustrative box plot for cell office 3N25-2013 of days per week.

From 9.4 it is clear that the majority of the data has a value of five, which explains why the median and the upper quartile are overlapping. The lower quartile has a value of 4. Out of the remaining values, only 9 of the values are lower than 4, which constitutes 18% of the total data. 4 of the remaining values are higher than 5 which constitutes 8% of the total data. This means that the box consists of 73.46% of the total data.

Two of the offices have an upper whisker at 7 days per week, while all the remaining offices have an upper whisker at 6 days per week. The lower whiskers for all of the offices are at 1 day per week. When studying the data it was discovered that the weeks with 7 days only occurred once for each of the two offices. Weeks with only one day occurred for 1 to 4 times for all the offices, except for office *3ø02-2014* where it occurred 6 times.

9.2.2 Variation of Days per Week for the Open Landscape Offices

The variation of the amount of days per week for 17 open landscape offices is shown in graph 9.5.

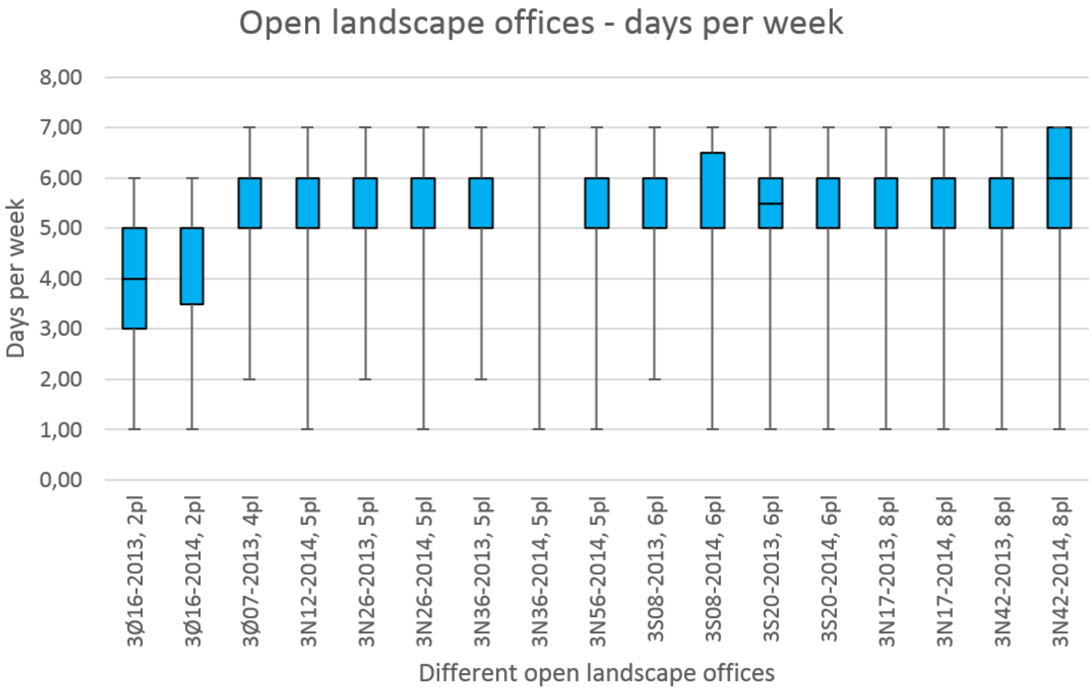

Figure 9.5. Box plot diagram of days per week for the different open landscape offices

It can be seen that all of the offices shows consistency to some extend except from the *3ø16-2013* and *3ø16-2014* which are the offices with only two people. The days per week for those two offices are lower than for the rest with a median of 4 and 3.5 days per week respectively. For the offices with no clearly visible median in the box, the median overlaps with the lower quartile. OLO5 *3N36-2014, 5pl* has a median, lower quartile and upper quartile all of 5 days per week, which is why this is pictured only as a straight line without a box.

It is clear that the majority of the offices have a median and lower quartile of 5 days per week, and an upper quartile of 6 days per week.

9.3 Establishing Days per Week for the Offices

In order to establish days per week for the offices frequency histograms and distribution curves are applied as for the hours per day in section 8.3.

9.3.1 Frequency of Days per Week for the Cell Offices

Graph 9.6 show the frequency of days per week and the distribution curve for the cell offices.

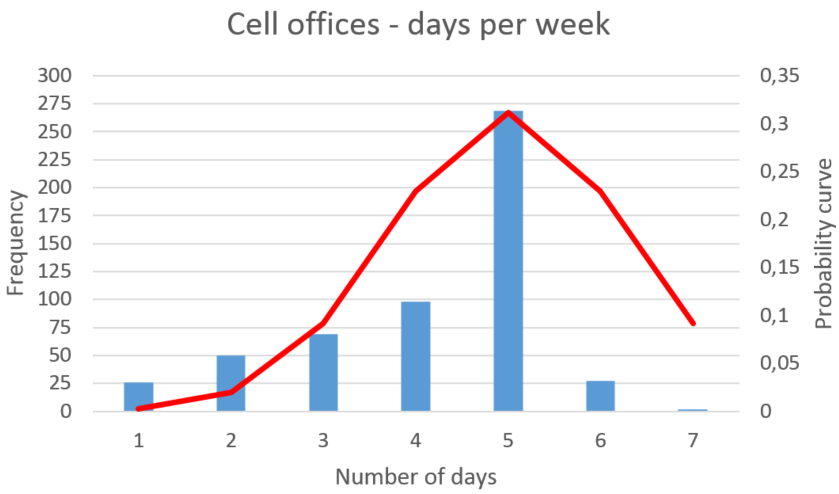

Figure 9.6. Frequency histogram and distribution curve for days per week for all the cell offices

- The mean is 4.15 days
- The median is 5 days
- The mode is 5 and occurs 269 times
- The standard deviation is 1.28 days

The data is skewed to the left, which means there is a higher frequency of lower values than the median than higher. As it is a skewed data set the median should be applied in order to establish the days per week for the occupancy profile as the mean may be distorted by the outliers.

As explained in section 8.3.1 on page 87 quite a few days consists of less than 30 minutes and should not be included as a regular working day when establishing the occupancy profile. 307 out of the total of 2246 days for all the cell offices during 2013 and 2014 are shorter than 30 minutes. This is a factor of approximately 1 to 7.5, which means that slightly less than 1 (0.96) day per 7 days is shorter than 30 minutes. Nevertheless, these 30 minutes cannot completely be excluded as artificial lighting is on for up to 30 minutes for these days and this will of course contribute to the total yearly electricity usage.

As seen in graph 9.6 there are some weeks consisting of six and seven days, 29 weeks out of the total of 541 weeks the occupants are present in the cell offices are weeks consisting of six or seven days. When stating that the cell offices are occupied five days per week due to the median and mode both at five, and extracting every seventh day due to a shorter day than 30 minutes and then adding the 29 weeks of six and seven days, a conclusion can be made stating that the cell offices are occupied for five days per week. Five days per week is representative for the variation of one to seven days per week with a median at five, and every seventh day shorter than 30 minutes.

9.3.2 Frequency of Days per Week for the Open Landscape Offices

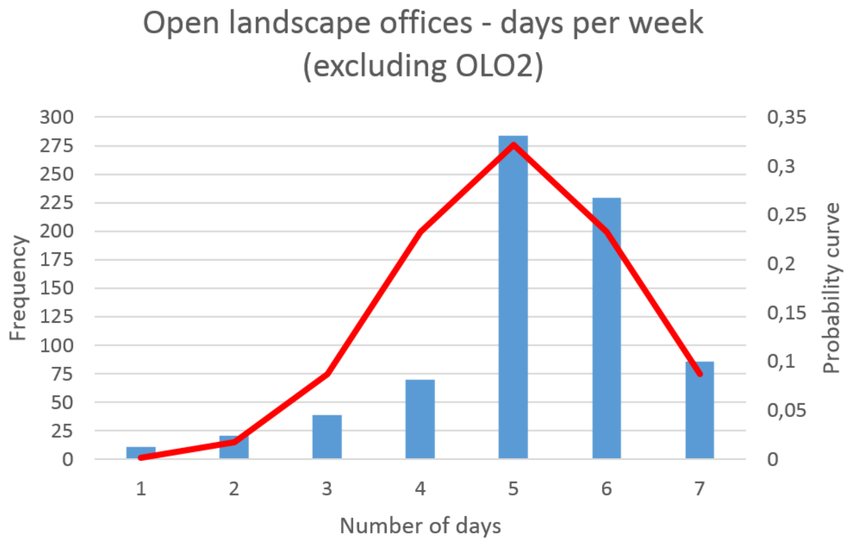

Figure 9.7. Frequency histogram and distribution curve for days per week for all the open landscape offices, excluding the two people open landscape offices

- The mean is 5.19 days
- The median is 5 days
- The mode is 5 and occurs 284 times
- The standard deviation is 1.239 days

The numbers just mentioned would indicate that the occupancy profile for open landscape offices can be stated to have five days per week, nevertheless when studying graph 9.7 this does not seam to be the case. The number of weeks with amount of days lower than 5 is 188, while the number of weeks above five is 321. This indicates that days per week should not be stated to be five.

In section 8.5.2 on page 93 the hours per day were investigated, it is interesting to establish if day six and seven are short days, shorter than 30 minutes. However, only 6 out of the total of 3846 days for all the open landscape offices, excluding OLO2, during 2013 and 2014 are days shorter than 30 minutes. These 6 out of 3846 days are so significantly few that they can be neglected. This means that day six and seven are indeed longer than 30 minutes. However, as mentioned in section 8.5.2 on page 93 these days are shorter than the "normal" working days varying between one to four hours. The distribution of hours for these days were shown in graphs 8.12 on page 94 and 8.13 on page 94.

When the OLO2 offices are included 272 out of the 4218 days are shorter than 30 minutes, which is similar as the result obtained for the cell offices in section 9.3.1.

Keeping in mind that the median and mode both are five days per week, and the mean right above 5, and also investigating the frequency histogram it can be concluded that days per week for the open landscape offices are 5 and $\frac{1}{2}$ days.

Weeks per Year 10

One of the inputs required in BSim is a schedule stating when a zone is occupied. Not only do hours per day and days per week need to be specified, months per year and weeks per year must also be specified as a part of this schedule. When studying the data is was concluded that months per year would not give an accurate schedule as it very rarely happened that someone was absent from their office for a full month, and if someone were absent it never followed the calendar months. Nevertheless, when studying the weeks it was clear that for some weeks throughout the year the occupants were absent. Therefore, the weeks were studied in detail to establish which weeks the occupants were not present. Then an occupancy profile dependent on which weeks the occupants where present were made.

10.1 Establishing Weeks per Year

It is of interest to establish the amount of weeks the occupants are absent from the office during one year, and if there is a correlation between which weeks these are for the different offices.

Arbeidsmiljøloven og ferieloven made by *Arbeidstilsynet* states that by law an employee must have at least 25 days vacation during a year where Saturdays are included as working days which means 4.16 weeks vacation (Arbeidstilsynet, 2007). This should mean that the occupants should be absent for at least four weeks every year.

In this study the data for the offices are divided between 2013 and 2014 in order study if there is a correlation between which weeks the occupants are absent for the two years.

10.1.1 Establishing Weeks per Year for the Cell Offices

Graphs 10.1 and 10.2 show the amount of weeks the occupants are absent from their cell office during 2013 and 2014.

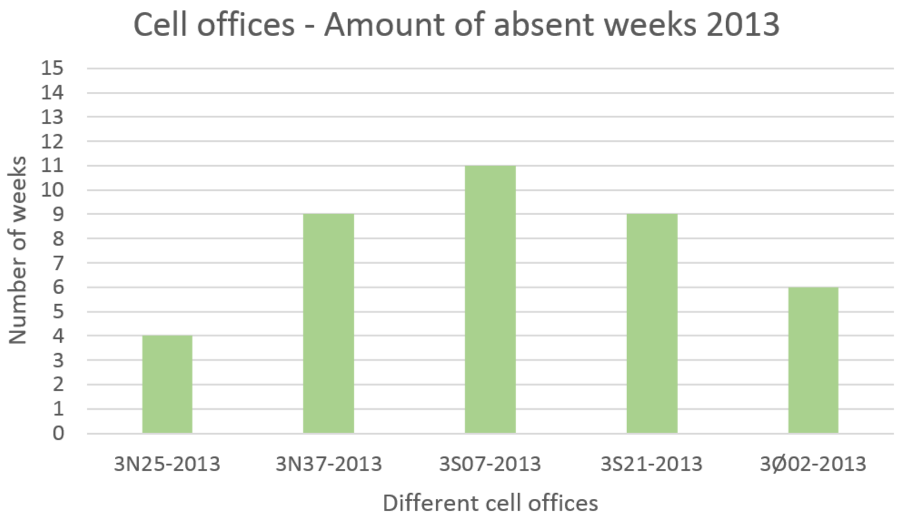

Figure 10.1. The amount of weeks the occupants are absent for the cell offices during 2013

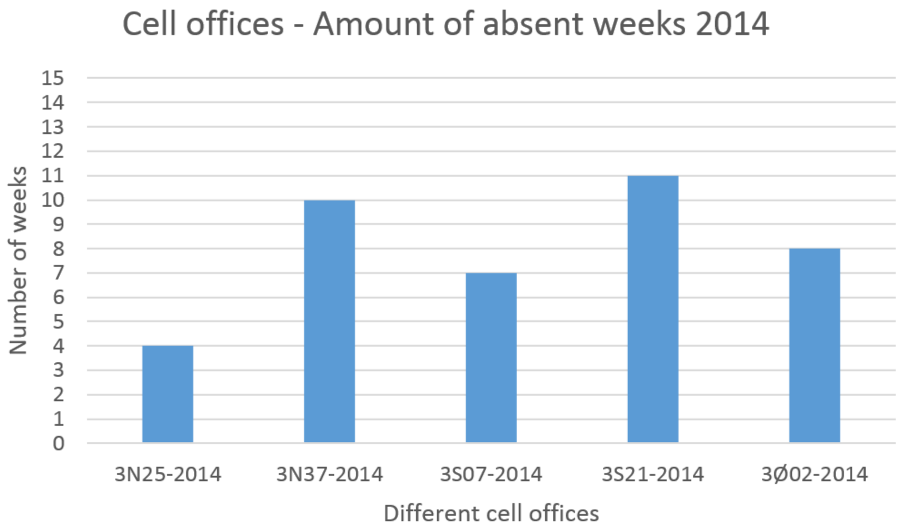

Figure 10.2. The amount of weeks the occupants are absent for the cell offices during 2014

The average amount of weeks the occupants in the cell offices are absent during 2013 is 7.8 weeks, while for 2014 it is 8 weeks. The average for both combined is 7.9 absent weeks during one year. In both 2013 and 2014 the amount of weeks varies from four to eleven weeks. A deviation of seven weeks between two of the offices is significant. One reason for this deviation may be that the occupant has small children or children in primary school and the occupant then must follow the holidays for the school, the holiday schedule for Oslo can be found in appendix M.0.4 on page 300. The holidays for the schools in the Oslo district may affect the weeks the occupants are absent from their office.

In Norway the recommended joint summer holiday, also called *byggeferien*, is the three following weeks; 28, 29 and 30, every summer. It is therefore expected that there is a correlation of absent weeks for 2013 and 2014 for these weeks.

The work tasks for the occupants in the case building may require some field work which might be the reason why some of the occupants are more absent than other. Another factor is that the employees in the case building can work from home if desired. An additional cause for the deviation of the amount of absent weeks can be sick leave.

The two following graphs 10.3 and 10.4 show the frequency of absent weeks for the cell offices.

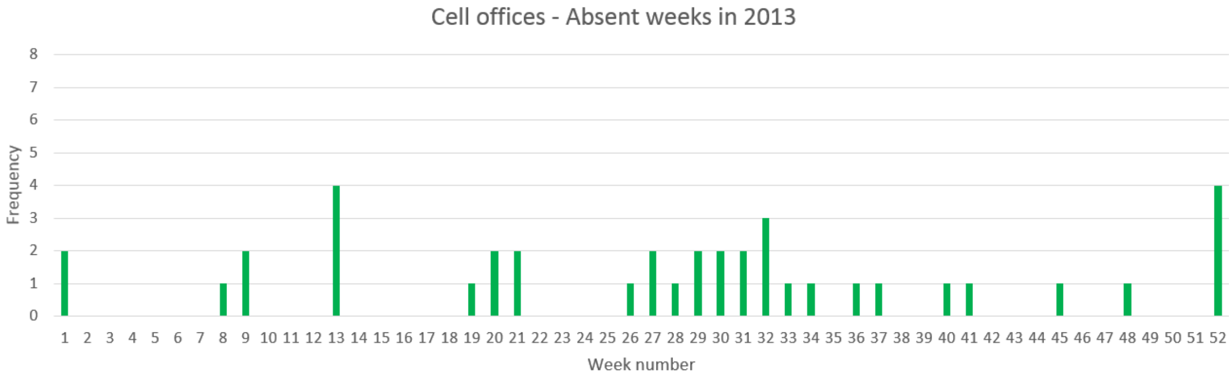

Figure 10.3. Frequency of weeks the occupants are absent for five cell offices during 2013

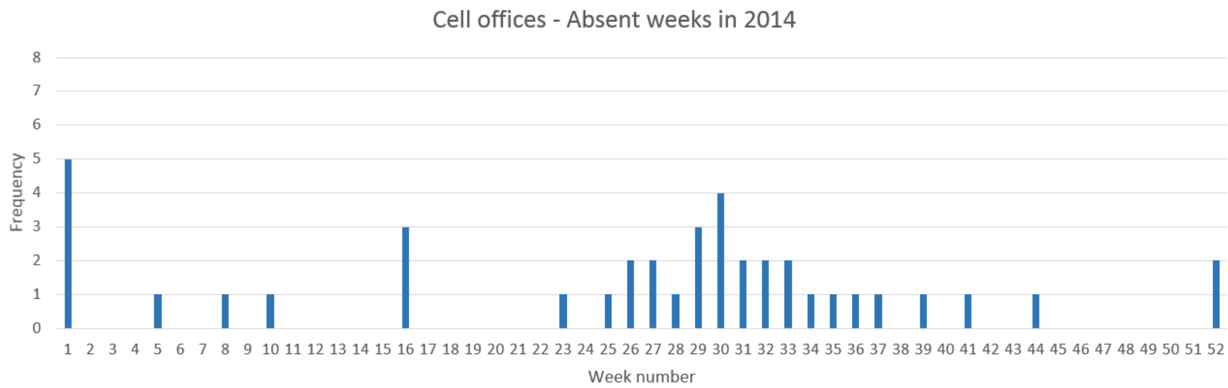

Figure 10.4. Frequency of weeks the occupants are absent for five cell offices during 2013

Graph 10.5 sum up the absent weeks for the two years. The Easter is in week 13 in 2013 and week 16 in 2014 and Christmas Eve and New Years Eve are one day later in 2014 compared to 2013. Other than that the fall, winter and summer holidays are during the same weeks for the two years.

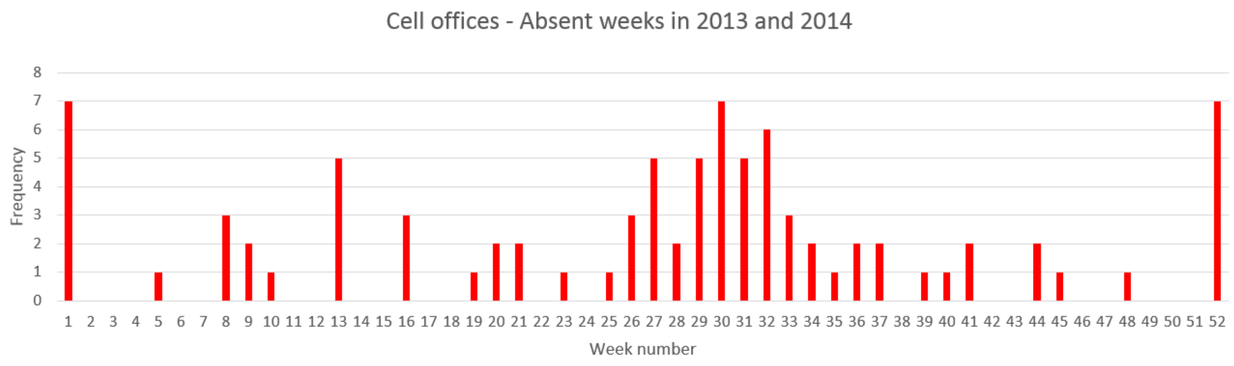

Figure 10.5. Frequency of weeks the occupants are absent for five cell offices during 2013 and 2014

When studying graph 10.5 and keeping in mind that the average weeks the occupants are absent from the cell offices are 7.9 absent weeks, the following eight weeks have the highest frequency:

- Week 1
- Week 13/16 - The Easter, it varies every year
- Week 27
- Week 29
- Week 30
- Week 31
- Week 32
- Week 52

Statistical data show that Easter has the highest frequency of occurrence in week 15 (Frost, March 2013), therefore it is concluded that week 15 will be an absent week and account for the Easter break.

10.1.2 Establishing Weeks per Year for the Open Landscape Offices

The open landscape offices are investigated in order to find the amount of absent weeks during one year and the frequency of occurrence for the same weeks for the two years.

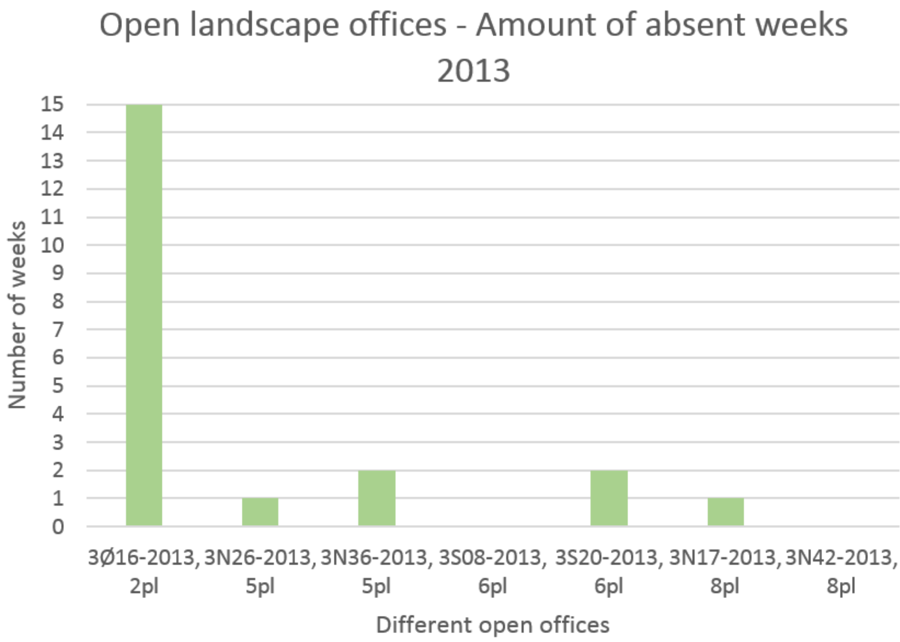

Figure 10.6. The amount of weeks the occupants are absent for the open landscape offices during 2013

The two people open landscape office has a total of 15 absent weeks in 2013, while one of the six and eight people open landscape offices has none.

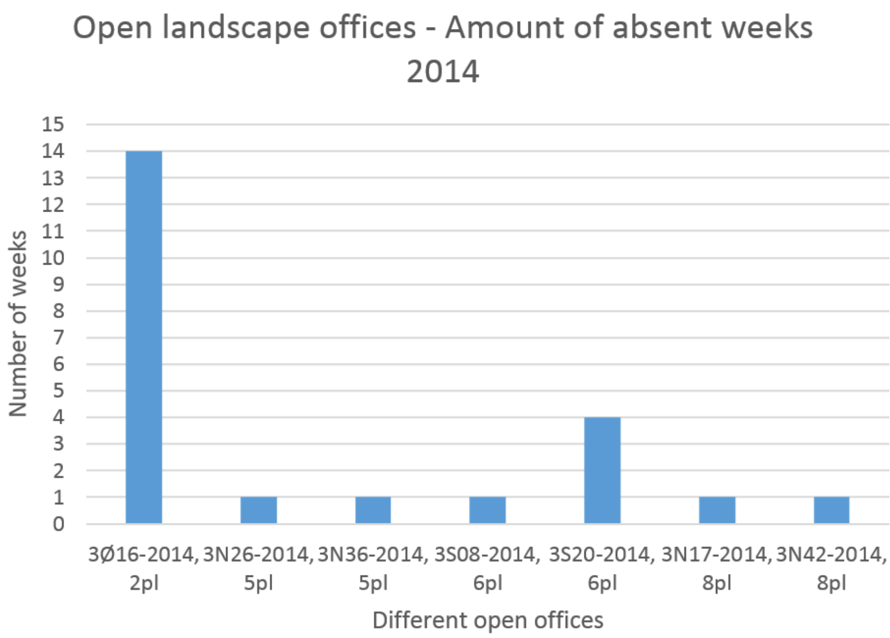

Figure 10.7. The amount of weeks the occupants are absent for the open landscape offices during 2014

Again, in 2014, the OLO2 has a significant larger amount of absent weeks compared to the other open landscape offices. It has therefore been decided to exclude the OLO2 as they are not representative for open landscape offices as explained in section 8.2.2.

The average of the amount of absent weeks for all the open landscape offices is 1.0 in 2013 and 1.5 in 2014.

As for the cell offices, the frequency of the absent weeks are studied for the open landscape offices. Graphs 10.8 and 10.9 show the frequency of absent weeks per year for the open landscape offices, except OLO2.

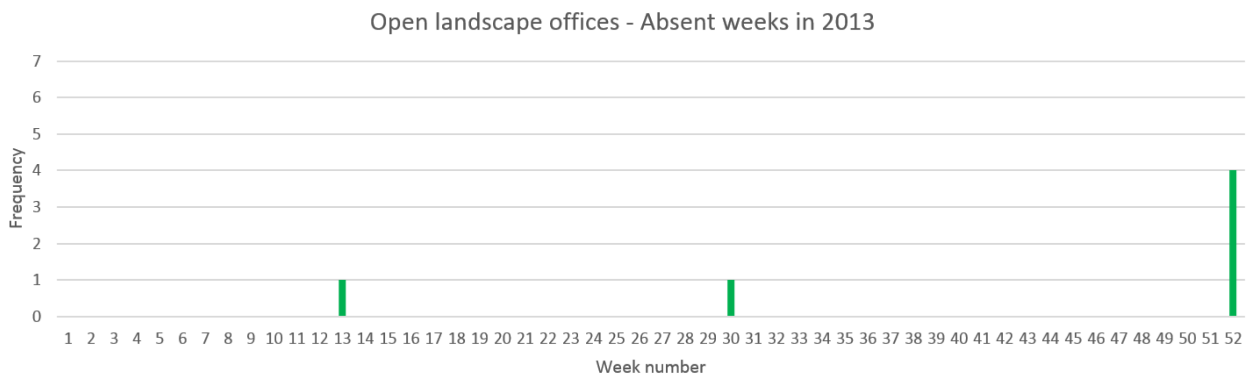

Figure 10.8. Frequency of weeks the occupants are absent for seven of the open landscape offices during 2013

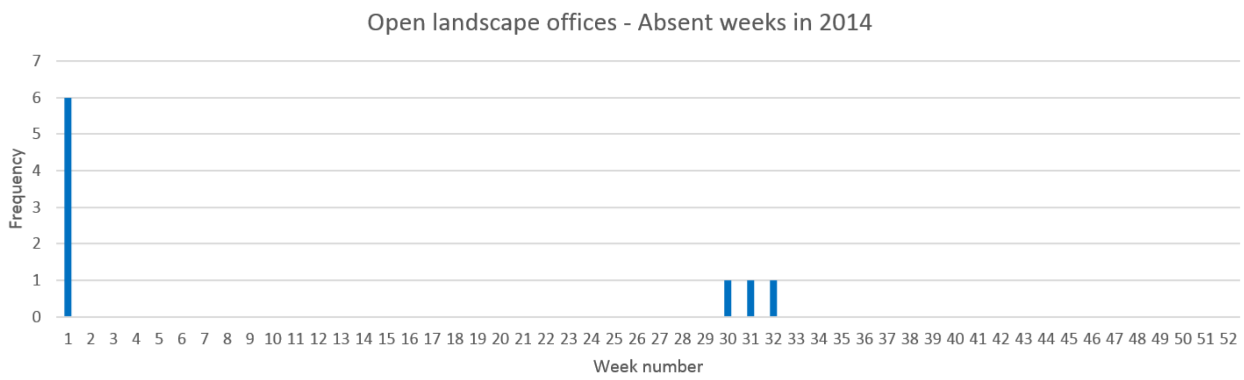

Figure 10.9. Frequency of weeks the occupants are absent for seven of the open landscape offices during 2014

The frequency of absent weeks for 2013 and 2014 are added together and shown in graph 10.10.

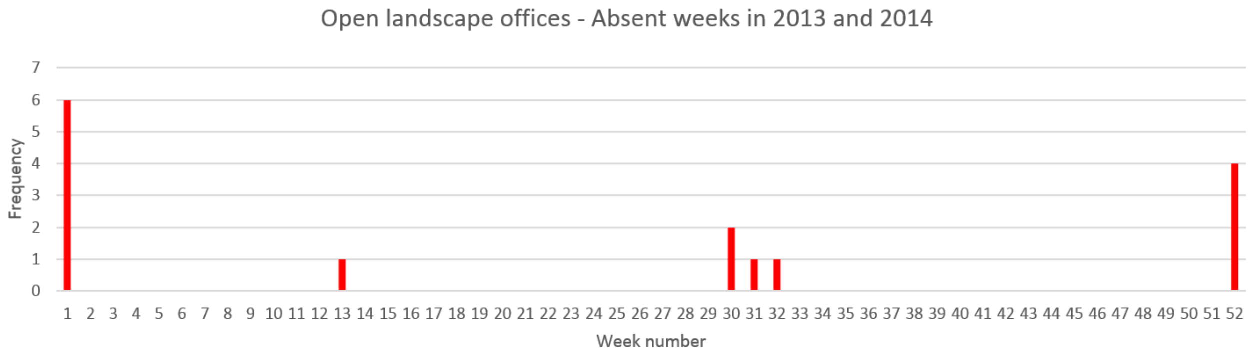

Figure 10.10. Frequency of weeks the occupants are absent for seven of the open landscape offices during 2013 and 2014

As the average of absent weeks in 2013 is 1.0, and 1.5 in 2014 the weeks of absence is week one it has a frequency of six in 2014, and the three first days of week 52 as it has a frequency of 4 in 2013.

The weeks with with the highest frequency of absence for the open landscape offices:

- Week 1
- 3 days in week 52

The Dependency on Number of People 11

The differences between cell offices and open landscape offices seen in chapters 8, 9 and 10 are investigated by looking at the hours per day, days per week and weeks per year for offices dependent on the number of people in the offices. It is of interest to establish if there is a connection between the number of people in an office and the occupancy time. The 11 cell offices and 17 open landscape offices of varying size are investigated. The cell offices are not interesting as they always have the same number of people, however they included for comparison.

11.1 Hours per Day, Days per Week and Weeks per Year Dependent on Number of People

Graph 11.1 shows the average of hours per day an occupant is present in the office over a year and how this is different for the different amount of people in the office. The 11 cell offices and 17 open landscape offices are included in graph 11.1, but many of the offices have the same median and the results are overlapping.

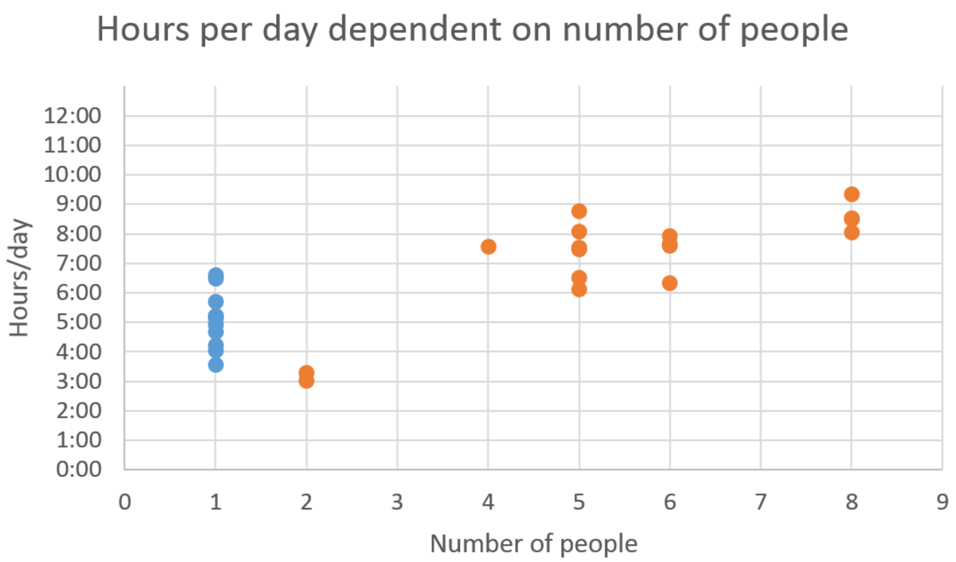

Figure 11.1. The average of hours per day for the offices dependent on number of people in the office

A slight increase of the average hours per day with an increase in number of people from the cell offices to the eight people open landscape offices. Nevertheless, there is not a clear increase from four to six people, the hours per day stay more or less the same. As there is only one OLO4 included in the data set the result for this one office is not completely representative for all four people open landscapes, but it can give an idea of the occupancy of four people open landscape offices. It is unanticipated that both OLO2 has a lower average of hours per day than all the cell offices. It was expected that the OLO2 would have a higher average hours per day than the cell offices as there is two people compared to only one, but as explained in section 8.3.2 on page 89, it is believed that the occupants in OLO2 has an abnormal working day.

The median of days per week the occupants are present in the offices is shown in graph 11.2.

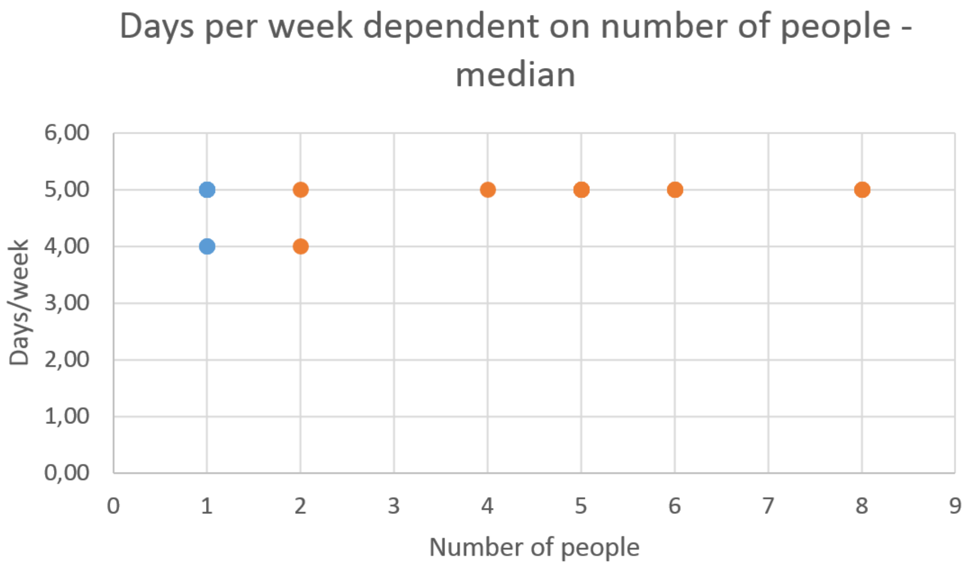

Figure 11.2. The median of days per week for the offices dependent on number of people in the office

The established days per week for the cell office occupancy profile in section 9.3 on page 100 states five days per week for both the cell offices and the open landscape offices. Some of the OLO8 has a median of six days per week, but as stated in section 8.5.2 these days only lasts for about 12 minutes to one hour. From graph 11.1 it is noted that the CO and OLO2 both have varying days per week between four and five, while open landscape offices from four to eight people are constant at five days per week.

The sum of weeks per year the occupants are present is shown i graph 11.3 for all the offices. The amount of weeks shown in graph 11.3 are the amount established after extracting days of less than 30 minutes and weeks only consisting of one to three days of 30 minutes.

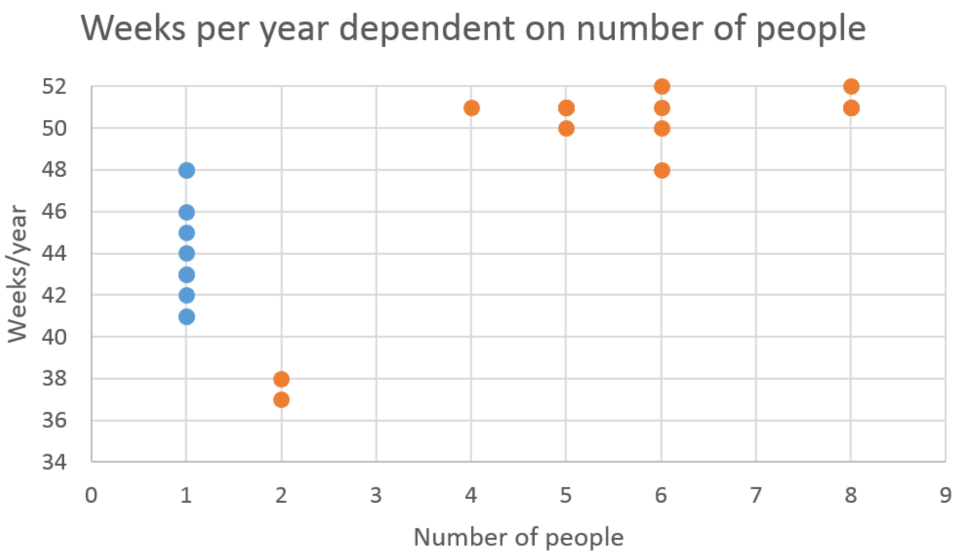

Figure 11.3. Weeks per year dependent on number of people in the office

For the cell offices a clear variation of weeks per year can be seen, the occupancy profile for weeks per year for cell offices established in section 10.1.1 on page 103 have 44 weeks per year for the cell offices. Again, the OLO2 has a significantly lower amount of weeks per year than the other offices. For the four to eight people open landscape offices the amount of weeks are for all, except one OLO6, above 50 weeks per year.

11.2 Established Dependency on Number of People

The three previous graphs 11.1, 11.2 and 11.3 does not illustrate a significantly clear trend for the offices dependent on the number of people. However, it can be slightly noticed that four to six people offices partially have the same amount of hours per day. It is of interest to establish the dependency for the open landscape offices with varying occupant number. The open landscape offices with only two occupants clearly show a lower average for hours per day compared to the other offices.

The interested reader can see appendix M.0.7 on page 302 for graphs of the sum of hours and sum of days over a year for the offices dependent on number of people.

The average of hours per day and average of days per weeks show a vague dependency of the number of people. The open landscape offices can be divided in sizes of:

- 2 people
- 4 - 6 people
- 8 people

This division of the open landscape offices dependent on the number of people is not completely trustworthy as only 17 open landscape offices are included in the study. Nonetheless, the division can give an idea of how the time in the offices may vary due to the number of people.

The average of days per week and weeks per year for the offices within the people interval are applied in graphs 11.5 and 11.6.

The median is applied for hours per day, as the data is skewed as explained in section 8.2 on page 85, in graph 11.4.

The established dependency for hours per day, days per week and weeks per year are shown in graphs 11.4, 11.5 and 11.6.

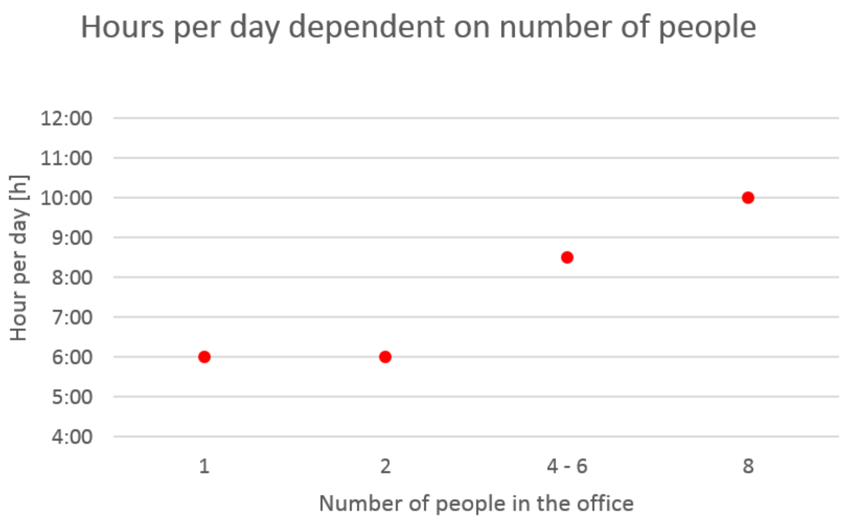

Figure 11.4. Established hours per day dependent on number of people

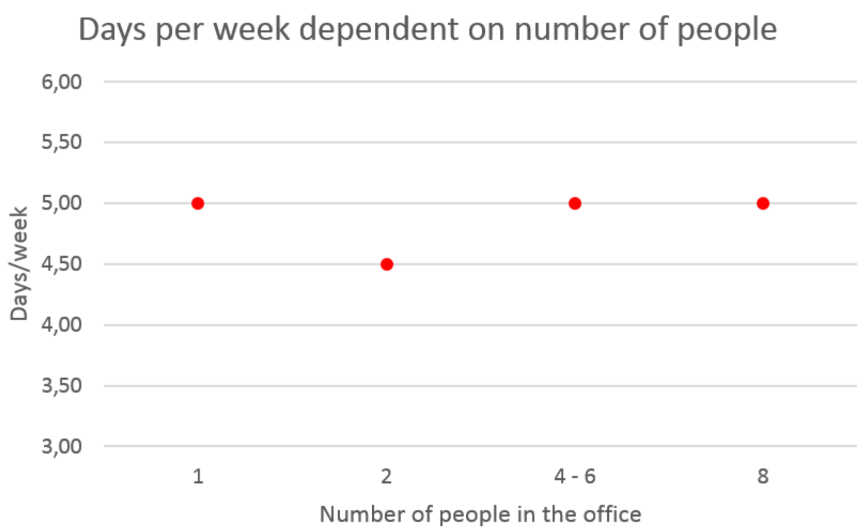

Figure 11.5. Established days per week dependent on number of people

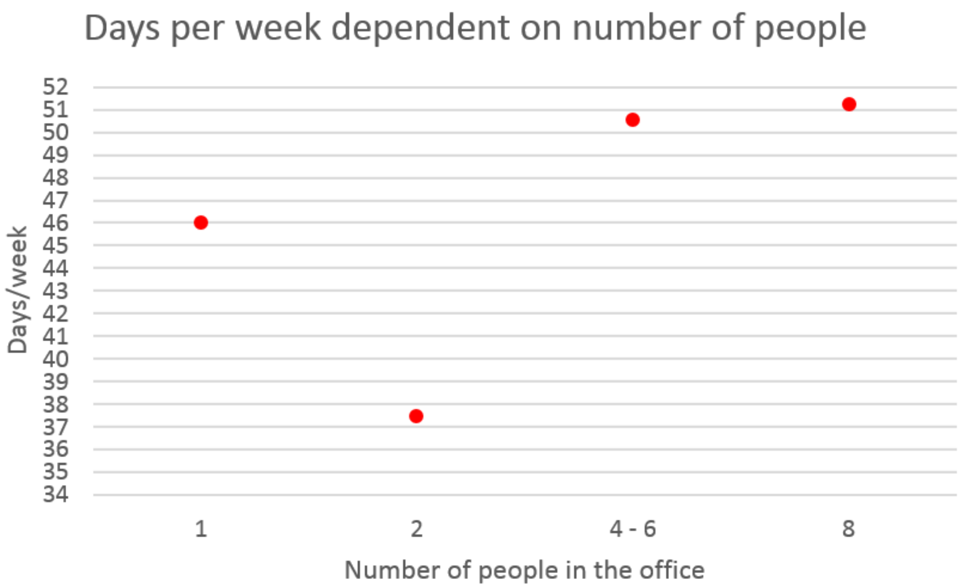

Figure 11.6. Established weeks per year dependent on number of people

This stated dependency may hold inaccuracies as it only include eight different open landscape offices investigated for two separate years, 2013 and 2014, treated as 17 different open landscape offices. The sample only include open landscape offices of two, four, five, six and eight. It is only one four person open landscape office which is only investigate for one year, this is inaccurate as only one four people open landscape office might not be representable for all four people open landscape offices. It is not known who the occupants are during these two years and what their position in the company. The position of a person might influence how much time they send at their working station.

Established Occupancy Profiles 12

One occupancy profile for cell offices and one for open landscape offices (from four to eight people) are obtained from the previous sections 8, 9 and 10. The obtained occupancy profiles are shown in table 12.1.

Occupancy	Cell office	Open landscape office
Hours per day	6:00	9:00
Days per week	5 days	5 and $\frac{1}{2}$
Weeks per year	44 weeks	50 and $\frac{1}{2}$

Table 12.1. Established occupancy profile.

The absent weeks for the cell offices are:

- Week 1
- Week 15
- Week 27
- Week 29
- Week 30
- Week 31
- Week 32
- Week 52

Absent weeks for the open landscape offices are:

- Week 1
- 3 days in week 52

The occupancy profiles from *NS 3031* and SBi as well as the newly obtained occupancy profile can be seen in table 12.2.

Regulation	Note	Hours	Days per week	Weeks per year	Hours of use every year
NS 3031	"Kontorbygning, driftstid for oppvarming og belysning", table A.43 page 40	12	5	52	3120
SBi 184	"Enkeltpersoner", table 14 page 93	8	5	45	1800
Obtained occupancy profile	Cell office	6	5	44	1320

Table 12.2. Occupancy profiles from *SBi 184 Bygningers Energibehov* and *NS 3031 Beregning av bygningers energiytelse Metode og data* and the obtained occupancy profile for cell offices.

The occupancy profile is inserted in BSim and the electricity usage for the cell office in the case building is calculated. The result from BSim with the three different occupancy profiles are shown in graph 12.1.

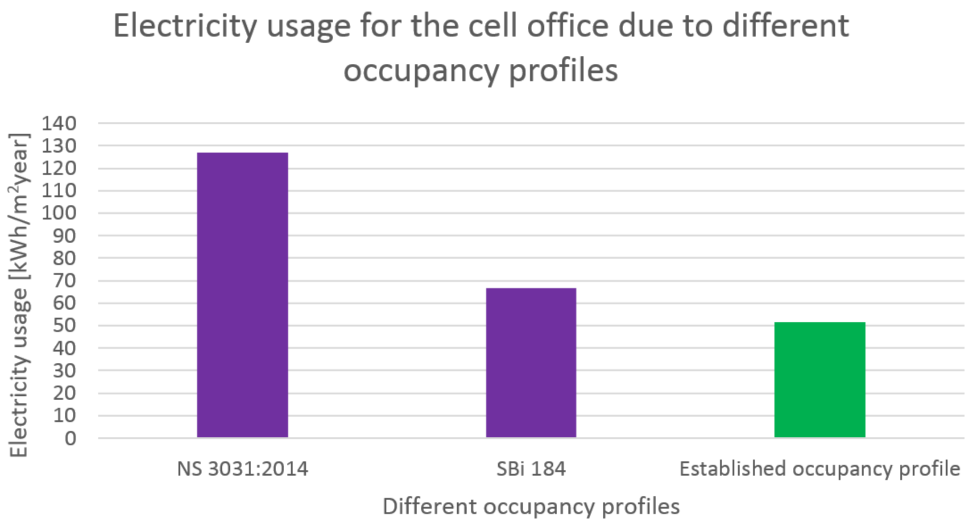

Figure 12.1. Yearly electricity usage for the cell office obtained for the established occupancy profile for cell offices compared to occupancy profiles from NS3031:2014 and SBi 184

The calculated electricity usage when applying the established occupancy profile for the cell offices is 51.51 $kWh/m^2 * year$, which is 22.9 % lower than the electricity usage obtained with the occupancy profile from *SBi 184 Bygningers Energibehov*.

12.1 Limitations and Recommendations

As mentioned in section 7.5 there are a some errors in the central operating system, these are extracted and replaced by the average from that office. Nevertheless, the actual occupancy profile for these periods are lost and might cause a slight inaccuracy in the result. These errors occurred as mentioned in section 7.5 for three weeks for all the offices and six days, then additional up to six days for three of the cell offices and up to one week and three days for seven of the open landscape offices. These errors do not sum up to a significant amount of time as the rest of the two years were without errors for all the offices. Nevertheless, some errors might still be present in the data which have not been noticed.

For the cell offices the five days are not restricted to only during the work week, only five days during a week, which means that some days might be during the weekend. In the distribution of hours in section 8.3.1 on page 87 the days for the two selected cell offices are from Monday to Friday, however if several cell offices were investigated it could be established with higher certainty that the five days are indeed during the work week. When these five days occur during the week will not influence the total electricity usage, but establishing when they occur can give a better understanding of the distribution of days in the occupancy profile for cell offices.

For further inspection separate occupancy profiles for the weekends and holidays can be established. Especially for the open landscape offices where there are 50 $\frac{1}{2}$ weeks of occupancy throughout the year, and some of these weeks occasionally consisted of up to seven days. It can be of interest to establish an occupancy profile for holidays such as Easter, as well as an occupancy profile of the weekends where people are present.

The obtained occupancy profile is obtained for open landscape offices of size of four to eight people. As seen in chapter 11 there is a slight difference between the time spent in the offices from a OLO4 to a OLO8. For further investigation different occupancy profiles for the different sizes of open landscape offices can be established.

The occupancy profile for cell offices will be applied in the new estimation methodologies in part IV, and will thereby be validated for a short period throughout the year. Nevertheless, it is recommended to validate the occupancy profiles by measuring the electricity usage for the offices over a year. The occupancy profiles can be further investigated by studying the time of occupancy for another office building for comparison.

Seasonal variations of the time of occupancy might occur throughout the year. For further investigation of the occupancy profiles it is recommended to consider seasonal variations. The year can be divided down to the four seasons, and one occupancy profile for every season can be established.

Part IV

Obtained Estimation Methodologies

Two estimation methodologies for calculating the electricity usage of daylight and occupancy controlled artificial lighting are presented in this part. The two methods are called the CIE Sky Method and the Hourly Average Method.

Initially the electricity usage of the artificial lighting in the cell office is calculated with the estimation methodology in NS 3031:2014, thereafter the electricity usage is calculated with the established methods. The results obtained with the three estimation methodologies are compared to the measured electricity usage for the measurement period for validation. Lastly, one estimation methodology is concluded upon due to how accurate and rapid it is.

Norwegian Standard 13

13.1 Requirement of Available Daylight in Norway

It is recommended that the average daylight factor should be 5 % if a working station shall only be lit by daylight (Norsk Lysteknisk Komité, 2014). If artificial lighting will be applied in combination with daylight then the required daylight factor is 2 % (Norsk Lysteknisk Komité, 2014). In rooms with normal occupancy it is required that the daylight factor is at least 2 % or that the daylight surface, the glazed area of the window, is at least 10 % of the usable floor area (Direktoratet for byggkvalitet (DiBK), 2011).

13.2 Norwegian Standard NS 3031:2014

The Norwegian Standard NS 3031:2014 provides a simple estimation methodology for the electricity usage for artificial lighting.

Tillegg A (normativt)
Standardiserte inndata for kontrollberegning

Tabell A.1 – Netto effekt- og energibehov – standardverdier for gjennomsnittlig effektbehov i driftstiden og årlig energibehov for belysning, utstyr og varmtvann

Bygningskategori	Belysning [a]		Utstyr [b]		Varmtvann [b, c]	
	W/m²	kWh/(m²·år)	W/m²	kWh/(m²·år)	W/m²	kWh/(m²·år)
Småhus [d]	1,95	11,4	3,00	17,5	5,1	29,8
Boligblokk	1,95	11,4	3,00	17,5	5,1	29,8
Barnehage	8	21	2	5	3,8	10
Kontorbygning	8	25	11	34	1,6	5
Skolebygning	10	22	6	13	4,5	10
Universitets- og høgskolebygning	8	25	11	34	1,6	5
Sykehus	8	47	8	47	5,1	30
Sykehjem	8	47	4	23	5,1	30
Hotellbygning	8	47	1	6	5,1	30
Idrettsbygning	8	21	1	3	18,9	50
Forretningsbygning	15	56	1	4	2,7	10
Kulturbygning	8	23	1	3	3,5	10
Lett industribygning, verksted	8	19	10	23	4,3	10

[a] Verdiene for belysning skal som hovedregel benyttes ved kontrollberegning mot offentlige krav. Dersom det benyttes styringssystem for utnyttelse av dagslys eller styringssystem basert på tilstedeværelse, kan energibehovet til belysning reduseres med 20 %. Eventuelt kan andre verdier for belysning dokumenteres gjennom beregninger etter NS-EN 15193 eller tilsvarende. Varmetilskuddet fra belysning i tabell A.2 skal da reduseres tilsvarende.

[b] Verdiene for utstyr og varmtvann brukes for kontrollberegning mot offentlige krav.

[c] Dersom det benyttes avtrekksvarmepumpe, kan netto energibehov til varmt tappevann reduseres etter reglene i tillegg N.

[d] Småhus omfatter enebolig, to- til firemannsbolig og rekkehus.

MERKNAD 1 Verdiene i tabellen er utarbeidet for kontrollberegning mot offentlige krav og representerer ikke nødvendigvis reelle forhold.

MERKNAD 2 Årlig energibehov for belysning og utstyr er gitt som gjennomsnittlig effektbehov i driftstiden multiplisert med driftstiden, gitt i tabell A.3.

Figure 13.1. Table showing standard values for electricity demand for different building types (Standard Norge, 2007).

As seen in the table in figure 13.1, the standard values for the energy demand for artificial lighting in an office building is

- $8\,\mathrm{W/m^2}$
- $25\,\mathrm{kWh/m^2} \cdot \mathrm{year}$

If the building uses either daylight or occupancy control system, the energy demand can be reduced by 20% (Standard Norge, 2007). The flow of the input required by the user and the obtained output with the *NS 3031:2014* calculation method is shown in figure 13.2.

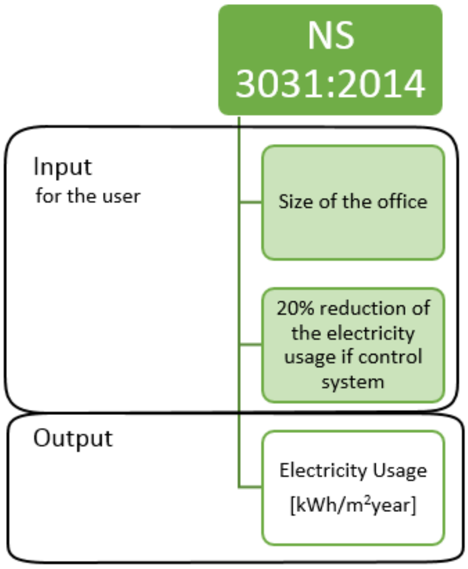

Figure 13.2. Illustration of the flow of inputs and output in the method from *NS 3031:2014*.

13.3 Applying *NS 3031:2014* on the Case Building

The cell office in the case building is 8.26 m^2 which gives a yearly electricity usage, with the 20 % reduction due to daylight control or occupancy, of 20.0 $\text{kWh/m}^2 \cdot \text{year}$. This electricity usage is calculated according to *NS 3031:2014*, and the occupancy profile from *NS 3031:2014* is seen in table 13.1 is applied.

Regulation	Hours	Days of week	Weeks per year	Hours of use every year
NS 3031	12	5	52	3120

Table 13.1. Occupancy profiles from *NS 3031 Beregning av bygningers energiytelse Metode og data.*

13.4 Validation of the Method in *NS3031:2014*

The electricity usage for the artificial lighting in the cell office during the measurement period is shown in figure 13.3. As mentioned in section 6.1 the occupant was only present for six of the days in the fourteen day measurement period. Therefore a period of six days are considered.

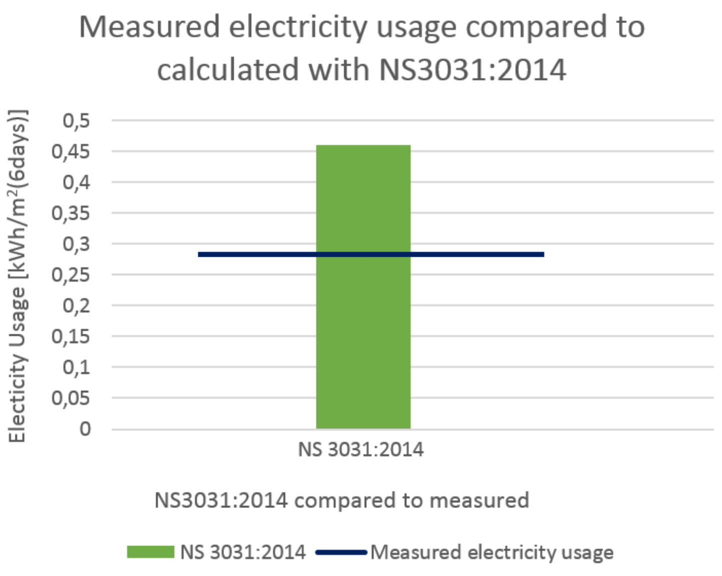

Figure 13.3. The calculated electricity usage for the measurement period with the method from *NS3031:2014* compared to the measured electricity usage.

The electricity usage for the artificial lighting system in the cell office is $0.46\,\mathrm{kWh/m^2} \cdot 6\mathrm{days}$. Comparing this to the measured electricity usage for the measurement period of $0.28\,\mathrm{kWh/m^2} \cdot 6\mathrm{days}$, from section 6.1 on page 69, it can be stated that the estimation methodology from *NS 3031:2014* calculates an electricity usage which is 39 % higher than the actual electricity usage. The hours of occupancy in *NS 3031:2014* is 12 hours per day, this is twice as many as the six hours per day in the developed occupancy profile for cell offices. This deviation in the occupancy is probably the most certain reason why the electricity usage calculated with the method from *NS 3031:2014* over estimates the electricity usage. Another reason is that the method in *NS 3031:2014* does not take available daylight into account. The external sky conditions, the geometry of the cell office nor parameters of the materials in the cell office is accounted for in the method in *NS 3031:2014*.

14 Introducing the Two New Estimation Methodologies for the Electricity Usage of Artificial Lighting

The established estimation methodologies will be introduced in this section. The two methods are called the *CIE Sky Method* and the *Hourly Average Method*. The two established estimation methodologies both require inputs which the estimation methodology from *NS3031:2014* do not. The parameters which are needed in the estimation methodologies are presented in this section. The estimation methodology from *NS3031:2014* and the two established estimation methods all calculate the electricity usage of daylight and occupancy controlled artificial lighting. Nevertheless, how the electricity usage is obtained is different for all methods.

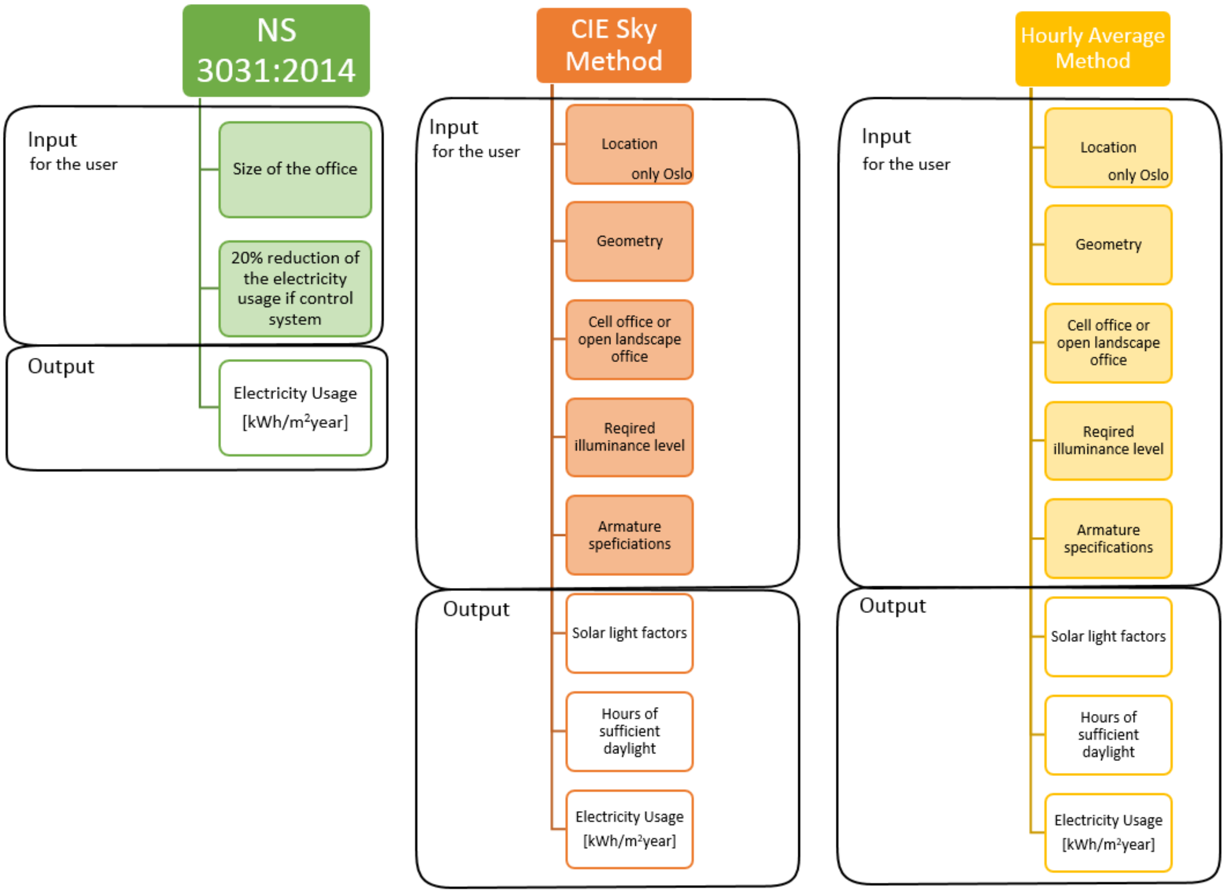

Figure 14.1. Illustration of the flow of inputs and output in the three estimation methodologies

The two established estimation methodologies require more inputs for the user compared to the estimation methodology from *NS3031:2014*. More outputs are also obtained in the two established estimation methodologies compared to *NS3031:2014*. The *CIE Sky Method* and the *Hourly Average Method* require the same inputs and obtain the same outputs. However, how the outputs are obtained and what the output is, is the deviation between the two methods. Figure 14.1 is an illustration of the inputs and outputs for the three estimation methodologies.

One Excel spread sheet is made for the *CIE Sky Method* and one for the *Hourly Average Method* in order to calculate the electricity usage for daylight and occupancy controlled artificial lighting. The yearly electricity usage is obtained by applying an hourly average for the 8760 hours throughout a year for both methods. In the next chapters 15 and 16 the *CIE Sky Method* and the *Hourly Average Method* respectively, are applied to calculate the electricity usage of the artificial lighting in the cell office in the case building. Last, in chapter 17 the result from the three calculation methods are compared to the measured electricity usage and the methods are then ranked according to accuracy and computational time.

14.1 Electricity Usage, Solar Irradiance and Occupancy Profile During the Measurement Period

The occupant was in his office seven days during the two weeks of measurements. However, due to the snowstorm on March the 26^{th} the irradiance measurements cannot be applied for this day, as explained in appendix D. Therefore there are only six days where the occupant is present and the solar irradiance is measured simultaneously. These six days are applied for comparison between the measured electricity usage and the calculated electricity usage with the three different methods.

The average hours per day the occupant spent in the office was six hours, which correspond well with the occupancy profile for a cell office obtained in III on page 75. Nevertheless, which hours during the day the occupant was present varied and did not correspond exactly with the obtained cell office occupancy profile. The exact hours the occupant is present during the six days are stated and inserted into the Excel spread sheets for the two methods.

The measured electricity usage for the armature in the cell office during the six days the occupant was present is $0.28\,\mathrm{kWh/m^2} \cdot 6\mathrm{days}$. Together with the exact occupancy profile obtained for the user in the cell office, the measured solar irradiance and the total electricity usage for these six days of $0.28\,\mathrm{kWh/m^2} \cdot 6\mathrm{days}$ is applied in order to validate the two established estimation methodologies in chapters 15 and 16.

14.2 Necessary Parameters for the *CIE Sky Method* and the *Hourly Average Method*

In the following sections, the illuminance and irradiance at different planes will be applied frequently. In order to clearly specify if it is exterior or interior, horizontal or vertical as well as if it is diffuse, direct or reflected, abbreviations have been made. These are presented in the following table 14.1.

Diffuse, direct and reflected illuminance and irradiance	Abbreviation
Total vertical exterior illuminance on the façade	TotVEI
Diffuse vertical exterior illuminance on the façade	DiffVEI
Direct vertical exterior illuminance on the façade	DirVEI
Reflected vertical exterior illuminance on the façade	RefVEI
Total horizontal interior illuminance on the working plane	TotHII
Diffuse horizontal interior illuminance on the working plane	DiffHII
Direct horizontal interior illuminance on the working plane	DirHII
Reflected horizontal interior illuminance on the working plane	RefHII
Total interior illuminance on the referent point	TotIIRP
Total vertical exterior irradiance on the façade	TotVEIrr
Diffuse vertical exterior irradiance on the façade	DiffVEIrr
Direct vertical exterior irradiance on the façade	DirVEIrr
Reflected vertical exterior irradiance on the façade	RefVEIrr

Table 14.1. The abbreviation for the different types illuminance and irradiance

The simulation model in BSim is the same as the model applied for calculation of the electricity usage for artificial lighting due to occupancy profiles in part III. The parameters in the BSim model is listed in table 14.2.

Component	Value
Transmittance of glazing	70%
Reflectance of the three white walls	0.4 (Statens Byggeforskningsinstitut, 2008)
Reflectance of the wooden wall	0.30 (RELUX Informatik AG, 2007)
Reflectance of the ceiling	0.9 (Statens Byggeforskningsinstitut, 2008)
Reflectance of the floor	0.1 (Statens Byggeforskningsinstitut, 2008)
Orientation	128°
Size of glazed area	0.8 m^2 (1.6 m^2 for both)
Area of the cell office	8.26 m^2
Height of room	2.85 m
Depth of room	3.931 m
Width of room	2.102 m

Table 14.2. Inputs in Bsim.

The necessary parameters for the *CIE Sky Method* and the *Hourly Average Method* will now be presented.

14.3 The Orientation of the Façade

DiffVEI, DIrVEi and refVEI varies with the orientation. Eight different orientations are therefore included in the Excel spread sheets. The orientations are seen in table 14.3.

Orientation	Degrees [°]	Interval in degrees [°]
North	0	$337.5 < ° \leq 22.5$
North-East	90	$22.5 < ° \leq 67.5$
East	45	$67.5 < ° \leq 112.5$
South-East	135	$112.5 < ° \leq 157.5$
South	180	$157.5 < ° \leq 202.5$
South-West	225	$202.5 < ° \leq 247.5$
West	270	$247.5 < ° \leq 292.5$
North-West	315	$292.5 < ° \leq 337.5$

Table 14.3. Orientations in the hourly average method.

DiffVEI, DIrVEi and refVEI are obtained for every orientation in the Excel spreads sheet by specifying the orientation of the façade. DiffVEI, DIrVEi and refVEI will be given for the interval the orientation, specified by the user, is within. The case building has an orientation of 128 °. Since this is in the South-East interval, the values for the illuminance components for an orientation of 135 ° will be applied in the calculation.

14.4 Geometry and Materials of the Office

The area of the office must be specified, as well as the geometry such as the height, width and depth. The total area of the glazing and the light transmittance must be stated. The user must also insert parameters specifying the reflectance of the materials in the office.

14.5 Occupancy Profiles

The occupancy profiles obtained in part III on page 75 for cell office or open landscape office is inserted in the excel spread sheet. The user must state if it is a cell office or an open landscape office in the pull down menu and the spread sheet will automatically give the correct occupancy profile for the office.

14.6 Set Point for the Armature and Required Illuminance Level on the Horizontal Working Plane

The user must know at what illuminance level on the working plane the armature switches on, the set point for the armature to switch on artificial light when there is not sufficient available daylight. The user must also know if the armature switches completely off when there is sufficient daylight in the room or if there is a minimum level for the power.

The required illuminance on the reference plane in the case building is 500 lux as it is an office building where Norwegian requirements apply (SINTEF Byggforsk, 1997). The maximum power of the armature in the cell office when there is not sufficient daylight available is 74.4 W. When there is sufficient daylight in the cell office the armature will not turn completely off as long as the occupant is present, the armature will go to a minimum power of 20.1 W. Therefore the the "off" state of the armature is said to be 20.1 W which is 27 % of the maximum power at 74.4 W.

Even thought the available daylight provide 500 lux on the working plane, and the required illuminance level on the working plane is 500 lux, the armature in the cell office does not switch to "off" due to a delay explained in section 6.1 on page 69. It is not until there is 700 lux on the working plane, due to available daylight, that the armature switches to 20.1 W. This means that the set point for the armature in the cell office to go to its minimum value is 700 lux.

14.7 Solar Light Factor

The daylight factor is used to determine the minimum value of interior illumination by daylight during overcast days, and this is not suited for energy calculations nor for control of artificial lighting (Statens Byggeforskningsinstitut, 2010). The daylight factor is by its definition independent on the orientation of the window. It is therefore needed to express the interior illuminance in comparison to the actual incident light on the window (Statens Byggeforskningsinstitut, 2010), this ratio is the solar light factor.

For dynamic calculations more detailed calculations of the variation of the daylight is needed, as well as the actual variation due to the seasons and the orientation. Sunlight, either direct through the window or reflected from the ground or other surfaces, is significant for the contribution to the actual daylight level in the room and must therefore be included in the calculations (Statens

Byggeforskningsinstitut, 2003). The solar light factor and its connection with the daylight factor can be seen in equation 14.1.

$$SF = \frac{E_{Ref.point}}{E_{Glazing}} \cdot DF \tag{14.1}$$

Where:

SF	Solar light factor
$E_{Ref.point}$	The illuminance on the internal reference point - TotIIRP [lux]
$E_{Glazing}$	The exterior vertical illuminance on the glazing - TotVEI [lux]
DF	Daylight factor

The definition of solar light factor at a point on a given plane is the ratio between the illuminance at that point to the illuminance outdoors on the surface of the façade without shadows (Statens Byggeforskningsinstitut, 2010). For the solar light factor there are three "light sources", those are; light from the sun, light from the sky and the reflected light from external surfaces (Statens Byggeforskningsinstitut, 2003). Light hitting a point in the room is divided into light which is directly from the "light source", and light which is reflected from internal surfaces inside the room from the "light source" before hitting the point (Statens Byggeforskningsinstitut, 2003).

The solar light factor is divided down to four different contributions. The three first account for the three contributions to illuminance, one for the direct light, another accounts for the diffuse light from the sky, while the third accounts for the reflected light. The last component accounts for the solar light factor if solar shading is present.

- SF1 - The solar light factor for direct sunlight
- SF2 - The solar light factor for light from the sky
- SF3 - The solar light factor for reflected light
- SF4 - The solar light factor for the window, when this is equipped with sunshades

These four contributions consist of two components, the direct component and the inter-reflected component. The direct component consist of the light which comes directly to the point from the source of illumination (the sky or shading) (Statens Byggeforskningsinstitut, 2010). While the inter-reflected component consist of the light which is first reflected at least one time from other surfaces.

Only the the average value of the inter-reflected contribution of direct sunlight is applied in SF1. The amount of incident light for SF2 is calculated according to CIE-overcast sky or uniform cloudy sky. The contribution from reflected radiation from the ground including both diffuse sky radiation and direct sunlight, are accounted for in SF3 (Statens Byggeforskningsinstitut, 2010). SF4 is used to account for the light being diffused after passing through the sun-shading.

The point inside the room where direct solar light hits directly is very dependent on the height and azimuth angle of the sun. This causes the SF1 to not be a constant value from hour to hour. BSim, however, only calculated one value for SF1 which is considered representative for the entire year (Statens Byggeforskningsinstitut, 2010). This is only dependent on the distance from the window (Statens Byggeforskningsinstitut, 2003). The solar light factors becomes slightly higher with less deep rooms, especially in the back of the room, this is due to the inter-reflected light becomes more concentrated in the back of the room, or it is spread over a smaller total area of surfaces (Statens Byggeforskningsinstitut, 2010).

SF1 is normally not critical for cases with unshaded windows, as the remaining illuminance in the room usually is high enough to ensure enough daylight in the room so no additional artificial light is needed. In real life situations, direct sunlight in the room will lead to the solar shading to be activated (Statens Byggeforskningsinstitut, 2010).

14.7.1 Solar Light Factor Direct Light - SF1

The periods where the sun directly hits the internal reference point is not of interest as it does not represent the general lighting conditions in the room. Therefore, the direct sunlight component for SF1 is excluded when calculating the solar light factor (Statens Byggeforskningsinstitut, 2003) and only the indirect sunlight is included as seen in figure 14.2.

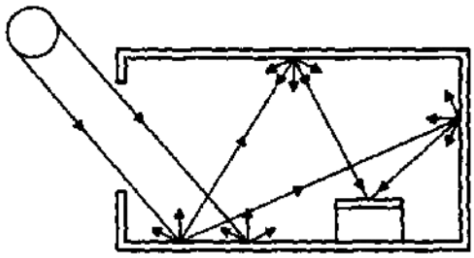

Figure 14.2. The indirect component for SF1 (Statens Byggeforskningsinstitut, 2010)

SF1 can be calculated according to equation 14.2 (Statens Byggeforskningsinstitut, 2008), only the inter reflected component is included.

$$SF1 = \frac{GP \cdot LT \cdot R_f}{A(1-R)} f(x) \tag{14.2}$$

Where:

$SF1$	Solar light factor for the direct light
GL	The percentage of the glazed area on the façade. [%]
R	The average reflectance of the surfaces of the room, weighted according to areas
R_f	The reflectance of the surface the direct sunshine strikes (the floor)
A	The area of the surfaces of the room $[m^2]$
R	The average reflectance of the surfaces of the room, weighted according to areas

The equation for the function *f(x)*, determining the distance for the reference point to the window, is different for a room with a depth larger or smaller than 7.5m (Statens Byggeforskningsinstitut, 2008).

The equation for a room with a smaller depth than 7.5 m, such as the cell office in the case building:

$$f(x) = 0.11x^3 - 1.46x^2 + 3.1x + 14.0 \tag{14.3}$$

The equation for a room with a depth larger than 7.5 m

$$f(x) = 17.2x^{-1.2} \tag{14.4}$$

14.7.2 Solar Light Factor for Diffuse Sky Light - SF2

How the diffuse light from the sky reaches the point on the internal reference plane is seen in figure 14.3.

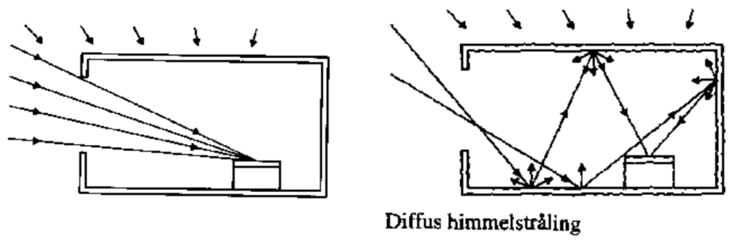

Figure 14.3. The direct component to the left and the indirect component to the right for SF2 (Statens Byggeforskningsinstitut, 2010)

SF can be calculated according to equation 14.5 Statens Byggeforskningsinstitut (2008), only the inter reflected component is included.

$$SF2 = \frac{DF2}{0.396\,(1 - \cos\gamma) + \cos\gamma} \tag{14.5}$$

Where:

$SF2$	Solar light factor for diffuse sky light
$DF2$	The daylight factor for CIE overcast sky
γ	The angle of the slope of the surface compared to the horizontal surface

DF2 is the daylight factor where only the contribution from the diffuse sky illuminance is included, and not the exterior reflected component. DF2 can be calculated with SimLight (Statens Byggeforskningsinstitut, 2008).

14.7.3 Solar Light Factor for Reflected Light - SF3

The reflected radiation from the surface of the ground cannot strike the point on the horizontal reference point directly and does not contribute to SF3 (Statens Byggeforskningsinstitut, 2010), therefore only the indirect component is included in SF3 as seen in figure 14.4. The direct and diffuse light from the sky contributes to SF3 (Statens Byggeforskningsinstitut, 2008). The reflectance from the ground is assumed to be completely diffuse. SF3 is therefore included in the inter reflected SF2 in the interior reference point as SF3 becomes diffuse after hitting the exterior ground, and does not strike the interior reference point before it is inter reflected.

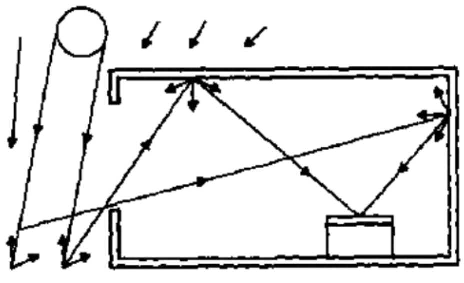

Figure 14.4. The indirect component for SF3 (Statens Byggeforskningsinstitut, 2010)

SF3 can be calculated according to equation 14.6 (Statens Byggeforskningsinstitut, 2010), only the inter reflected component is included.

$$SF3 = \frac{1.5 \cdot G \cdot R_{avg}}{A\,(1 - R)} \tag{14.6}$$

Where:

$SF3$	Solar light factor for reflected light
G	The area of the glazing $[m^2]$
R_{avg}	The average reflectance of the surfaces of the room above the reference point
A	The area of the surfaces of the room $[m^2]$
R	The average reflectance of the surfaces of the room, weighted according to areas

SF3 will not contribute to the illuminance level on the horizontal reference point when the reference point in the cell office in the case building is 850 mm above the floor and the height of the window above the floor is 1020 mm. The reference point was placed right below the ceiling in order to study the influence from SF3 on the interior illuminance level. When SF3 was placed close to the ceiling it became 0.03 instead of 0. The reference point is normally on the height of the working plane, 850 mm above the floor, and SF3 is therefore not contributing to the interior illuminance level if the height of the window in the room is above the working plane.

14.7.4 Solar Light Factor for Solar Shading - SF4

Lastly the contribution when solar shading is applied is seen in figure 14.5. For the case building the solar shading is not active and SF4 is neglected.

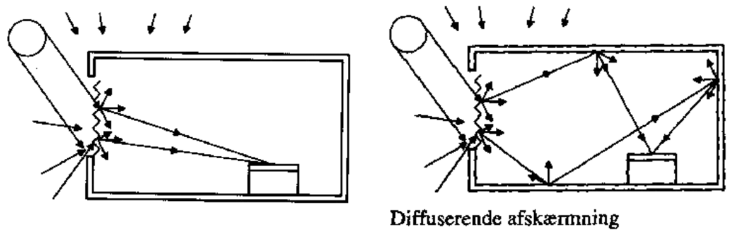

Figure 14.5. The direct component to the left and the indirect component to the right for SF4 (Statens Byggeforskningsinstitut, 2010)

When determining the available interior illuminance level due to daylight the direct, sky diffuse and ground reflected solar light factors will be calculated. The solar light factor accounting for solar shading is included in the cases where solar shading is present.

14.7.5 Total Solar Light Factor

The interior illuminance distribution between the three different solar light factors, direct (SF1), sky diffuse (SF2) and ground reflected (SF3), is dependent on the vertical exterior illuminance intensity on the glazing. This exterior illuminance intensity varies significantly with the sky condition. Figure 14.6 illustrates typical illuminance intensities on a vertical plane in June for a clear and overcast day.

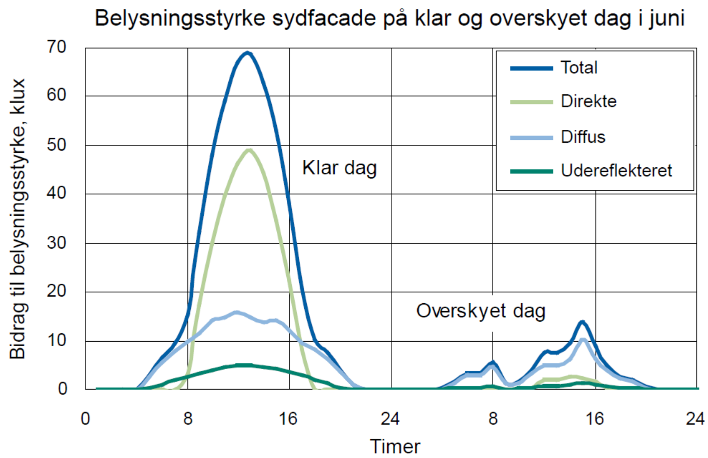

Figure 14.6. Typical values of illumination intensity on the South façade for a clear and overcast day in June (Statens Byggeforskningsinstitut, 2008)

As clearly seen in figure 14.6 the illuminance intensity is very different from the clear to the overcast day, and this must be taken into account when calculating the total solar light factor. This means the total solar light factor actually varies with the intensity of the exterior illuminance on the vertical plane. The equation for the total solar light factor is shown in equation 14.6.

$$SF = \frac{E_{Ref.point}}{E_{Glazing}} = \frac{SF1 \cdot E_{Dir} + SF2 \cdot E_{Diff} + SF3 \cdot E_{Refl}}{E_{Dir} + E_{Diff} + E_{Refl}} \tag{14.7}$$

Where:

SF	Solar light factor
$E_{Ref.point}$	The illuminance on the internal reference point [lux]
$E_{Glazing}$	The exterior vertical illuminance on the glazing - TotVEI [lux]
E_{Dir}	The exterior vertical illuminance on the glazing due to direct sunlight - DiffVEI [lux]
E_{Diff}	The exterior vertical illuminance on the glazing due to diffuse light from the sky - DIrVEI [lux]
E_{Refl}	The exterior vertical illuminance on the glazing due to exterior reflectance [lux] - RefVEI
$SF1$	Solar light factor for direct light
$SF2$	Solar light factor for diffuse sky light
$SF3$	Solar light factor for reflected light

14.7.6 Obtaining the Solar Light Factors

The *CIE Sky Method* and the *Hourly Average Method* require the user to calculate the solar light factors for the specific room. The solar light factors must be calculated as explained in section 14.7 on page 131. The user must establish the solar light factor for direct sunlight (SF1), diffuse sky light (SF2) and the reflected light (SF3). These three solar light factors adds up to the total solar light factor dependent on the specific office at hand. The solar light factor due to solar shading is not included in this method.

The user can either determine the solar light factors with a simulation software or calculate it manually in the Excel spread sheet made for the two methods. If the user chose to calculate the solar light factors by applying the Excel spreadsheet, the daylight factor must be calculated.

Solar Light Factors Obtained with SimLight

SimLight is a BSim module which can calculate solar light factors in the reference point in the room. However, SimLight does not give values for the inter reflected component, and SF3 is therefore zero. This is correct for the direct component of reflected illuminance from the ground to the reference point, but not for the inter reflected component. The total SF3 should include the inter reflected component for the cell office.

SimLight applies the equations for SF1 14.2, SF2 14.5 and SF3 14.6. For calculations of the solar light factors in SimLight the Bsim model with parameters from table 14.2 is applied, but the light transmittance is set to 1.0 for calculation of the solar light factors (Statens Byggeforskningsinstitut, 2010).

Solar light factors calculated for the cell office in the case building in SimLight with light transmittance of the glazing 1.0:

- SF1: 0.007
- SF2: 0.042
- SF3: 0

These solar light factors are inserted in the calculation of the electricity usage in the Excel spread sheet for the hourly average method during the measurement period. The results obtained with the Excel spread sheet for the hourly average method are explained in detail in chapter 16. The measured electricity usage for the armature in the cell office during the six days the occupant was present is $0.28\,\mathrm{kWh/m^2} \cdot 6\mathrm{days}$. When the solar light factors obtained with SimLight, with a transmittance of 1.0 for the glazing, is inserted in the hourly average Excel spread sheet, the calculated electricity usage is $0.24\,\mathrm{kWh/m^2} \cdot 6\mathrm{days}$. As the calculated result is 15 % lower than the measured it was decided to calculate the solar light factors with a light transmittance of 0.7, which is the light transmittance of the glazing in the case building, to see if the calculated electricity usage would then be closer to the actual electricity usage.

The solar light factors calculated for the cell office in the case building with SimLight with light transmittance of the glazing of 0.7:

- SF1: 0.007
- SF2: 0.029
- SF3: 0

The calculated electricity usage is $0.27\,\mathrm{kWh/m^2} \cdot 6\mathrm{days}$ which is significantly closer to the measured value with a deviation of only 5 %. However, SF3 is zero which is incorrect as the inter reflected component of reflected light should be included. Therefore it was decided to obtain the solar light factors manually.

Solar Light Factors Calculated Manually

The user can calculate the solar light factor for their office by filling in parameters for the office in the Excel spread sheet. A screen shot of the *Solar Light Factors*-tab in the Excel spread sheet for both the *CIE Sky Method* and *Hourly Average Method* can be seen in figure 14.7.

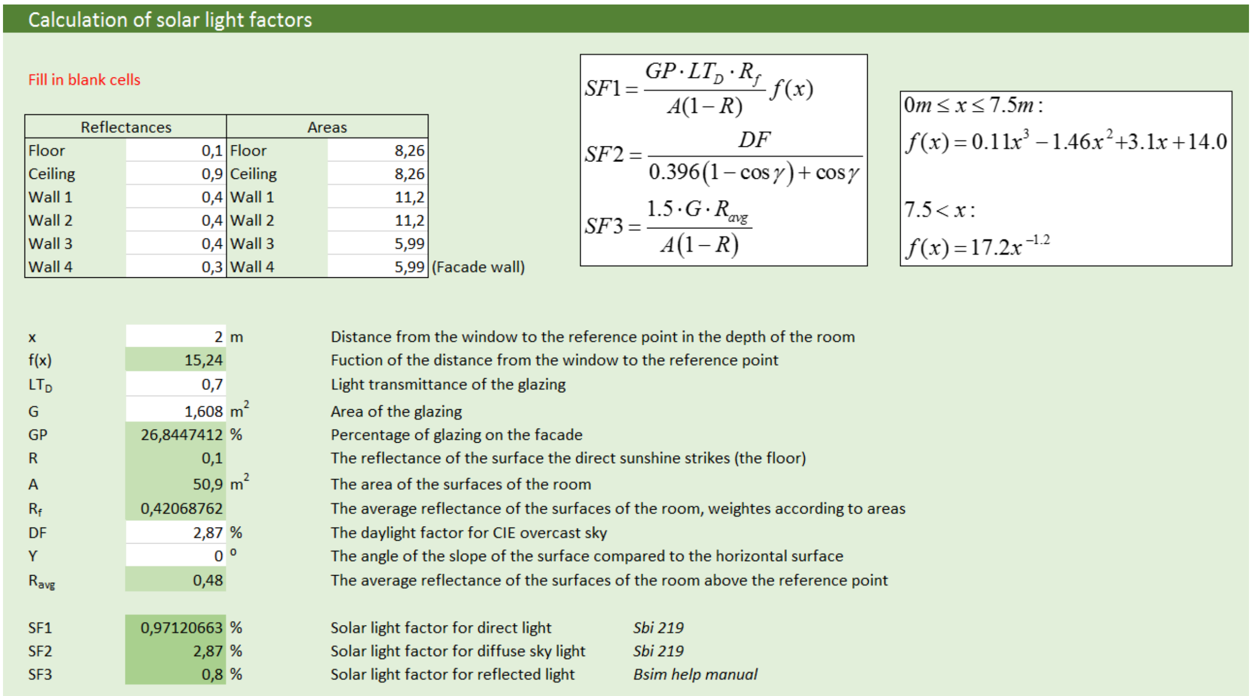

Calculation of solar light factors

Fill in blank cells

Reflectances		Areas	
Floor	0,1	Floor	8,26
Ceiling	0,9	Ceiling	8,26
Wall 1	0,4	Wall 1	11,2
Wall 2	0,4	Wall 2	11,2
Wall 3	0,4	Wall 3	5,99
Wall 4	0,3	Wall 4	5,99 (Facade wall)

$$SF1 = \frac{GP \cdot LT_D \cdot R_f}{A(1-R)} f(x)$$

$$SF2 = \frac{DF}{0.396(1-\cos\gamma)+\cos\gamma}$$

$$SF3 = \frac{1.5 \cdot G \cdot R_{avg}}{A(1-R)}$$

$0m \leq x \leq 7.5m$:

$$f(x) = 0.11x^3 - 1.46x^2 + 3.1x + 14.0$$

$7.5 < x$:

$$f(x) = 17.2x^{-1.2}$$

x	2	m	Distance from the window to the reference point in the depth of the room
f(x)	15,24		Fuction of the distance from the window to the reference point
LT_D	0,7		Light transmittance of the glazing
G	1,608	m^2	Area of the glazing
GP	26,8447412	%	Percentage of glazing on the facade
R	0,1		The reflectance of the surface the direct sunshine strikes (the floor)
A	50,9	m^2	The area of the surfaces of the room
R_f	0,42068762		The average reflectance of the surfaces of the room, weightes according to areas
DF	2,87	%	The daylight factor for CIE overcast sky
Y	0	º	The angle of the slope of the surface compared to the horizontal surface
R_{avg}	0,48		The average reflectance of the surfaces of the room above the reference point

SF1	0,97120663	%	Solar light factor for direct light	*Sbi 219*
SF2	2,87	%	Solar light factor for diffuse sky light	*Sbi 219*
SF3	0,8	%	Solar light factor for reflected light	*Bsim help manual*

Figure 14.7. Screen shot of the Excel spread sheet calculating the solar light factors in the hourly average method

For the cell office in the case building the reference point is 2 m from the window in the depth of the room on the working plane, 0.85 m above the floor, and in the middle of the width of the room. The reference point can then be calculated according to equation 14.3 or 14.4 (dependent on the depth of the room), and then be inserted in the *f(x)* function in SF1.

The solar light factors are calculated by applying the equations obtained from (Statens Byggeforskningsinstitut, 2008) for SF1 and SF2, and from (Statens Byggeforskningsinstitut, 2010) for SF3. The results calculated manually with the excel spread sheet for the cell office in the case building are:

- SF1: 0.0097
- SF2: 0.029
- SF3: 0.0080

The results for SF2 obtained with SimLight and manually calculated are the same, while the result for SF1 is remarkably close. As expected the results for SF3 are different, SF3 calculated manually gives a value of 0.008 compared to the value of 0 obtained with SimLight.

14.7.7 Interior Illuminance Obtained with Solar Light Factor Compared to Measured Illuminance

TotIIRP at 12:00 on March the 22^{nd} is calculated with solar light factor and the measured irradiance inserted into BSim. TotIIRP is placed in different locations from the window. Graph 14.8 shows the result for the calculated TotIIRP by solar light factors for the cell office compared to the measured TotIIRP. It should be remembered that the calculation of TotIIRP with solar light factor assumes that TotIIRP is placed in the middle of the width of the room. Measurement points 2B and 4B are not in the middle of the room, they are 20 cm from the wall as seen in figure 5.12 on page 51.

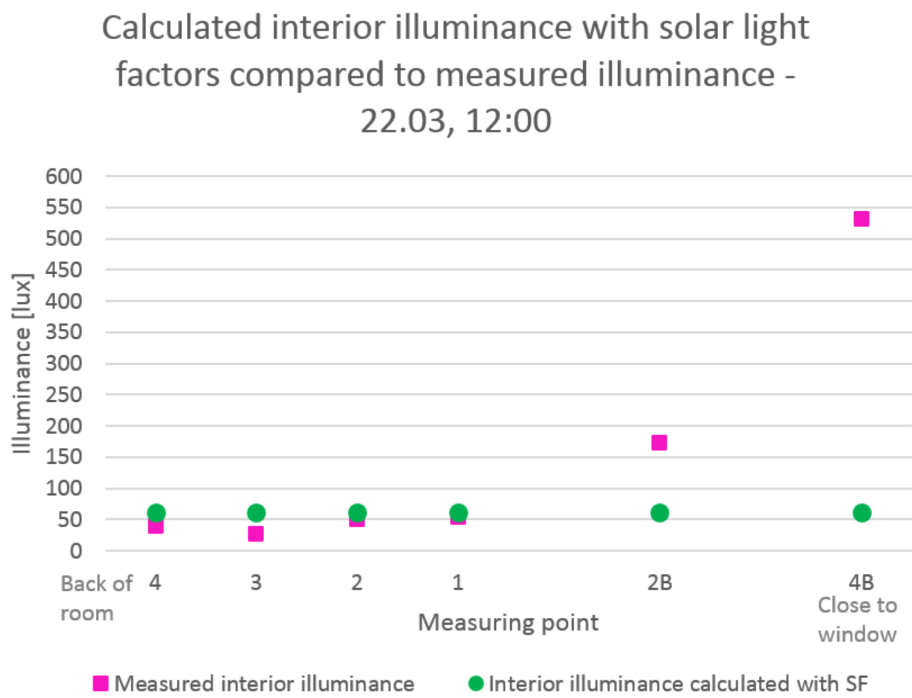

Figure 14.8. Calculated interior illuminance with solar light factors for the cell office in the case building compared to measured illuminance at 12:00 on March the 22^{nd}

As clearly seen in graph 14.8, the calculated TotIIRP is almost the same in the whole depth of the cell office. This is due to only SF taking into account the distance from the window. For measurement points 2B and 4B the calculated TotIIRP is significantly lower to the actual TotIIRP.

However, in the depth of the room TotIIRP obtained with the solar light factor show good agreement with the measured TotIIRP. SF1 does not take into account the direct component, even though the sky conditions during March the 22^{nd} is assumed to be overcast as stated in section 5.1.2, the significantly lower calculated TotIIRP might be due to the direct component of SF1 not being accounted for. Graph 14.9 show the calculated and measured TotIIRP for March the 14^{th} which is assumed to be a clear day as explained in section 5.1.1.

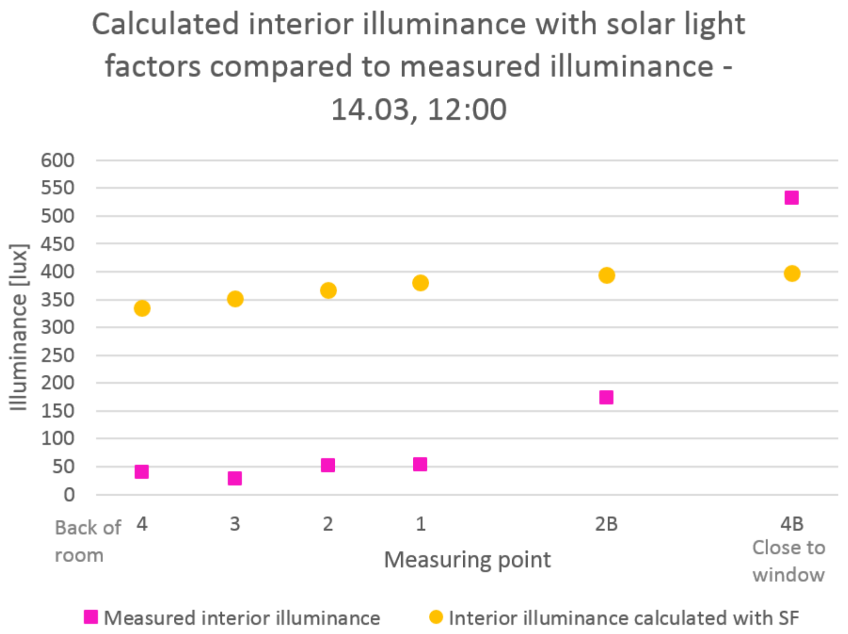

Figure 14.9. Calculated interior illuminance with solar light factors for the cell office in the case building compared to measured illuminance at 12:00 on March the 14^{th}

As graph 14.9 show, TotIIRP is rather constant in the depth of the room, but a slight decrease can be noticed. For measurement point 4B close to the window TotIIRP obtained with the solar light factor is lower than the measured TotIIRP, while for the rest of the measurement points the calculated TotIIRP is higher than the measured TotIIRP. Even though TotIIRP obtained by the solar light factor do not correspond well with the measured TotIIRP, the solar light factor is applied to obtain TotIIRP from TotVEI in the two established methodologies.

Further investigation of TotIIRP obtained from solar light factors due to the distance from the window is recommended for a clearer perception of how this affects the calculated total interior illuminance for different reference points throughout the room.

14.8 Establishing Direct, Diffuse and Reflected Exterior Illuminance

The hourly average of the 8760 hours of a year is included. The diffuse and direct solar irradiance from the *NS 3031* Norwegian reference year is inserted in BSim and TotVEI is obtained.

To find the interior illuminance, totVEI must be multiplied with the solar light factor for the room of interest. The total solar light factor is divided into components dealing with diffuse, direct and reflected illuminance. Therefore, TotVEI should also be divided into direct, diffuse and reflected component.

14.8.1 Obtaining Diffuse and Direct External Vertical Illuminance - DiffVEI & DirVEI

Both the diffuse and direct component changes with the orientation of the façade and is therefore obtained for every orientation as explained in section 14.3. The diffuse component must not be mistaken with overcast sky, the diffuse component is diffuse light which can still occur for clear days as seen from the solar irradiance measurements explained earlier in section 5.1.1 on page 43. The Norwegian reference year from *NS 3031* shows that there are more diffuse light during the warmer months compared to the cold months.

The *NS 3031:2014* weather data file for the Norwegian reference year inserted in BSim contains direct and diffuse solar irradiance. TotVEI can be calculated by BSim, but is not divided into the different components of illuminance. To solve this, two separate weather files are made. One where the direct solar irradiance is set to zero, and one where the diffuse solar irradiance is set to zero. Thereby DIffVEI and DirVEI were obtained.

When the simulation results from the two weather files were added together, it was discovered that the sum of DiffVEI and DirVEI was lower than TotVEI simulated with the initial weather file. This deviation was initially believed to be caused by the reflective component. It may be due to the reflective component being included in both the direct and the diffuse component.

14.8.2 Reflected External Vertical Illuminance - RefVEI

The reflective component is caused by the ground reflectance which is set to 0.1 as a default in BSim. The reflective component is included in both the direct and diffuse components and needs to be extracted to be multiplied with SF3. Two different methods were utilized to extract the reflective illuminance component from the diffuse and direct illuminance components.

Extracting RefVEI from the Percentage of the Irradiance Components

The first method to obtain RefVEI was to apply the percentage of refVEIrr from diffVEIrr and DirVEIrr and assume that this percentage would be the same for RefVEI of DiffVEI and DirVEI.

The default value of the ground reflectance of 0.1 was applied in BSim. Then the following steps were conducted:

1. Simulation in BSim with diffuse irradiance only in the weather file
2. Percentage of RefVEIrr from DiffVEIrr
3. Extract that percentage from DiffVEI

After the percentage of refVEirr from DiffVEIrr is obtained and the same percentage is extracted from DiffVEI, the same procedure is repeated, but not only the direct irradiance is inserted in the weather file in BSim.

1. Simulation in BSim with direct irradiance only in the weather file
2. Percentage of RefVEIrr from DirVEIrr
3. Extract that percentage from DirVEI

Now both the amounts of the reflectance from DiffVEI and DirVEI are obtained and the RefVEI can be retrieved by adding these amounts together:

$$Ref_{Diff} + Ref_{Dir} = RefVEI \tag{14.8}$$

The newly obtained RefVEI will of course vary for every hour, these equations are therefore inserted for every 8760 hours of the year. The new TotVEI can now be obtained for every hour:

$$DiffVEI_{Withoutreflectance} + DirVEI_{Withoutreflectance} + RefVEI = TotVEI \tag{14.9}$$

This TotVei varies with orientation, the orientations from table 14.3 is applied.

Extracting RefVEI from the Deviation Between DiffVEI and DirVEI With and Without Ground Reflectance

The second method applied in order to obtain RefVEI was to extract the deviation between the simulated result of DiffVEI with a ground reflectance of 0 and one with the default ground reflectance. The same procedure was then repeated to obtain the deviation between DirVEI with and without ground reflectance.

The steps in the method were:

1. Set ground reflectance to 0.1 in Bsim and simulation with diffuse irradiance only in the weather file to obtain $DiffVEI_{Groundreflectance=0.1}$
2. Set ground reflectance to 0.0 in Bsim and simulation with diffuse irradiance only in the weather file to obtain $DiffVEI_{Groundreflectance=0.0}$

The reflected component of DiffVEI is obtained with equation 14.10.

$$DiffVEI_{Groundreflectance=0.1} - DiffVEI_{Groundreflectance=0.0} = RefVEI_{Diff} \tag{14.10}$$

1. Set ground reflectance to 0.1 in Bsim and simulation with direct irradiance only in the weather file to obtain $DirVEI_{Groundreflectance=0.1}$
2. Set ground reflectance to 0.0 in Bsim and simulation with direct irradiance only in the weather file to obtain $DirVEI_{Groundreflectance=0.0}$

The reflected component of DirVEI is obtained with equation 14.11.

$$DirVEI_{Groundreflectance=0.1} - DirVEI_{Groundreflectance=0.0} = RefVEI_{Dir} \tag{14.11}$$

RefVEI is obtained by adding the reflected component form DiffVEI and DirVEI in equation 14.12.

$$RefVEI_{Diff} + RefVEI_{Dir} = RefVEI \tag{14.12}$$

TotVEI is obtained by summing DiffVEI and DirVEI without ground reflectance, and the newly obtained RefVEI.

$$DiffVEI_{Groundreflectance=0.0} + DirVEI_{Groundreflectance=0.0} + RefVEI = TotVEI \quad (14.13)$$

Setting the ground reflectance to 0.0 caused $DirVEI_{Groundreflectance=0.0}$ to become extremely high for some hours throughout the year. This caused a negative $RefVEI_{Dir}$ as DirVEI with ground reflectance was subtracted from DirVEI without ground reflectance. This can be due to a numerical error in Bsim. It seams that BSim does not cope with a ground reflectance of 0.0 and then gives extremely high values for $DirVEI_{Groundreflectance=0.0}$ in some cases.

Therefore it was decided to repeat the same procedure, but set the ground reflectance to 0.01 instead of 0.0. Applying 0.01 will give marginally small contribution of reflectance in DiffVEI and DirVEI as, the ground reflectance is not zero. However, it is extremely small and it is assumed that it can be treated as zero. Applying 0.01 instead of 0.0 does not give negative $Reflected_{Dir}$.

The results from the two methods of obtaining RefVEI by first extracting RefVEI from the percentage of the irradiance components, and the second method applying the deviation between DiffVEI and DirVEI with and without ground reflectance, and the last method tried twice with different values of "zero" ground reflectance are shown in graph 14.10.

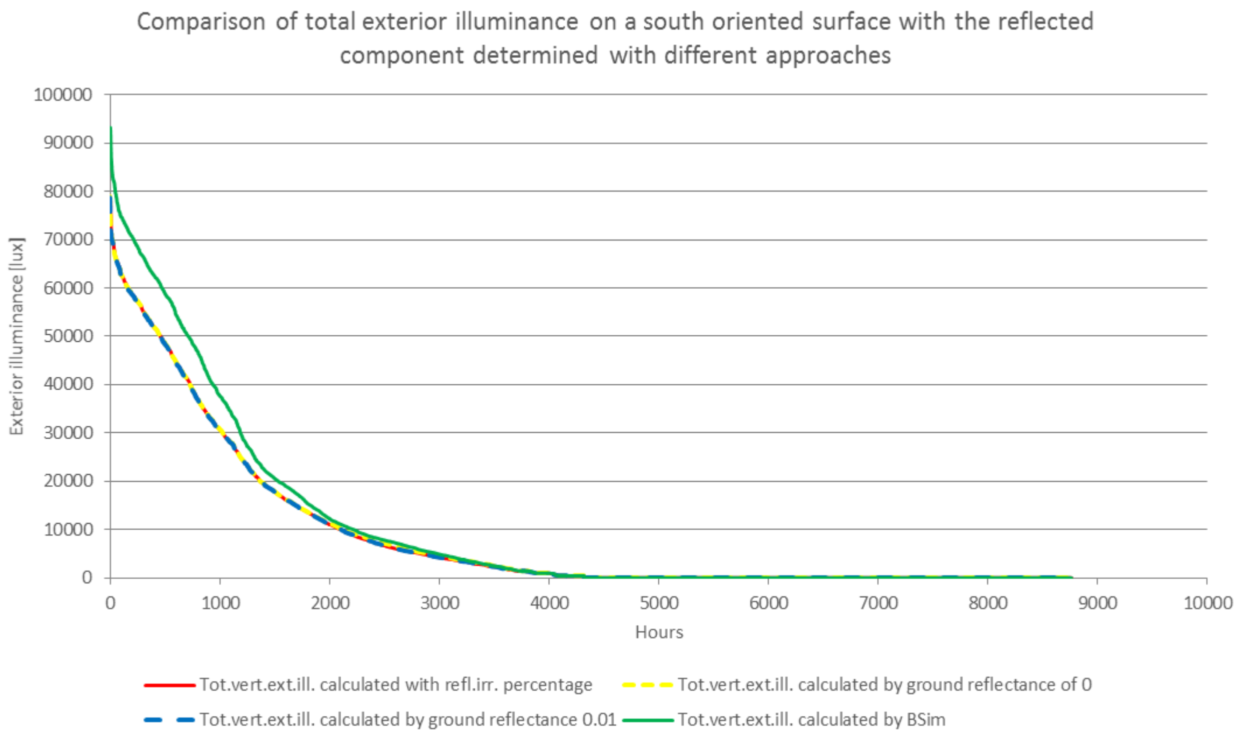

Figure 14.10. Extracting RefVEI from the percentage of the irradiance components and from the deviation between DiffVEI and DirVEI with and without ground reflectance

As seen in graph 14.10 the result for TotVei obtained with different methods of extracting RefVEI is fairly the same, the three results are overlapping. The different values of TotVEI obtained with these methods are not the same as TotVEI obtained directly with BSim, TotVEI obtained directly with BSim is higher. It is believed that additional work and a deeper understanding of the algorithms in BSim is required before this phenomenon can be understood completely.

The last method of extracting RefVEI from the deviation between DiffVEI and DirVEI with and without ground reflectance where the ground reflectance of "zero" is set to 0.01 is the method applied in order to obtain RefVEI in the *CIE Sky Method* and the *Hourly Average Method*.

14.9 Interior Illuminance Level in the Reference Point on the Horizontal Working Plane

The interior illuminance level in the office is calculated for the reference point on the working plane 0.85 above the floor and at a specified distance in the depth of the room, the distance from the window. It is assumed that it is in the middle of the width of the room.

The user must specify the required illuminance level on the horizontal working plane, which for office buildings in Norway is 500 lux (SINTEF Byggforsk, 1997). This means that TotIIRP should be at least 500 lux when the occupant is present. The required illuminance level of TotIIRP can be established due to sufficient available daylight, if there is not sufficient daylight then artificial lighting must be added.

14.9.1 Sufficient Daylight on the Interior Illuminance Level on the Horizontal Working Plane

TotIIRP due to daylight is obtained by multiplying the total solar light factor with TotVEI. It is the process of obtaining TotIIRP due to daylight which deviates the *CIE Sky Method* and the *Hourly Average Method*.

In the *CIE Sky Method* TotIIRP due to daylight is obtained by sorting the 8760 hours of a year into CIE sky intervals of TotVEI. Then TotVEI for every interval is muliplyied with the total solar light factor to obtain a TotIIRP for every interval. This will be explained in detail in chapter 15.

For the *Hourly Average Method* TotIIRP due to daylight is obtained for the hourly average of the 8760 hours throughout the year. The hourly average of TotVEI is multiplied for the total solar light factor to obtain an hourly average of TotIIRP throughout the year. This will be explained in detail in chapter 16.

Needed Artificial Light Level and Corresponding Electricity Usage

The deviation between TotIIRP and the set point of the armature, as explained in section 14.6, will establish when there is need for artificial lighting. The hours when the occupant is present, and there is not sufficient daylight for TotIIRP to reach the set point, the artificial lighting will be on. The electricity usage of the armature for these hours sum up to the total electricity usage for the artificial lighting in the office over a year per square meter.

14.10 Summary of Required Input for the User

The input parameters required for the user to insert in both of the methods are listed below.

- Geometry

    - The area of the office in [m^2]
    - The area of each of the different surfaces in the office [m^2]
    - The orientation of the façade in degrees [°]
    - The reflectance of each of the different surfaces in the office [-]
    - The light transmittance of the glazing [-]
    - The total area of the glazing in the façade [m^2]
    - The daylight factor for the reference point [%]
    - The distance from the window to the reference point in the depth of the room [m]
    - The angle of the slope of the surface where the reference point is located, compared to a horizontal surface [°]
- Cell office or open landscape office
- Armature
    - The required illuminance level on the working plane [lux]
    - The set point for the armature to switch from minimum to maximum [lux]
    - Minimum power of the armature [W]
    - Maximum power of the armature [W]

In order to establish the electricity usage for the artificial lighting, the occupancy profile, required illuminance level of TotIIRP, and TotVEI must be established initially. The two new estimation methodologies; the *CIE Sky Method* and the *Hourly Average Method* will now be explained in chapter 15 and 16. The two established methodologies will then be compared to the results of the methodology from *NS 3031:2014* in chapter 17.

CIE Sky Method 15

To determine the TotIIRP in the *CIE Sky Method*, the hourly TotVEI from the Norwegian standard reference year weather file sorted into intervals of CIE sky conditions. The intention of this method is to obtain a standardized set of TotVEI value intervals according to the definition of the CIE sky conditions, and classify the number of hours during a certain time period, when these intervals occur. The obtained number of hours with the corresponding illuminance value of the interval will then be used for calculating the TotIIRP, and thereby calculate the yearly electricity usage for the room in interest.

The following flow diagram 15.1 lists the inputs required for the user, and the outputs obtained from the *CIE Sky Method*.

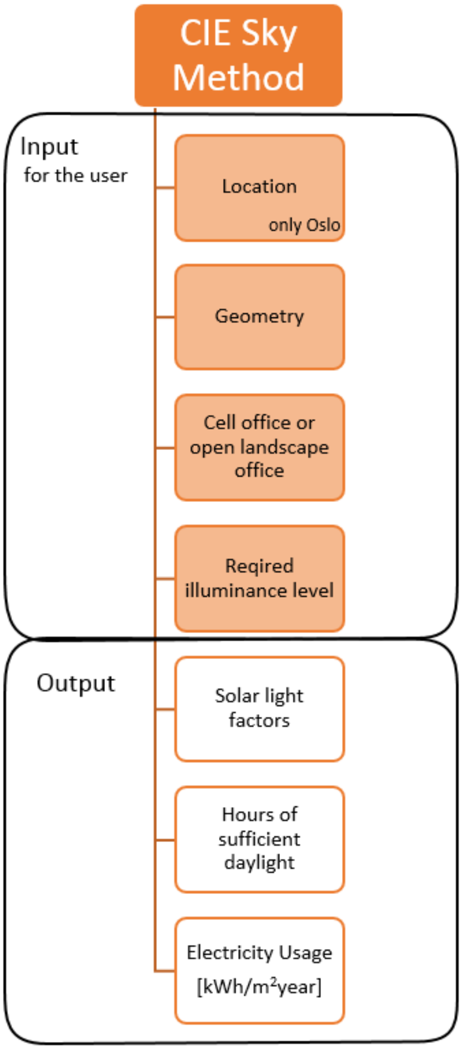

Figure 15.1. Illustration of the flow of inputs and output in the *CIE sky method*

The parameters and procedures explained in 14 on page 127 are applied in order to obtain the yearly electricity usage for the room of interest. The stepwise procedure of the method can be seen in figure 15.2.

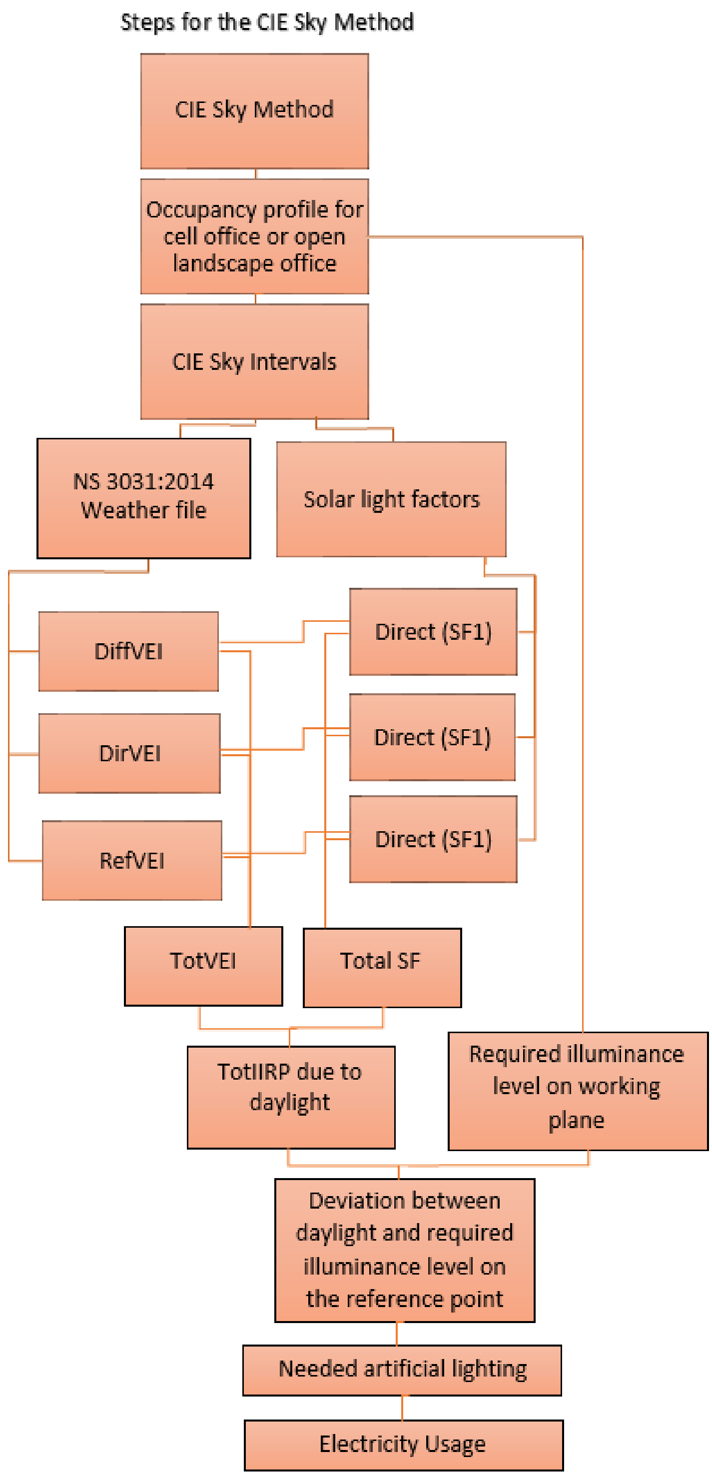

Figure 15.2. Illustration of the steps taken in the *CIE sky method*

An Excel spreadsheet is developed for the calculation of the electricity usage for the room. A screen shot of the spreadsheet can be seen in figure 15.3. The blank cells are the input cells where the user is required to insert information about the building geometry, orientation, type of office the method is applied for, as well as parameters for the armature. The solar light factors are also calculated in this spreadsheet according to the procedure explained in 14.7 on page 131.

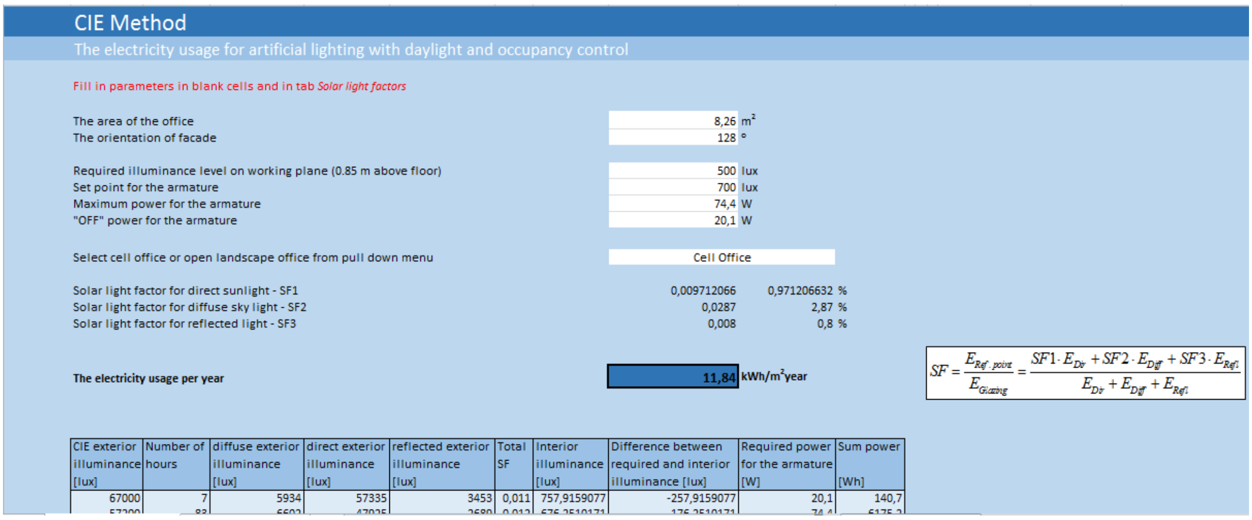

Figure 15.3. Screen shot of the Excel spreadsheet for the *CIE sky method*

15.1 Applying the *CIE Sky Method* on the Case Building

The yearly electricity usage for daylight and occupancy controlled artificial lighting in the cell office in the case building was calculated using the *CIE Sky Method*.

The ranges of CIE illuminance values were obtained by following the procedure explained in 5.3.1 on page 65. In this case, the obtained occupancy profile for a cell office is used, and the TotVEI from the *NS 3031:2014* weather file for these exact hours are extracted and inserted into graph 15.4 with the CIE illuminance intervals. The intervals between the top five lines represent different levels of TotVEI for CIE clear sky with sunlight. The blue line represents the CIE intermediate sky condition, while the remaining two green bottom lines are the TotVEI values obtained when simulating in Relux with CIE overcast sky conditions. The grey sloped line shows the hourly TotVEI from the Norwegian reference year.

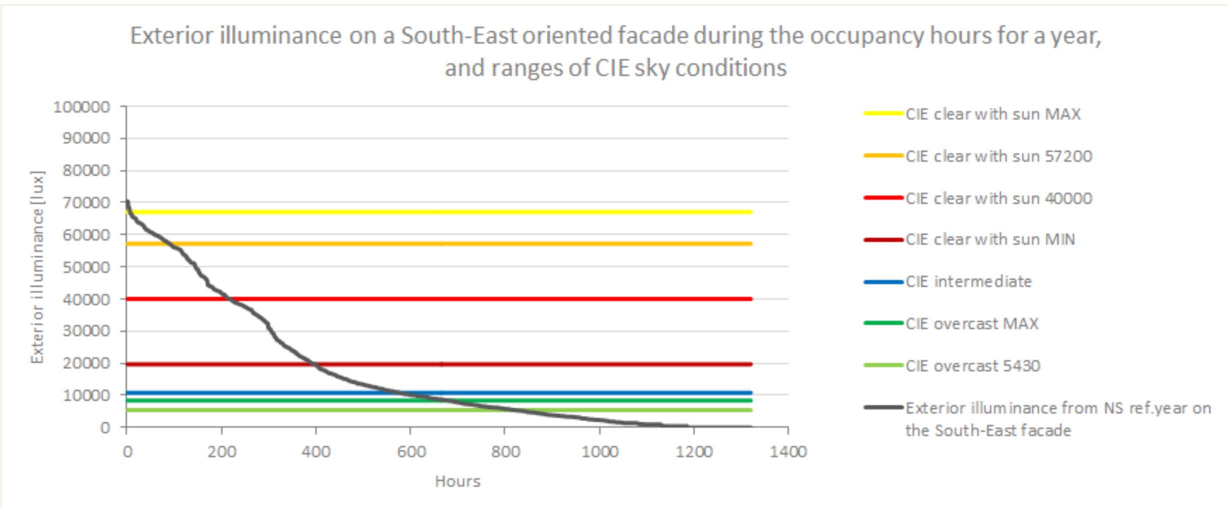

Figure 15.4. The yearly TotVEI from the Norwegian reference year weather file compared to the TotVEI from Relux for different CIE sky conditions on the façade with an orientation of 128 ° during occupancy hours

As seen on graph 15.4, the TotVEI from the Norwegian reference year consist of values from every CIE sky condition interval. It shows that CIE clear sky with sunlight, on the 128 ° oriented façade, has a range from 19700 lux to 67000 lux. The CIE intermediate sky has a range from 10800 lux to 19700 lux, while the CIE overcast sky has a range from 0 lux to 10800 lux.

In graph 15.5, TotVEI from the Norwegian reference year is divided into amount of hours where the different CIE sky conditions occur.

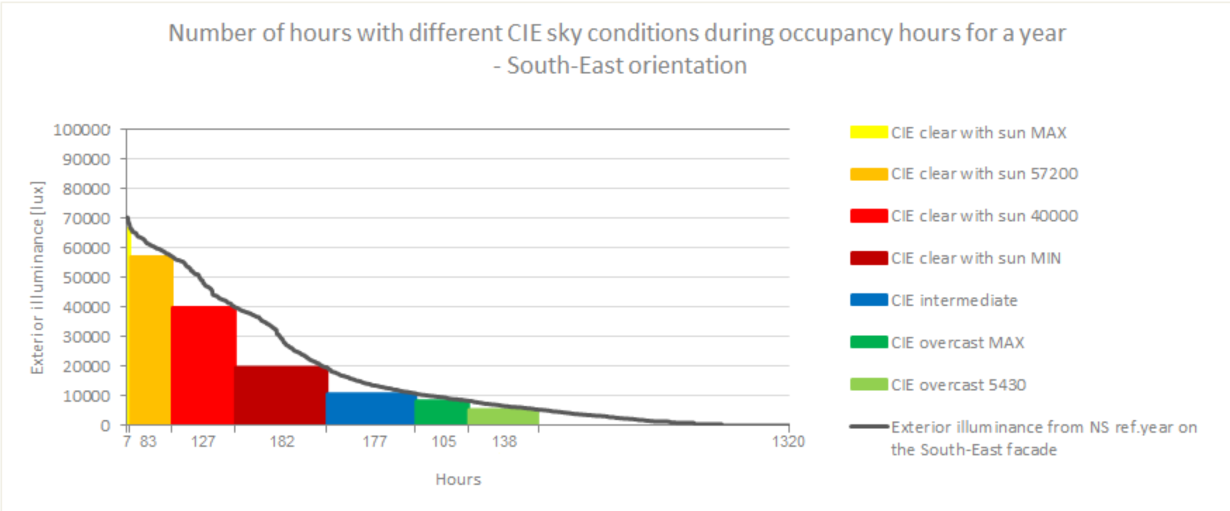

Figure 15.5. TotVEI from the Norweigan reference year weather data divided into intervals of hours where different CIE sky conditions occur

As seen in graph 15.5, the office will have 399 hours with clear sky conditions, 177 hours with intermediate sky conditions, and 744 hours with overcast sky conditions during occupancy hours for a year, according to the CIE definition. The results are inserted into the *CIE Sky Method* spreadsheet.

The yearly electricity usage for the cell office is, according to this method, 11.84 $\mathrm{kWh/m^2 \cdot year}$. This result will be compared to the yearly electricity usage obtained from the *Hourly Average Method* and *NS 3031:2014* in chapter 17 on page 165 When studying the calculation in the spreadsheet, it can be seen that for the CIE sky method, there are only seven out of 1320 occupancy hours of the year with sufficient daylight in the room. This is due to the *CIE Sky Method* sorting the hours into CIE sky intervals where all the hours within each interval does in fact has a higher TotVEI than the TotVEI of every interval. This will be discussed in section 15.3.

15.2 Validation of the *CIE Sky Method*

The *CIE Sky Method* is applied on the case office using the measured irradiance weather file and the actual occupancy profile for the office during the measurement period.

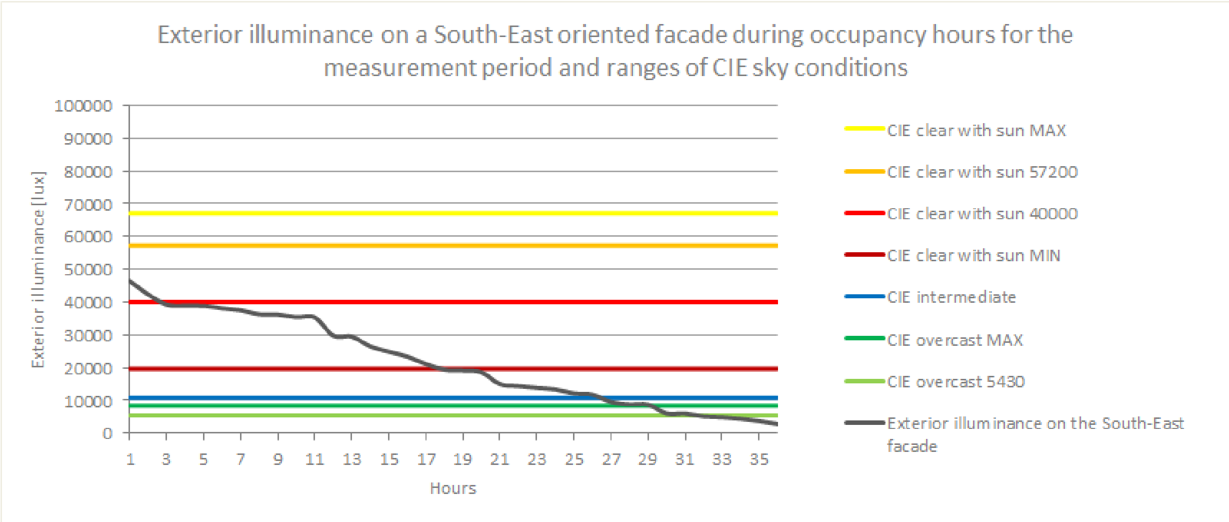

Figure 15.6. TotVEI from measurement period using irradiance weather data file for exact occupancy

As seen in the graph 15.6, the TotVEI from the measured irradiance weather file does not contain values from the two highest levels of CIE clear sky. In the following graph, the TotVEI is divided into amount of hours where the different CIE illuminance levels occurred during the measurement period.

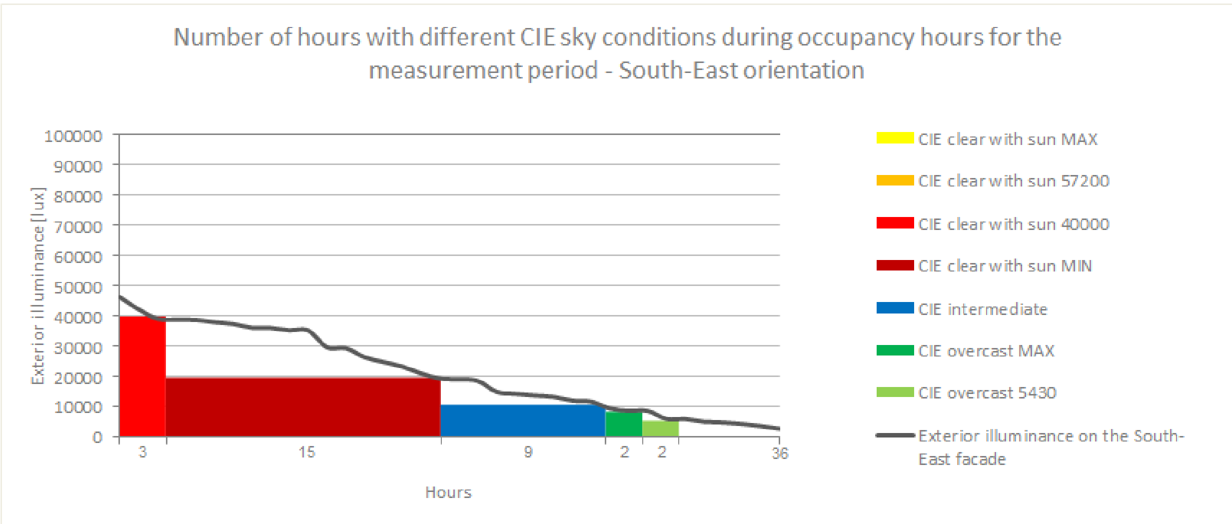

Figure 15.7. Number of hours from the Norwegian reference year weather data divided into different CIE sky conditions

As seen on graph 15.7, out of a total of 36 hours there is 18 hours with clear sky, nine hours of intermediate sky and nine hours of overcast sky conditions occurring during the occupancy hours in the measurement period. From the spreadsheet it can be seen that there is three out of 36 hours during the measurement period where there is sufficient daylight in the cell office.

The electricity usage for the measurement period, calculated in the spreadsheet, is $0.30\,\text{kWh/m}^2 \cdot 6\text{days}$. This is very close to the measured electricity usage for the cell office of $0.28\,\text{kWh/m}^2 \cdot 6\text{days}$. To validate the method, the electricity usage for six days is calculated with the Norwegian reference year weather file and obtained occupancy profile. This will give the electricity usage for the same amount of time as the occupant was present in the office during the measurement period. This results in an electricity usage of 0.32 $\mathrm{kWh/m^2} \cdot$ 6days. The different results are compared in figure 15.8.

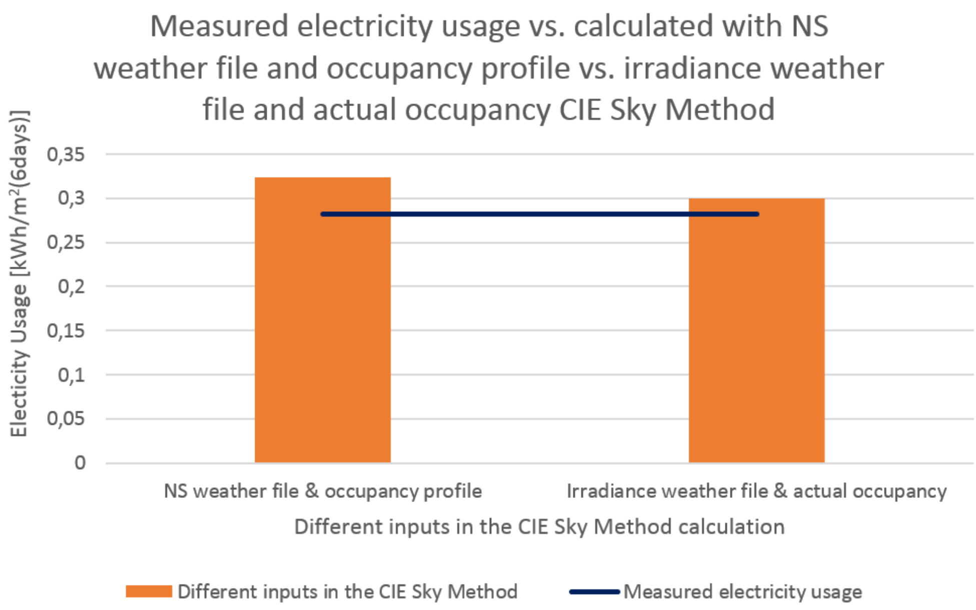

Figure 15.8. Comparison of the calculated electricity usage with the NS weather file and occupancy profile as an input in the *CIE sky method*, and the irradiance weather file and actual occupancy as an input to the measured electricity usage

As seen graph 15.8, the results obtained with the *CIE Sky Method* are close to the measured electricity usage for the cell office. However, both of the calculations leads to a slightly higher electricity usage than measured.

15.3 Discussing the CIE Sky Method

The *CIE Sky Method* appears to be a rapid and fairly accurate method for calculating the electricity usage for artificial lighting. The results obtained in the validation of the method are slightly higher, but still very close, to the measured electricity usage. The deviation is most likely due to the fact that a set of hours in each interval has one set exterior illuminance value, even though the majority of the hours in each interval in reality has a higher exterior illuminance. This leads to an overall lower interior illuminance level for the office in interest, which again results in a higher electricity usage.

The results showed that even with a high amount of hours with CIE clear sky with sun, the hours with sufficient daylight in the cell office was pretty low. This shows that CIE clear sky condition does not directly imply sufficient interior illuminance levels. When comparing the spreadsheet calculation for the yearly electricity usage to the spreadsheet calculation for the measurement period, a deviation was discovered. In the calculation for the measurement period, it was seen that an exterior illuminance level of 40000 lux provided sufficient daylight in the room. However, the same exterior illuminance level in the calculation for the yearly electricity usage, did not provide sufficient daylight in the cell office. This may be due to the fact that the measured irradiance weather file contains irradiance values with a higher number of decimals than the NS weather file, which can have an affect on the calculated DiffVEI, DirVEI, RefVEI and thereby TotVEI. In graph 15.9 the different illuminance components applied in the different calculations for the CIE illuminance level of 40000 lux is displayed.

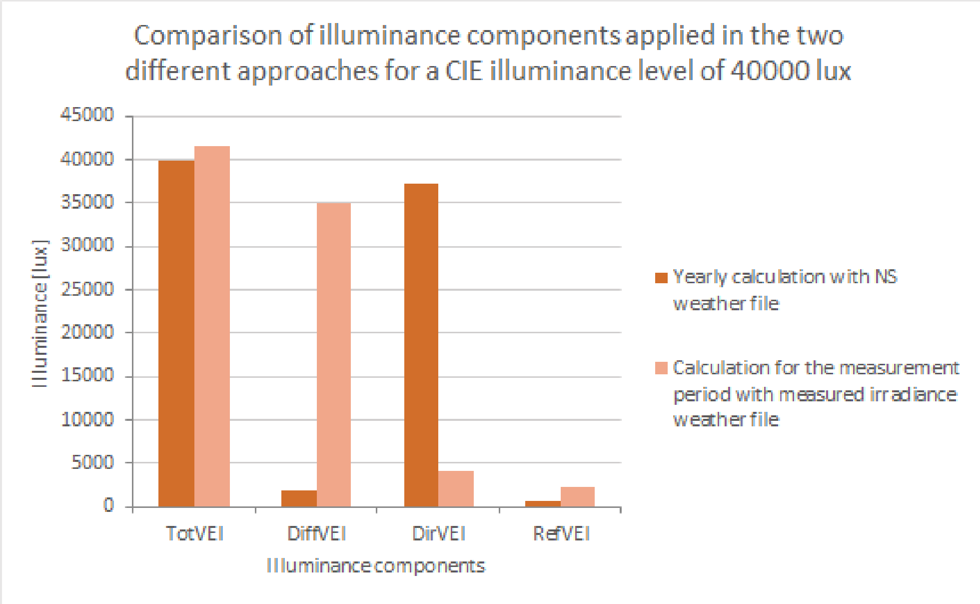

Figure 15.9. Comparison of the illuminance components applied in the different cases for a CIE illuminance level of 40000 lux

The two TotVEI values that were closest to the CIE sky illuminance level were extracted from the two different weather files. From the graph it is clear that the distribution between the different components are extremely different for the two values. The TotVEI from the NS weather file is mostly due to the direct component, while for the measured irradiance weather file, the opposite is the case. As these different components are multiplied with the specific solar light factor accounting for the direct and diffuse components, this may lead to a large difference in the calculated total solar light factor. For this TotVEI value in the yearly calculation, the total solar light factor becomes 0.011, while in the calculation for the measurement period it becomes 0.026. This is a relatively large difference that obviously has an impact on the calculation of TotHII. As mentioned in 14.8.2 on page 141 some uncertainties occurred when extracting the RefVEI from the different illuminance components was attempted. When studying the data, it seems like this complication occurs when the direct component is larger than the diffuse component. Graph 15.9 also indicates that this may be the case. It appears as if an inadequate understanding of the procedure of extracting RefVEI from TotVEI may be part of the reason for this distinction between the results.

It can be concluded that additional work should be conducted before the accuracy of this method can be fully determined. One of the inputs in the spreadsheet is the orientation of the building. As for now, the method can only be applied for offices with an orientation of 128 ° located in Oslo, Norway. For this specific orientation and location there is only eight intervals of CIE illuminance values. This will most likely vary from location to location, and for the different orientations. For the method to be applicable for buildings with other orientations and locations, simulations in Relux for each orientation is required to obtain illuminance levels for the different CIE sky conditions on the different façades.

Hourly Average Method 16

The purpose of this method is to increase the accuracy of the previous method as the previous method sorts TotVEI into different CIE intervals and then calculates the electricity usage for the artificial lighting due to the corresponding TotIIRP. The *Hourly Average Method* investigates every hour throughout the year. The average of every hour in the year is included in order to calculate the deviation between the required illuminance level of TotIIRP and the illuminance level due to available daylight. This deviation will then give the electricity usage for the armature in the office on a hourly average for the 8760 hours of a year.

The parameters explained in chapter 14 are applied in the *Hourly Average Method*. The inputs required to be filled out by the user and the outputs obtained by the method can be seen as a flow diagram in figure 16.1.

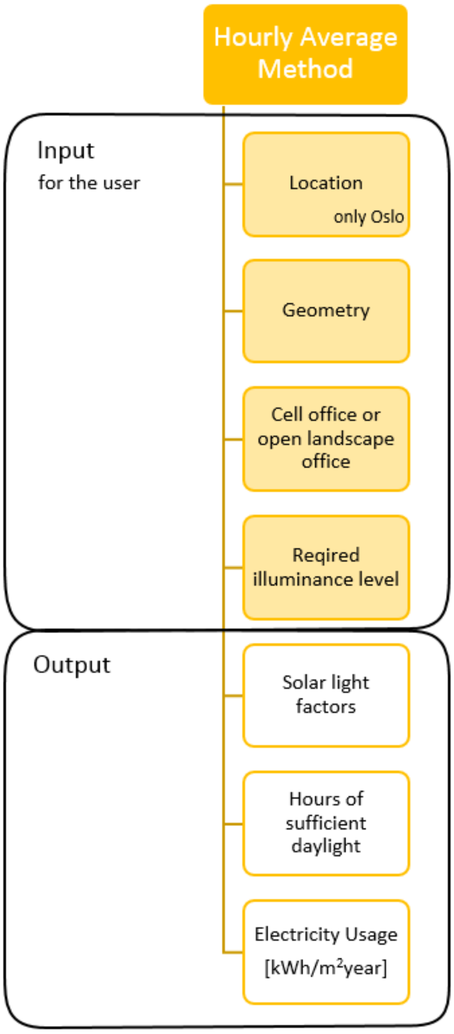

Figure 16.1. Illustration of the flow of inputs and output in the *Hourly Average Method*

As explained in section 14.9 what deviates the *CIE Sky Method* and the *Hourly Average Method* is how TotIIRP due to daylight is obtained. The steps of obtaining TotIIRP and the corresponding hours of artificial lighting and the yearly electricity usage is shown step by step in the illustration in figure 16.2.

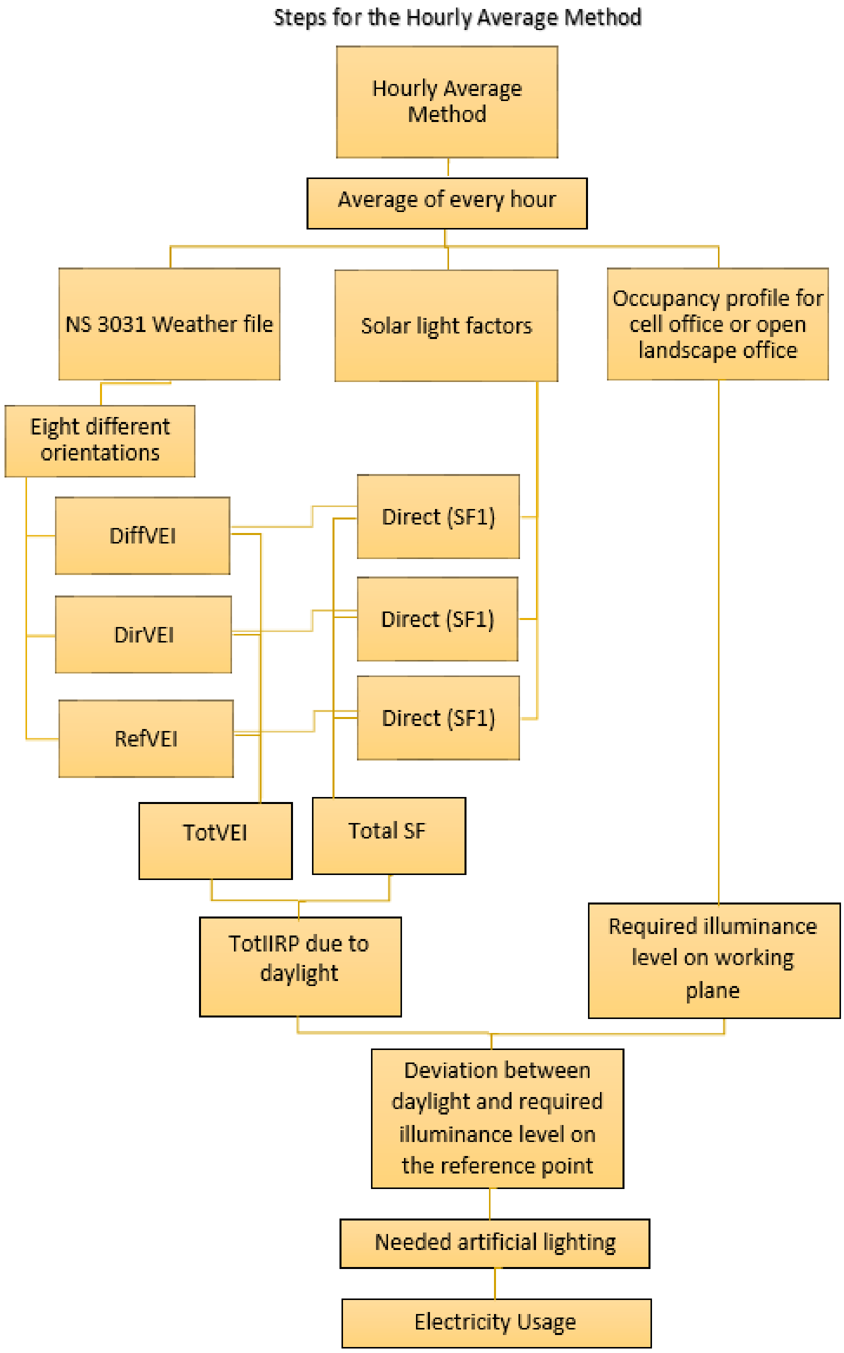

Figure 16.2. Illustration of the steps taken in the *Hourly Average Method*

16.1 Applying the *Hourly Average Method* on the Case Building

The hourly average method is applied on the cell office in the case building and the yearly electricity usage of the artificial light can been calculated.

A screen shot of the Excel spread sheet for hourly average method can be seen in figure 16.3. The inputs required by the user is inserted into the blank cells seen in the screen shots of the Excel spreadsheet. The solar light factors are obtained as explained in section 14.7 on page 131.

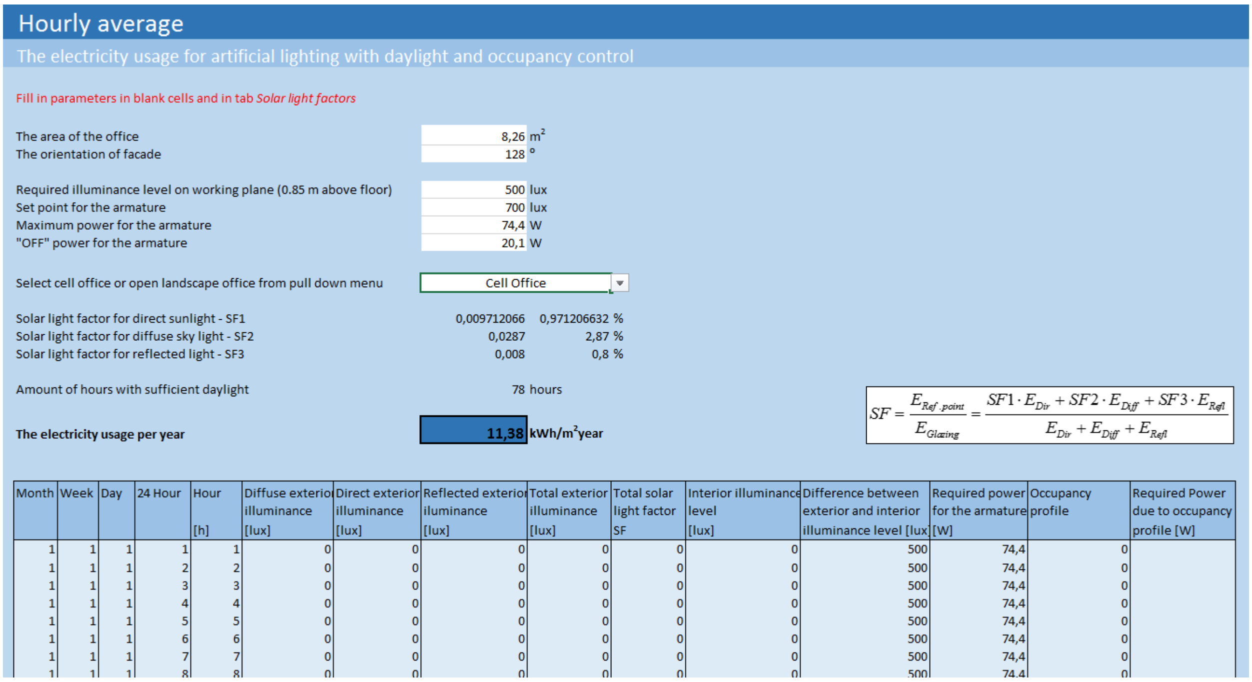

Hourly average

The electricity usage for artificial lighting with daylight and occupancy control

Fill in parameters in blank cells and in tab *Solar light factors*

The area of the office	8,26	m^2
The orientation of facade	128	°
Required illuminance level on working plane (0.85 m above floor)	500	lux
Set point for the armature	700	lux
Maximum power for the armature	74,4	W
"OFF" power for the armature	20,1	W
Select cell office or open landscape office from pull down menu	Cell Office	
Solar light factor for direct sunlight - SF1	0,009712066	0,971206632 %
Solar light factor for diffuse sky light - SF2	0,0287	2,87 %
Solar light factor for reflected light - SF3	0,008	0,8 %
Amount of hours with sufficient daylight	78	hours
The electricity usage per year	**11,38**	**kWh/m^2year**

$$SF = \frac{E_{Ref.point}}{E_{Glazing}} = \frac{SF1 \cdot E_{Dir} + SF2 \cdot E_{Diff} + SF3 \cdot E_{Refl}}{E_{Dir} + E_{Diff} + E_{Refl}}$$

Month	Week	Day	24 Hour	Hour [h]	Diffuse exterior illuminance [lux]	Direct exterior illuminance [lux]	Reflected exterior iluminance [lux]	Total exterior illuminance [lux]	Total solar light factor SF	Interior illuminance level [lux]	Difference between exterior and interior illuminance level [lux]	Required power for the armature [W]	Occupancy profile	Required Power due to occupancy profile [W]
1	1	1	1	1	0	0	0	0	0	0	500	74,4	0	
1	1	1	2	2	0	0	0	0	0	0	500	74,4	0	
1	1	1	3	3	0	0	0	0	0	0	500	74,4	0	
1	1	1	4	4	0	0	0	0	0	0	500	74,4	0	
1	1	1	5	5	0	0	0	0	0	0	500	74,4	0	
1	1	1	6	6	0	0	0	0	0	0	500	74,4	0	
1	1	1	7	7	0	0	0	0	0	0	500	74,4	0	
1	1	1	8	8	0	0	0	0	0	0	500	74,4	0	

Figure 16.3. Screen shot of the Excel spreadsheet calculating for the hourly average method

The yearly calculated electricity usage for the cell office in the case building by the *Hourly Average Method* is 11.38 $\mathrm{kWh/m^2 \cdot year}$. According to the calculation there is only 78 hours during the total of 1320 working hours, obtained from the occupancy profile for the cell office, throughout one year that there is sufficient daylight in the cell office for an orientation of 128 °.

The result obtained with this methodology will be compared to the methodology applying the CIE sky intervals and the methodology from *NS 3031:2014* in chapter 17.

16.2 Validation of the *Hourly Average Method*

The hourly average method was applied on the cell office in the case building for the same period as the measurements for the solar irradiance and electricity usage of the armature were conducted. As explained in section 14.1 the total electricity usage for the armature during the six days the occupant was present is 0.28 $\mathrm{kWh/m^2 \cdot 6days}$.

The electricity usage calculated with the *Hourly Average Method* for six days is 0.31 $\mathrm{kWh/m^2 \cdot 6days}$. This is obtained by dividing the yearly calculated electricity usage of 11.38 $\mathrm{kWh/m^2 \cdot year}$ by the 1320 hours of occupancy, and then multiplying this with 36 hours in order to obtain the electricity usage for the same amount of time the occupant spent in the office. This method gives a deviation of 8.9 % from the measured electricity usage of 0.28 $\mathrm{kWh/m^2 \cdot 6days}$.

The slightly larger calculated electricity usage from the *Hourly Average Method* may be due to that extracting six days out of the reference year does not correspond well with the actual weather condition during the measurement period. In this method of calculating the electricity usage the time of the year is not taken into consideration. Another reason might be that even though the occupant is present for an average of six hours per day for the six days, when these hours occur during the day does not correspond exactly with the obtained cell office occupancy profile. It should also be kept in mind that when inserting an orientation of 128 ° in the *Hourly Average Method*, the orientation in the calculation will be 135 ° due to the orientation intervals explained in section 14.3.

In order to further validate and study the hourly average method, the exact orientation of 128 ° and the corresponding DiffVEI, DirVEI and RefVEI obtained from the irradiance measurements, explained in appendix D on page 229, are inserted as a weather file in BSim. In order to get as close to the actual result for the electricity usage as possible the actual occupancy profile of the occupant during the measurement period is also inserted in the Excel spreadsheet.

The calculated result from the *Hourly Average Method* with an occupancy profile and TotVEI which correspond as much as possible to the real conditions is $0.27\,\mathrm{kWh/m^2} \cdot 6\mathrm{days}$. The deviation is 4.3 %, which means the *Hourly Average Method* underestimated the electricity usage. There are six out of the 36 hours with sufficient daylight. One possible reason for the deviation can be that the solar shading is activated at 14:30 on the 23^{rd} until 14:45 on the 24^{th}. On the 23^{rd} the sky condition was a combination of clear and overcast as explained in appendix D on page 229, and on the 24^{th} the sky condition was close to being clear.

The electricity usage obtained with the *Hourly Average Method*, with the *NS 3031:2014* weather file and developed occupancy profile, compared to the results obtained with the measured solar irradiance as a weather file and the exact occupancy, are seen in figure 16.4, together with the measured electricity usage.

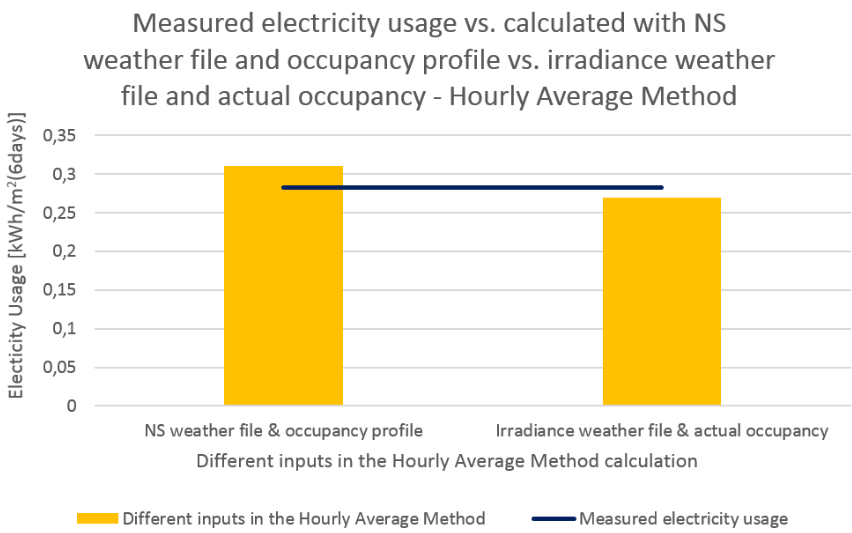

Figure 16.4. The calculated electricity usage with NS weather file and occupancy profile as an input in the *Hourly Average Method*, and the irradiance weather file and actual occupancy as an input, compared to the measured electricity usage.

16.3 Assessing the *Hourly Average Method*

In order to assess the *Hourly Average Method* the yearly electricity usage for the daylight and occupancy controlled artificial lighting in the cell office in the case building were calculated with different inputs. The set point, occupancy profile and orientation were varied one at a time.

The electricity usage of $11.38\,\mathrm{kWh/m^2} \cdot \mathrm{year}$ is obtained with a set point at 700 lux for the armature, explained in detail in section 14.6. This was compared to applying a set point of 500, which means there is no delay for the armature. This gives an electricity usage of 10.20 $\mathrm{kWh/m^2 \cdot year}$. Different values of the set point were tested to observe the corresponding electricity usage, the result is shown in graph 16.5. For these calculations only the set point is changed, the other parameters are kept the same as in the case building.

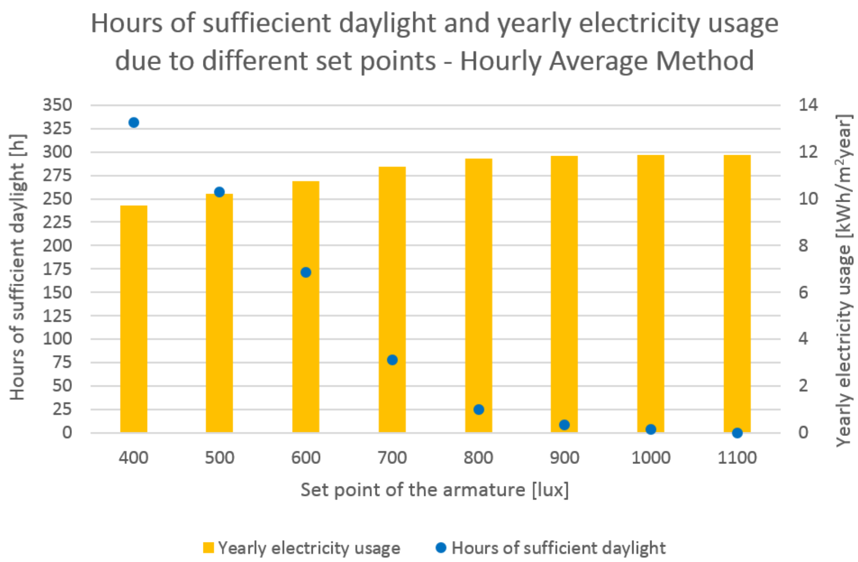

Figure 16.5. Hours of sufficient daylight and corresponding yearly electricity usage due to different set points for the armature calculated with the *Hourly Average Method*

As seen in graph 16.5 the amount of hours with sufficient daylight varies significantly with the different set points. With a set point of 400 lux there are 332 hours of sufficient daylight and an electricity usage of 9.71 $\mathrm{kWh/m^2 \cdot year}$, while for a set point of 500 lux there are 257 hours. With a set point of 1000 lux there are only three hours of sufficient daylight. On the other hand, the electricity usage does not vary significantly with the different amount of hours with sufficient daylight. With a set point of 1100 lux there are zero hours of sufficient daylight and the electricity usage is 11.89 $\mathrm{kWh/m^2 \cdot year}$. This only gives a deviation of 2.81 $\mathrm{kWh/m^2 \cdot year}$ between a set point of 400 and 1100 lux. This supports the statement from section 7.2.1 that the electricity usage is highly dependent on the occupancy profile compared to available daylight.

In order to assess the statement that the occupancy profile pays a huge role for the electricity usage, the electricity usage was calculated with the different occupancy profiles for the cell office and open landscape office in the *Hourly Average Method*. All other parameters were kept the same as in the case building. The results are displayed in figure 16.6.

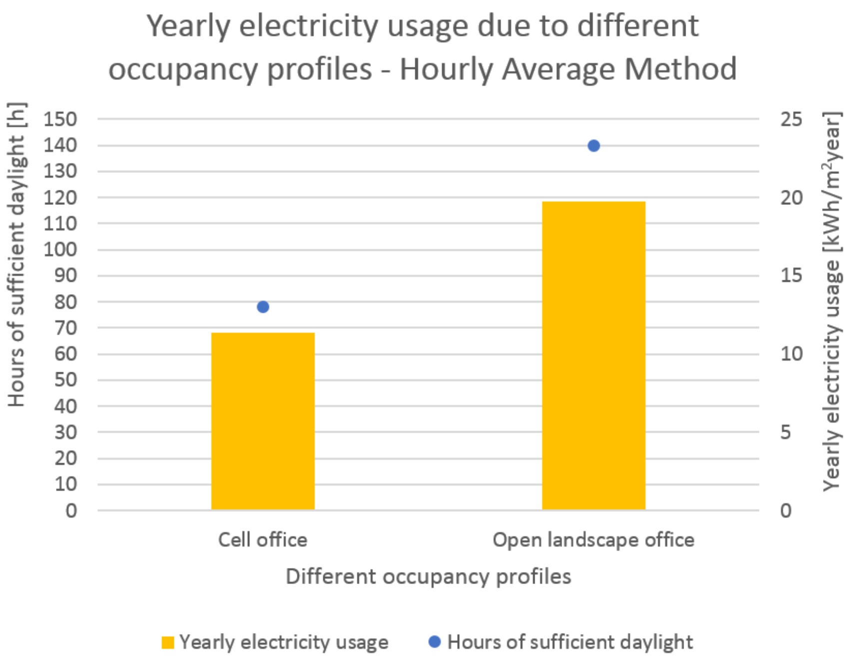

Figure 16.6. Hours of sufficient daylight and corresponding yearly electricity usage of the armature calculated with the Hourly Average Method with different occupancy profiles

When changing the occupancy profile from the cell office occupancy profile to the open landscape occupancy profile, the electricity usage becomes 19.75 $\mathrm{kWh/m^2 \cdot year}$ instead of 11.38 $\mathrm{kWh/m^2 \cdot year}$. The electricity usage obtained with the open landscape occupancy profile is almost twice as large as the electricity usage for the same office, but with the cell office occupancy profile. This clearly shows that the electricity usage is strongly dependent on the hours of occupancy, and the daylight control does not pay such a significant role for the electricity usage. This again supports the statement from section 7.2.1 that the electricity usage is highly dependent on the occupancy profile.

The last parameter investigated in the *Hourly Average Method* is the orientation. When the electricity usage due to the orientation is investigated, only the orientation is changed while the other parameters are kept the same as in the case building. The result for the four cardinal orientations are shown in graph 16.7.

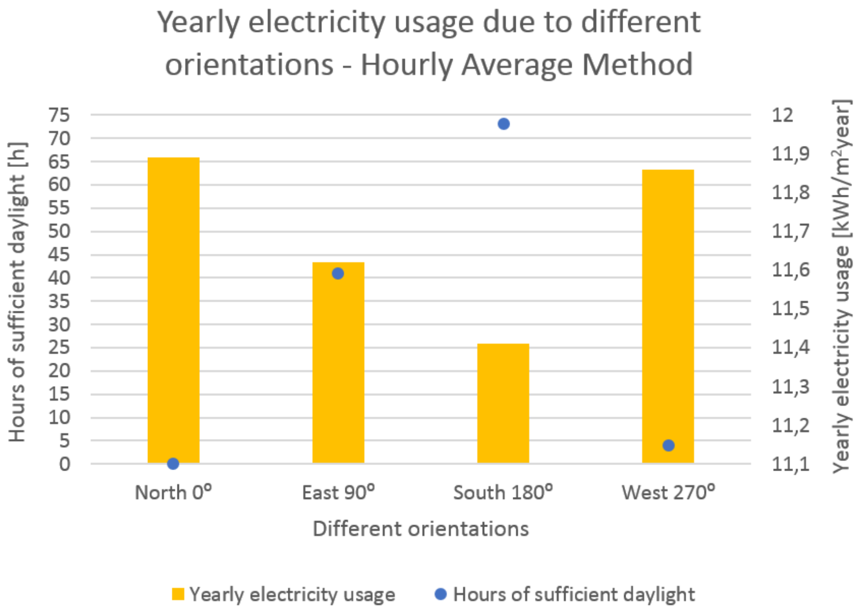

Figure 16.7. Hours of sufficient daylight and corresponding yearly electricity usage of the armature calculated with the *Hourly Average Method* with different orientations

When the office is facing directly South, the electricity usage becomes 11.41 $\text{kWh/m}^2 \cdot \text{year}$. The electricity usage becomes 11.89 $\text{kWh/m}^2 \cdot \text{year}$ when the cell office is facing directly North. The deviation of the electricity usage for a cell office facing directly South and North is only 0.48 $\text{kWh/m}^2 \cdot \text{year}$. As seen in graph 16.7 there are 73 hours of sufficient daylight when the cell office is facing South. If the cell office is facing East there are 41 hours of the occupied hours with sufficient daylight, compared to only 4 when the cell office is facing West. This is due to the morning hours of daylight for the East orientation corresponding with the occupancy profile. The occupant is not present when the evening sun strikes the West façade. It can be concluded that the amount of hours throughout the year with sufficient daylight is highly dependent on the orientation. However, 73 hours of sufficient daylight out of the 1320 hours of occupancy is not a significantly large amount.

In order to further assess the *Hourly Average Method*, the electricity usage due to different parameters such as the light transmittance of the glazing, the reflectance of the surfaces and the depth of the room could be investigated.

16.4 Discussing the *Hourly Average Method*

One limitation to this method is that it is only possible to insert one armature. If several armatures were to be placed in the office, which most likely would be the case for an open landscape office, the illuminance level on the working plane for the armatures added together in that office must be known. To further extend the hourly average method the correlation between the illuminance level on the working plane and the number of armatures should be established. If this is determined, the *Hourly Average Method* can then include several armatures.

Another limitation to this method is that only two set points for the armature is possible, either 100 % or 27 %. No dimming of the artificial light due to available daylight is accounted for. This means that it is, of now, not possible to calculate the electricity usage of an armature with dimming, only two set points can be inserted. In order to further extend the *Hourly Average Method* the possibility of dimming of the armature due to available daylight should be included.

This method is only applicable for Oslo, as of now. If the diffuse, direct and reflected exterior illuminance for other locations can be obtained, then this method can be employed for other locations.

The values obtained with the *Hourly Average Method* does not include variations which might occur within one hour. In reality the exterior illuminance can change rapidly due to varying sky conditions. These variations will not be accounted for. Nor will the small variations in the hours of occupancy. As stated in section 8 on page 83 the hours of occupancy per day included variations within one full hour, these variations are not included in the *Hourly Average Method*.

Solar shading is not included in the *Hourly Average Method*. This holds a significant limitation as in real life solar shading will be activated, if installed in the building, when the exterior illuminance on the façade is high. Nevertheless, the direct component of SF1 is not included, only the inter reflected is, which means that direct sunlight will not hit the working plane directly, and thereby increase the interior illuminance correspondingly which then decreases the electricity usage. On the other hand, when solar shading is active not only the direct illuminance from the sun will be cut off, but also the diffuse and reflected components. How much, depends in the cut off angle of the solar shading. If further investigation in this field is carried out, it is recommended to include solar shading in the hourly average method as this might be the largest weakness of the method. As shown in appendix I.0.1 on page 275, the interior illuminance on March the 23^{rd} were significantly low, even though there were a great amount of solar irradiance simultaneously as the sky was clear. The low amount of interior illuminance in the cell office was due to the solar shading. If the *Hourly Average Method* should be further developed, it should be investigated if there will be a reduction in the electricity usage for artificial light controlled by daylight if solar shading is active.

The *Hourly Average Method* was assessed by studying the calculated electricity usage when the different parameters in section 16.3 were changed. The different results for the electricity usage indicated that the electricity usage calculated by the *Hourly Average Method* is realistic.

It is concluded that the *Hourly Average Method* can accurately and rapidly calculate the electricity usage of daylight and occupancy controlled artificial lighting.

Ranking of the Estimation Methodologies 17

The ranking of the estimation methodologies for determining the electricity usage of artificial lighting is done with regard to two qualifications:

- Rapidity
- Accuracy

17.1 Ranking the Estimation Methodologies due to Rapidity and Accuracy

The estimation methodology should accurately determine the electricity usage of daylight and occupancy controlled artificial lighting. However, the calculated electricity usage should also be rapidly established which means that the method should not require the user to perform measurements or simulations prior to using the method.

The yearly electricity usage for the cell office in the case building is calculated with the method from *NS 3031:2014* explained in chapter 13, the *CIE Sky Method* explained in chapter 15 and the *Hourly Average Method* explained in chapter 16. The result for the yearly electricity usage is shown in graph 17.1.

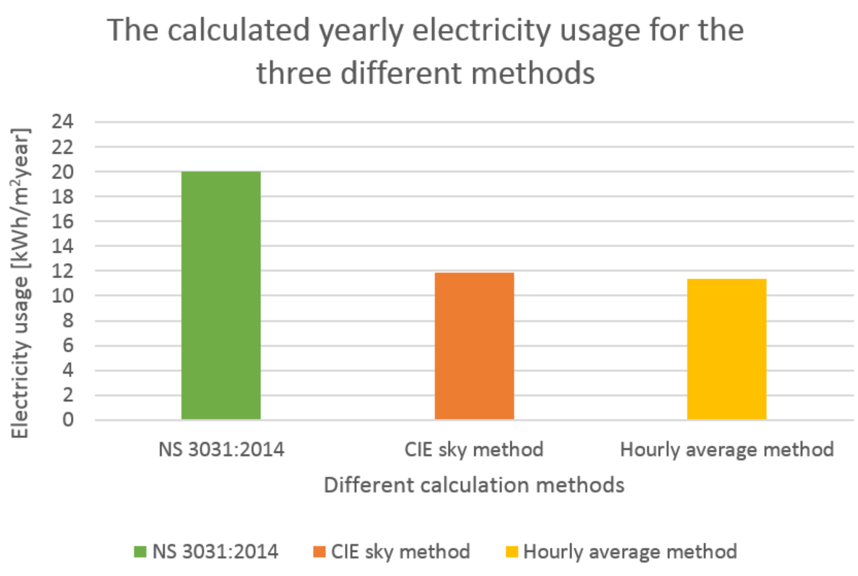

Figure 17.1. The calculated yearly electricity usage from the three different

The electricity usage calculated with the method from *NS 3031:2014* is nearly twice as large as the electricity usage calculated with the *CIE Sky Method* and *Hourly Average Method*. The results obtained with the two established methods are fairly close to each other with values at 11.84 kWh/m^2 · year for the *CIE Sky Method* and 11.38 kWh/m^2 · year for the *Hourly Average Method*.

In order to validate the methods and determine their accuracy, electricity usage for the same period as the measurements were calculated, as was done in section 13.4 for the method in *NS 3031:2014*, in section 15.2 for the *CIE Sky Method* and in section 16.2 for the *Hourly Average Method*. The obtained result for the three different methods are compared and shown in graph 17.2. The results shown in graph 17.2 are obtained with the *NS 3031:2014* weather file, and the developed occupancy profile from part III, for the *CIE Sky Method* and the *Hourly Average Method*.

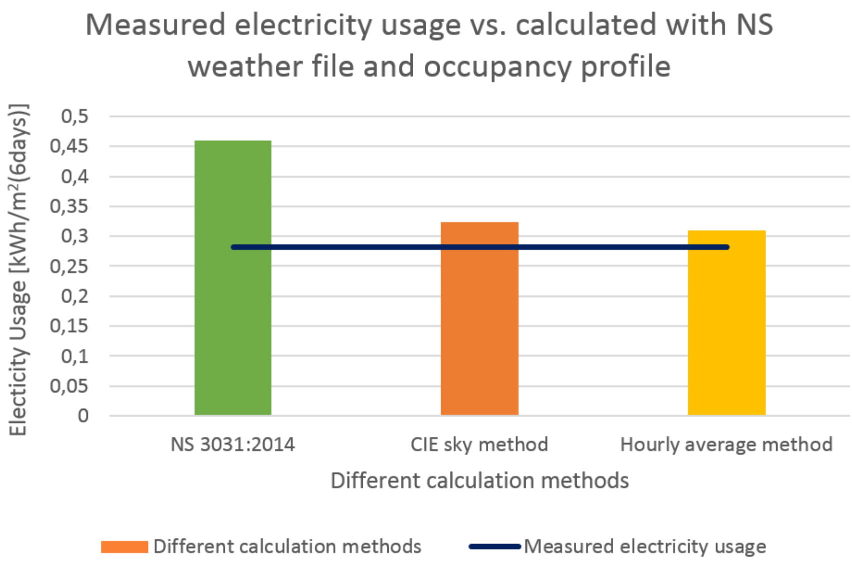

Figure 17.2. The calculated electricity usage from the three different methods for the measurement period of 6 days compared to the measured electricity usage

The results obtained with the *CIE Sky Method* and the *Hourly Average Method* seen in graph 17.2 are fairly close to the measured electricity usage. Both the developed methods slightly over estimates the electricity usage. The *CIE Sky Method* by 12.9 % and the *Hourly Average Method* by 9.0 %.

The electricity usage calculated with the method in *NS 3031:2014* clearly over estimates the electricity usage, possible reasons are explained in section 13.4. The method from *NS 3031:2014* is proved to be inaccurate with a deviation of 39 % from the actual electricity usage. However, the method is more rapid than the *CIE Sky Method* and the *Hourly Average Method* as only the size of the office need to be stated. The method do not require parameters such as the daylight factor, the reflectance of the surfaces, the light transmittance of the glazing, the orientation and the set point and power of the armature which is required in the *CIE Sky Method* and the *Hourly Average Method*. Therefore, the method from *NS 3031:2014* can be stated to be more rapid than the two obtained methodologies. However, as the inaccuracy of the method is high it is preferred to apply the *CIE Sky Method* and the *Hourly Average Method*. The *CIE Sky Method* and the *Hourly*

Average Method both hold the same rapidity as the parameters are required by the user. The two obtained methodologies are further investigated and compared.

The results shown in graph 17.3 are obtained with the measured irradiance weather file, and the actual occupancy during the measurement period.

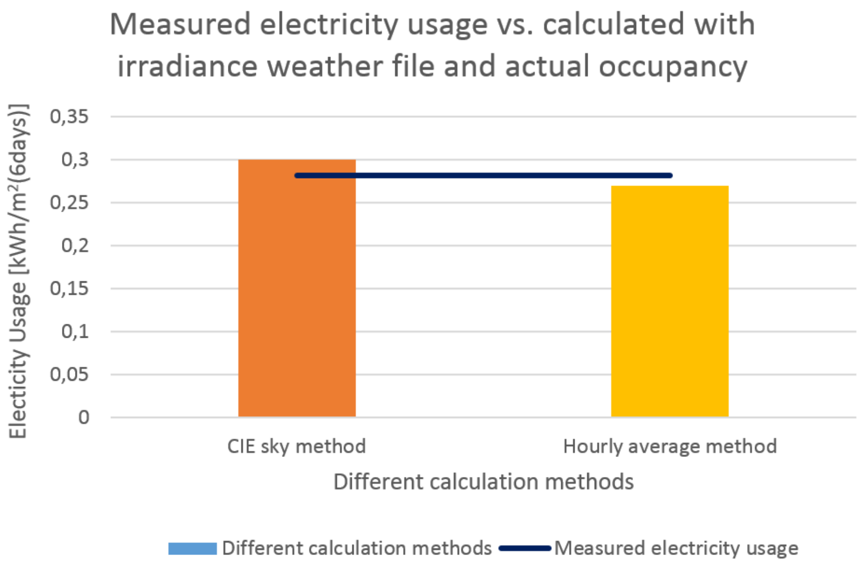

Figure 17.3. The calculated electricity usage by *CIE Sky Method* and *Hourly Average Method* with irradiance weather file and actual occupancy, compared to the measured electricity usage

As seen in graph 17.3 the *Hourly Average Method* underestimates the electricity usage by 4.3 %. Possible reasons for the under estimation are described in section 16.2. The *CIE Sky Method* sky method over estimated the electricity usage by 6.0 %, possible reasons for this deviation are described in section 15.3. With this it can be argued that the deviation between the actual electricity usage and the calculated with the *Hourly Average Method* is smaller than the calculated result with the *CIE Sky Method* and thereby the *Hourly Average Method* is the most accurate methodology.

Even though the *Hourly Average Method* under estimates the measured electricity usage, the *Hourly Average Method* is stated to be the most accurate. The presumably reason for this under estimation is that solar shading is not included in the methodology as discussed in section 16.4.

Another factor which supports the statement that the *Hourly Average Method* is the most accurate methodology is as stated in section 15.3, that the *CIE Sky Method* only takes into account different CIE sky intervals. While the *Hourly Average Method* takes into account the average of every hour throughout the year. This, of course, proves that the *Hourly Average Method* will be the most accurate estimation methodology.

All in all, it can therefore be concluded that the *Hourly Average Method* can rapidly and accurately determine the electricity usage of daylight and occupancy controlled artificial lighting.

17.2 Discussing the *CIE Sky Method* and the *Hourly Average Method*

A deviation of only 4.3 % for the *Hourly Average Method* and 6.0 % for the *CIE Sky Method* is remarkably small, and can be due to a coincidence as there are several uncertainties in the estimation methodologies.

A weakness for both the estimation methodologies is that neither include solar shading. Additional research is needed to implement solar shading.

The parasite load of the control system in the armature in the cell office is not known. This means that there is an uncertainty to the measured electricity usage. If the methodologies were to be further developed, then this uncertainty should be reduced by assessing the parasite load.

Obtaining the interior illuminance with the solar light factor proved to not correspond well with the actual interior illuminance as explained in section 14.7.7. Further investigation of obtaining the interior illuminance level with solar light factors should be conducted for a higher certainty of the methodology.

The reflected component of the exterior illuminance obtained with BSim holds a very high uncertainty. Further exploration is required in order to fully understand this complication.

All these uncertainties, or some of them, can work in the favour of the obtained estimation methodologies causing the obtained estimation methodologies to seam more accurate than they actually are.

Part V

Conclusion

The conclusion is found in this part, the conclusion sums up all significant findings throughout this thesis.

Conclusion 18

The research conducted in this thesis is performed based on the following research question:

How can the electricity usage be rapidly and accurately determined for daylight and occupancy controlled artificial lighting?

The electricity usage of the daylight and occupancy controlled artificial lighting in the cell office in the case building proved to be more dependent on occupancy than daylight.

Stating one specific occupancy profile for all office buildings will include large inaccuracies as there were individual variations in every occupancy profile for every office in the case building. However, after analysing the data one occupancy profile is established for cell offices, and another for open landscape offices varying of size from four to eight people. The obtained occupancy profile is assumed applicable on other office buildings.

As expected the occupancy profile for open landscape offices has a higher amount of weeks per year and hours per day in office, compared to the occupancy profile for a cell office, as a higher number of occupants will prolong the time of presence in the office. It is noteworthy that the statistical data showed that open landscape offices were occupied for $5\frac{1}{2}$ days per week.

As the artificial lighting was controlled by daylight, the available daylight was established prior to calculation of the electricity usage. Different approaches was tried to obtain the available daylight.

Daylight simulation software such as Relux and VELUX Daylight Visualizer require a specified CIE sky condition, and thereby determines the interior illuminance. However, specifying the real sky conditions as different CIE skies proved to be problematic as the variations in the real sky condition is highly complex. Therefore another approach, applying the solar light factor and exterior illuminance obtained with BSim, was utilized in order to obtain the interior illuminance level.

As the total solar light factor is divided down to a diffuse, direct and reflected component the corresponding exterior diffuse, direct and reflected components are required. When obtaining the reflected component in BSim a numerical error was encountered, further investigation of the algorithms in BSim is necessary before this problem can be solved.

The amount of hours where there is not sufficient daylight in the office sums up to the electricity usage of the armature. These hours are calculated differently in the two obtained estimation methodologies; the *CIE Sky Method* and the *Hourly Average Method*.

In the first obtained estimation methodology, the *CIE Sky Method*, the hourly exterior illuminance over a year is sorted into CIE sky intervals. The set illuminance level of the different CIE sky intervals were then applied together with the solar light factor of the cell office to obtain interior illuminance level.

The weakness of the *CIE Sky Method* is that it only takes into account the variation between the CIE sky intervals. The *Hourly Average Method* is therefore developed to increase the accuracy and take into account the average of all 8760 hours of a tear. The interior illuminance level is obtained by applying the solar light factor and the hourly average of the exterior illuminance.

The calculated electricity usage of the daylight and occupancy controlled artificial lighting, in the cell office in the case building, from the method in *NS 3031:2014*, the *CIE Sky Method* and the *Hourly Average Method* are compared to the measured electricity usage. The result showed that the method from *NS 3031:2014* significantly overestimated the electricity usage, while both the *CIE Sky Method* and the *Hourly Average Method* are fairly close to the actual result. It is concluded that the *Hourly Average Method* can accurately and rapidly calculate the electricity usage of daylight and occupancy controlled artificial lighting. This method can for now only be applied for offices in Oslo, but the idea is that it can be developed to included different types of buildings and locations throughout the world.

Bibliography

Adobe, February 2015. Adobe. *The RGB (CMY) Color Model.* URL `http://dba.med.sc.edu/price/irf/Adobe_tg/models/rgbcmy.html`, February 2015. Downloaded: 27-02-2015.

Advanced Buildings, December 2014a. Advanced Buildings. *Useful Daylight Illuminance.* URL `http://patternguide.advancedbuildings.net/using-this-guide/analysis-methods/useful-daylight-illuminance`, December 2014. Downloaded: 10-12-2014.

Advanced Buildings, December 2014b. Advanced Buildings. *Daylight Autonomy.* URL `http://patternguide.advancedbuildings.net/using-this-guide/analysis-methods/daylight-autonomy`, December 2014. Downloaded: 10-12-2014.

Arbeidstilsynet, 2007. Arbeidstilsynet. *Veiledning om Arbeidsmiljøloven og ferieloven*, 2007.

Arvid Skartveit og Tuft, 1998. Jan Asle Olseth Arvid Skartveit og Marit Elisabet Tuft. *An Hourly Diffuse Fraction Model with Correction for Variability and Surface Albedo*, 1998.

Daysim, December 2014a. Daysim. *Engineering Guide.* URL `http://daysim.ning.com/page/program-structure`, December 2014. Downloaded: 10-12-2014.

Daysim, December 2014b. Daysim. *Daysim Subprograms.* URL `http://web.mit.edu/SustainableDesignLab/projects/Daysim/Daysim_flowchart.html`, December 2014. Downloaded: 10-12-2014.

l'Eclairage, May 2015. Comission Internationale de l'Eclairage. *Spatial Distribution of Daylight - CIE Standard General Sky.* URL `http://www.cie.co.at/index.php?i_ca_id=476`, May 2015. Downloaded: 14-05-2015.

Delta-T Devices Ltd, 2007. Delta-T Devices Ltd. *User Manual for the Sunshine Pyranometer typeSPN1*, 2007.

Dementia Enabling Environments, January 2011. Dementia Enabling Environments. *About Lighting.* URL `http://www.enablingenvironments.com.au/AdaptaHome/Lighting.aspx`, January 2011. Downloaded: 28-01-2015.

DIAL GmbH, December 2014a. DIAL GmbH. *DIALux 4.7 - Planning and calculation of skylights with DIALux.* URL `http://www.dial.de/DIAL/en/company/press-announcement/dialux/dialux-47-planning-and-calculation-of-skylights-with-dialux.html?no_cache=1&sword_list%5B0%5D=consumption`, December 2014. Downloaded: 11-12-2014.

DIAL GmbH, **2012**. DIAL GmbH. *DIALux evo 1 User Manual*, 2012.

DIAL GmbH, **December 2014b**. DIAL GmbH. *DIALux Software History*. URL http://www.dial.de/DIAL/en/dialux/software-history.html, December 2014. Downloaded: 11-12-2014.

DIAL GmbH, **December 2014c**. DIAL GmbH. *Software. DIALux*. URL http://www.dial.de/DIAL/en/dialux/about.html, December 2014. Downloaded: 11-12-2014.

Direktoratet for byggkvalitet (DiBK), **2011**. Direktoratet for byggkvalitet (DiBK). *§ 13-12. Lys*, 2011.

Dubois og Blomsterberg, **2011**. Marie-Claude Dubois og Blomsterberg. *Energy and Buildings*, 2011.

al., **2001**. Jens Christoffersen et al. *Dagslysberegninger med SimLight*, 2001.

al., **2009**. Rahul Athalye et al. *Comparison of Results From the Daylighting Simulation of a Side-Lit Classroom Using Daysim With Actual Measured Annual Illuminances*, 2009.

EXTECH Instruments, **2013**. EXTECH Instruments. *User Guide Heavy Duty Digital Light Meter (HD400)*, 2013.

Frost, **March 2013**. Jim Frost. *When is Easter*. URL http://blog.minitab.com/blog/adventures-in-statistics/when-is-easter-for-the-next-2086-years, March 2013. Downloaded: 10-04-2015.

Halsted, **February 2015**. Charles P. Halsted. *Brightness, Luminance, and Confusion*. URL http://www.crompton.com/light/index.html, February 2015. Downloaded: 02-02-2015.

Helvar, **2014a**. Helvar. *DALI Network Router (910)*, 2014a.

Helvar, **2014b**. Helvar. *iDim Sense System and Standalone (315)*, 2014b.

Henderson, **January 2015**. Tom Henderson. *The Electromagnetic and Visible Spectra*. URL http://www.physicsclassroom.com/class/light/Lesson-2/The-Electromagnetic-and-Visible-Spectra, January 2015. Downloaded: 26-01-2015.

Indiana University Bloomington, **January 2015**. Indiana University Bloomington. *Energy Filtered Transmission Electron Microscopy*. URL http://sites.bio.indiana.edu/~cryo/eftem.html, January 2015. Downloaded: 26-01-2015.

Jensen, **1996**. Henrik Wann Jensen. *Global Illumination using Photon Maps*, 1996.

Jones, **January 2015**. Andrew Zimmerman Jones. *What is a Photon?* URL http://physics.about.com/od/lightoptics/f/photon.htm, January 2015. Downloaded: 26-01-2015.

Karlsen, **2014**. Line R. Karlsen. *Lyskrav og energibruk til belysning LENI*. 2014, 2014.

Kolb, **October 2011**. Helga Kolb. *Simple Anatomy of the Retina*. URL http://webvision.med.utah.edu/book/part-i-foundations/simple-anatomy-of-the-retina/, October 2011. Downloaded: 26-01-2015.

Larsen og Shakespeare, 1998. Greg Ward Larsen og Rob Shakespeare. *Rendering with Radiance, The Art and Science of Lighting Visualization.* ISBN:1-55860-499-5, The Morgan Kaufmann Series in Computer Graphics and Geometrical Modeling. Morgan Kaufmann Publishers, Inc., 1. udgave, 1. oplag edition, 1998.

Lighting Ever, February 2015. Lighting Ever. *Basic Lighting Interation Terminology.* URL `http://www.lightingever.com/kbase/learninglighting/basic-lighting-interation-terminology.html`, February 2015. Downloaded: 02-02-2015.

Lund og Lund, May 2015. Dr. Adam Lund og Mark Lund. *Measures of Central Tendency.* URL `https://statistics.laerd.com/statistical-guides/measures-central-tendency-mean-mode-median-faqs.php`, May 2015. Downloaded: 15-05-2015.

Luxlak, December 2014. Luxlak. *NCS farver.* URL `http://luxlak.dk/farver/ncs-farver/`, December 2014. Downloaded: 07-12-2014.

Moon, 2010. Kee S. Moon. *Residential Scale Helium Solar Stirling Engine*, 2010.

Norges vassdrags- og energidirektorat (NVE), September 2011. Norges vassdrags- og energidirektorat (NVE). *Bilder av NVE-bygget i Middelthunsgate 29.* URL `http://www.nve.no/no/Om-NVE/Presserom/Bilder-av-NVE-bygget-i-Middelthunsgate-29/`, September 2011. Downloaded: 11-12-2014.

Norsk Lysteknisk Komité, 2014. Norsk Lysteknisk Komité. *Lyskultur faktaark Dagslysfaktor*, 2014.

NREL Buildings Research, July 2014. NREL Buildings Research. *Solar Irradiance Measurements.* URL `https://buildingsfieldtest.nrel.gov/solar_irradiance_measurements`, July 2014. Downloaded: 12-02-2015.

NVE, December 2014. NVE. *Karakterskalaen.* URL `http://www.energimerking.no/no/Energimerking-Bygg/Om-energimerkesystemet-og-regelverket/Energimerkeskalaen/`, December 2014. Downloaded: 07-12-2014.

NVE og Entra, 2011. NVE og Entra. *Det nye NVE-huset*, 2011.

Pernigotto et al., 2014. Pernigotto et al. *Multi-year and Reference Year Weather Data for Building Energy Labelling in North Italy Climates*, 2014.

Piatt, January 2015. Meagan Piatt. *Photoelectric Effect.* URL `http://chemcanbecool2.weebly.com/the-electron.html`, January 2015. Downloaded: 26-01-2015.

Programme, March 2015. United Nations Environment Programme. *Why Buildings.* URL `http://www.unep.org/sbci/AboutSBCI/Background.asp`, March 2015. Downloaded: 03-03-2015.

Prolys, December 2014. Prolys. *Lysrør.* URL `http://www.prolys.no/?aid=9060561`, December 2014. Downloaded: 04-12-2014.

Quaschning, May 2003. Prof. Dr. Volker Quaschning. *The Sun as an Energy Resource*. URL `http://www.volker-quaschning.de/articles/fundamentals1/index.php`, May 2003. Downloaded: 02-02-2015.

R. Labayrade et al., 2009a. R. Labayrade et al. *Assessment of Velux Daylight Visualizer 2 Against CIE 171:2006 Test Cases*, 2009a.

R. Labayrade et al., 2009b. R. Labayrade et al. *Validation of Velux Daylight Visualizer 2 Against CIE 171:2006 Test Cases*, 2009b.

Radsite, Radiance-online, December 2014. Radsite, Radiance-online. *Detailed Description*. URL `http://www.radiance-online.org/about/detailed-description.html`, December 2014. Downloaded: 08-12-2014.

Reinhart og Breton, 2009. Christoph Reinhart og Pierre-Felix Breton. *Experimental Validation of Autodesk 3ds Max Design 2009 and Daysim3.0*, 2009.

RELUX Informatik AG, 2012. RELUX Informatik AG. *Relux Suite flyerl*, 2012.

RELUX Informatik AG, 2007. RELUX Informatik AG. *Relux Professional 2007 Manual*, 2007.

RELUX Informatik AG, 2011. RELUX Informatik AG. *Relux Raytracing Manual*, 2011.

RELUX Informatik AG, 2013. RELUX Informatik AG. *Relux Suite 2013 Manual*, 2013.

Saint Gobain Glass, 2014. Saint Gobain Glass. *Solavskärmanda energispareglad*, 2014.

Satel-Light, April 2015. Satel-Light. *Advanced User Guide - The Satel-Light Project*. URL `http://www.satel-light.com/guide/advsatel.htm`, April 2015. Downloaded: 13-04-2015.

SINTEF Byggforsk, 1997. SINTEF Byggforsk. *Byggforskserien Byggdetaljer 421.610 Krav til lys og belysning*, 1997.

SINTEF Byggforsk, 2004. SINTEF Byggforsk. *Byggforskserien Byggdetaljer 421.625 Dagslysinnfall og sparepotensial for belysningsenergi*, 2004.

Skanska Norge AS, 2014. Skanska Norge AS. *Middelthunsgate 29 - NVE, FVD-instruks, 1.Forvaltning*, 2014.

S.L. Energiteknik ApS, 2015. S.L. Energiteknik ApS. *Power KWh Detective User Manual*, 2015.

Standard Norge, 2007. Standard Norge. *Norsk Standard NS 3031:2007+A1:2011, Beregning av bygningers Energiytelse, Metode og Data*, 2007.

Statens Byggeforskningsinstitut, 2010. Statens Byggeforskningsinstitut. *BSim User's Guide*, 2010.

Statens Byggeforskningsinstitut, 2008. Statens Byggeforskningsinstitut. *SBi-anvisning 219, Dagslys i Rum og Bygninger*, 2008.

Statens Byggeforskningsinstitut, 2013. Statens Byggeforskningsinstitut. *Daylight Calculations in Practice*, 2013.

Statens Byggeforskningsinstitut, **2003**. Statens Byggeforskningsinstitut. *Anvisning 203 Beregning af dagslys i bygninger*, 2003.

Taylor, **2009**. Dr. Jeffrey L. Taylor. *Reflectance Measurements of Materials Used in the Solar Industry*, 2009.

Technical Committee CEN/TC 169, **2006**. Technical Committee CEN/TC 169. *PrEN 15193: Energy performance of buildings and Energy requirements for lighting*, 2006.

Time og AS, **March 2015**. Time og Date AS. *Oslo, Norway - Sunrise, Sunset and Daylength, Marts 2015*. URL `http://http://www.timeanddate.com/sun/norway/oslo?month=3&year=2015`, March 2015. Downloaded: 04-06-2015.

Tom Henderson, **January 2015**. Tom Henderson. *Light Absorption, Reflection, and Transmission*. URL `http://www.physicsclassroom.com/class/light/Lesson-2/Light-Absorption,-Reflection,-and-Transmission`, January 2015. Downloaded: 26-01-2015.

Tsangrassoulis og Bourdakis, **2002**. A. Tsangrassoulis og V. Bourdakis. *Comparison of Radiosity and Ray-tracing Techniques with a Practical Design Procedure for the Prediction of Daylight Levels in Atria*, 2002.

U.S. Department of Energy, **2011**. U.S. Department of Energy. *Building Energy Software Tools Directory*. URL `http://apps1.eere.energy.gov/buildings/tools_directory/software.cfm/ID=415/pagename_submenu=energy_simulation/pagename_menu=whole_building_analysis/pagename=subjects`, 2011. Downloaded: 11-12-2014.

VELUX Daylight Visualizer, **2014a**. VELUX Daylight Visualizer. *Manual 3D Importer*, 2014a.

VELUX Daylight Visualizer, **2014b**. VELUX Daylight Visualizer. *Manual 3D Modeller*, 2014b.

Voltimum, **2015**. Part L. Voltimum. *LENI - what it means and what it does*, 2015.

Witzel, **2012**. Daniel Witzel. *DIALux evo - new calculation method*, 2012.

Part VI

Appendix

Detailed Building Description A

A.1 The Façades

The main façade with the main entrance is facing towards west. The façade has a curved shape as seen in picture A.1. The Frogner Park is on the west side of the building, which means that the west façade is rather exposed to the sun. There is no shading from adjacent buildings, and only a few planted threes on the west side of the building as well as the road Middelthunsgate.

Figure A.1. The West façade of the NVE-building

The North and South façades can be seen on figures A.2 and A.3.

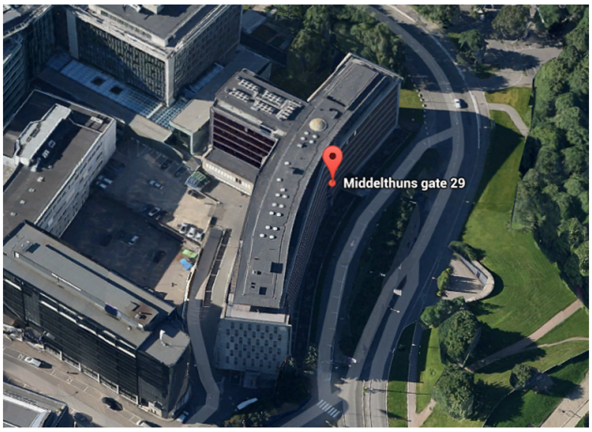

Figure A.2. 3D view of the North façade from Google Maps

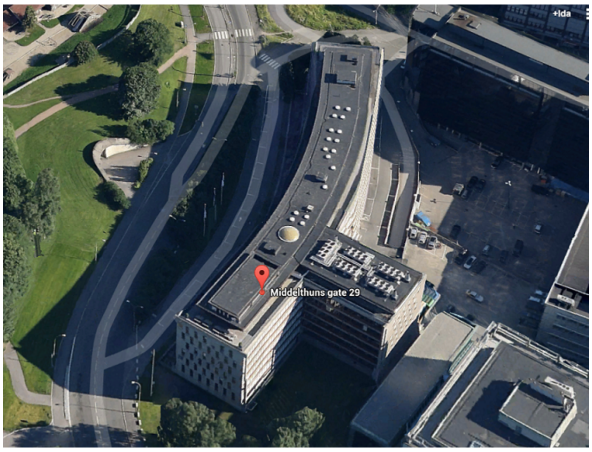

Figure A.3. 3D view of the South façade from Google maps

The East and West façades can be seen on figures A.4 and A.5.

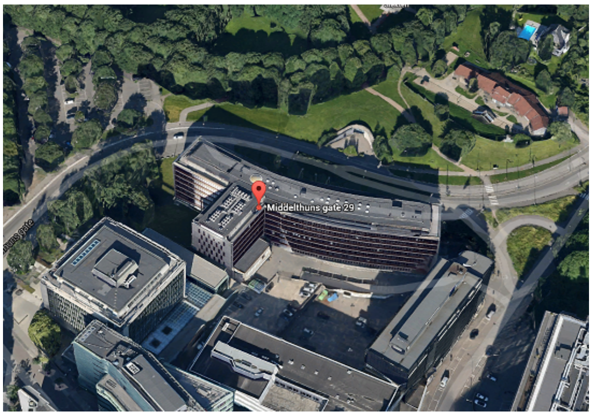

Figure A.4. 3D view of the East façade from Google Maps

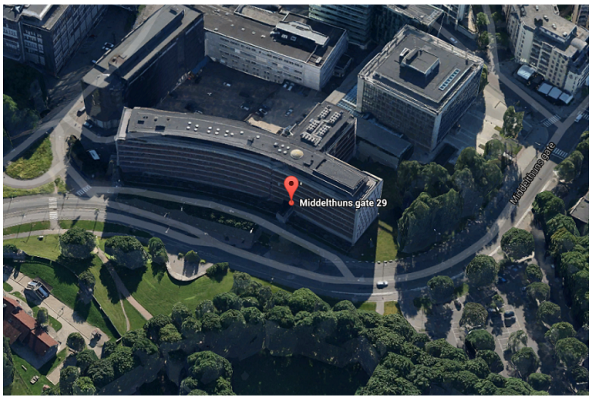

Figure A.5. 3D view of the West façade from Google maps

Towards the North there is no obstacles, which means the building is exposed. On the East side of the building there is a wing, this wing is close to the neighbouring building towards the East which means that the East façade on this wing will not be exposed to the sun. The rest of the east façade was initially exposed to the sun as it was a parking lot there, but at the time of writing there is a construction site on the east side of the NVE-building. There will be built a new office building that will be approximately 3 m higher than the NVE building, marked with red in figure A.6. This will ensure less direct sunlight at the east façade. On the south side of the building there a few rather tall trees which ensure shade on the lowest floors on the south façades.

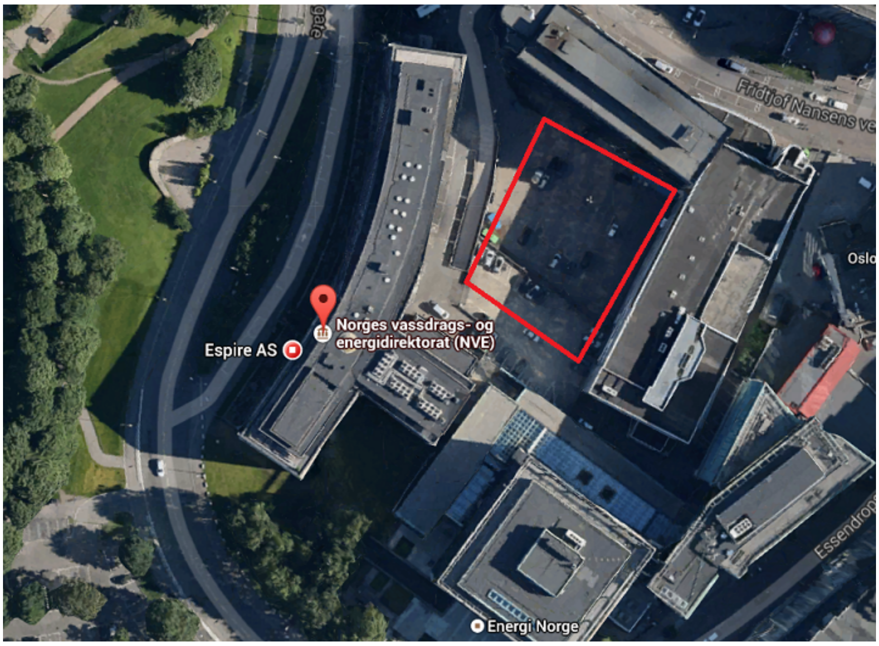

Figure A.6. The construction site on the East side of the building

Most of the surrounding buildings have a glazed façade, there have been complaints form the occupants due to glare, and especially from the black building to the East of the office building see A.9.

A.2 Floor Description

Figure A.7 show a section view of the case building, the location of the cell office is marked with yellow.

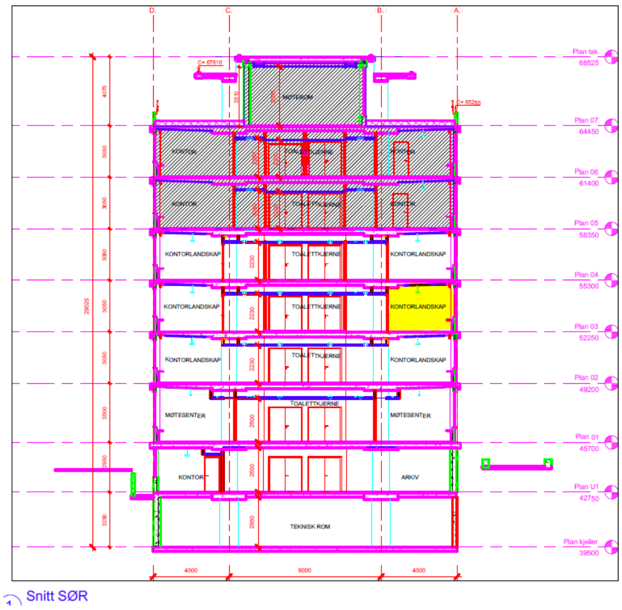

Figure A.7. Section view from South.

Figure A.8 is an elevation view of the East façade, the two windows for the cell office is marked with yellow.

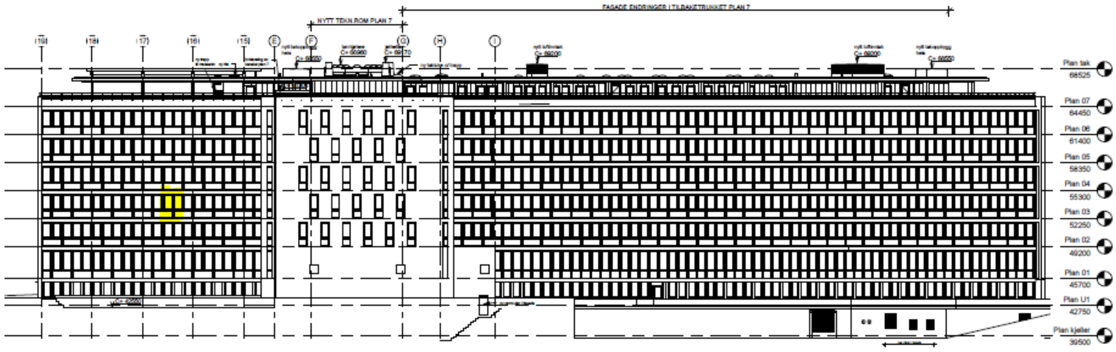

Figure A.8. Elevation view of the East façade.

A.3 The Zones

The measurements for the electricity usage are performed for the whole building, as well it is divided down to the floor level. The third floor is further divided into four zones, it is focused on the south zone for the measurements. The south zone is the smallest and least complex zone which mainly consist of cell offices and open landscape offices. In the south zone cell office for further investigation is located, cell office 3S21 facing east.

Figure A.9 illustrates the location of the south zone on the third floor marked with yellow.

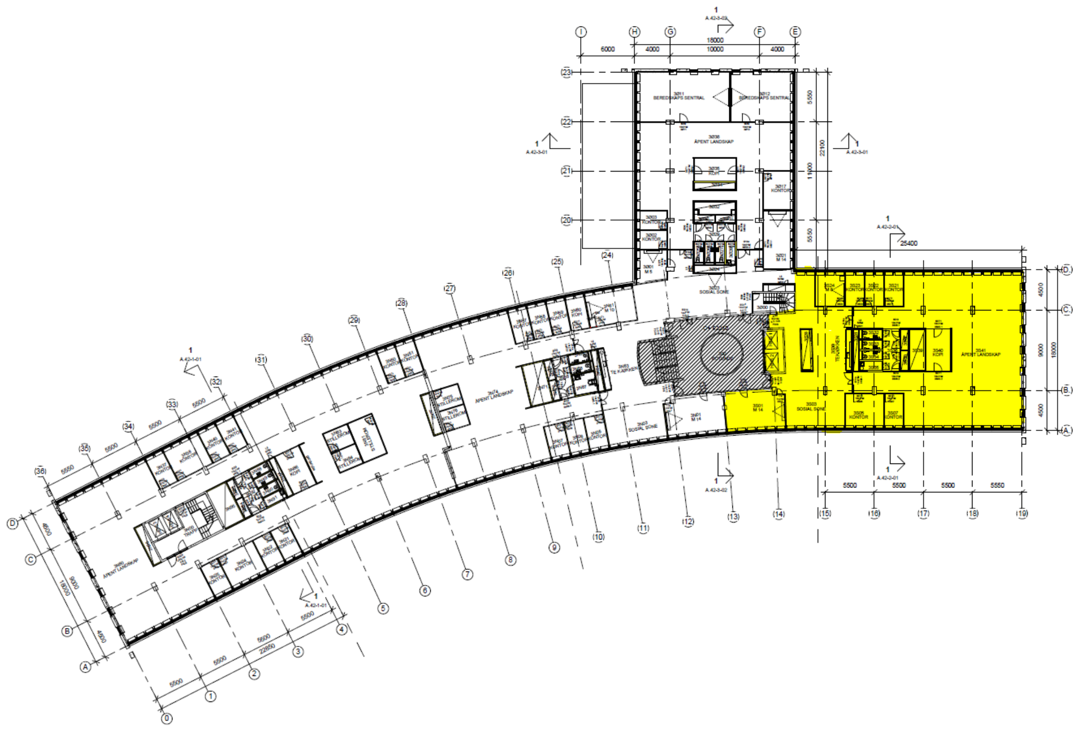

Figure A.9. The south zone marked with yellow on the 3^{rd} floor.

Figure A.10 shows the south zone and the cell office is marked with yellow.

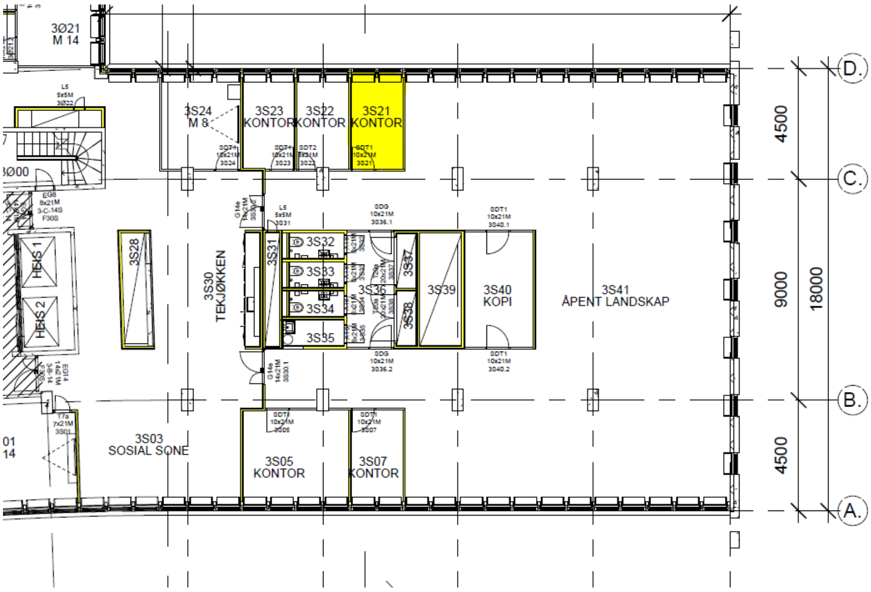

Figure A.10. Cell office 3S21 facing east in the south zone on the 3^{rd} floor.

Figure A.11 shows a furniture plan of the south zone, and the cell office is marked in yellow.

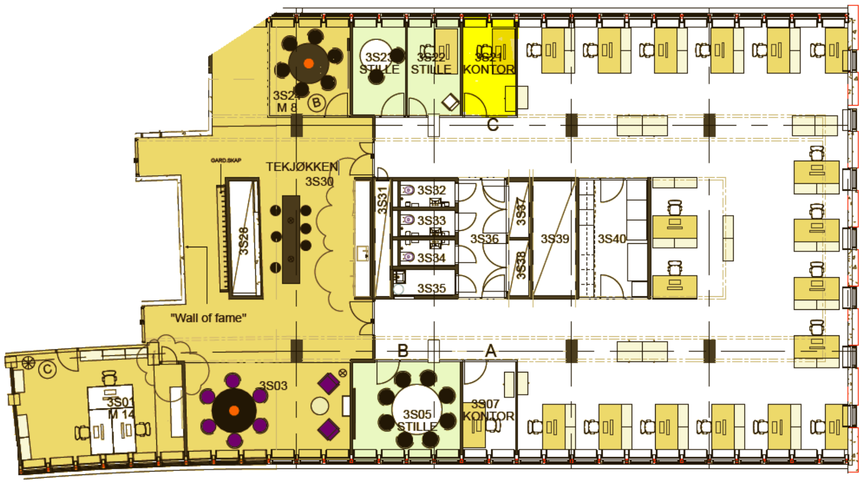

Figure A.11. Furniture plan of the south zone on the 3^{rd} floor.

The orientation of the east, south and west façades are illustrated in figure A.12.

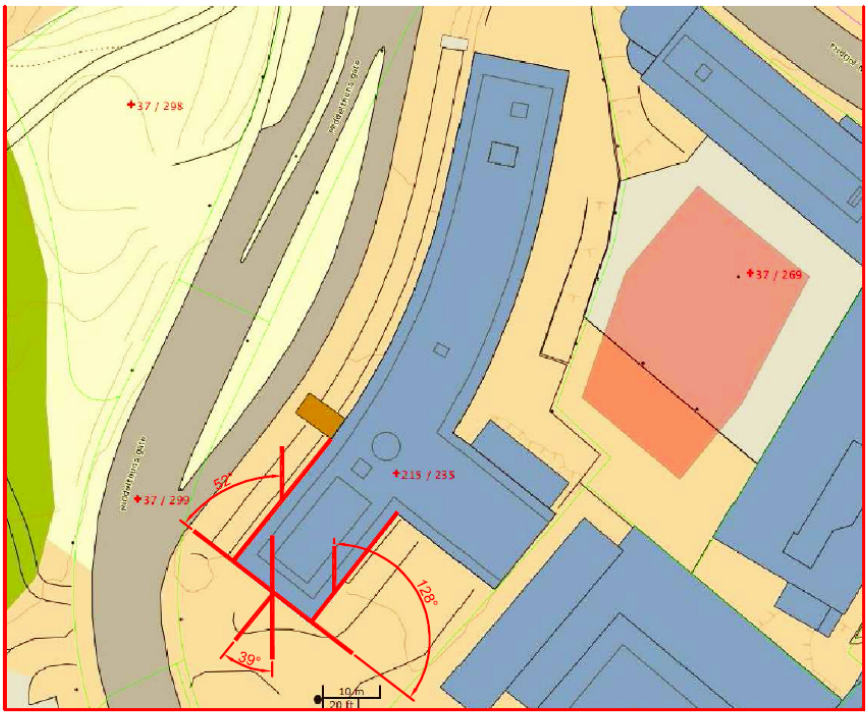

Figure A.12. The orientation of the façades measured with AutoCAD on the map obtained from Kartverket

The cell office facing east can be seen in figure A.13.

Figure A.13. Cell office 3S21 facing east, towards the façade

Figure A.14. Cell office 3S21 facing east, towards the corridor

A.4 Simulation Model

A single cell office was simulated in different simulation software. The dimensions of the cell office can be seen in figure A.15 and A.16.

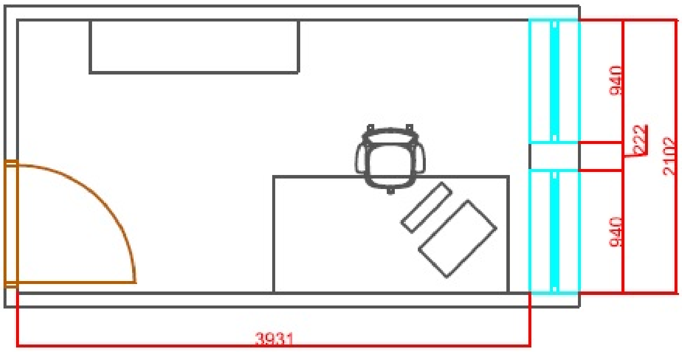

Figure A.15. Cell office plan with dimensions

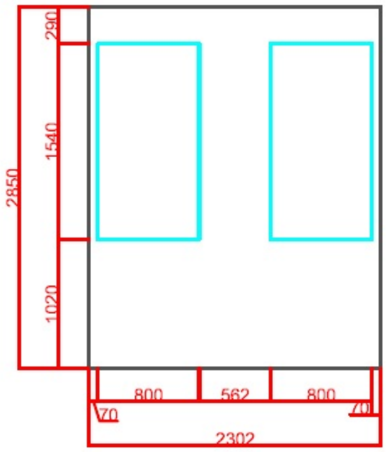

Figure A.16. façade with dimensions

Figure A.15 and figure A.16 are applied in Relux and Velux. The exact same AutoCAD or Sketchup model has been applied in order to reduce inaccuracy in different model geometries in the simulation results.

A.5 Renovation

The renovation was performed in order to ensure an improved energy efficiency for the building. It was important for both the building owner an the tenant.

The main focuses for the renovation besides improved energy efficiency was universal design, correct lighting and well defined traffic zones (NVE og Entra, 2011).

The main focuses for improved environmental effects were replacement of electrical heating radiators by radiators running on district heating, heat recovery on the ventilation system and improved thermal envelope. In order to ensure improved thermal envelope the following were performed:

- 2000 m^2 of glazing are replaced by grazing with krypton gas in the spacing with a U-value of 0.9.
- Grouting and sealing of external walls
- External walls on the seventh floor are replaced by new well isolated walls
- Improved insulation on the roof by replacing Leca with 30 cm of insulation
- Improved insulation in the garage

Preservation

The Directorate for Cultural Heritage preserved parts of the building in 2004, therefore parts of the building were preserved during the renovation:

- The cafeteria
- The main entrance
- The staircase in the core of the building and the rotunda
- Two office wings on the fifth and sixth floor on the south and south-east wings
- Meeting room on the south wing on the seventh floor
- Both inside and outside of the façade

In order to ensure improved energy efficiency and keep the architectural expression of the building which the Directorate for Cultural Heritage desired, the windows were rehabilitated as explained in section A.8.

A.6 Floor description

The building has a total usable area (BRA) of 16 874 m^2. Its curved shape and the use of materials, such as exposed concrete, glass and teak wood gives it a distinctive look. All these materials are preserved both on the inside and outside of the façades (NVE og Entra, 2011). Outside the west façade, on the first floor where the main entrance is located, it is a small pool following the shape of the building.

Figure A.17. West façade with main entrance and pool seen from the roof terrace.

The building has seven floors, with one floor and a basement below the ground, as seen in picture A.18.

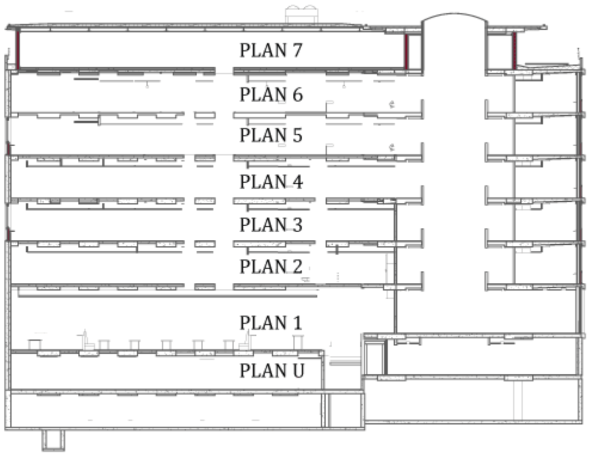

Figure A.18. Section view of the building seen from the North side

The area of each floor and their different room heights can be seen in the following tables: A.1 and A.2. All areas and room heights are measured by Skanska Norge AS (Skanska Norge AS, 2014)

Floor	Area [m^2]
Basement	3595
Underground floor	2425
1^{st} floor	1485
2^{nd} floor	2716
3^{rd} floor	2716
4^{th} floor	2715
5^{th} floor	2715
6^{th} floor	2715
7^{th} floor	965
Total	22047

Table A.1. Area of each floor.

The east part of the underground floor and the 1^{st} floor is elevated half a stair up due to the room height in the canteen located on the 2^{nd} floor. The room height of each floor can be seen in table A.2

Floor	Room height [m]
7th floor	2.42
7th floor corridor	2.21
2nd-6th floor, east wing	2.74
2nd-6th floor, the rest of the floor	2.23
6th and 5th floor, preserved areas	2.38
1st floor east wing	3.20
1st floor, the rest of the floor	2.60
Underground floor, east wing	2.60
Underground floor, the rest of the floor	2.21
Basement/Garage	1.95

Table A.2. Room height of each floor.

The second to sixth floor is the office floors. They all contain both cell offices and open landscape offices. A typical workspace module can be seen in picture A.19.

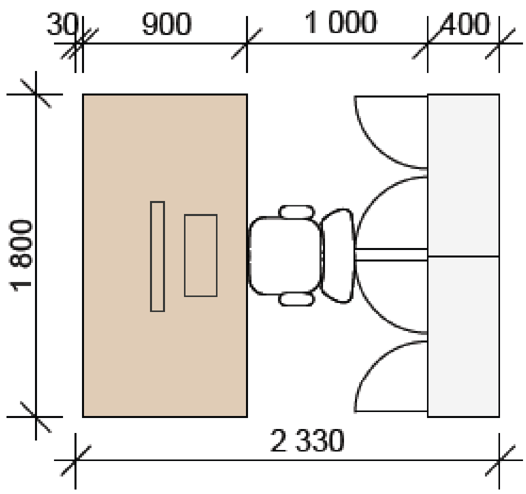

Figure A.19. A typical workspace module with measurements

A staircase and elevators are located in the north wing of the building from the basement to the seventh floor. Every floor from the underground to the seventh floor has a little kitchen area.

A.7 Energy Labelling

The Norwegian standard states that all commercial buildings over 1000 m^2 must be energy labelled. The energy label describes the buildings energy standard and is represented by a colour and a letter.

The energy rank, from A to G, is based on the calculated supplied energy. The calculations are made out of normal use in average climate conditions. An A means that the building is energy efficient, while a G means that the building is not very energy efficient. A building constructed after the 2007 standard regulations will normally receive a C.

The heating rank is divided into four grades from red to green and represents how much of the heating demand is covered by electricity, oil or gas. Green means a low amount of the heating demand is covered by electricity, oil or gas, while red means a high amount of the heating demand is covered by one of the above mentioned sources. The building must cover the heating demand with electricity by less than 30% to obtain the green label. The purpose of the heating grade is to lead to an increased use of renewable energy sources for heating such as heating pumps, solar energy, biomass and district heating.

There is no correlation between the energy rate (the letter) and the heating rate (the colour), so a good energy rate does not necessarily mean a good heating rate and vice versa (NVE, December 2014).

This building was labelled with a green B as 30% or less of the heating demand is covered by electricity, and the rest by district heating. The building has a supplied energy per m^2 heated usable area (BRA) of 120 kWh/m^2, which is close to the regulation for office buildings A.21 (NVE, December 2014).

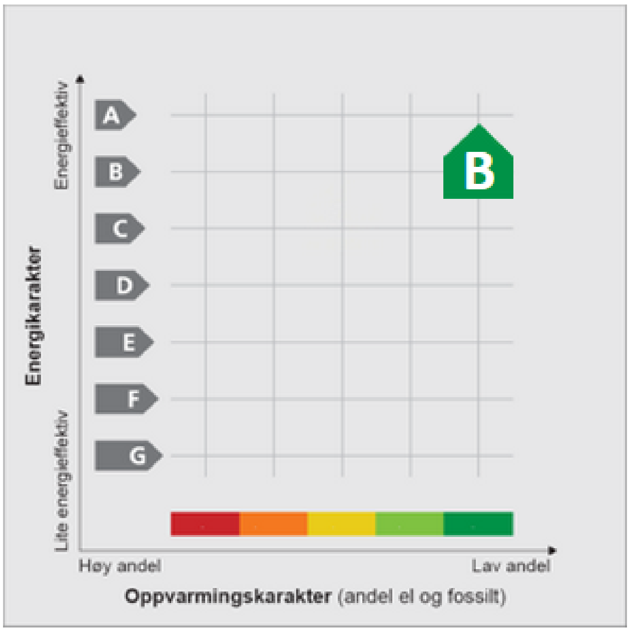

Figure A.20. Energy label for this building

Bygningskategorier	Levert energi pr m^2 oppvarmet BRA (kWh/m^2)						
	A	B	C	D	E	F	G
	Lavere enn eller lik	Lavere enn eller lik	Lavere enn eller lik	Lavere enn eller lik	Lavere enn eller lik	Lavere enn eller lik	Ingen grense
Småhus	**85,00+800/A**	**115,00+1600/A**	**145,00+2500/A**	**175,00+4100/A**	**205,00+5800/A**	**250,00+8000/A**	**> F**
Leiligheter (boligblokk)	**75,00+600/A**	**95,00+1000/A**	**110,00+1500/A**	**135,00+2200/A**	**160,00+3000/A**	**200,00+4000/A**	**> F**
Barnehage	80,00	110,00	145,00	180,00	220,00	275,00	> F
Kontorbygning	85,00	115,00	145,00	180,00	220,00	275,00	> F
Skolebygning	70,00	100,00	135,00	175,00	220,00	280,00	> F
Universitets- og høgskolebygning	85,00	125,00	160,00	200,00	240,00	300,00	> F
Sykehus	165,00	235,00	305,00	360,00	415,00	505,00	> F
Sykehjem	140,00	190,00	240,00	295,00	355,00	440,00	> F
Hotellbygning	125,00	185,00	240,00	290,00	340,00	415,00	> F
Idrettsbygning	115,00	160,00	205,00	275,00	345,00	440,00	> F
Forretningsbygning	105,00	155,00	210,00	255,00	300,00	375,00	> F
Kulturbygning	85,00	130,00	175,00	215,00	255,00	320,00	> F
Lett industribygning, verksted	100,00	140,00	185,00	250,00	315,00	405,00	> F

Figure A.21. The Norwegian energy rating scale per 01.07.2013

A.8 The windows

There are three window types in the building, two of the types are constructed by Norgesvinduet Bjorlo AS and the last type is the original window that is then renovated. All windows in the office areas on the second to the sixth seventh floor is renovated original windows, this is because the façade is preserved by The Directorate for Cultural Heritage. These windows are renovated by Edvarsson Entreprenor Bygg AS. During the renovation of the building, the glazing and frame of the windows were kept original. They were reconstructed with krypton gas filling with a spacing of 10mm and improved sealing of the frame with silicone and EPDM-list in order to ensure a break of cold bridges. The frames are teak and they are the original from 1964.

The window type for second to sixth floor is "4mm cool-lite SKN178 + 10 krypton varm kant + 4 mm", and the window type on the first and seventh floor, and in the cafeteria, are safety glazing "8mm laminert cool-lite + 10 krypton varm kant + 6 mm."

The window type which will be considered in this report is the type for second to sixth floor, the SKN178 with 10mm krypton. The different glazing properties are as seen in figure A.22.

Egenskaper	SGG COOL-LITE® SKN 178 SGG PLANILUX®
Dagsljus (EN410)	6-15-4
Reflektion utvändig LR%	12
Reflektion invändig LR%	13
Transmission LT%	70
Ra-index	96,4
Solenergi (EN410)	
Primär transmission	38
Absorbtion (Total)	31
Solfaktor SF	0,40
U-värde W/m² K (EN673)	
Luft	1,4
Argon	1,1
Krypton (gäller 12 mm)	1,0

Figure A.22. The SKN178 10 mm krypton (Saint Gobain Glass, 2014)

The window type for second to sixth floor are pictured in figure A.23 from the outside of the building.

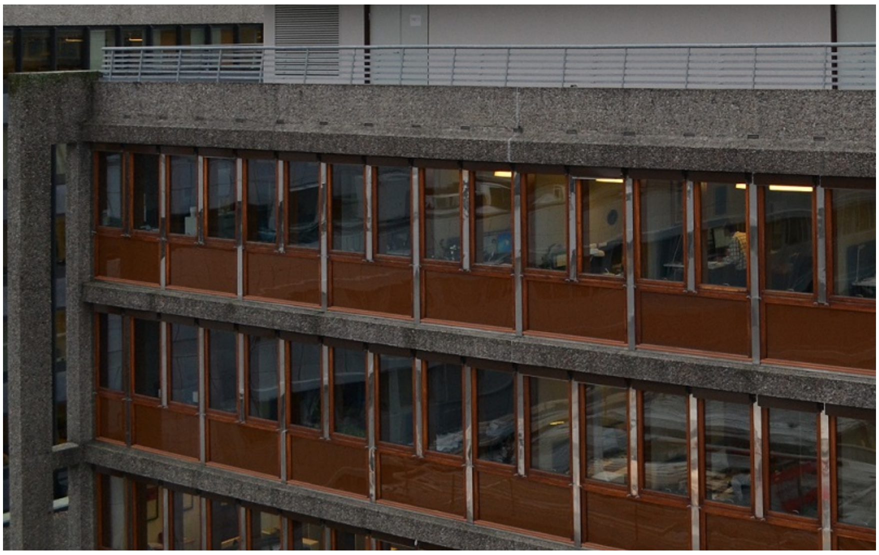

Figure A.23. The windows on fifth and sixth floors

None of the windows in the building can be opened due to the external venetian blinds which will be described in section A.9. The windows are professionally cleaned twice a year by Resco AS.

A.9 Technical Installations

short description of all the technical installations

The Zones

In total there are eight measuring devices for artificial lighting in the office building, four of these are placed on the third floor. The third floor consist of cell and open space offices, as well as meeting rooms, toilets, changing rooms, kitchen areas, printer rooms, corridors and common areas.

As mentioned, the measurements for distributed electrical usage have four measuring devices on the third floor, and the third floor is therefore divided into four zones. Two are in the north wing, and one is located in each of the south and East wings. The different zones are illustrated on figure A.24 with the furnishing plan.

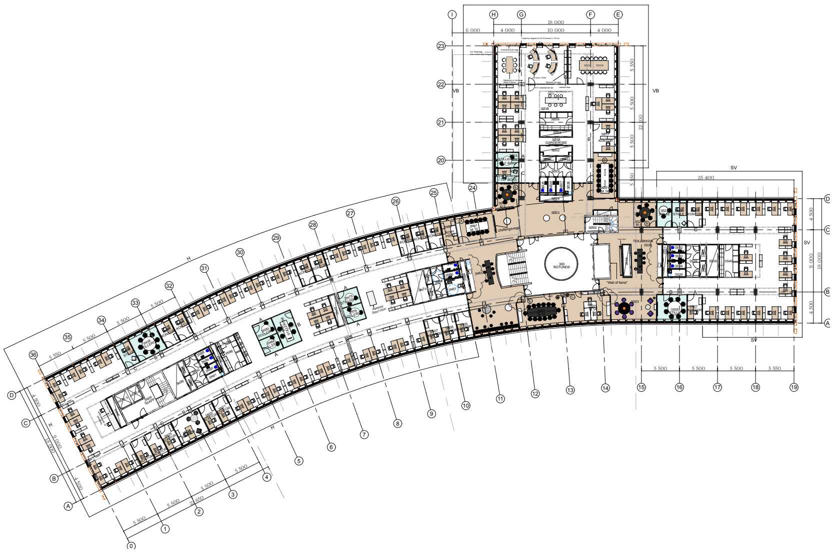

Figure A.24. The zones and the furnishing

As seen in figure A.25 the intersection of the middle zone and the East zone is not in an internal wall as most of the other intersections. There are two armatures in this corner as seen in figure A.25, where the armature to the North belongs to the middle zone and the armature to the East belongs to the East zone. The same goes for the intersection between the East and South zones. The following figures illustrate the zones with electrical installations.

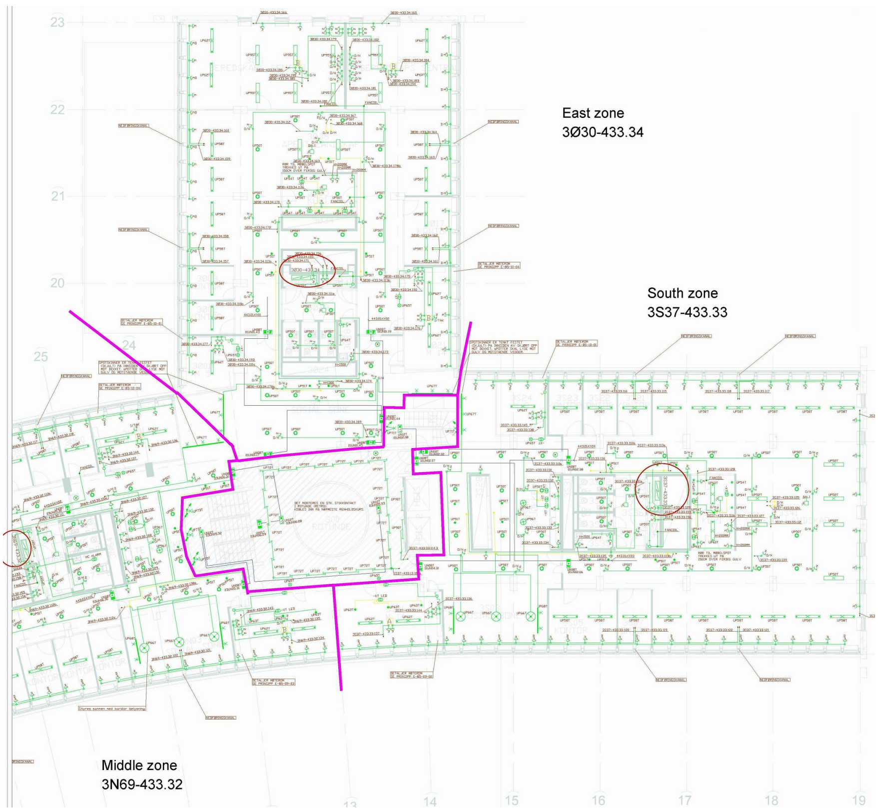

Figure A.25. The middle, the East and the South zones with electrical installations

The North zone is illustrated on figure A.26 with the adjacent zone, the middle zone.

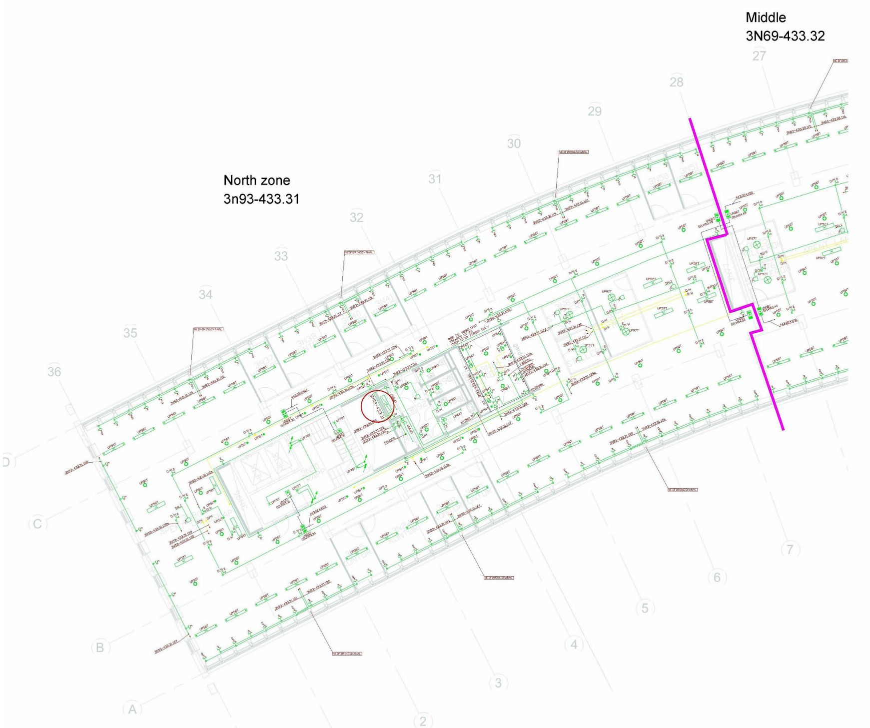

Figure A.26. The North and the middle zone with electrical installations

The North Zone

The zone furthest to the North include open office areas along the external walls toward East and West, and in the North end. There are six cell offices on the West side, and five on the west as well as a meeting room. In the middle of the wing there are three meeting rooms, changing rooms and toilets as seen in figure A.26. The measuring device for this zone is labelled 3N93-433.31.

The Middle Zone

The zone in the North wing but closer to the core of the building is named the middle zone and it consist of an open office area on the East and one on the West side, as well as three cell offices. The zone also has three meeting rooms, a printer room, toilets and a kitchen and common room area as seen in figures A.26 and A.25. The measuring device for this zone is labelled 3N69-433.32.

The East Zone

The zone in the East wing includes three cell offices, one towards South and two towards North. It has five meeting rooms, one towards South, two towards North and two rather large meeting rooms facing South. In the centre it is an open office space, and towards the core of the building it is a common area as seen in figure A.25. The measuring device for this zone is labelled 3ø30-433.34.

The South Zone

The last zone is facing south, the zone has three meeting rooms where one is facing West and the other to towards East. The zone also has two cell offices towards the East and one towards the south, and closer to the core of the building is has a large common area with kitchen. In the South end it has a large open office space area as illustrated on figure A.25. The measuring device for this zone is labelled 3S30-433.33.

The Control System

In this office building it is only the open landscape offices and the cell offices by the windows that are controlled with both presence detectors and light sensors. The open landscape offices deeper into the building, the corridors, the meeting rooms, toilets and kitchens are controlled only by presence detectors. There are no light switches in this office building.

The sensors are installed in the armature as seen in picture A.27. The sensors are luminaire-based DALI sensors which include a passive infrared presence detector and a light sensor for constant light function (Helvar, 2014b).

Figure A.27. The sensor is installed in the armature

All the sensors are connected to the DALI network router which controls how the system should operate. This system will provide energy-saving due to presence detectors and constant light functionality (Helvar, 2014a). The DALI sensor can be seen in figure A.28.

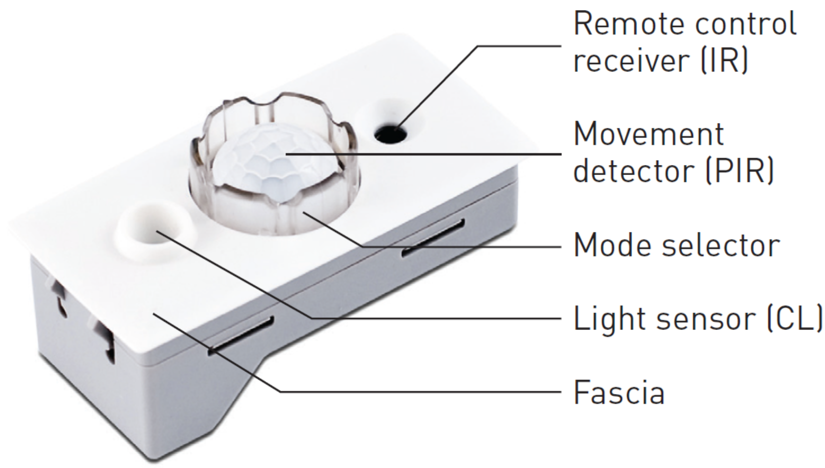

Figure A.28. The DALI sensor (Helvar, 2014b)

The presence detectors also control the ventilation system and heating in the building. The OPC server controls the ventilation and heating system. The OPC server receives signals from the KNX system which communicates with the DALI sensors through a Wago controller. The OPC sensor controls the set point for heating and ventilation and sends the signals back to the KNX system, while DALI controls the armature.

The system is set to operate for 15 minutes. If there is no presence detected, then the artificial light, heating and ventilation will turn off. In some cell offices and meeting rooms it turns off after 20 minutes due to complaints from the occupants.

Each of the four zones in the building is divided further down into several zones for control of the artificial lighting, ventilation and heating. One open office area is one zone, as well as one cell office is one zone, the toilets is another and the common area is one zone. The corridors are divided into traffic zones. This means that if a person enters the corridor there will be artificial light in that traffic zone the persons enter, as well as the traffic zones which leads to the closest toilet and exit.

Types of Armatures

The fluorescent lights are not LED as one would expect in an energy efficient office building, but as this building is preserved it was chosen to use T5 fluorescent. The T5 fluorescent are both energy efficient and has a high efficiency, they also have a warmer colour of the light beam (Prolys, December 2014).

Solar Shading

The sensor for the control system for the external venetian blinds are on the façade of the building, the building is divided into twelve vertical zones as seen in figure A.29.

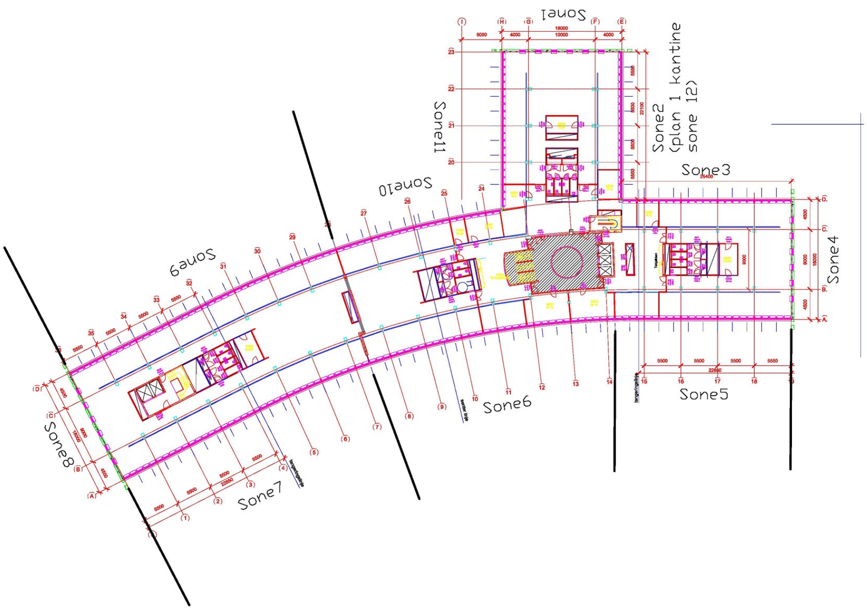

Figure A.29. The twelve zones for the control system of the solar shading

Initially a weather station on the roof controlled the external venetian blinds, but due to complaints of glare from surrounding buildings from the occupants, the solar shading is now controlled with sensors installed on the façade for every zone. The blinds have a central control system, which means that the occupants cannot adjust the blinds after their particular needs.

As mentioned earlier, there have been complaints due to glare from the black glazed building to the East of the office building, as well as from direct sunlight hitting the working station of the occupants.

A.10 Materials and Surfaces

Walls

The cell offices, meeting rooms and silent rooms are made out of module walls delivered by Modulvegger Oslo AS. The cell offices has a glazed wall with 6 mm tempered glazing and white frames and two walls with a 13 mm plasterboard surface on both sides, painted in white. For the glazed walls in the meeting- and silent rooms, the glazing is 8.76 mm laminated glass.

All teak wood on the inside and outside of the façade, as well all teak elements in doors and doorframes, is preserved due to the historical protection of the building, and is only treated with varnish: 60% Benar Matt and 40% Benar UVR which leads to a matt surface.

The walls facing the the middle core of the third floor are made out of painted gypsum and plastered concrete and are painted light grey (NCS S 2502-Y). The wall dividing the large silent room with the two smaller silent rooms in the north part of the building is painted in a darker shade of grey (NCS S 6000-N). All remaining walls are painted in white (NCS 0500-N).

A colour chart of the NCS colours can be found at (Luxlak, December 2014).

The wall tiles in all the bathrooms have a matt white surface and one wall being grey (agrob buchtal, Type plural plus 1. Farge 1529 ativweis matt og farge 1503 azkentgrau) Existing yellow brick walls and natural stone concrete walls are preserved.

Ceiling

The ceiling in the cell offices and social zones is white mineral wool boards. The open landscape offices have a ceiling made out of white painted gypsum.

Floor

The floors in the cell offices and open landscape offices are carpeted (Ege, Epoca Globe GM 210410-05) and have a dark grey colour as seen in picture

Figure A.30. Dark grey carpets in cell offices and open landscape offices.

Furniture

The desks at the work stations have a white linoleum surface. The back wall of the workstation is made of blue matt fabric. A typical workspace can be seen in picture A.31.

Figure A.31. Surfaces on the workstations.

Blinds

The external blinds are made of aluminium (colour RAL 7038) and has a shading factor of 0.85 when the conditions are optimal. The internal blinds are also made of aluminium (colour RAL 8014).

Aluminium is quite a reflective surface material, and can cause issues such as glare.

Simulation software B

pros and cons for some daylight simulation software programs

In this chapter the different simulation programs are described. It is desired to simulate the light levels inside the building as accurate as possible. It must be kept in mind that no matter what simulation program applied, the software will always represent a simplified model of the physical reality. A software can therefore never provide 100% accuracy of the results (Witzel, 2012).

B.0.1 The Light Simulations Programs

The six programs described and compared in this thesis are as follows:

- Radiance
- Relux
- DaySim
- Velux Daylight Visualizer 2
- DIAlux evo 4
- SimLight

The description and comparison of the programs include:

- Input (illuminance vs. radiance)
- Output
- Type of weather data
- Calculation frequency
- Calculation period
- Computation time
- Limitations
- Accuracy
- Availability

Afterwards a conclusion on which programs should be applied for further study and simulations are conducted.

B.0.2 Criteria for the Simulation Programs

CAD input easily obtained so the method can easily be applied later for everybody, should not have complex inputs which are hard to measure/obtain.

B.0.3 Daylight Factor Comparison for the Simulation Programs

In (Statens Byggeforskningsinstitut, 2013) ten different programs are investigated, the programs are:

- Radiance
- Desktop Radiance
- Relux Radiosity
- Relux Raytracing
- DaySim
- Velux Daylight Visualizer
- DIAlux
- LightCalc
- Ecotect
- IESve

The ability of the programs to calculate the daylight factor on the working plane and the depth of the daylight penetration are compared (Statens Byggeforskningsinstitut, 2013). Table C.24 shows the results for the five programs investigated in this report, the results are obtained from (Statens Byggeforskningsinstitut, 2013). SimLight is not included as it was not a part of this research project.

The mean daylight factor [DF_{mean}]	Radiance	Relux Radiosity	Relux Raytracing	DaySim	VELUX Daylight Visualizer	DIALux
Simple room	3.3	3.4	3.5	3.4	3.0	3.2
Deep room	1.9	1.9	2.1	1.9	1.7	1.7
Room with obstruction	0.8	0.9	0.9	0.8	0.7	0.7
Room with light shelf	2.5	2.4	2.6	2.5	2.2	2.2
Room with borrowed light	2.1	-	1.7	2.1	2.2	2.4

Figure B.1. The mean daylight factors for the software programs (Statens Byggeforskningsinstitut, 2013)

As seen in table C.24 Relux Raytracing is the software which obtain the highest mean daylight factors for the first four room types, this may imply that Relux Raytracing generally calculates too high values of the daylight factor. Velux Daylight Visualizer is the software which calculates the lowest daylight factor for the first four room types, this may imply that Velux Daylight Visualizer calculates too low values of the mean daylight factor.

For the room with borrowed light Relux Radiosity cannot be applied as it is not possible to insert a window in an interior wall (Statens Byggeforskningsinstitut, 2013). For this room type the trend has turned, and it is now Velux Daylight Visualizer which estimates the high values of the mean daylight factor, while Relux Raytracing obtained the lowest value. This can suggest that for a room type with borrowed light the results obtained are inaccurate.

Radiance

The theory in this section can be found in (Larsen og Shakespeare, 1998) and (Radsite, Radiance-online, December 2014).

Radiance is a simulation software for analysis and visualization of lighting in building design. Its intention is to assist engineers and architects by predicting the light levels and appearance of a space in an early design phase .

The package includes programs for modeling and translating scene geometry, luminaire data and material properties, all of which are needed as input to the simulation.

Input

The input of the program includes:

- Scene geometry
- Materials
- Luminaires
- Time
- Date
- Sky conditions (for daylight calculation)

The geometry is usually conversed from CAD-files. The only requirement *Radiance* has, is that there has to be some way to associate the different materials with the different surfaces in the model.

The lighting simulation uses backwards ray tracing and the Monte Carlo method to compute radiance values (the quantity of light passing through a specific point in a specific direction) which then creates a photographic quality image that may be analysed. The backward ray tracing method starts at a measurement point and traces rays of light backwards to the sources. The calculation can be divided into three parts:

- The direct component: The light hitting a surface directly from light sources
- The specular indirect component: Light hitting a surface from other surfaces and being reflected off or transmitted through in a certain direction
- The diffuse indirect component: Light hitting a surface and being reflected or transmitted with no specific direction

Output

Radiance is a package of programs intended for different usages, dependent on what you want out of it. It can also be used in combination with a lot of other programs such as CAD-programs and photo editing programs. The simulation results may be represented by a rendered image, numerical values and contour plots, which then may be analysed.

Output parameters may include:

- Luminance
- Radiance
- Daylight factor

- Glare

It can accurately model both daylight and electric light. Modelling daylight accurately means following the initial intense solar radiation and redistributing it through reflections from other surfaces, and scattering from clouds. Accurately modelling electric light means using measured and/or calculated output data for light fixtures in the building.

Computational time

The computational time is very dependent on the number of light sources, the complexity of the space geometry, the desired accuracy, the importance of indirect illumination and how good you want the quality of the rendered image to be.

Accuracy

The accuracy of the luminance or radiance calculation is very dependent on the accuracy of the surface reflectance model. *Radiance* includes 25 different surface material types, but it is also possible to insert other material types by conducting measurements. These measurements may, however, be very time consuming.

The accuracy of the output is very dependent on the accuracy of the input. It is possible to obtain very accurate results with *Radiance*, but it will be on the expenses of long computational time.

Availability

Radiance is free to download for everyone.

Conclusion

Radiance is a software that can give almost any parameter desired with the right inputs. It is free to download, and is available for anyone. The accuracy can be very high, depending on how detailed and accurate the input is. However, this program is fairly complicated and has a steep learning curve. It might take a long time to master it on a high enough level if it is never used before.

B.1 Relux

Relux is developed by Relux Informatik AG, situated in Switzerland, in 1998. The ReluxSuite program package contains ReluxPro, ReluxSensor, ReluxOffer and ReluxEnergy.ReluxPro is the main program, also known as "Relux Professional", and it is the planning software. ReluxSensor estimates the optimum coverage for sensor detection range in the zones. ReluxOffer uses the price of the selected products and estimates an offer for the project. ReluxEnergy establishes the energy consumption for lighting by use of the EN15193 and DIN18599 standards.

Calculation Engine - Radiosity and Ray Tracing

In ReluxPro, the radiosity method carry out the calculations and simulations, but if professional visualisation is desired it can be performed by the raytracing method (RELUX Informatik AG, 2012).

The standard calculation engine in ReluxPro is radiosity, when choosing visualization with the raytracing calculation the same steps need to be followed as for the default radiosity method (RELUX Informatik AG, 2013).

Input

The location for the project is important in order to calculate the available daylight (RELUX Informatik AG, 2007). Either a known location can be selected, or a new location can be created. If a new location is created then the geographical longitude and latitude together with the time zone must be entered as this determines the luminance distribution of the sky. The rotation of the building must also be specified by establishing the North Angle.

External obstructions are added by inserting a ”cube” as desired outside the window. The lenght from the window to the cube as well as the height of the cube can be specified.

Either CIE clear sky or CIE overcast sky models are applied in the calculation. The daylight factor must be calculated with the CIE overcast sky, after this is performed other values can be calculated such as illuminance and luminance levels and the electricity usage of the armature.

The input geometry can either be created in ReluxPro, or it can be imported from AutoCAD as a dxf file (RELUX Informatik AG, 2007). Room elements such as doors, windows, skylights and pictures are entered in the model geometry, the glazing transmittance must be specified for the windows. Armatures are inserted in the model as luminaries.

The different inputs for the geometry:

- Reflectances and colours for the floor, ceiling and walls etc.
- Planning, reduction or maintenance factors
- Height of reference plane
- Distance between reference plane and wall
- Maintenance factor for each luminaire typeÂ”

The maintenance factor, the reduction in light levels over time, must also be specified. The appropriate furniture is selected from the Relux furniture library.

The color of the material must be selected, and Relux then gives the composition of the colors in terms of percentage of red, green or blue. It is possible to either type in the surface reflectance of the wall, ceiling and floor directly, or Relux will calculate a proposed reflectance due to the color chosen (RELUX Informatik AG, 2007). The thickness of both the walls and roof is necessary in order to calculate the correct daylight.

The utilization profile must be specified in Relux Energy, but prior to this the type of room must be specified. There are 34 different room types to choose from ranging from classrooms and hotel rooms to cell offices and open landscape offices. Every room as a default utilization profile.

The default utilization profile for a one person cell office and open landscape office are:

- Annual operating hours - day: 2543 hours.
- Annual operating hours - night: 207 hours.
- Relative absence: 0.3
- Reduction factor for building operation time.

Output

The daylight factor is calculated and it is independent of the time of the day and year (RELUX Informatik AG, 2007).

The glare can be rated by entering obverses in the model (RELUX Informatik AG, 2007). The luminous intensity of each luminaire in the direction of the observer is calculated.

Different calculation variants can be chosen, such as:

- Daylight calculation variant
- Artificial and daylight calculation variant
- Emergency lighting calculation variant
- Sensors calculation variant
- Solar altitude graph

For the sensor calculation variant ReluxPro will estimate the detection range for a presence detector (RELUX Informatik AG, 2007). In the artificial light variation it is possible to calculate the efficiency for different luminaire types. The solar altitude graph take the clear sky condition into account and shows the period of the year where direct sunlight reaches a specific point inside the room.

Accuracy

Both the calculation precision and number of raster points can be selected for each calculation.

Number of Interreflections

The precision is the number of interreflections, more interreflections will increase the precision of the calculation.

ReluxPro ensures a recommendation of the precision which is adapted to the specific room and luminaires within it. The recommendation precision ensures sufficiently accurate result as well as the computing time is optimised (RELUX Informatik AG, 2007).

There are four different settings for the number of interreflections:

- Only direct fraction
- Low indirect fraction
- Average indirect fraction
- High indirect fraction

An increase in the indirect fraction means an increase in the number of interreflections in the calculation. By setting high indirect fraction the most accurate result are achieved, but this will increase the computing time. It is therefore recommended to apply the proposed number of indirect fractions (RELUX Informatik AG, 2007).

Number of Raster Points

If the number of raster points are increased, this will increase the accuracy, nevertheless it is recommended to apply the default raster settings in ReluxPro as this will ensure sufficient accuracy along optimised computing time (RELUX Informatik AG, 2007). It is recommended to activate the dynamic raster, when this is active ReluxPro will establish which surfaces that need addition raster points incorporated. ReluxPro established this during the calculation by estimating the luminous fluxes and illuminance gradients and then establishes where additional raster points are needed. The dynamic raster can be set to coarse, medium or fine, where fine ensures the most accurate results (RELUX Informatik AG, 2007).

Pre-calculation

It is recommended that a pre-calculation is run in order to accurately simulate the illumination through windows and skylights, also known as daylight openings. Each daylight opening must be treated individually as the illumination is highly dependent on the incoming daylight which is again dependent on the sky model and external obstructions. It is important that the level of external interreflections is sufficient so the amount of light through the daylight openings are both directly from the sun and also reflected by external objects (RELUX Informatik AG, 2013). A pre-calculation will ensure a correct number of external interreflections to be chosen, it must at least be two.

Calculation Frequency

For reluxVivaldi: At the moment it is only possible to choose hours and minutes as intervals, and the whole period must not exceed one day. (RELUX Informatik AG, 2013).

Calculation Period

The results obtained from ReluxPro are annual (RELUX Informatik AG, 2007).

Computational Time

The computing time is hight influenced by the number of raster points, the diner the raster-point monitoring is, the longer the computing time will be. It is therefore recommended to apply the default setting for raster points (RELUX Informatik AG, 2007).

Some longer calculations can be running for a long period of time, ReluxPro will therefore save the results after the calculations are finished so the user to not have to wait by the computer (**?**).

Availability

ReluxPro is available free of charge, due to the contributions from the Relux members, and it can be downloaded here: *http://www.relux.biz/*.

Some extra add-ons can be installed for a fee, the add-ons are: ReluxVivaldi, ReluxEnergy CH, ReluxCAD, ReluxTunnel. Relux Vivaldi visualizes the light ambient concepts over time, the software also calculated the energy consumption. ReluxEnergy CH calculates and verifies the light according to the SIA Standard 380/4 ”Electrical Energy in Buildings”. ReluxCAD assist in transfering data directly between AutoCAD and ReluxPro, the plans drawn in AutoCAD can be transferred to ReluxPro and afterwards the calculated light data can be transferred directly back to AutoCAD. The last add-on is ReluxTunnel, this software assists in planning of light tunnels.

Conclusion

Relux proved has many possibilities to customize the calculations to be in good accordance with the project, the desired accuracy compared to computational time can be selected.

Relux uses illumination as input in order to calculate the daylight factor.

The results from the calculations can be shown directly on a pdf, this enables persons who do not have Relux installed nor uses it to read the results which is advantageous.

DAYSIM

The theory described in this chapter is mainly extracted from (Daysim, December 2014a).

DAYSIM is a *Radiance*-based daylight analysis software. It models the annual amount of daylight in and around buildings. It also allows the user to model dynamic façade systems such as venetian blinds and can model complex electric lighting systems and control strategies, including manual switches, occupancy sensors and photocell controlled dimming.

Calculation Engine

DAYSIM and radiance is a calculation engine for calculating different metrics.. maybe call section something else? Calculation method or something?

To calculate the annual amount of daylight available in and around a building, DAYSIM operates with the Perez all weather sky model combined with a daylight coefficient approach and the *Radiance* backwards ray tracer.

Daylight coefficients are a mathematical construct that describes how much a sky patch contributes to the daylight at a sensor point within a building. When a complete set of daylight coefficients has been calculated for each sensor point, the daylight coefficients can be combined with any sky condition, and the amount of daylight at the sensor point can be determined for any particular sky condition.

The resulting time series of illuminance, luminance, radiance and irradiance at the sensor points can be used to derive climate-based daylight metrics and/or to calculate electric lighting use for different lighting controls based on the daylight available.

DAYSIM consists of a series of command line subprograms. It is based on different models and concepts that can be seen in the chart on picture B.2. The subprograms are marked in orange, and the related input and output files are marked in grey.

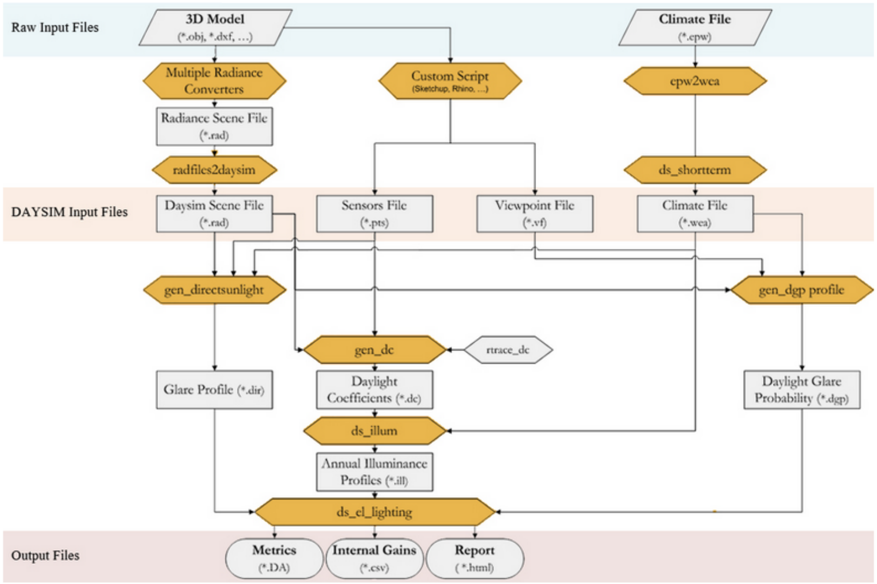

Figure B.2. Chart showing input, output and subprograms used in DAYSIM (Daysim, December 2014b).

Input

The input files required to conduct and annual daylight and electric lighting analysis in DAYSIM are:

- 3D model
- Climate file
- *Radiance* geometry and material files
- Sensor file

The 3D model is usually converted from a CAD-program into *Radiance*, resulting in a Radiance scene file. The weather file is usually downloaded or purchased. EPW weather files can be downloaded from the US Department of Energy.

Output

The main output from DAYSIM is:

- Daylighting metric distributions
- Electric energy use
- Internal gain

Two daylight metrics that are calculated by DAYSIM are Daylight Autonomy and Useful Daylight Illuminance. Daylight Autonomy is presented as a percentage of annual daytime hours that is above a certain illumination level specified by the user (Advanced Buildings, December 2014b). Useful Daylight Illuminance is a modified version of the Daylight Autonomy metric which sorts the hourly values into three illumination ranges, 0-100 lux, 100-2000 lux, and over 2000 lux. The values outside this range is considered not useful (Advanced Buildings, December 2014a).

To predict how the occupants will use the electric lighting controls and shading system, DAYSIM uses a model called Lightswitch that is based on annual illuminance profiles and occupancy schedules. Out from this, the model can predict the electric lighting energy use in the building.

DAYSIM can also model dynamic shading systems such as venetian blinds and roller shades. Initially, DAYSIM generates annual illuminance profiles with the shading system in a fixed position throughout the year. In the next process it uses the Lightswitch model to predict in which state the shading system is going to be during the year.

Discomfort glare due to daylight can be predicted by the use of the daylight glare probability metric. It predicts glare for different viewpoints in the building throughout the whole year. The different shading device settings are also taken into account in this prediction.

Daysim also outputs an Internal Gains schedule which can be used by energy simulation programs such as EnergyPlus and eQuest to conduct an integrated thermal lighting analysis of a space if desired.

Accuracy

The accuracy for typical daylight design with DAYSIM has in previous studies been proved to be sufficient even with complex geometry. When compared to measurements, DAYSIM seems to produce lower values of incoming light flux for cases where more complicated surfaces such as venetian blinds or light shelves are introduced to the model. The sky conditions also have an influence on the accuracy, where clear sky and sunny conditions will decrease the accuracy (et al., 2009).

A classic *Radiance* simulation only simulates lighting conditions under one sky condition at a time, and each calculation usually takes several minutes, and even some times hours. Compared to this, DAYSIM is a very good alternative since its analysis is over a whole year and includes a big variation of sky conditions (Reinhart og Breton, 2009).

Computational time

DAYSIM was initially developed to calculate illuminance or luminance more efficiently than Radiance. Because of the use of the daylight coefficient approach it is able to analyse lighting conditions within a reasonable time.

However, just because DAYSIM have a shorter computational time than Radiance, it is still not very fast. Simulations in DAYSIM can take hours dependent on the complexety of the geometry, light sources and surfaces,

Availability

DAYSIM is free to download and available for anyone.

Conclusion

DAYSIM is sufficient for daylight simulations, and is proven to be very accurate even with complex geometry. However, it seems as the accuracy decrease when systems such as blinds or light shelves are introduced to the model, and under clear sky conditions. It is easily available as it can be downloaded by anyone for free without any required licence. It is not possible to make a geometrical model within the program, which means it must be imported from another software. The computational time is improved compared to *Radiance*, but is still quite long as one simulation can take up to hours. The graphical treatment of the results are not very good, and the user interface is quite difficult to understand if the user is new to the program (Statens Byggeforskningsinstitut, 2013).

B.2 VELUX Daylight Visualizer 2

Velux Daylight Visualizer 2 is a software which predicts the daylight levels, it simulates daylight transport in building (R. Labayrade et al., 2009a). Velux Daylight Visualizer 2 is dedicated to the simulation of natural lighting (R. Labayrade et al., 2009b).

Velux Daylight Visualizer 2 can predict daylight levels accurately as well as show the appearance of a space lit with natural light before the building is built (?). It is therefore an important tool for architects, engineers and designers.

Calculation Engine

The calculation engine is photon mapping as described in chapter 4.4. In addition, there are different light transport algorithms applied, they are bidirectional path tracing and irradiance caching. The settings for each algorithm will influence the simulation accuracy and the rendering time (R. Labayrade et al., 2009b).

Input - Boundary Conditions

Either the building can be drawn up in VELUX Daylight Visualizer, or it can be imported from a CAD-software such as AutoCAD or ArchiCAD (VELUX Daylight Visualizer, 2014b).

Surrounding obstructions should be modelled in VELUX Daylight Visualizer in order to improve the accuracy of the simulations (VELUX Daylight Visualizer, 2014a).

The type of windows and doors can be found in the roof and façade database. The sky conditions can be selected between 15 different sky types (VELUX Daylight Visualizer, 2014b).

The location and orientation must be specified, as well as the date and time of the simulation (R. Labayrade et al., 2009a). The reflectance of the interior and exterior surfaces should be specified in percent [%] (R. Labayrade et al., 2009b).

Output - Result

Velux Daylight Visualizer 2 produces a photo-realistic rendering,and in addition the simulation results are luminance, illuminance and daylight factor maps (R. Labayrade et al., 2009b).

Accuracy

The three different algorithms applied in Velux Daylight Visualizer 2 as mentioned in B.2. The settings of these will influence the simulation accuracy as well as the rendering time. It is reommended to apply a custom detailed setting (R. Labayrade et al., 2009a).

The user can set a parameter which then rules the global simulation quality. There are six settings for the light transport algorithms (R. Labayrade et al., 2009b):

- Ambient - indicates whether indirect illumination is simulated
- Trace level - is the number of bounces of all types of lighting

- Ambient trace level - is the number of bounces of ambient (indirect) lighting
- Ambient precision - relates to the image based sampling used
- Ambient complexity - describes the lighting complexity. It influences the number of samples used. Higher values equals higher precision
- Ambient feature size - relates to the image interpolation quality

The accuracy of Velux Daylight Visualizer 2 to predict the daylight levels and the appearance of an inbuilt space lit with natural light was validated in (R. Labayrade et al., 2009b). The simulation software was tested with different cases, and the maximal error found was below 5.54 %, while the average error was below 1.63 %. These errors are fairly low, thus Velux Daylight Visualizer 2 proves to establish accurate results for daylight levels and visualisation of the appearance of an inbuilt space lit with natural light.

The simulation time and the rendering quality depends on the global setting, QR, it can be set to low, medium or high (R. Labayrade et al., 2009b). The low value will ensure optimised rendering time and an acceptable accuracy. On the other hand, the high value of the global setting will ensure a long rendering time, but very accurate result. The medium value is a compromise between the the two.

Computational Time

According to (R. Labayrade et al., 2009b) are the simulation times reasonable for Velux Daylight Visualizer 2.

When unsure if a simulation with a particular rendering quality is realistic and reasonable, then the simulation time analysis can be a useful tool to decide whenever the simulation with that quality should be performed (R. Labayrade et al., 2009b).

Calculation Period

Have to use the program and figure this out... but think it is annual..

Availability

Velux Daylight Visualizer 2 can be downloaded free of charge from *http://viz.velux.com/*.

Conclusion

Velux Daylight Visualizer 2 has been validated to be an accurate simulation tool for daylight levels as explained in B.2, with reasonable simulation time. The simulation software is a user-friendly tool which can import models from CAD-software.

On the other hand, information about the algorithms applied and other setting such as weather data are not easily found. The impression that Velux Group is secretive of what is behind the calculations was obtained, detailed information was found through other research reports, if information was found at all. If Velux Daylight Visualizer 2 is an appropriate tool for this project is unsure, as information about the calculations in the program are hard, if even not possible, to obtain.

DIALux evo 4

DIAL GmbH is the company behind DIALux. Initially the software was different and improved versions of DIALux, but in 2012 the new and highly improved version DIALux evo was launched. The latest version of DIALux evo 4 has many improvements and modifications, such as the possibility to calculate daylight levels (DIAL GmbH, December 2014b).

DIALux estimates the energy consumption for artificial lighting as well as establishes photo-realistic visualizations of daylight and artificial light scenarios (DIAL GmbH, December 2014c).

Calculation Engine

Previously the radiosity method was applied, but as this method has a long calculation time for complex geometries and only take diffusely reflecting materials into consideration, it was decided to apply photon shooting a the calculation method for DAILux evo (Witzel, 2012).

Input

It is possible to import building drawings as .dwg or .dxf files from a CAD program. The site must be specified and luminaries and objects inserted, objects such as furnitures can be inserted as .sat, .3ds and .m3d files (DIAL GmbH, 2012). The texture and colors of the surfaces must either be specified or chosen in the DIALux material catalogue (DIAL GmbH, 2012). The transmission degree and reflection factor must also be specified.

The luminaires from the leading manufacturers are available (DIAL GmbH, December 2014c), which ensures the model to be adapted to the specific project.

The daylight calculations are performed with CIE models. The three models applied are clear, overcast or cloudy skies (DIAL GmbH, December 2014b).

Output

The total energy consumption for all the artificial lighting can be calculated annually (DIAL GmbH, December 2014a).

Different results can be obtained for the surfaces in the geometry (DIAL GmbH, 2012):

- Horizontal illuminance
- Vertical illuminance
- Unified glare rating
- Glare rating
- Cylindrical and semi-cylindrical illuminance
- Hemispherical illuminance
- Adaptive perpendicular illuminance
- Perpendicular illuminance

Accuracy

If desired, the rooms can be divided further down into zones is desired, this ensures opportunities for more accurate and adoption to the specific project (DIAL GmbH, 2012).

DIALux evo 4 provides accurate results compared to standardized test procedures (Witzel, 2012). If very exact results are required on a large surface it is recommended to place calculation points here as the number of photons are limited (Witzel, 2012).

Computational time

If one calculation is performed in DIALux evo, and afterwards changes are done, then DIALux evo will apply previous results and thereby must not perform the complete calculation again (DIAL GmbH, 2012). This shortens down the computational time. In DIALux evo very complex scenes can be calculated within a reasonable period of time (Witzel, 2012).

Availability

DIALux can be installed free of charge from *http://www.dial.de/DIAL/en/dialux/about.html*.

Limitations

The calculations can only be performed for thee different ICE sky models, which limits the results for different weather conditions.

The material model is very simplified which decreases the accuracy of the results. The number of photons applied in the simulation is restricted due the available storage capacity and it must be limited within an acceptable computational time (Witzel, 2012).

Conclusion

DIALux evo 4 has is intuitive and user friendly with reasonable computational time. It can be applied on complex geometries, and easily adapted to the specific project. However, the accuracy of the program has not been validated by other sources than DIAL GmbH themselves, which limits the credibility of the accuracy results.

B.3 SimLight

The theory in this chapter is found from (et al., 2001) and (U.S. Department of Energy, 2011).

SimLight is an application which is a part of the BSim-package. It can calculate the daylight factor in any point on a horizontal, vertical or angled plane in a room.

The program can calculate the illumination in the specific point respectively from direct solar radiation, externally reflected radiation and internal reflected radiation both for cloudy sky conditions and CIE overcast sky.

Calculation Engine

SimLight uses the Finite Element Method (FEM) for calculating daylight. Since FEM-based radiation calculation can have a very long computational time, the application has implemented functions that permits dynamical altering of the finite element grid. This is of particular significance for internally reflected illuminance calculations.

Input

The input for SimLight is:

- Building geometry: Rooms and thermal zones
- Weather data
- Constructions and materials: Type of materials and their different parameters
- Systems and functions: Internal loads, ventilation system etc.
- Automatic control strategies

The 3D model is made in the BSim application SimView, so there is no need for importing it from another software.

Output

The output is:

- Calculated data from climate file
- Daylight factor
- Solar light factors

The output can be calculated on an hourly, weekly, monthly or yearly basis and comes in either tabular or graphic form. Outputs can also be copied and transferred into other programs.

Accuracy

SimLight produce reasonable results for simple geometrics. However, it does not take shading from outdoor obstructions into account, and the sky model is assumed to be of uniform illuminance which can decrease the accuracy compared to actual measurements.

The thermal simulation core has been validated in the IEA (International Energy Agency) Task 12 / Annex 21 "Empirical validation of thermal building simulation programs using test room data" activity. Any additions to the program since then have been validated individually by external experts (U.S. Department of Energy, 2011).

Computational time

The computational time is only a few minutes on an up to date computer.

Availability

BSim have to be purchased to get the SimLight tool since it is an application in BSim.

The start charge of BSim is 20 000 DKK. A student licence is available per adress for 7000 DKK annualy.

Limitations

Limitations to the programs are:

- Does not take shading from outdoor obstructions into account
- The sky must be of uniform luminance

- The reference plane must be perpendicular to the window plane
- It does not support import of 3D models from CAD tools

Conclusion

BSim with SimLight is able to conduct simulations on complex building geometries. It takes every aspect of indoor climate into account, which is important for daylight calculations. It does not support any CAD files from other programs, which is a weakness since the construction of a 3D model for a large and complex building can be very time consuming. Users must have some general knowledge on building design and how buildings behave thermally in order create the building model.

Assessing Relux and VELUX Daylight Visualizer C

C.1 Relux

Inputs in Relux

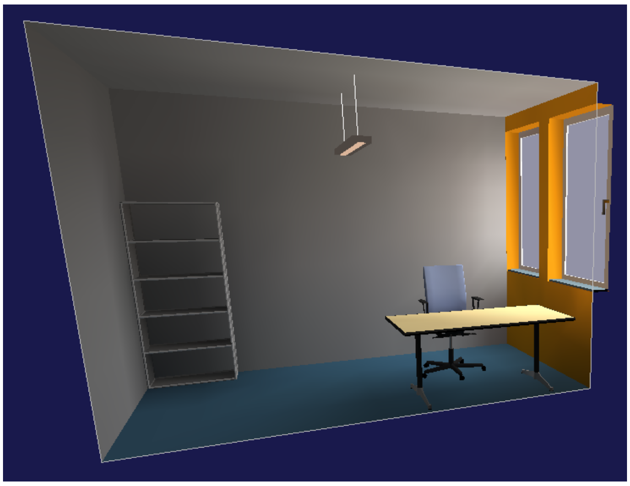

Figure C.1. Illustration of the cell office in Relux with furniture

The properties of the windows can be exactly stated, such as the transmission of the glazing in the test building given from the manufacturer of 77%.

The red, green and blue proportional colour of every material must be inserted. These colours make up the RGB-color model, the RGB-color model is the main model applied in TV, computers and other mediums which projects color (Adobe, February 2015). The RGB-color model is closely related to the way humans preceive color with the R, G and B receptors in the retinas of the eye (Adobe, February 2015).

As a default will Relux calculate with the radiosity model, it must be stated if the ray-tracing model should be applied.

The date and time must be entered in order to determine the solar altitude and the luminance in the sky (RELUX Informatik AG, 2007).

Outputs in Relux

All results obtained from Relux are shown for the reference plane at 0.8 m above the floor. The reflectance of the surfaces applied in Relux are from SINTEF Byggforsk as explained in 3.4.1.

The Radiosity Method

The daylight factor is an important value when considering the daylight level inside a room, the daylight factor is therefore calculated in Relux using the radiosity method.

All results here are shown with no outside surrounding reflecting surfaces such as neighbouring buildings. All results are obtained for the cell office facing east.

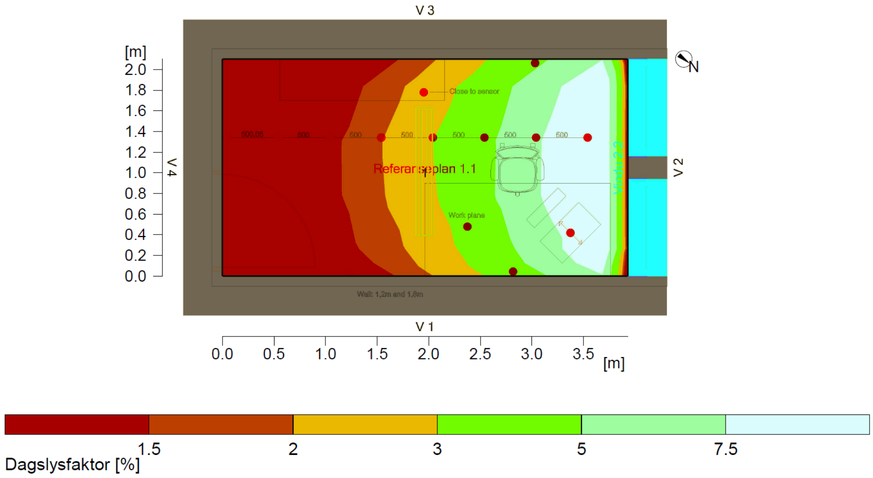

Figure C.2. Daylight factor from Relux obtained with the radiosity method for the cell office without furniture

As seen in figure C.2 the daylight factor is above 2 % until about 2.5 m from the façade wall which correspond to about half of the depth of the room.

A 3D graphical representation of the daylight factor is shown in figure C.3.

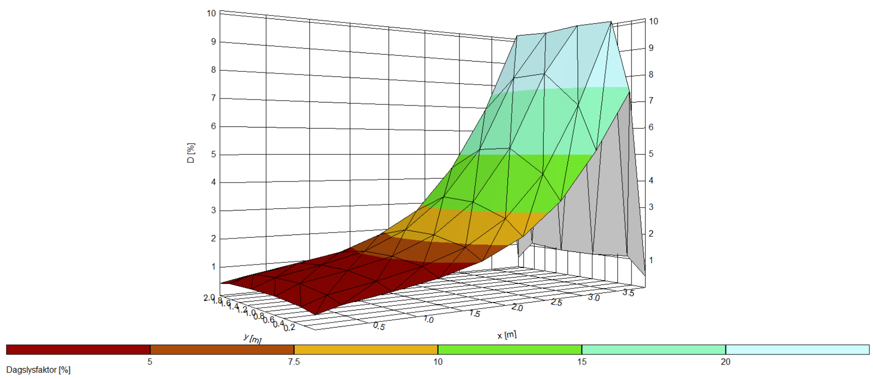

Figure C.3. 3D graph of the daylight factor from Relux obtained with the radiosity method for the cell office without furniture

The 3D graph illustrates the same result for the daylight factor obtained with the radiosity method for the reference plane at 0.8 m above the floor.

Figure C.4 a 3D view of the illuminance obtained with the radiosity method is shown.

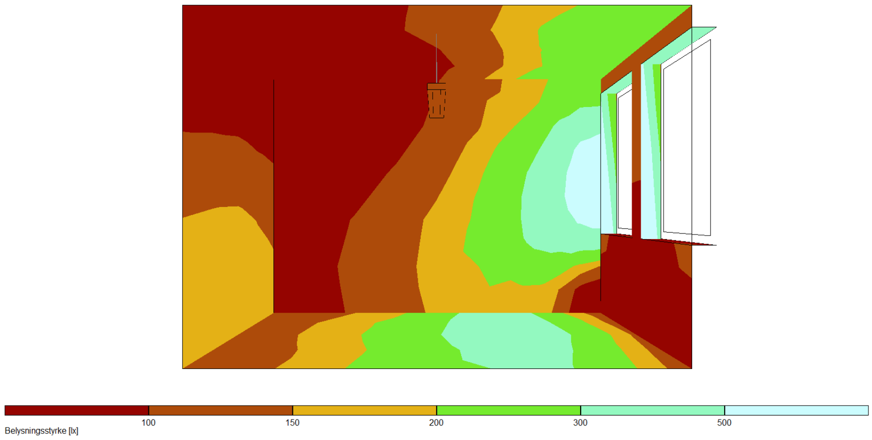

Figure C.4. 3D view of the illuminance obtained with the radiosity method in Relux for the cell office without furniture

Figure C.5 shows the luminance obtained with the radiosity method in Relux.

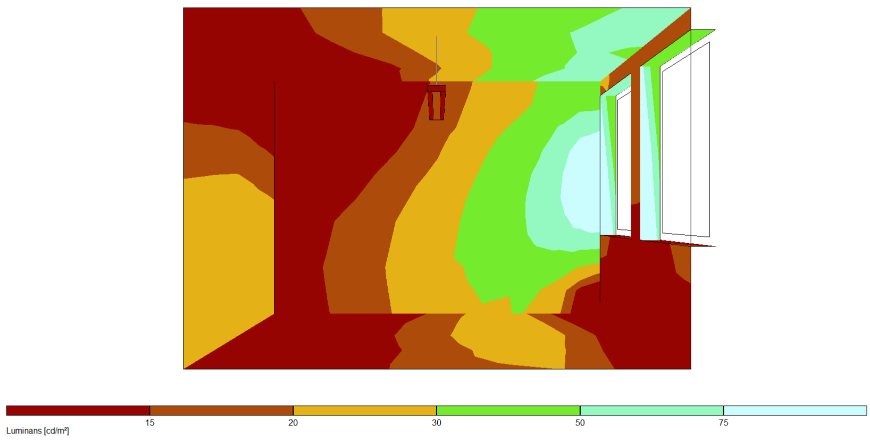

Figure C.5. 3D view of the luminance obtained with the radiosity method in Relux for the cell office without furniture

Figure C.6 shows the daylight factor obtained with the radiosity method with furniture inside the cell office.

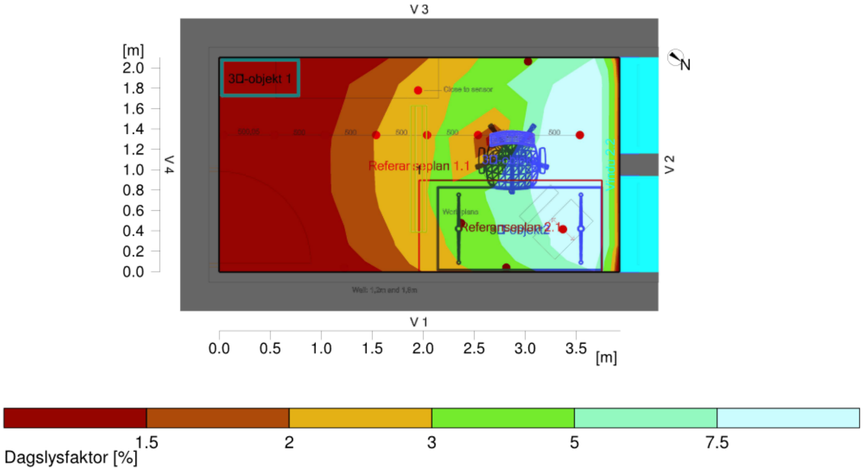

Figure C.6. Daylight factor from Relux obtained with the radiosity method for the cell office with furniture

Figure C.6 shows that the furniture clearly cause shading, but the daylight factor is still above 2% for about half of the room length for the reference plane at 0.8 m above the floor.

The Raytracing Method

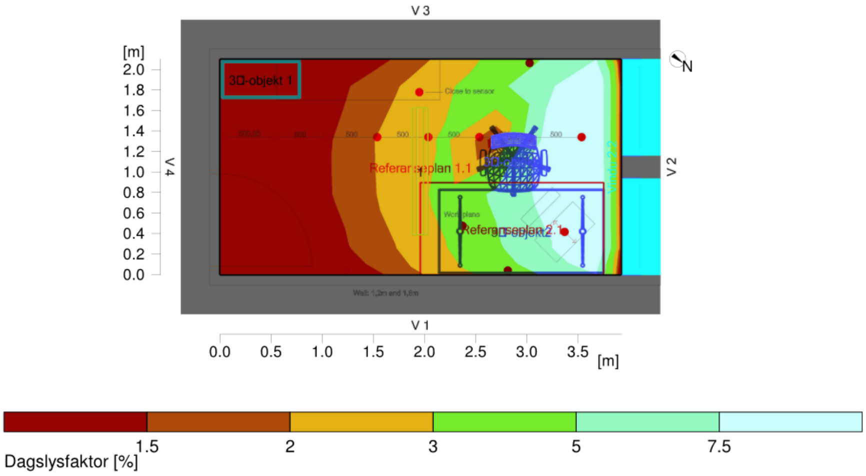

Figure C.7. Daylight factor from Relux obtained with the raytracing method for the cell office with furniture

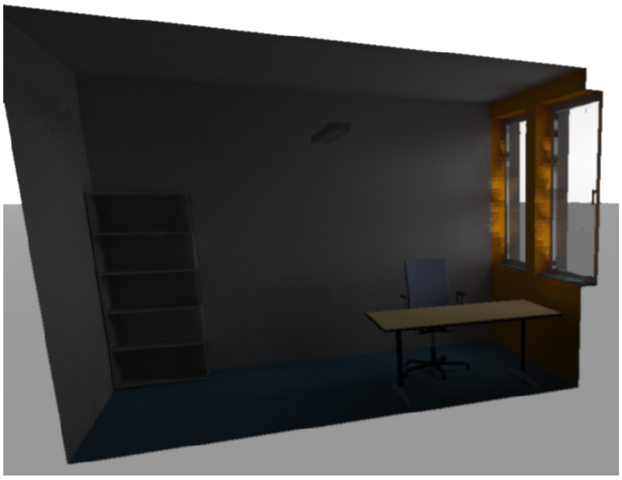

Figure C.8. 3D illustration of the luminance from Relux obtained with the raytracing method for the cell office with furniture

Electricity Usage

Figure C.9 shows the monthly and yearly electrcity usage for the armature in the cell office. The armature if Glamox Luxo C10-S1 150 with two 35 W fluorescent light tubes. In Relux the exact same armature is inserted but with two 28W fluorescent light tubes as 30W did not exist.

Måned:	Totalenergi		
	Andel [%]	[kWh]	[kWh/m²]
Januar	9.37	5.03	0.61
Februar	8.54	4.59	0.56
Mars	7.92	4.26	0.52
April	7.51	4.03	0.49
Mai	7.23	3.89	0.47
Juni	7.16	3.85	0.47
Juli	7.30	3.92	0.47
August	7.58	4.07	0.49
September	8.06	4.33	0.52
oktober	8.75	4.70	0.57
November	9.64	5.18	0.63
Desember	10.68	5.74	0.69

Vurderte soner:

Navn:	Andel [%]	Energiforbruk [kWh/år]	Areal [m²]
Sone 1	100.00	53.74	8.26

Figure C.9. The electricity usage for the armature in the cell office obtained with ReluxEnergy

Figure C.9 shows that the electricity usage is less for the summer months compared to the winter months which is as expected as there is more available daylight in Oslo during summer compared to the winter which then means reduced electricity usage for artificial lighting during the summer. The yearly electricity usage for the cell office is 53.74 kWh/year.

C.2 VELUX Daylight Visualizer

Simulation of a Single Cell office

A single cell office has been simulated facing east, west and south. The geometry of the cell office corresponds to a single cell office in the case building in the south zone on the third floor. The cell office is also simulated facing north for comparison purposes.

All simulations for luminance and illuminance are performed for 12:00 in February, while the daylight factor is an annual value.

Inputs in VELUX Daylight Visualizer 2

Limitation in the Geometry The dimensions of the glazing is 800 mm wide and 1540 mm high in the building, but it is not possible to have a window which is taller than 1500 mm in the model. The window dimensions which is specified in the model is including the window frame, but the size of this frame is not know. The frame thickness in the building is 70 mm, the width of the window in the model is set to 940 mm, and it is assumed that the frame is 7 mm in the model as well. The height of the window in the model is set to 1500 mm as this is the maximum size for a wall which is 2230 mm high.

It is not possible to specify the light transmission quality of the glazing. This is a significant limitation as the actual glazing properties are not an input in the model, nor is any information about what glazing properties which the model applies available.

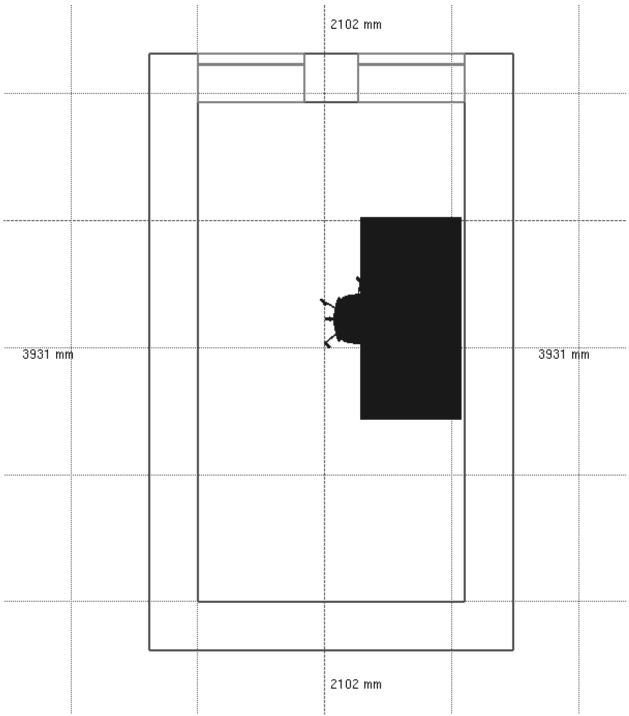

Figure C.10. Plan view of the single cell office in VELUX Daylight Visualizer 2

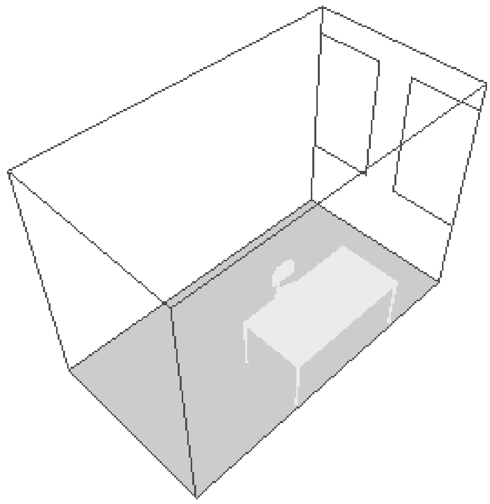

Figure C.11. 3D view of the single cell office VELUX Daylight Visualizer 2

Outputs in VELUX Daylight Visualizer 2

The daylight factor, luminance and illuminance are obtained with VELUX Daylight Visualizer 2, in a grey-and-white illustrative picture, ISO contour or a false colour map can be added for illustrative purposes.

- Daylight factor
- Illuminance
  - CIE 1 Overcast
  - CIE 7 Intermediate
  - CIE 12 Sunny
- Luminance
  - CIE 1 Overcast
  - CIE 7 Intermediate
  - CIE 12 Sunny
    - Without sunlight
    - With sunlight

It was chosen to focus on the overcast sky as this will be the worst-case-scenario for luminance and illuminance values inside the cell office.

Results - Daylight Factor The average daylight factor should be at least 2 % (Direktoratet for byggkvalitet (DiBK), 2011), it is therefore desired to study the results obtained for the daylight factor for the cell office facing the four different cardinal coordinates. The daylight factor is calculated as an annual value, and it is for a CIE overcast (1) sky condition. In figure

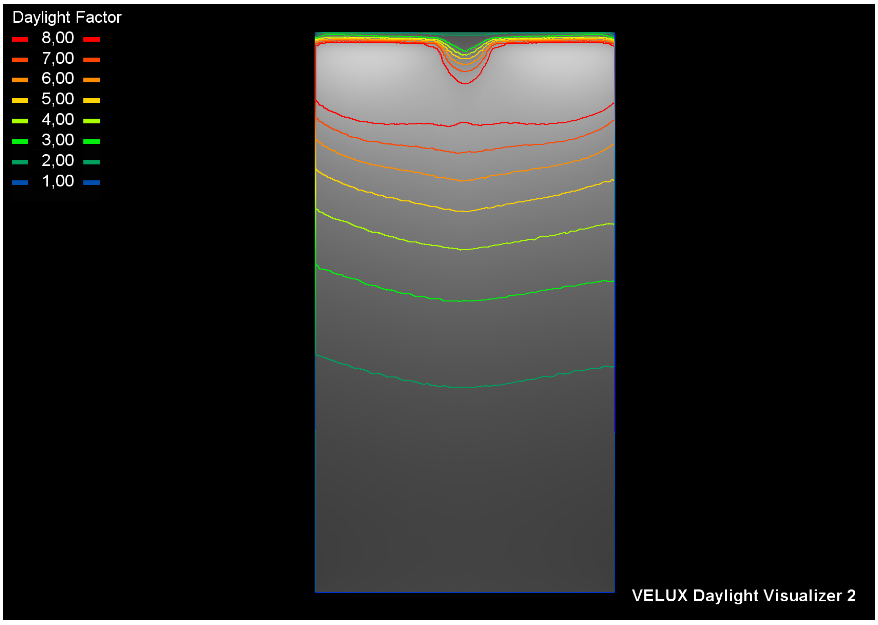

Figure C.12. Daylight factor for a single cell office

The ISO contour shows that the daylight factor is above the average of 2 % for the single cell office. This means that the office will according to VELUX Daylight Visualizer 2 satisfy the requirement stated by TEK 10.

Results - Luminance The Luminance for the three different CIE sky conditions; overcast, intermediate and sunny are obtained. The sunny CIE sky can be simulated with and without sunlight.

In figure C.13 the simulation result for luminance in February at 12:00 with overcast sky facing west is shown, the result is shown with ISO contour.

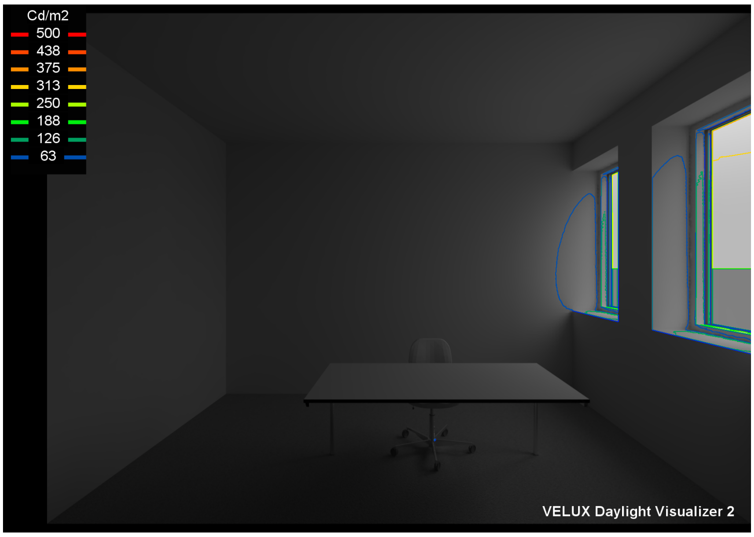

Figure C.13. Luminance for single cell office facing west - ISO contour

On the left wall there should be a door to the corridor, but it is excluded from the simulation as it is not significant for light simulation.

For better understanding of the results the following results are shown with false colour. The results for the four cardinal coordinates are compared. In figures C.14 and C.15 simulation results of the luminance for overcast sky in February at 12:00 from VELUX Daylight Visualizer 2 for a single cell office facing east and west can be seen in.

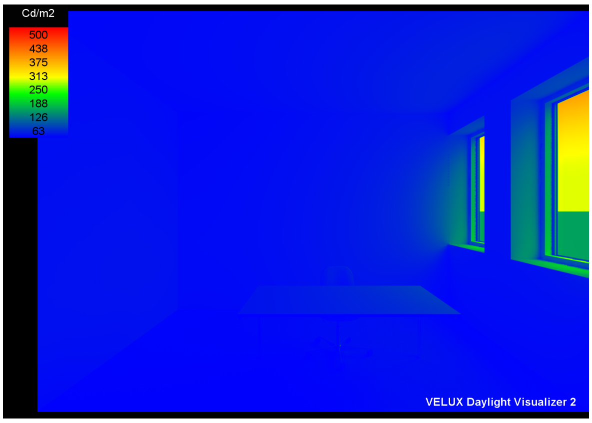

Figure C.14. Luminance for a single cell office facing east - February, 12:00, overcast sky - false colour

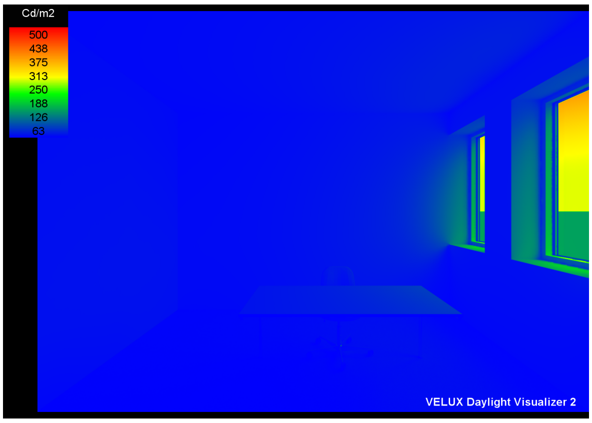

Figure C.15. Luminance for a single cell office facing west - February, 12:00, overcast sky - false colour

In figure C.16 and C.17 simulation results of the luminance for February at 12:00 for overcast sky from VELUX Daylight Visualizer 2 for a single cell office facing south and north can be seen in.

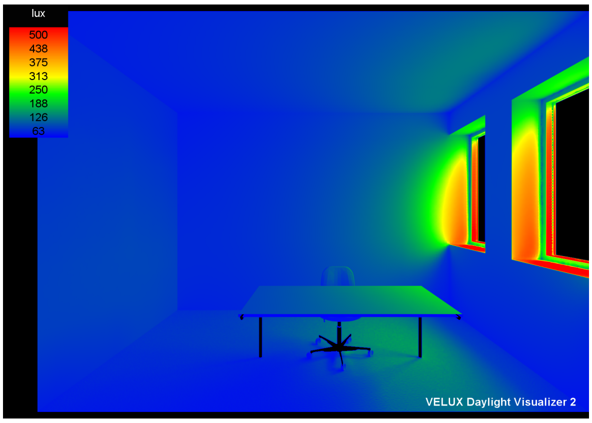

Figure C.16. Luminance for a single cell office facing south - February, 12:00, overcast sky - false colour

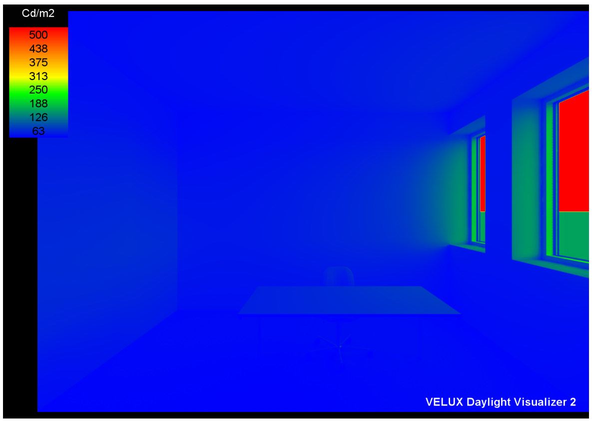

Figure C.17. Luminance for a single cell office facing north - February, 12:00, overcast sky - false colour

The four false colour images clearly illustrates the difference in the illuminance for north and south facing offices. The offices facing east and west are not showing significant difference. The results shows that the cardinal direction of the façade strongly influence the illuminance value in the cell office.

The sunny CIE sky condition with and without sunlight for the cell office facing south at 12:00 in February is shown in figures C.18 and C.19.

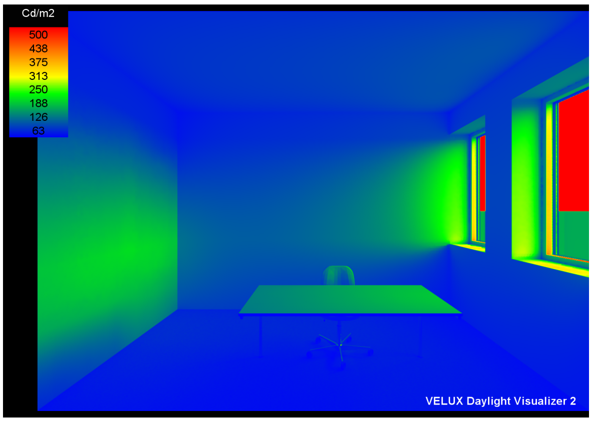

Figure C.18. Luminance for a single cell office facing south - February, 12:00, sunny without sunlight - false colour

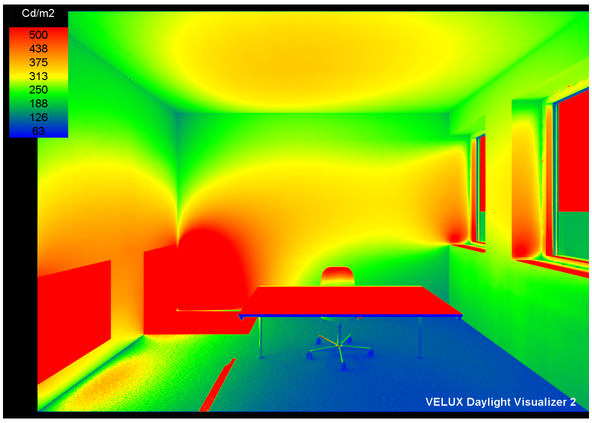

Figure C.19. Luminance for a single cell office facing south - February, 12:00, sunny with sunlight - false colour

Figures C.18 and C.19clearly shows the importance of available sunlight for luminance calculation. Figure C.19 shows high values of candelas per square meter.

Illuminance Illuminance for overcast, intermediate and sunny CIE skies can be obtained. The values for overcast and sunny for a cell office facing west and east are shown. False color illuminance map for sunny condition with sunlight are shown for comparison purposes for the overcast sky condition.

The illumination values for overcast sky condition for cell offices facing west and east are shown in figures C.20 and C.21.

Figure C.20. Illuminance for a single cell office facing west - February, 12:00, overcast sky - false colour

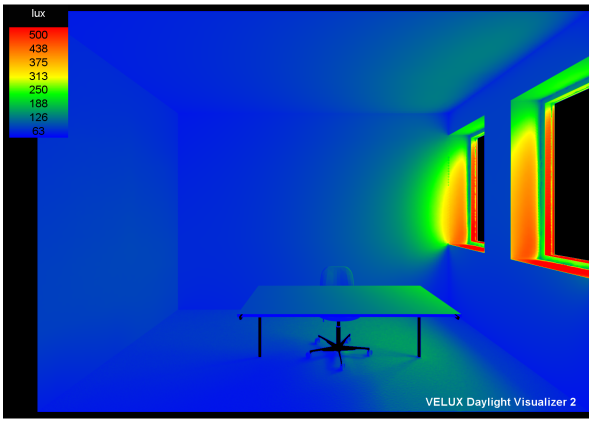

Figure C.21. Illuminance for a single cell office facing east - February, 12:00, overcast sky - false colour

Illumination values for a sunny sky for cell offices facing west and east are shown in figures C.22 and C.23.

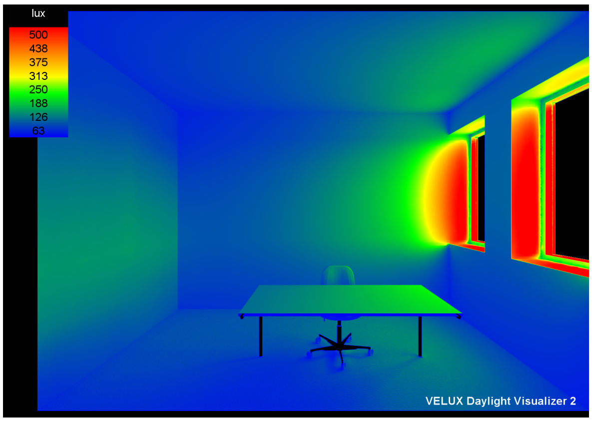

Figure C.22. Illuminance for a single cell office facing west - February, 12:00, sunny sky - false colour

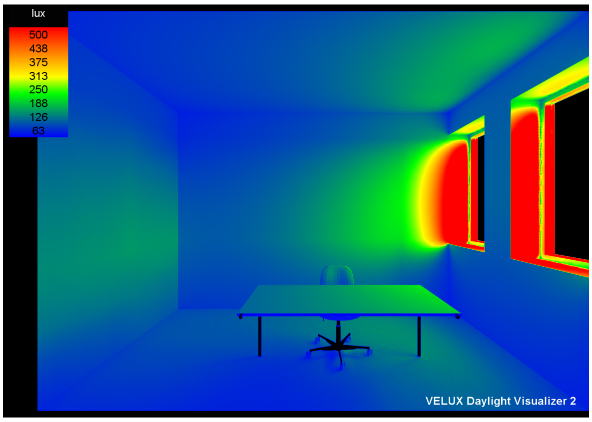

Figure C.23. Illuminance for a single cell office facing east - February, 12:00, sunny sky - false colour

A comparison of the illumination results for the cell offices facing east and west shows that difference between the cardinal coordinates from east to west do not influence the illumination result significantly in February at 12:00. On the other hand, the difference between overcast and sunny sky conditions is clearer, the sunny sky clearly has higher lux values thought the room compared to the overcast sky. All in all, this shows that the sky condition will significantly influence the illuminance value inside the cell office.

C.3 Comparison of the Simulation Programs

	Radiance	Relux	DaySim	Velux Daylight Visualizer	DIALux	SimLight (BSim)
Import from CAD	Yes	Yes	Yes	Yes	Yes	No
Can be applied on complex geometries?	Yes	Yes	Yes	Yes	Yes	Yes
Calculation period	Annual	Annual	Annual	Annual	Annual	Annual
Calculation frequency						
Calculation engine	Backwards ray tracing	Radiosity and ray tracing	Backwards ray tracing	Photon mapping	Photon mapping	Finite Element Method
Illuminance input?	Yes	No	Yes	No	No	No
Radiance input	Yes	No	Yes	No	(No)	No
Weather data needed?	Yes	No	Yes	No	(No)	(Yes)
Applies CIE sky models?	Yes	Yes	Yes	Yes	Yes	Yes
Availability	Free	Free	Free	Free	Free	Purchase
Take surroundings into consideration?	Yes	Yes	Yes	Yes	Yes	No
Daylight factor as output?	Yes	Yes	Yes	Yes	Yes	Yes
Illuminance as output?	Yes	Yes	Yes	Yes	Yes	Yes

Figure C.24. Comparison of the Simulation Programs

Solar Irradiance D

The global irradiance was measured by a pyranometer. This, as mentioned in 3.1 on page 13, includes measurements of both direct and diffuse irradiance.

D.1 Purpose of Solar Irradiance Measurements

As weather data is usually obtained from weather stations and not the specific location of the building at interest, they do not give completely accurate results especially when the sky conditions are in the range between clear sky and overcast. Nearby obstacles and reflectance from other buildings are also naturally not taken into account in these data. Therefore, for better accuracy, the solar irradiance should be measured for the building.

These readings can later be made into a climate file and used in simulation programs.

D.2 Conduction of Solar Irradiance Measurements

Because of the preservation of certain parts of the building, it was not possible to mount the pyranometer to the façades of the building. Therefore the pyranometer was placed on the roof of the seventh floor. The pyranometer was placed on the middle of the roof as this was the place with the least shade from the obstacles on the roof as seen in picture D.1. It was ensured that the pyranometer was levelled for accurate results.

Figure D.1. The placement of the pyranometer on the roof

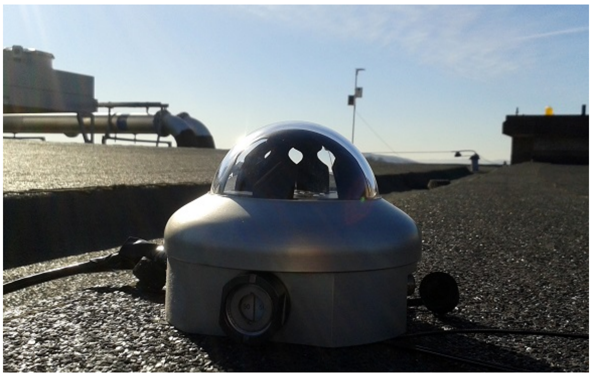

Figure D.2. The pyranometer

D.2.1 The Pyranometer

A pyranometer, as seen in picture D.3 on the next page, uses a black-coated thermopile that absorbs solar radiation in a wide spectrum of wavelengths. A glass dome ensures that the radiation is limited to only short wavelengths. A thermopile generates a voltage signal that is proportional to the solar radiation at that moment (NREL Buildings Research, July 2014). This voltage signal is logged by a data logger and results in solar irradiance $\mathrm{k\,wh/\,m^2}\cdot$

To measure the diffuse solar irradiance, a small shading disc can be applied. This means that the pyranometer is always shaded and eliminates the direct beam component of the solar irradiance. The sensor for diffuse irradiance is shaded with a 6 cm diameter shading disk at 30 cm distance (Arvid Skartveit og Tuft, 1998).

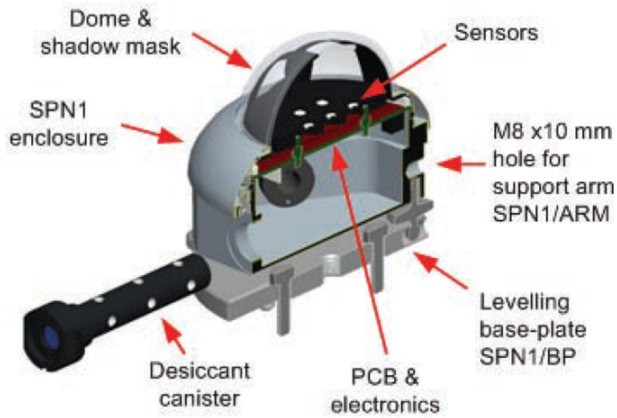

Figure D.3. Section of the SPN1 sunshine pyranometer

The SPN1 pyranometer measures short wave radiation between 400 nm and 2700 nm (Delta-T Devices Ltd, 2007).

D.2.2 Measuring Period and Frequency

The irradiance was measured for 13 days from Friday the 13^{th} of March to Wednesday the 25^{th} of March.

In order to determine in what time interval the solar irradiation needed to be measured a test measurement was performed the afternoon and evening of Thursday the 12^{th}, figure D.4 displays the result. Initially a time interval of five minutes was set as recommended time interval for measurements lasting over days is two and a half or five minutes (Delta-T Devices Ltd, 2007).

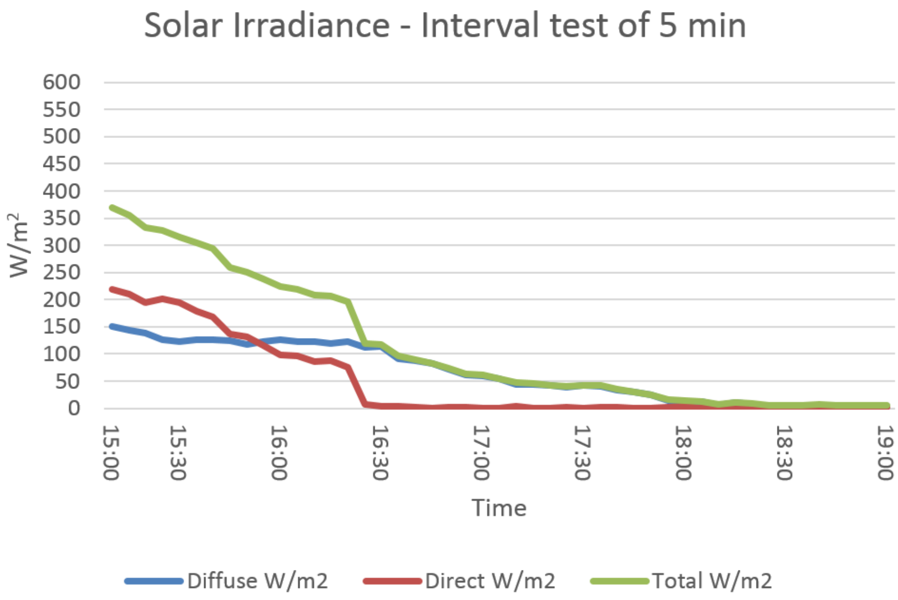

Figure D.4. Solar irradiation interval test of five minutes.

As seen in figure D.4, the solar irradiation curves for total, diffuse and direct components are not smooth. The variation in the curves happens in rather big steps at a time, and it is believed that this interval was not sufficient to capture the changes in the solar irradiation and give a reasonable illustration of the change in solar irradiation over time.

Therefore, one minute was chosen for the next day, Friday the 13^{th}, in order to evaluate a shorter time interval. The result are displayed in figure D.5.

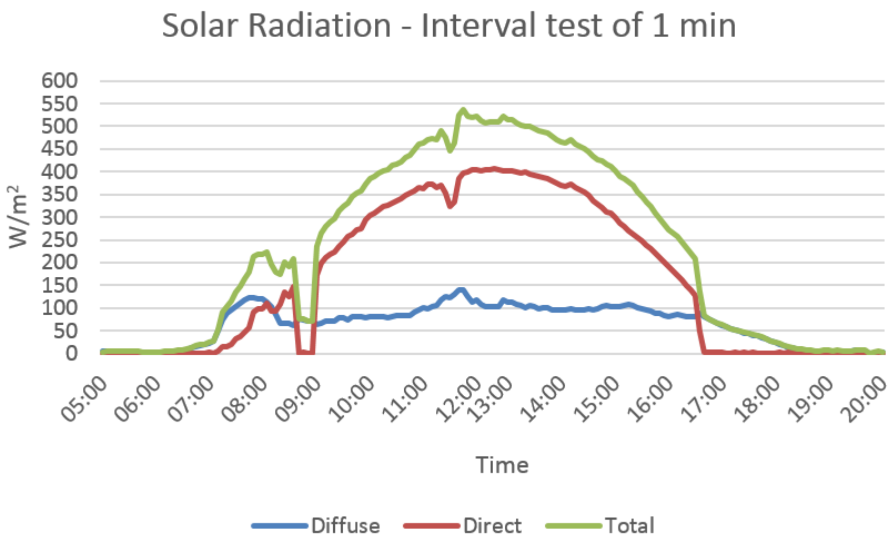

Figure D.5. Solar irradiation interval test of one minute.

As shown in figure D.5 the curve for the three different solar irradiation components is sufficiently smoother compared to the previous time interval of five minutes. As a time interval of two and a half or five minutes are recommended (Delta-T Devices Ltd, 2007), it was chosen to apply a time interval of one minute as this will certainly be sufficient enough.

The time interval of all the solar irradiation measurements was one minute. This time interval is short enough to ensure significant data which will cover every change on the sky dome.

D.2.3 Direct and Diffuse solar Irradiation

The output obtained with pyranometer are one maximum and minimum radiation. Three simple equations are applied to obtain the diffuse, direct and total radiation as seen in equations D.1, D.2 and D.3 (Delta-T Devices Ltd, 2007).

$$Diffuse = 2 \cdot MIN \tag{D.1}$$

$$Direct = MAX - MIN \tag{D.2}$$

$$Total = Direct + Diffuse = MAX + MIN \tag{D.3}$$

Where:

MAX	The maximum radiation output [$\mathrm{w\,m^2}$]
MIN	The minimum radiation output [$\mathrm{w\,m^2}$]

D.2.4 Inaccuracies and Offsets

The SPN1 pyranometer will miss out some of the blue part of the solar spectrum due to the spectral response which goes from 400nm and upwards (Delta-T Devices Ltd, 2007). This may cause an under-reading of the diffuse component of the radiation under very clear blue skies.

During night the SPN1 thermopile pyranometer may give negative output due to radiative cooling, but this effect should be rather small. During nights where it is completely dark the output may still have a small positive output due to noise in the system (Delta-T Devices Ltd, 2007). The noise will be below 3 $\mathrm{w\,m^2}$.

The output is based on readings from seven individual sensors. These should have identical readings, but they will not obtain exactly identical values. This difference in the output value from the seven sensors may be shown as small steps in the output (Delta-T Devices Ltd, 2007).

As the SPN1 pyranometer holds the *WMO Good Quality Pyranometer Classification* the accuracy of the pyranometer is 95 % under normal climatic conditions (Delta-T Devices Ltd, 2007).

The range of the SPN1 pyrnometer is from 0 to 2000 $\mathrm{w\,m^2}$, the resolution is from 0.6 $\mathrm{w\,m^{-2}}$ to 0.6 $\mathrm{m\,V}$. The accuracy is ± 5 % for daily integrals , while the accuracy is ± 5 %, which means ± 10 $\mathrm{w\,m^{-2}}$, for daily and hourly averages. For individual readings the accuracy is ± 8 % ± 10 $\mathrm{w\,m^{-2}}$ (Delta-T Devices Ltd, 2007).

D.3 Sunrise and sunset

The following table shows the time of sunrise, sunset and the hours of daylight for the measuring period (Time og AS, March 2015).

Day	**Sunrise**	**Sunset**	Hours of daylight
Friday 13.03.2015	06:41	18:13	11:32
Saturday 14.03.2015	06:38	18:16	11:38
Sunday 15.03.2015	06:35	18:18	11:43
Monday 16.03.2015	06:32	18:21	11:49
Tuesday 17.03.2015	06:29	18:23	11:54
Wednesday 18.03.2015	06:26	18:26	12:00
Thursday 19.03.2015	06:23	18:28	12:05
Friday 20.03.2015	06:20	18:31	12:11
Saturday 21.03.2015	06:17	18:33	12:16
Sunday 22.03.2015	06:14	18:35	12:21
Monday 23.03.2015	06:11	18:38	12:27
Tuesday 24.03.2015	06:08	18:40	12:32
Wednesday 25.03.2015	06:05	18:43	12:38
Thursday 26.03.2015	06:02	18:45	12:43

Table D.1. Sunrise and sunset during the measurement period.

Interior Illuminance E

The interior illuminance was measured in the cell office facing east. A detailed description of the measurements follows in this chapter.

E.1 Purpose of Interior Illuminance Measurements

The purpose of measuring the interior illuminance was to establish the illuminance distribution in the room under varying sky conditions. Simultaneously the exterior illuminance was measured, see F on page 239. The relation between the interior and exterior illuminance can be defined by solar light factors. The interior illuminance measurements was applied in analysis of interior illuminance distribution due to different values of reflectance.

The illuminance measurements was conducted on days with the occupant in the room, as well as days when the occupant was not present, see H.1 on page 256. In this way it was possible to study the illuminance levels for daylight and artificial light together, and also the illuminance levels for daylight only. To further investigate this, a correlation factor between the amount of artificial light and daylight was made, see G on page 245.

The power of the armature was measured simultaneously as the interior illuminance to find a relation between illuminance level on the working plane and the power of the armature.

E.2 Luxmeters

11 Hagner SD2 luxmeters measuring interior illuminance were applied. They were attached to wooden stand with a height of 0.85 m as seen in E.1 on the next page. The calibration file for the luxmeters can be found in the electronic appendix.

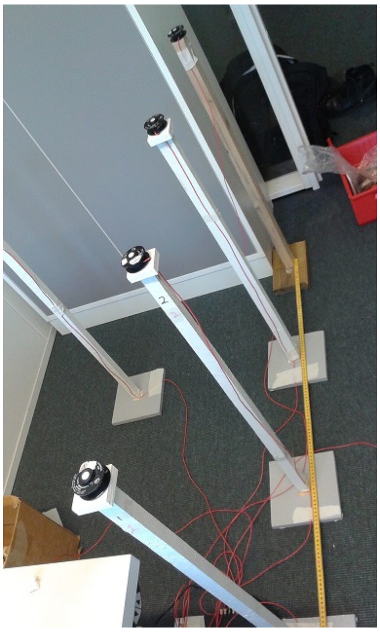

Figure E.1. Hagner SD2 luxmeters attached to wooden stands

The luxmeters were connected to a Hagner multi-channel amplifier MCA-1600, which then was connected to a Grant Squirrel SQ2040 datalogger. The amplifier sends a voltage signal to the datalogger, and the data is then exported to a computer via Squirrelview software.

E.3 Conduction of Interior Illuminance Measurements

In total 11 luxmeters were placed inside the cell office as seen in figure E.2.

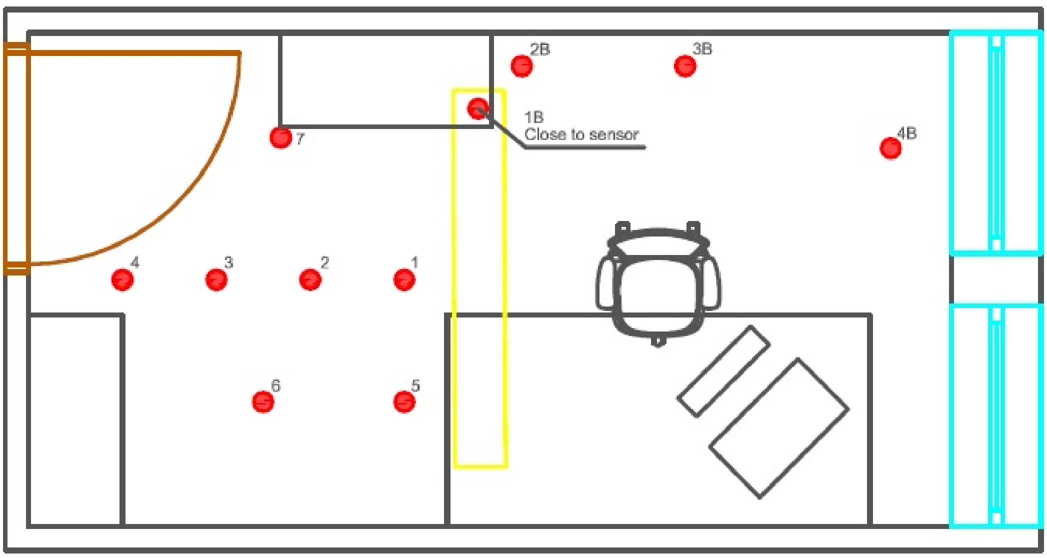

Figure E.2. Illuminance measurement points in the single cell office.

Ten of these were placed 85 m above the floor level as this is defined as the work plane (**?**). One luxmeter was placed close to the daylight sensor on the armature as seen in E.3, to measure the illuminance that the sensor receives.

Figure E.3. Luxmeter attached to the armature close to the daylight sensor

Most of the luxmeters were placed in the back of the room as this is the area where the least amount of daylight will reach. For an office, a daylight factor of 2% in the work area is required (**?**). In this case, the entire office is considered as the work area so the results can be used for an estimation of any office regardless of the placement of the desk. A daylight factor of 2% will therefore be required for the whole room, which makes the illuminance measurements for the area in the back of the office most crucial.

E.4 Measuring Period and Frequency

The interior illuminance was measured from 13.03.2015 to 26.03.2015 with a 10 second interval.

Exterior Illuminance F

F.1 Purpose of Exterior Illuminance Measurements

The exterior illuminance was measured, vertically as well as horizontally. The purpose of the measurements was to define the CIE sky conditions by looking at the relation between the horizontal and vertical illuminance, and comparing it to the relation in the CIE sky models. In this way a division between clear-, intermediate- and overcast sky conditions would be made.

F.2 Illuminance meter

The outdoor illuminance was measured with an EXTECH Instruments HD400 Digital Light Meter as seen in figure F.1, it is a hand-hold illuminance meter. The illuminance meter contains of a light sensor and a meter which shows the measured illuminance at a point in lux or klux ·

Figure F.1. Hand-held illuminance meter used for the reflectance measurements

The illuminance meter can be set to different ranges, the ranges vary from 400.0 to 400.0k with varying resolution and accuracy. For the range of 400 the resolution is 0.1, while for the resolution of 4000 the resolution is 1, for both ranges the accuracy is $\pm(5\%+10digits)$ (EXTECH Instruments, 2013). This means that the reading is off by $\pm 5\%$ and that the least significant digit may vary with up to 10 digits. For the range of 40.00k the resolution is 0.01k and for the range of 400.0k the resolution is 0.1k, for both ranges the accuracy is $\pm(10\% + 10digits)$.

F.3 Conduction of Exterior Illuminance Measurements

The exterior illuminance was measured as point measurements with a hand-held illuminance meter as seen in F.1 on the previous page. The measurements were conducted on the roof of the case building, or in a open space close to the case building, at certain times of the day when changes in the sky condition was observed. As seen in F.2 and F.3 the illuminance was measured both vertically and horizontally.

Figure F.2. Horizontal outdoor illuminance measurement

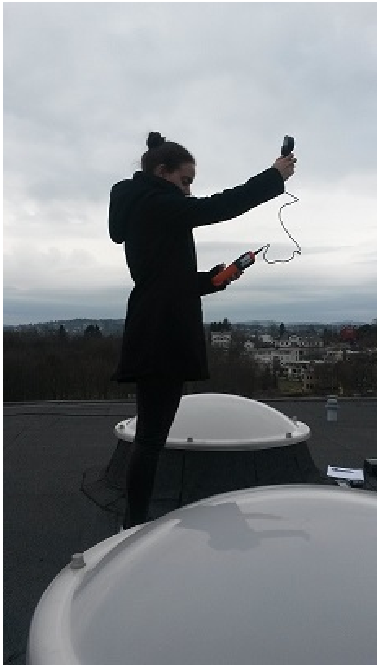

Figure F.3. Vertical outdoor illuminance measurement

F.4 Measuring Period and Frequency

The exterior illuminance was conducted as point measurements when changes in the sky condition was observed. The date and time, as well as the location, when the measurements were conducted can be seen in the table F.4.

F.5 Measurement Results

Table F.4 on the facing page shows the results from the exterior illuminance measurements.

Date	Time	Location	Recieved Horizontal Illuminance [lux]	Receieved Vertical Illuminance [lux]			
				North	South	East	West
16.mar	16:00	Case building	3539	1457	1902	Not measured	Not measured
17.mar	11:00	Open space	12474	Not measured	Not measured	Not measured	6991
17.mar	11:15	Open space	13804	Not measured	Not measured	Not measured	7411
17.mar	13:30	Open space	54607	11339	47652	27091	14305
17.mar	15:30	Open space	22642	7503	27388	7810	21926
18.mar	07:50	Case building	1822	1821	1831	1728	1890
19.mar	08:00	Case building	5938	2531	3053	2685	2409
21.mar	09:55	Case building	47140	7452	80282	7554	74452
21.mar	14:30	Case building	26682	8168	77009	7145	75884
21.mar	16:20	Case building	13896	6020	10827	6531	80998
23.mar	08:00	Case building	3155	1519	1519	1621	1519
23.mar	13:00	Open space	24974	7063	20616	9508	19062
24.mar	11:50	Case building	66984	8168	98899	23716	9191
26.mar	15:30	Case building	12177	10305	9477	9774	9549

Figure F.4. Results from the exterior illuminance measurements

The luminance distribution in the standard CIE clear sky is dependent on the position of the sun. Since the exterior illuminance was measured by a hand-held illuminance meter only, the solar angle was not measured. The exterior illuminance measurements were therefore not taken into account when defining the clear sky.

CIE's definition of an overcast sky is that the luminance in the zenith is 3 times higher than in the horizon. This relationship is investigated for the exterior illuminance measurements for each day. As seen in table F.4, the vertical illuminance in the different cardinal directions vary a lot for each measurement point. Therefore the relationship between the horizontal illuminance (zenith) and the vertical illuminance is calculated separately for each cardinal direction. The results can be seen in table F.1.

Day	Time	Zenith:North	Zenith:South	Zenith:East	Zenith:West
16. March	16:00	2.4	1.9	-	-
17. March	11:00	-	-	-	1.8
17. March	11:15	-	-	-	1.9
17. March	13:30	4.8	1.1	2.0	3.8
17. March	15:30	3.0	0.8	2.9	1.0
18. March	07:50	1.0	1.0	1.1	1.0
19. March	08:00	2.3	1.9	2.2	2.5
21. March	09:55	6.3	0.6	6.2	0.6
21. March	14:30	3.3	0.3	3.7	0.4
21. March	16:20	2.3	1.3	2.1	0.2
23. March	08:00	2.1	2.1	1.9	2.1
23. March	13:00	3.5	1.2	2.6	1.3
24. March	11:50	8.2	0.7	2.8	7.3
26. March	15:30	1.2	1.3	1.2	1.3

Table F.1. Relationship between measured illuminance in zenith and horizon in the different cardinal directions

Figure F.5. Snapshot of the sky from the cell office on Tuesday 17.03.2015 at 15:30 o'clock

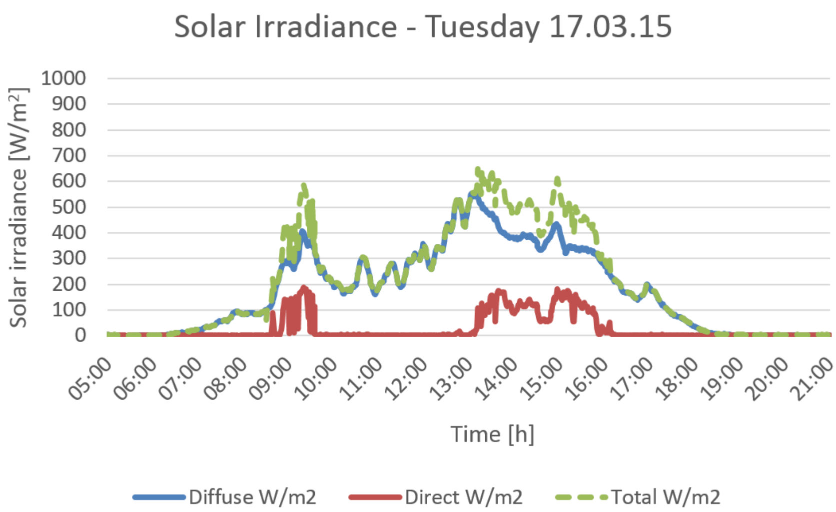

Figure F.6. The diffuse, direct and total irradiation for Tuesday 17.03.2015

Since the pictures of the sky is taken from the cell office facing East, the luminance relation between zenith and horizontal in the East direction is considered when validating the CIE definition.

As seen in the table F.1, the relation between the luminance in zenith and the east direction is 2.9 on the 17^{th} of March at 15:30. This means that, according to the CIE definition, the sky should be overcast. This is confirmed by picture F.5 which shows the sky seen from the cell office on the 17^{th} of March at 15:30. The solar irradiance measurements seen in I.16 shows that the direct component of the irradiance at 15:30 is much lower than the diffuse component, which also indicates that the sky was overcast at that point. However, graph I.16 also shows that the direct irradiance is varying throughout the day, which means that the sky conditions were also changing. Looking at the values in table F.1 it can also be seen that the luminance relation was varying during the day and also for the different cardinal directions.

This shows that the CIE standard definition for an overcast sky, in this case, is accurate. However, the fact that the exterior illuminance varies so much from one cardinal direction to the other, shows that in reality the sky is much more complex than what CIE has defined. It should be mentioned that the exterior illuminance only was measured at certain times of the day on some days, and at different locations where the surroundings might have caused inaccurate readings.

F.6 Accuracy

To determine the daylight factor in the room, the exterior illuminance should have been measured simultaneously as the interior illuminance and not just as point measurements. Due to the lack of equipment this was not possible. This will lead to somewhat inaccurate results.

The exterior illuminance was measured in an open space on ground level on some days. The buildings surrounding this space might have blocked and/or reflected the daylight to some extend, which might have caused inaccuracy in the readings.

A cause of error may be the cosine response of the illuminance meter. A illuminance meter is calibrated for exactly vertical light, therefore when angular incident light hits the photo cell a larger part of the light will be reflected and the illuminance meter will show a too low light value (Statens Byggeforskningsinstitut, 2008). The cosine response of the EXTECH Instruments HD400 light meter is $f_2' \leq 2\%$ (EXTECH Instruments, 2013).

Correlation Between Illuminance and Electricity Usage G

G.1 Purpose of Experiment

To be able to determine the available daylight in a room, measurement of the interior- and exterior illuminance should be conducted without any artificial light in the room. This can however be difficult when measuring in a room where the occupant is present during the day and the artificial light cannot be turned off. In this case the measurements first have to be conducted with both daylight and artificial light in the room, and then the measurements should be performed again, at night time, with only artificial light in the room (**?**). A correlation factor between the illuminance from the daylight and the artificial light can then be made.

As the armature in the case building never turns off even when there is sufficient daylight in the cell office, but turns to a set minimum power. It is of interest to investigate what this power is and at what illuminance level this occurs.

G.2 Equipment

A small light bulb as seen in G.1 was used for controlling the illuminance received by the armature.

Figure G.1. Light bulb used to manipulate the daylight sensor

The light bulb was connected to a Labor-Netzgerat EA 3031S transformer that was used for regulating the light bulb.

A tube was used to shield the daylight sensor from any surrounding light. One end of the tube was placed over the daylight sensor while the light bulb was inserted at the other end. In this way the illuminance level received by the armature could be controlled.

A sparometer was used for measuring the kilowatt hours for the armature. A description of the sparometer can be found in H on page 253.

The illuminance from the artificial light was measured by the luxmeters as seen in E on page 235. An illuminance meter as seen in F.1 on page 239 was placed on the desk right below the armature for additional illuminance readings at this certain point.

G.3 Conduction of Measurements

The lightbulb was inserted into one end of the tube while the other end of the tube was covering the daylight sensor on the armature as seen in G.2.

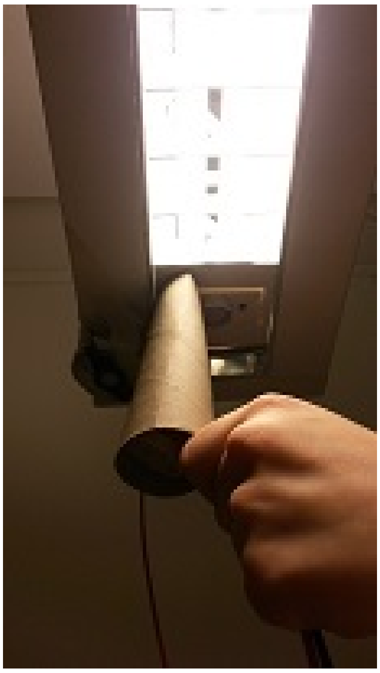

Figure G.2. Measurement conducted with the small tube

The light bulb was dimmed to different illuminance levels to observe the dimming level and time, and to see at which illuminance level the armature would give maximum and minimum power.

G.4 Measurement Results

Graph G.3 on the facing page shows the correlation between the voltage received by the light bulb and the illuminance received by the sensor.

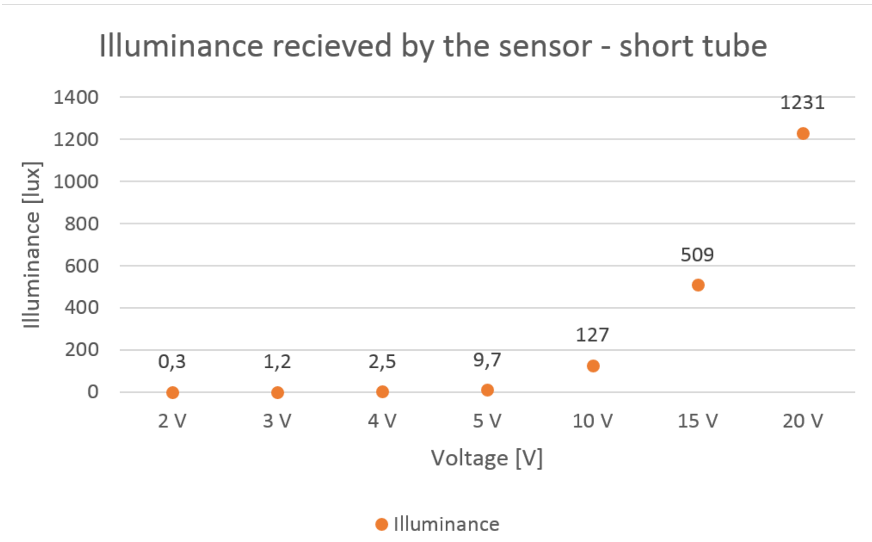

Figure G.3. Correlation between voltage input to the light bulb and illuminance received by the sensor

The illuminance measured by the hand-held illuminance meter on the work plane is displayed in graph G.4.

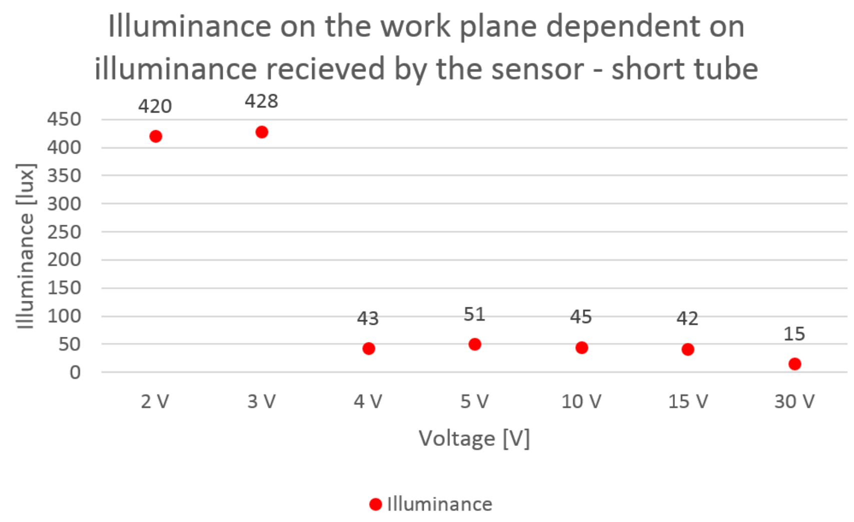

Figure G.4. Illuminance measured by the hand-held illuminance meter on the work plane

The graph shows that when the armature receives more than 3 V which corresponds to an illuminance level of 1.2 lux, the armature starts dimming the light.

Graph G.5 on the following page shows the illuminance measured by the luxmeters when the daylight sensor is covered and the armature generates maximum power.

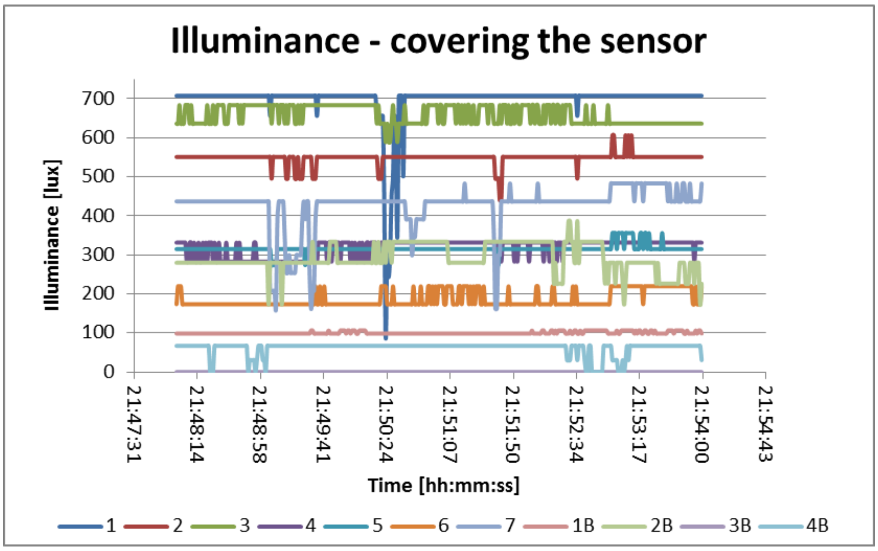

Figure G.5. Illuminance measured by the luxmeters in the room when the daylight sensor is covered

Sensor number 1 is clearly the sensor receiving the highest levels of illuminance with values over 700 lux. The disturbances seen in the graph is created by our presence in the room while conducting the measurements.

The lightbulb was then tuned to 15 V which corresponds to an illuminance level of 509 lux. This causes the armature to generate minimum power. The illuminance measured by the luxmeters can be seen in graph G.6

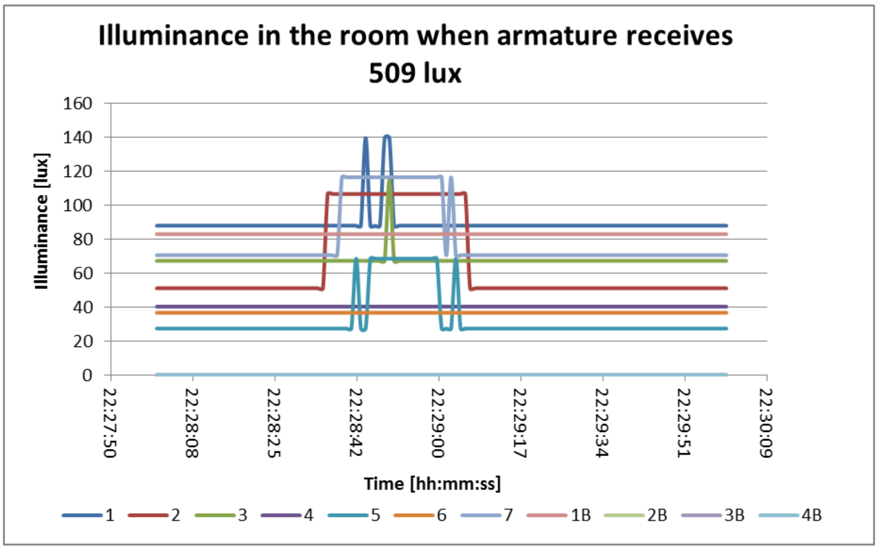

Figure G.6. Illuminance measured by the luxmeters in the room when the daylight sensor receives 509 lux

All the luxmeters receives below 100 lux when the armature is set on minimum power.

The light bulb was tuned to be able to observe at which illuminance levels the armature generates maximum and minimum power. The graphs G.7 on the facing page, G.8 on the next page and G.9 on page 250 shows the illumiance measured by the luxmeters when the armature receives 0.3 lux, 1.2 lux and 2.5 lux respectively.

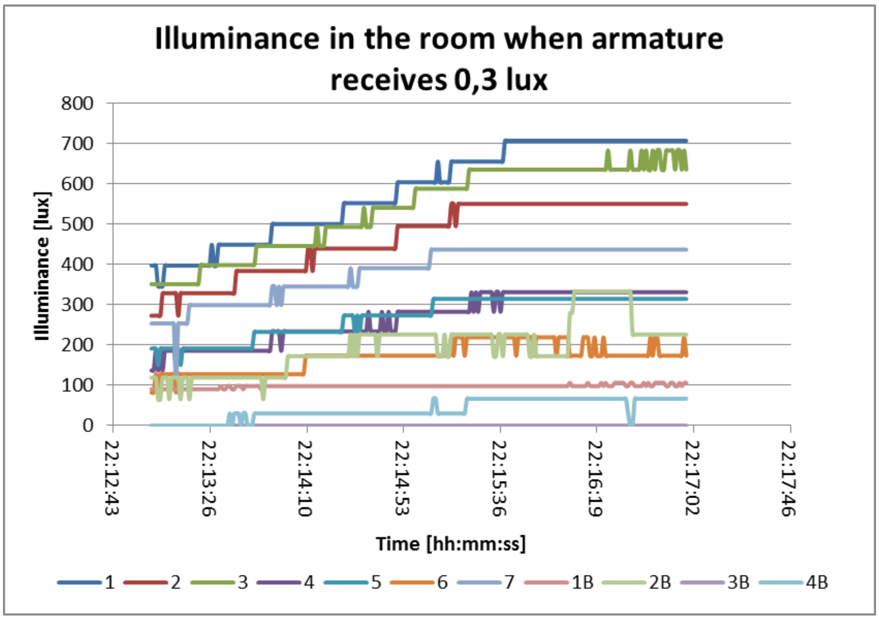

Figure G.7. Illuminance measured by the luxmeters in the room when the daylight sensor receives 0.3 lux

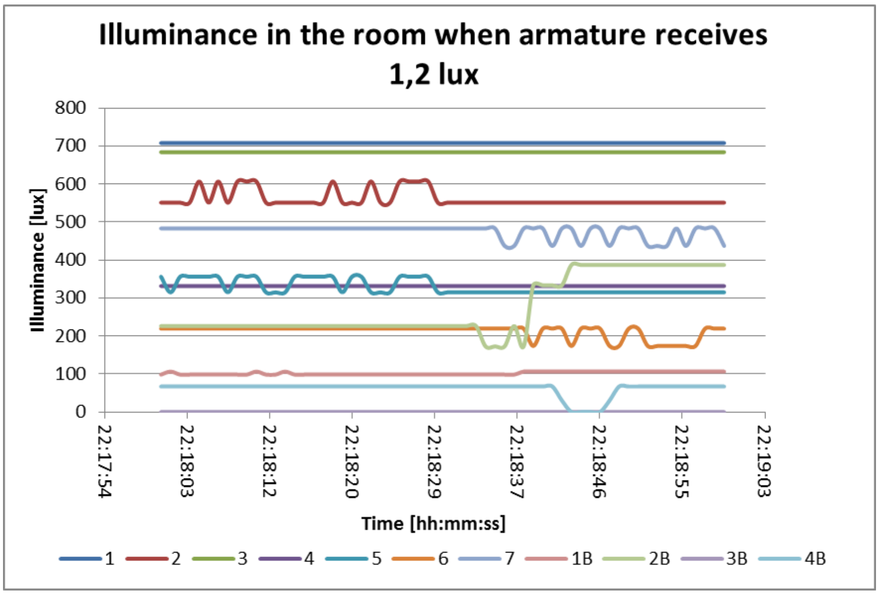

Figure G.8. Illuminance measured by the luxmeters in the room when the daylight sensor receives 1.2 lux

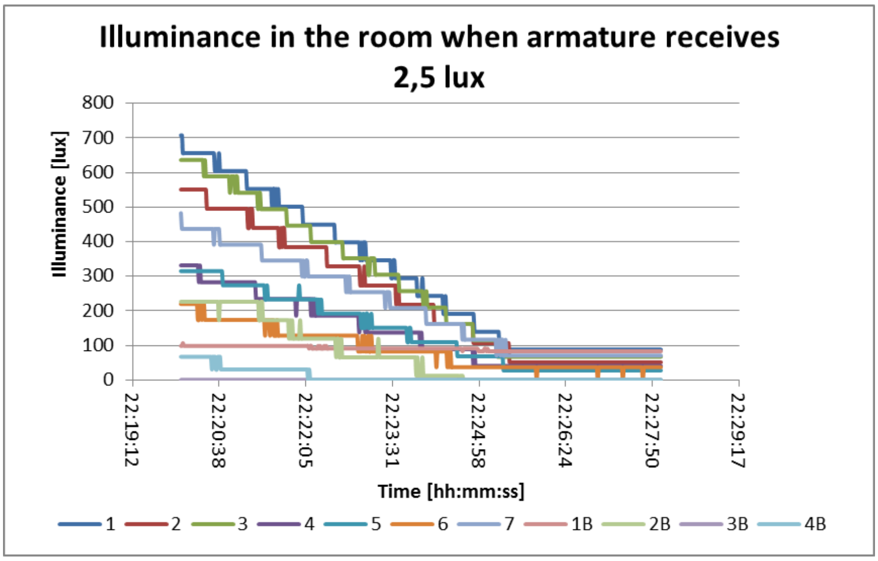

Figure G.9. Illuminance measured by the luxmeters in the room when the daylight sensor receives 2.5 lux

It takes approximately 5 minutes for the light to be switched from minimum to maximum and vice versa. When the bulb is tuned to 3 V the armature receives 1.2 lux, and this is is the illuminance level which causes the armature to generate maximum power. When the bulb is tuned to 4 V, which corresponds to 2.5 lux, the armature dims the light down to the minimum. The experiment shows that in reality the armature goes from maximum power to minimum power and it takes five minutes. The armature does in fact not have dimming, it only has two steps; maximum and minimum as seen in graph G.10.

Simultaneously with the illuminance measurements, the power of the armature was measured by the SparOmeter. The results are shown in the following graph G.10.

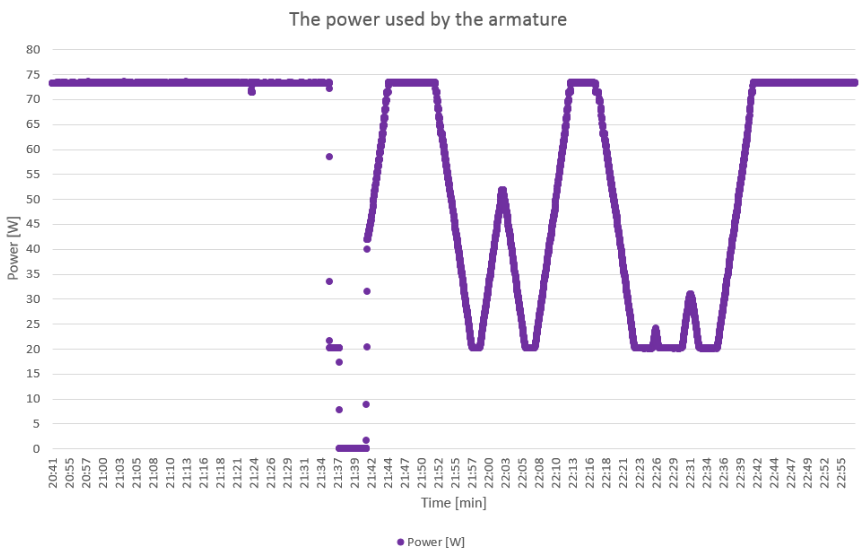

Figure G.10. Measured power for the SparOmeter during the experiment

The graph shows that the maximum power of the armature is 74.4 W, while the minimum power is 20.1 W. The "dimming" is only the armature increasing or decreasing the power. It can therefore be concluded that the armature in the case building only has two steps: 74.4 W and 20.1 W.

Sensor 1 on the working plane of 0.85 m above the floor is applied when investigating

G.5 Accuracy

Since the daylight- and occupancy sensor on the armature cannot be turned off, this experiment requires someone to be present in the room during the measurements. This causes disturbance in the measurement results. As seen in the presented graphs, sensor number 3B almost consistently shows 0 lux. This is due to the sensor being located right next to where the person holding the tube has to stand, which leads to the sensor being blocked during the experiment.

Electricity Usage for the Artificial Lighting on Room Level H

There is one armature in each cell office as seen in figure H.1, every armature has two fluorescent light tubes with 35 W in each, so every armature has 70 W as seen in figure H.2.

Figure H.1. The armature in the cell office

Figure H.2. The two 35W fluorescent light tubes in the armature

The ampere is calculated with the following equation H.1.

$$\frac{P}{U} = I \tag{H.1}$$

Where:

P	Power [W]
U	Voltage [V]
I	Current [A]

As the armature has 70 W and the electricity net in the building is 230 V and one phase, the ampere is then 0.304 A.

H.1 The SparOmeter

The kWh was measured with a SparOmeter as seen in figure H.3.

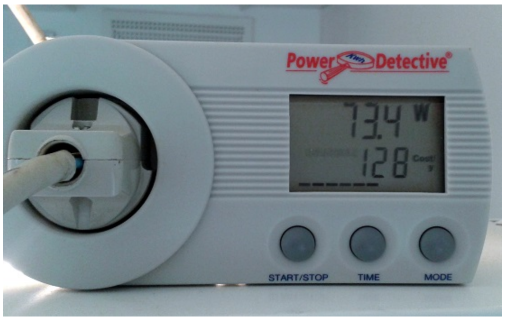

Figure H.3. Power Detective SparOmeter measuring the KWh

The SparOmeter was attached in the conjunction point as seen in figure H.4.

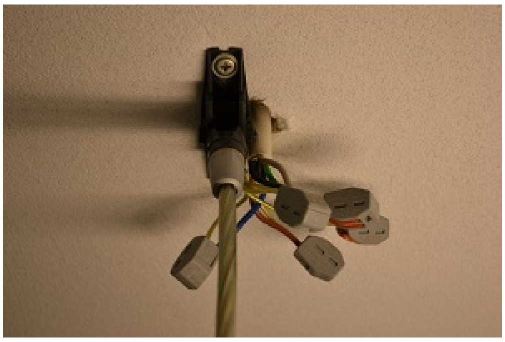

Figure H.4. Conjunction point for the armature where the power meter was attached

Figure H.5. The placement and attachment of the SparOmeter on the armature

H.2 Errors and Inaccuracies

The SparOmeter works with voltage at 230 [V] and the maximum power is 2 300 [W] (S.L. Energiteknik ApS, 2015). The range is from 0.2 - 2 300 [W]. The SparOmeter uses 0.4 [W], which means 0.0024 [kWh] for a period of 6 hours. As the SparOmeter always uses 0.4 [W] it has been decided to neglect this impact in the measurements as the value is fairly small and the impact will be equal for all measurements and therefore even out.

H.3 Measurement Period and Frequency

The kWh was logged during the measurements of exterior and interior illuminance. The kWh was logged every minute from Friday the 13^{th} of March 2015 until Thursday the 26^{th} of March 2015. The time interval of one minute was chosen as the options on the SparOmeter was once every 24 hours, every hour or every minute. The shortest time interval of every minute was chosen as this gives the opportunity to properly investigate the electricity usage. Once every hour would not have shown how the effect will go up an down with available daylight as well as when the occupant leaves the office for lunch or meetings.

H.4 Yearly Electricity Usage

The electricity usage for the short measurements period will not give an accurate answer of the yearly electricity usage. In order to obtain the electricity usage for a year, two methods were applied.

- Relux and Daysim
- Norwegian Reference year

The electricity usage obtained through the measurements with the three different CIE sky conditions was compared to results obtained from Relux and Daysim for the same time period. If the kWh obtained from the two simulation programs are in agreement with the measured kWh, then the simulation program which correspond the most will be applied to simulate the yearly kWh usage.

From NS-EN ISO 15927-4 the Norwegian Reference Year is applied in order to establish the percentage throughout the year where clear, partly cloudy and overcast sky conditions occur. Then the electricity usage for each of the three sky conditions obtained from the measurements will be scaled up with the corresponding percentage of occurrence thorough the reference year.

The 14 days the measurements were conducted for are listed in table H.1. he occupant is not present in the office room for six of the days, and the first day measurements were performed included some errors, therefore seven days are analysed.

Day	**Hours in Office**	**Arrived**	**Left**
Friday 13.03.2015	Measurement error	-	-
Saturday 14.03.2015	Not in office	-	-
Sunday 15.03.2015	Not in office	-	-
Monday 16.03.2015	06:52	08:09	15:36
Tuesday 17.03.2015	04:52	08:07	15:27
Wednesday 18.03.2015	Not in office	-	-
Thursday 19.03.2015	Not in office	-	-
Friday 20.03.2015	04:45	08:00	13:48
Saturday 21.03.2015	07:13	08:21	16:27
Sunday 22.03.2015	Not in office	-	-
Monday 23.03.2015	Not in office	-	-
Tuesday 24.03.2015	04:38	08:23	15:16
Wednesday 25.03.2015	07:03	06:59	15:02
Thursday 26.03.2015	06:43	08:00	15:24

Table H.1. Overview of the days in the measurement period.

Sky Condition, Interior Illuminance and Corresponding Electricity Usage I

In order to determine the sky conditions during the measurements a web cam was installed in the window of the cell office. The web cam was facing the sky outside the cell office. The web cam is filming the sky and registering when the solar shading is active. Snapshots are taken of the sky at 08:00, 10:00, 12:00, 14:00, 16:00 and 18:00.

Pictures of the sky alone is not sufficient when determining the sky conditions. The components of diffuse and direct solar irradiance will help establish the sky conditions. It is of interest to investigate the light level inside the cell office and how it varies with varying sky conditions. The interior illuminance was investigated for every day. It is also of interest to study the corresponding electricity usage of the armature and how the different sky conditions will affect the electricity usage for artificial lighting.

I.0.1 The Sky Condition, Solar Irradiance, Interior Illuminance and Electricity Usage for every day of the Measurement Period

Pictures of the sky for every day as well as solar irradiance graphs are displayed in this section. The results from the interior illuminance measurements from each day of the measurement period is described in this section. The following graphs contain data from 07 : 00 to 17 : 00 o'clock every day. Corresponding electricity usage is also displayed for every day. The results are displayed in graphs showing the increase of the electricity use throughout the day and the effect the armature is using. The effect is varying from 0 W when the armature is off to 74.0 [W], which is maximum. The effect can never be exactly 0 as explained in 6.1 on page 69.

Friday 13.03.15

The sky during Friday 13.03.15 can be seen in picture I.1.

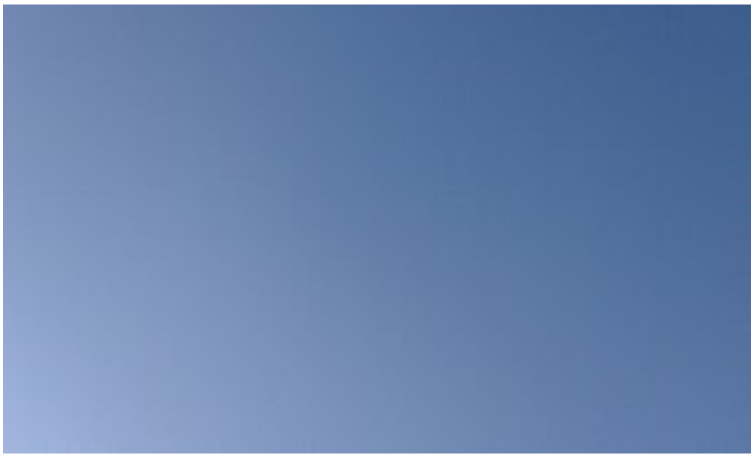

Figure I.1. The sky during Friday 13.03.15

Throughout the whole day the sky was clear sky with mostly no clouds. There was some very small and transparent clouds in the distance. This can be seen in the graph I.2 where the direct component of the irradiance is significantly higher than the diffuse component. From 08:30-09:00 the direct component of the irradiance drops to about zero, and the total component then becomes equal to the diffuse component. This is due to shade from obstacles on the roof hitting the pyranometer, the placement of the pyranometer on the roof is where there is the least shade as it was not possible to completely avoid shade. Therefore the results from 08:30 to 09:00 will be neglected from all measurements.

The results are varying a little bit which may be due to the small and transparent clouds.

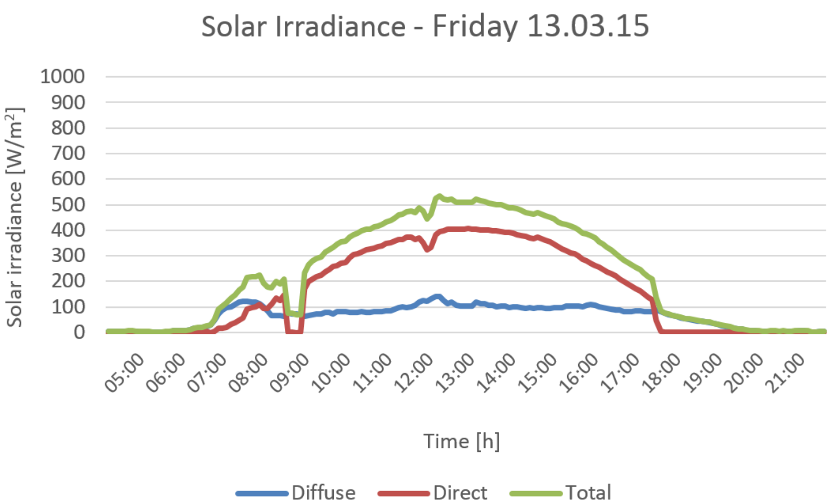

Figure I.2. The diffuse, direct and total irradiation for Friday 13.03.2015

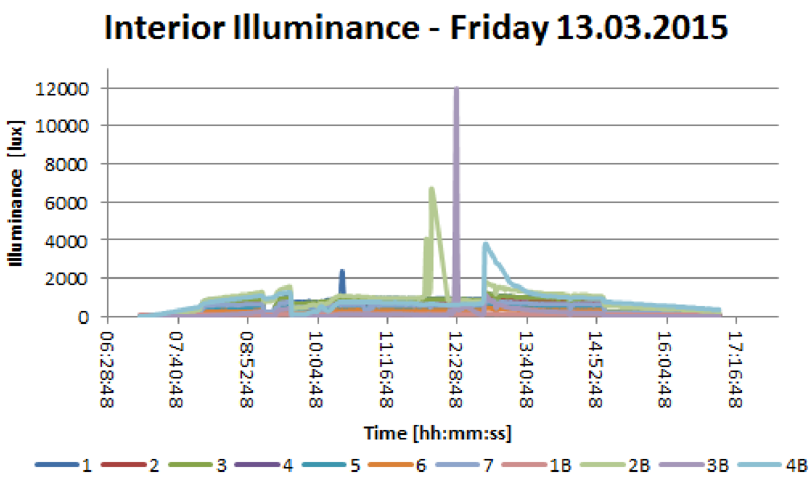

Figure I.3. Results from the interior illuminance measurements, Friday the 13.03.15

The illuminance levels were fairly stable, except from some peaks at some points during the day. As seen in I.2 on the preceding page this was a day with clear sky with just a transparent layer of clouds. The peaks occurred for the sensors close to the window at the time of the day when direct sunlight hit the back wall of the office.

The results for the electricity usage for Friday the 13^{th} are only every hour due to an error with the settings of the SparOmeter. This results are not very representative for a working day as it can not be seen when the occupant leaves the office for example lunch or a meeting. In figure I.4 the increasing used electricity usage is shown with the orange line, effect is shown with blue marks. By the end of the working-day the armature had used 0.074 $[KWh/m^2]$.

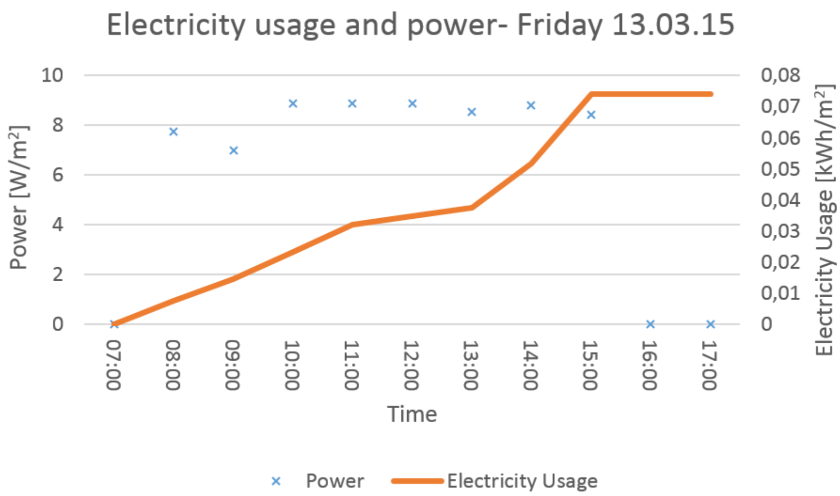

Figure I.4. The effect and electricity usage of the armature during Friday 13.03.15

The results for this Friday the 13^{th} is therefore neglected in the analyses.

Saturday 14.03.15

The sky during Saturday 14.03.15 can be seen in picture I.5.

Figure I.5. The sky during Saturday 14.03.15

The sky during Saturday the 14^{th} of March was fairly similar as Friday the 13^{th} of March. Throughout the whole day the sky was completely clear sky with no clouds. The graph I.6 looks very similar to I.2, but it is more smooth and the results are more stable due to absolutely no clouds on the whole sky dome.

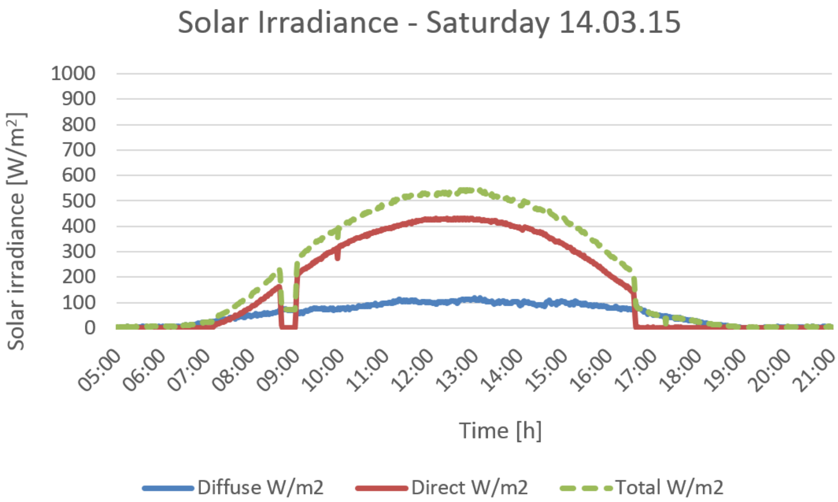

Figure I.6. The diffuse, direct and total irradiation for Monday 14.03.2015

During Saturday the 14^{th} the maximum direct solar irradiation reached 433 W/m^2.

As seen in I.6, the sky was completely clear as the direct component of the irradiance was significantly higher than the diffuse component. This can also be seen in I.7.

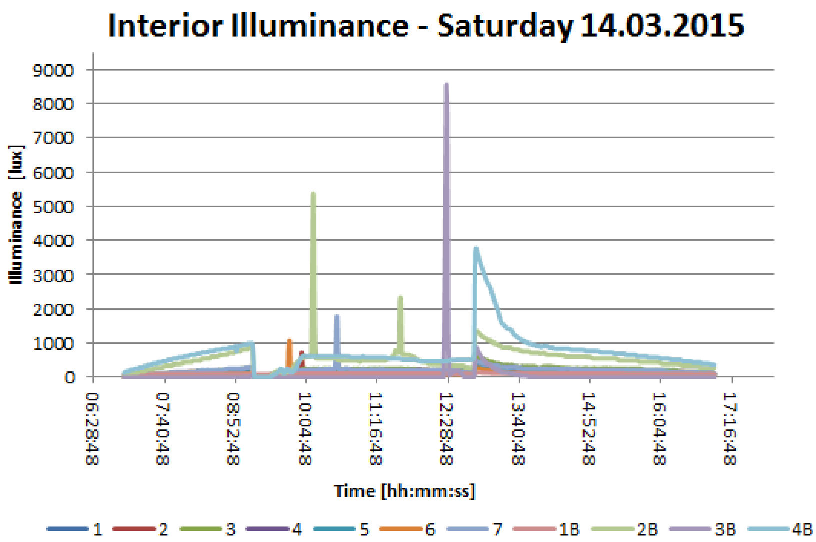

Figure I.7. Results from the interior illuminance measurements, Saturday 14.03.15

The illuminance levels in the room were very low throughout the day. This is because the occupant was not present in the office on this day, which means the illuminance is from the daylight only. The peaks show when the different sensors were hit by direct sunlight entering the room. The maximum peak value reached approximately 8520 lux at 12 : 30.

There was no one in the office throughout this Saturday, therefore the results for both effect and electricity usage were 0 all day.

Sunday 15.03.15

The sky during Saturday 15.03.15 can be seen in picture I.8.

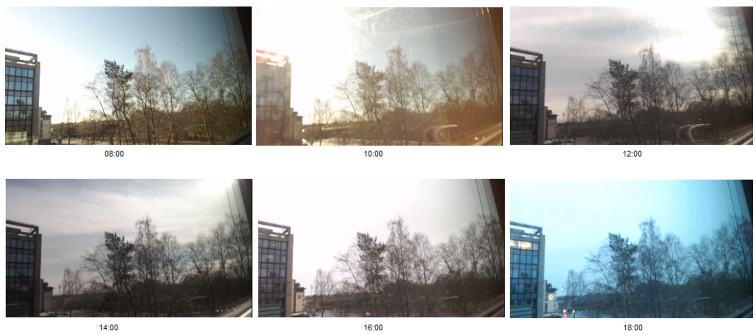

Figure I.8. The sky during Sunday 15.03.15

The sky during Sunday the 15^{th} of March was blue sky with some see through white scattered clouds in the morning from 08:00-12:00. Then thicker and whiter clouds during the afternoon from 12:00-16:00, but still squinting when looking at the sky.

The results for Sunday the 15^{th} of March shows some oscillating results in graph I.9. This may be due to the conditions that day which was blue sky with some small white clouds.

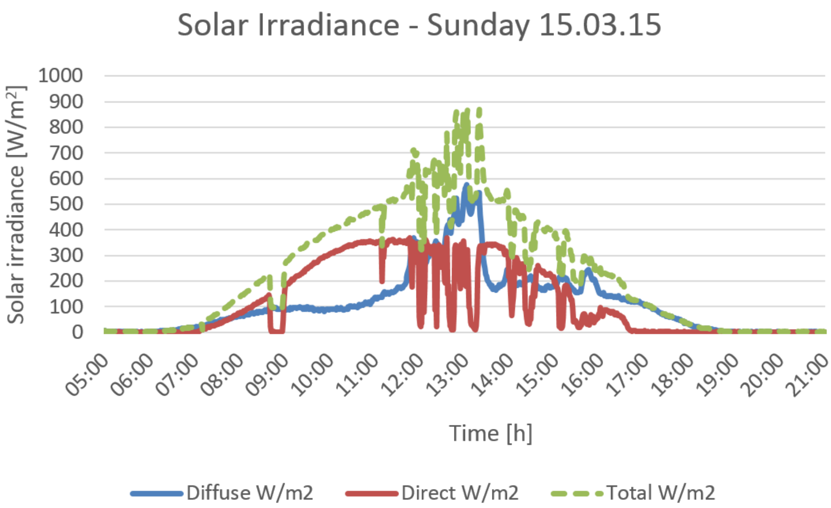

Figure I.9. The diffuse, direct and total irradiation for Sunday 15.03.2015

Due to the varying sky conditions during this day, as seen in I.9, the interior illuminance in the room was varying correspondingly.

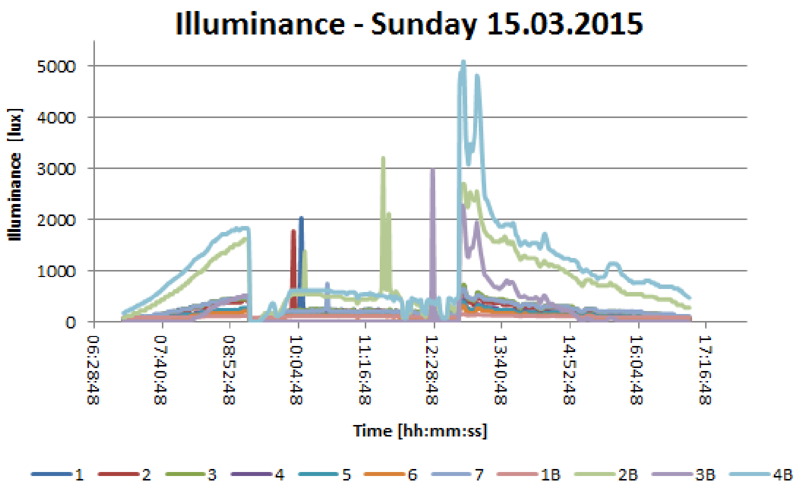

Figure I.10. Results from the interior illuminance measurements, Sunday 15.03.15

The peaks have lower illuminance levels compared to the previous days. The maximum peak value reached approximately 5080 lux at 13 : 00.

As well as for the previous day there was no one in the cell office for this Sunday therefore both effect and electricity usage were 0 all day.

Monday 16.03.15

The sky during Monday 16.03.15 can be seen in picture I.11. Thick white clouds which covered the whole sky dome. Could not see the placement of the sun. The clouds where white, not grey. Had to squint a little when looking at the sky.

Figure I.11. The sky during Monday 16.03.15

The conditions this day was thick with clouds, this can be seen in graph I.12 as the direct component of the irradiation is close to zero while the diffuse component is oscillating and for most of the day the only component of irradiation which was present.

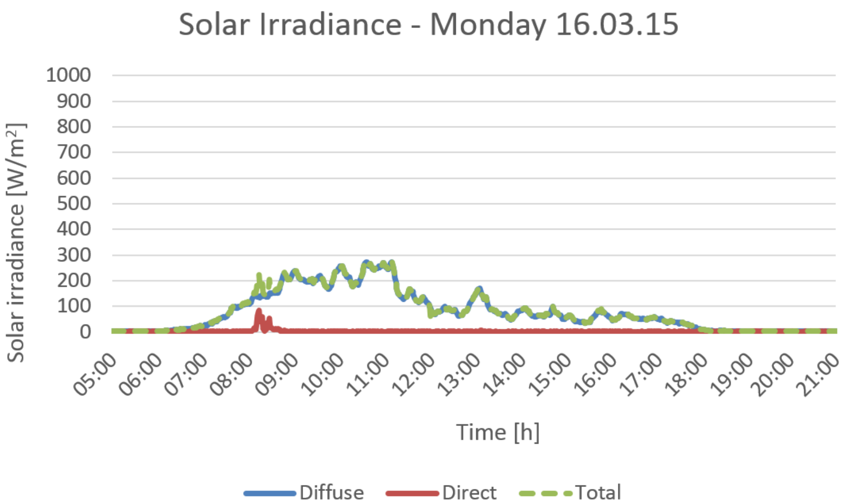

Figure I.12. The diffuse, direct and total irradiation for Monday 16.03.2015

The corresponding illuminance levels can be seen in graph I.13.

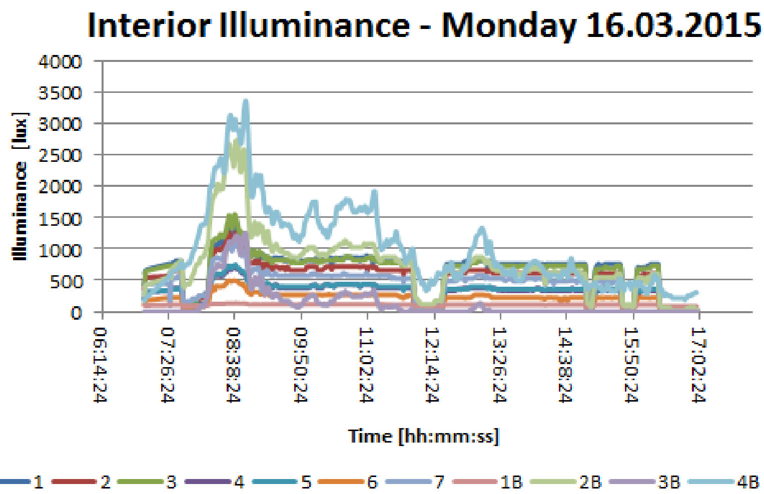

Figure I.13. Results from the interior illuminance measurements, Monday 16.03.15

As seen in the graph, the illuminance levels were much lower on this day. This is due to the overcast sky conditions as seen in I.12 on the preceding page. The maximum peak value was just below 3500 lux at 08 : 50.

The user arrived at his office at 08:09 and left at 15:36 this Monday. The effect was either on maximum or off throughout the day as seen in graph I.14. The increasing used electricity usage is shown with the orange line, effect is shown with blue marks. The grey area underneath the marks for the effect is for illustration of the increasing or decreasing effect to give a better view of when the armature is turned on or off. When the armature turns on or off it has some steps with different levels of effect before it is fully turned on or off.

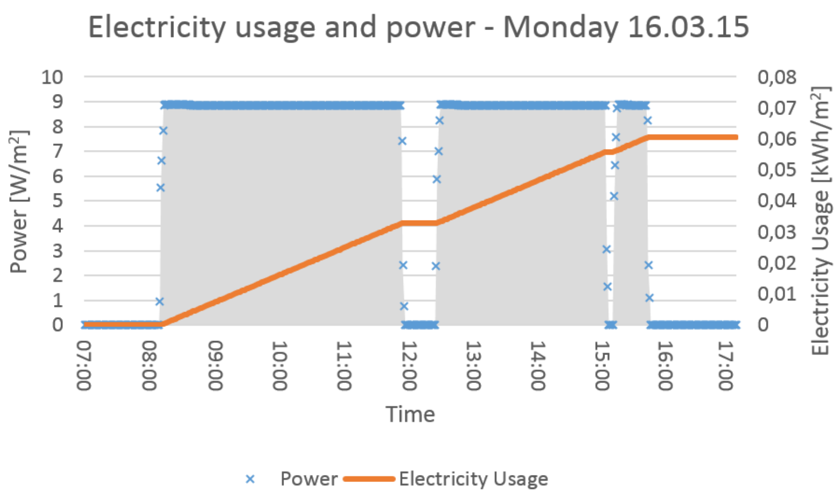

Figure I.14. The effect and electricity usage of the armature during Monday 16.03.15

Effect and electricity usage for Monday 16.03.15:

- Total time the armature was on: 6 hours and 52 minutes.
- Total electricity used by the armature: 0.0605 $[kWh/m^2]$.
- Average effect: 8.557 $[W/m^2]$.

- Maximum effect: 8.907 $[W/m^2]$.
- Electricity usage per hour: 0.00881 $\frac{\text{KWh}}{\text{hm}^2}$

Tuesday 17.03.15

The sky during Tuesday the 17^th of March was shifting from fairly cloudy to almost clear as seen in figure I.15.

As seen in figure **??** the sky had Scattered white clouds with some visible blue sky from 08:00-11:00.

Figure I.15. The sky during Tuesday 17.03.15

From 11:00 to 13:00 white thick clouds covered the whole sky dome as seen in figure I.15. The position of the sun was not visible. As seen in figure I.15 the sky was blue with small scattered transparent white clouds between 13:00-16:00, and the sun was visible.

During Tuesday the 17^{th} the sky conditions was shifting from fairly cloudy to almost clear throughout the day and these shifting conditions can be seen in graph I.16 as the diffuse solar irradiance is significantly higher than the direct component. There is a peak from 08:30 to 10:00 with some rise in the direct component, there is also another peak in the afternoon from 13:10-16:30 when the sky cleared.

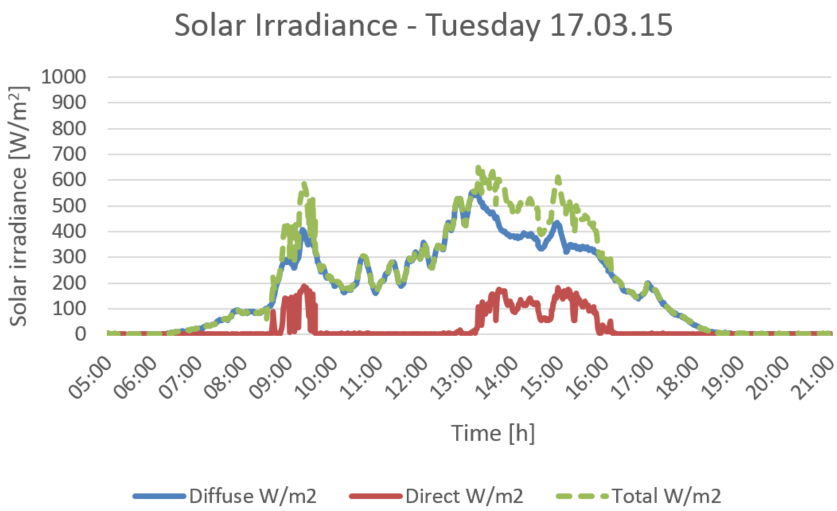

Figure I.16. The diffuse, direct and total irradiation for Tuesday 17.03.2015

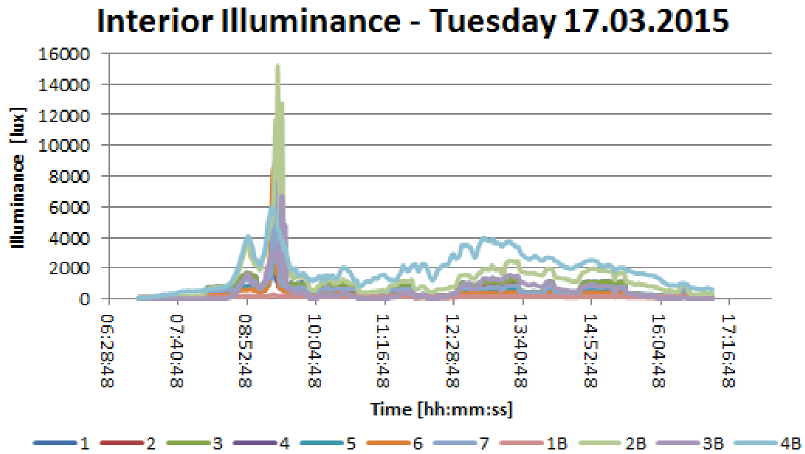

Figure I.17. Results from the interior illuminance measurements, Tuesday 17.03.15

According to I.16 on the previous page the weather was shifting throughout the day. The peak at 09 : 30 reaching approximately 15 000 lux, corresponds to the rise in the direct component in graph I.16 on the preceding page.

As seen in graph I.18 the occupant leaves his office quite often this day. From approximately 09:00 to 09:30 the armature is only using 2,420 W/m^2 which is due to direct sunlight hitting the cell office, the interior illuminance can be seen in graph I.17.

This Tuesday the occupant arrived at 08:07 and left at 15:27.

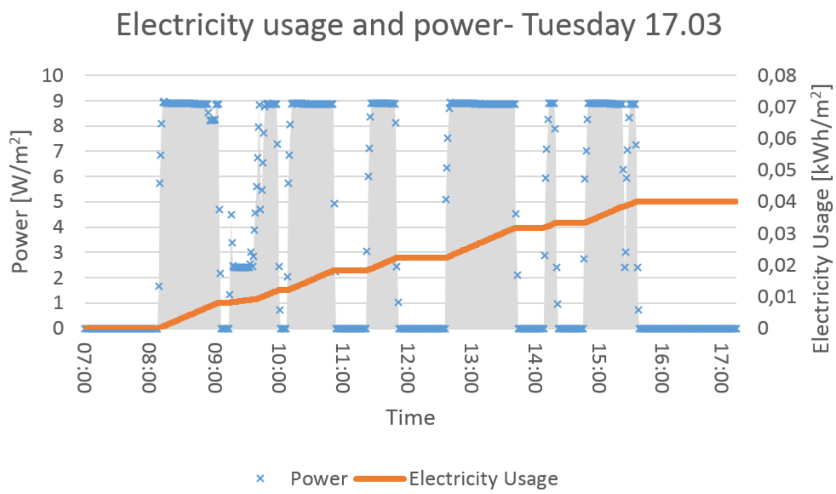

Figure I.18. The effect and electricity usage of the armature during Tuesday 17.03.15

Effect and electricity usage for Tuesday 17.03.15:

- Total time the armature was on: 4 hours and 52 minutes.
- Total electricity used by the armature: 0.0401 $[\frac{\mathrm{KWh}}{\mathrm{m}^2}]$.
- Average effect: 7.589 $[W/m^2]$.
- Maximum effect: 8.956 $[W/m^2]$.
- Electricity usage per hour: 0.00823 $\frac{\mathrm{KWh}}{\mathrm{hm}^2}$

Wednesday 18.03.15

Stable conditions throughout the day. Even sky layer covering the whole sky dome. Drizzle throughout the whole day.

Figure I.19. The sky during Wednesday 18.03.15

During Wednesday it was an even sky layer and drizzle throughout the day, and this condition is also seen in the solar irradiation graph where the direct component of the solar irradiation is close to zero and the diffuse component is dominant and the total component mostly only exist of the diffuse component.

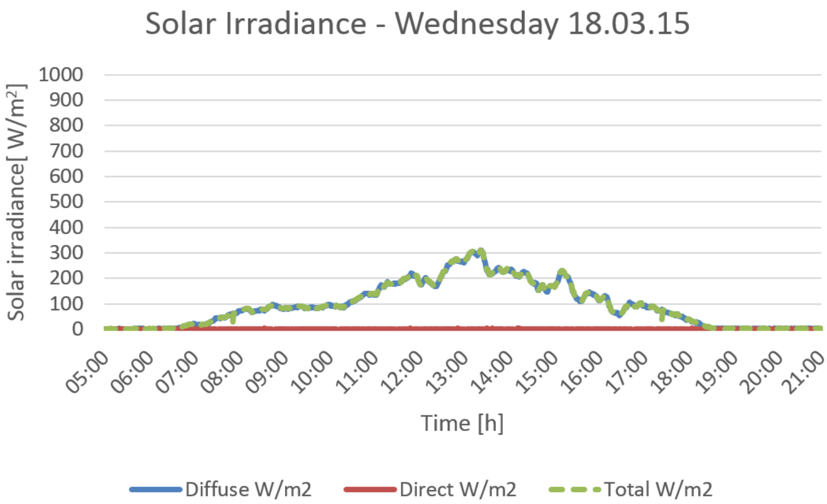

Figure I.20. The diffuse, direct and total irradiation for Wednesday 18.03.2015

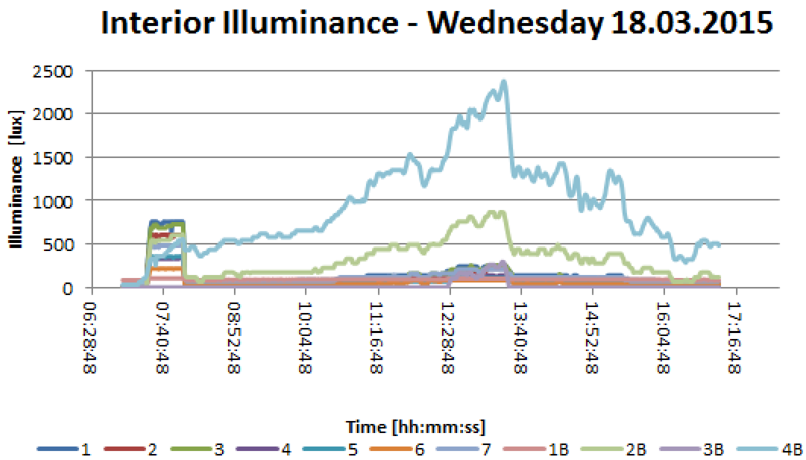

Figure I.21. Results from the interior illuminance measurements, Wednesday 18.03.15

As seen in H.1 on page 256, the occupant was not present in the room on this day, meaning that the illuminance is from daylight alone. This explains the low illuminance levels. The maximum peak value reached approximately 2380 lux at 13 : 20.

The occupant was not using his office during this Wednesday, therefore the results for both *Watt* and *KWh* were 0 all day.

Thursday 19.03.15

Even sky layer covering the whole sky dome. Stable conditions throughout the day.

Figure I.22. The sky during Thursday 19.03.15

During Thursday the 19th of March the sky had an even cloud layer, this can be seen in graph I.23. The sky layer is more compact than for Wednesday the 18th as the solar irradiation graph for Thursday the 19th has a lower vale of diffuse and therefore direct solar irradiation. Less solar irradiation is let through the sky layer.

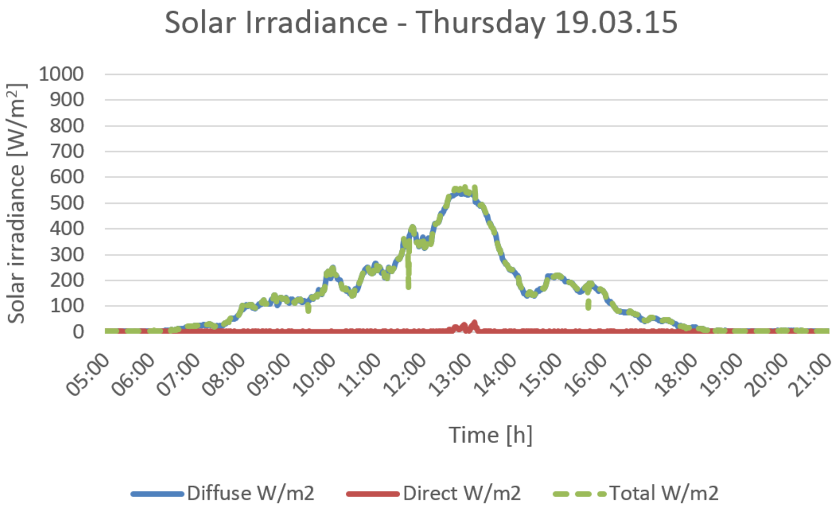

Figure I.23. The diffuse, direct and total irradiation for Thursday 19.03.2015

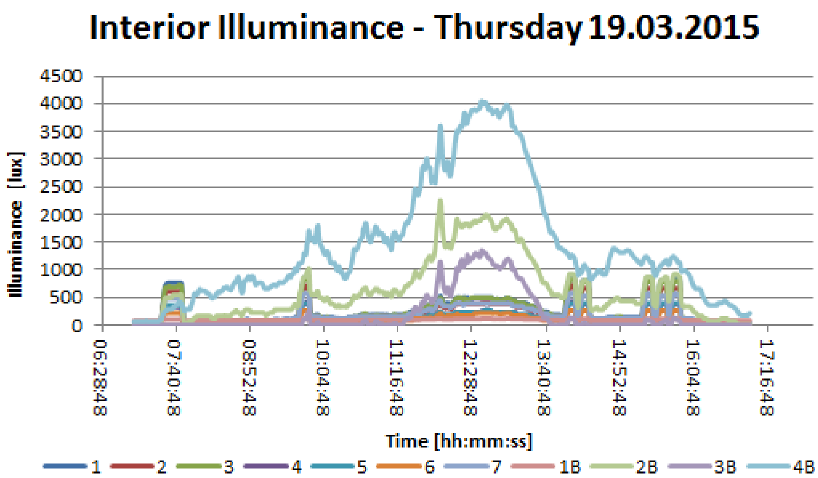

Figure I.24. Results from the interior illuminance measurements, Thursday 19.03.15

The sky had an even cloud layer throughout this day as seen in I.23. The occupant was not present in the room this day. This resulted in fairly low illuminance levels on I.24. The maximum peak value reached approximately 4000 lux at 12 : 40.

The user was not in his office during Thursday the 19^{th}, but still the office is used occupationally by someone as seen in graph I.25. It may be the cleaning staff and it may be some of his colleagues borrowing his office, and by the end of the day the armature had used 0.00883 $\frac{\text{KWh}}{\text{m}^2}$. The results from this Thursday is neglected in further analysis as the occupant is not in his office.

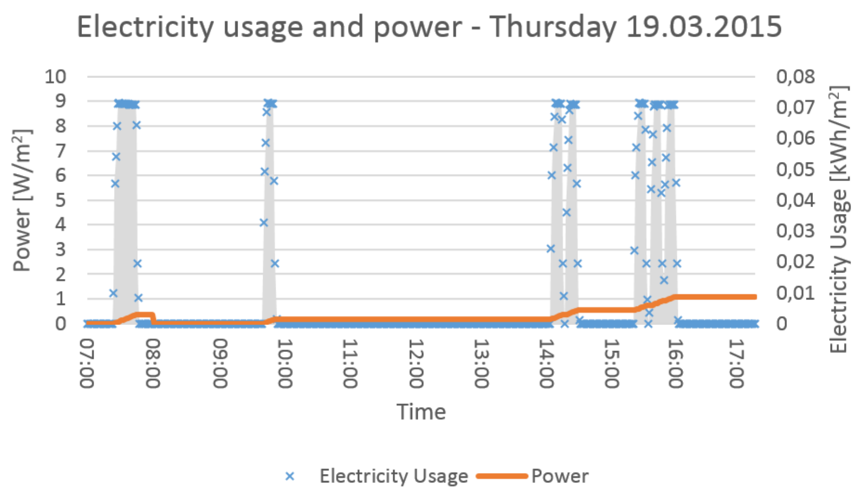

Figure I.25. The electricity usage shown in Watt and KWh for Thursday 19.03.15

Friday 20.03.15

Shifting conditions thorough the day. In the morning between 09:00-11:30 it was a solar eclipse. It was thick white clouds which were moving slowly. During the solar eclipse it was considerably darker.

Figure I.26. The sky during Friday 20.03.15, 13:00-16:00

Later in the afternoon between 11:30 and 17:00 the sky cleared a little towards the afternoon. Still thick white clouds, but some glimpses of the blue sky in between.

Shifting conditions throughout the day with clouds in the morning and then the sky cleared in the afternoon as mentioned in I.0.1.

Between 09:00-11:30 it was a solar eclipse and it was considerably darker as seen by a low value of the total solar irradiation, the total solar irradiation is only represented with the diffuse component as it was cloudy during the solar eclipse.

Later in the afternoon the sky cleared a little and the diffuse component of the solar irradiation became higher as the clouds were not so compact. The direct component is still very close to zero except around 13:30 where there is a small peak in the direct solar component which may be due to a glimpse of the sun when the direct solar component reach the pyranometer.

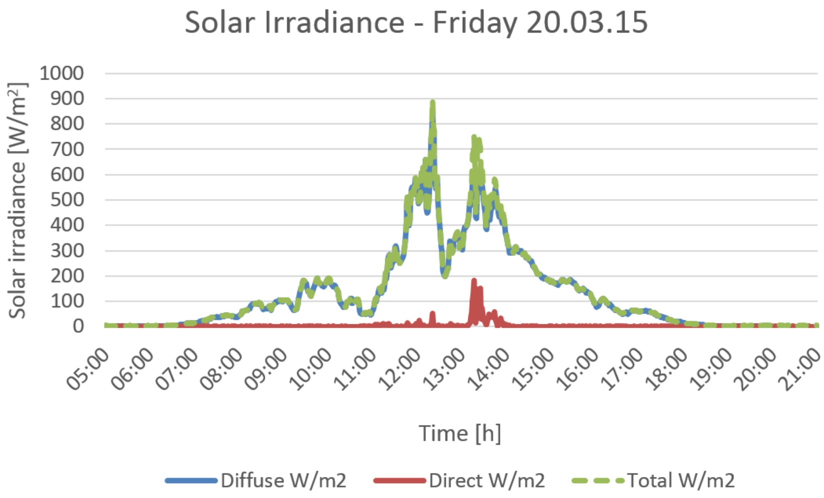

Figure I.27. The diffuse, direct and total irradiation for Friday 20.03.2015

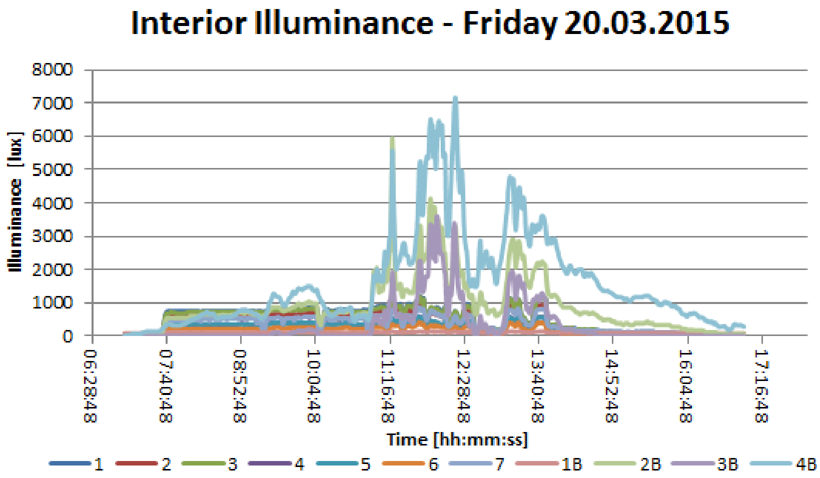

Figure I.28. Results from the interior illuminance measurements, Friday 20.03.15

The sky was cloudy during the first part of the day but brightened up later during the day as seen in I.27. From 09 : 00 to 10 : 30 there was a solar eclipse, which is showing on the illuminance results from 10 : 00 to 10 : 30. The maximum peak value reached approximately 7000 lux at 12 : 20.

The occupant arrived in the morning at 08:00 this day, but then after lunch he was mostly in meetings and then left early for the weekend as seen in graph I.29, the used left at 13:48.

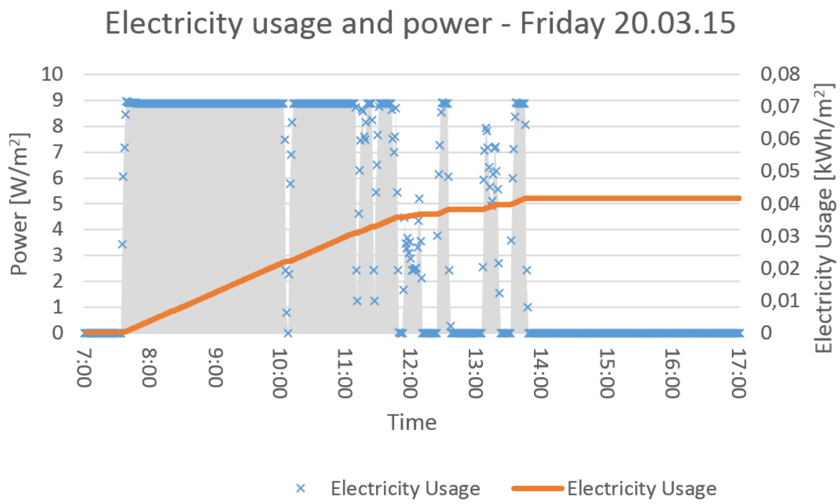

Figure I.29. The effect and electricity usage of the armature during Friday 20.03.15

As seen in graph I.29 from 11:09 to 11:14 and from 11:25 to 11:31 the *Watt* of the armature drops to 10.3 and 10.2 respectively. This may be due to the user leaving the office for a short period or sitting too still so the movement sensor did not recognise any movement.

Effect and electricity usage for Friday 20.03.15:

- Total time the armature was on: 4 hours and 45 minutes.
- Total electricity used by the armature: 0.0380 $[\frac{\text{KWh}}{\text{m}^2}]$.
- Average effect: 6.642 $[W/m^2]$.
- Maximum effect: 8.895 $[W/m^2]$.
- Electricity usage per hour: 0.00800 $\frac{\text{KWh}}{\text{hm}^2}$

Saturday 21.03.15

Throughout the whole day from 07:00-20:00 it was completely clear and blue sky, no clouds, as seen in figure I.30.

Figure I.30. The sky during Saturday 21.03.15

From 09:00-12:00 the sun hit the cell office directly, but the solar shading did not go down. The illuminance on the inside of the glazing was measured with the handheld luxmeter, it was 58.2 klux. The illuminance on the desk was also measured with the handheld luxmeter, it was 22.87

klux. As the sun was moving the places within the cell office which was hit with direct sunlight changed, this can be seen on the luxmeters placed around inside the cell office I.32. During this time the armature only used 20.0 W.

From 12:00 to 14:25 there was still some direct sunlight on the back wall of the office. Lux meter 2B is hit by sunlight from around 13:00 lasting for about 15-20 min as seen in figure I.32. After 14:25 there was no direct sunlight in the cell office.

During Saturday the 21^{st} the sky was completely clear and blue as seen in figure I.30. This can be seen in graph I.31 where the direct component is significantly larger than the diffuse component.

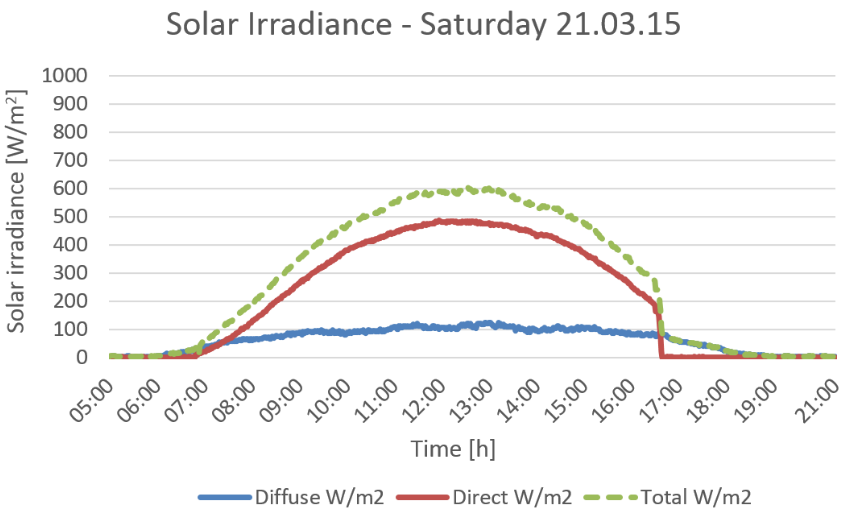

Figure I.31. The diffuse, direct and total irradiation for Saturday 21.03.2015

During Saturday the 21^{st} the direct solar irradiation maximum reached 487 W/m^2.

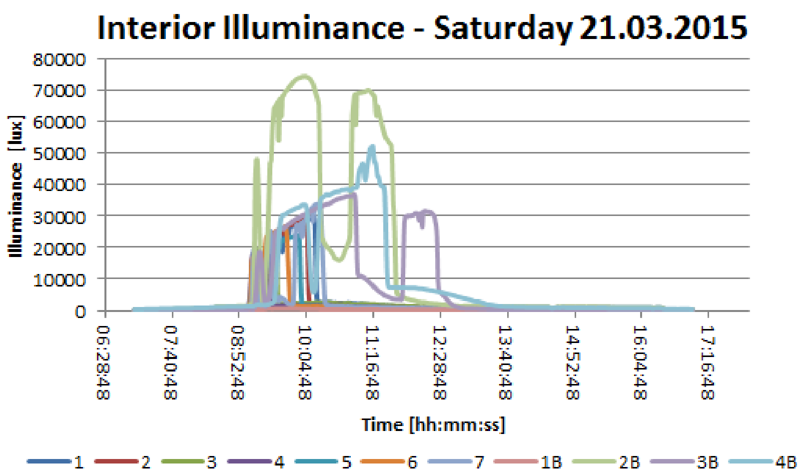

Figure I.32. Results from the interior illuminance measurements, Saturday 21.03.15

The sky was completely clear and sunny on this day according to I.31. The graph I.32 clearly shows when the direct sunlight hit the different sensors throughout the day. The maximum peak value reached approximately 7000 lux at 12 : 20.

As seen in graph I.33 between approximately 09:00 to 12:50 the armature only used about 20 [W]. This was the same time period as the direct sunlight hit the cell office as explained in I.0.1 and the solar shading did not go down as explained in I.32.

The armature did not need to deliver maximum illuminance as the illuminance level in the cell office was rather high as explained in L on page 291.

This Saturday the user arrived at 08:21 and left at 16:27.

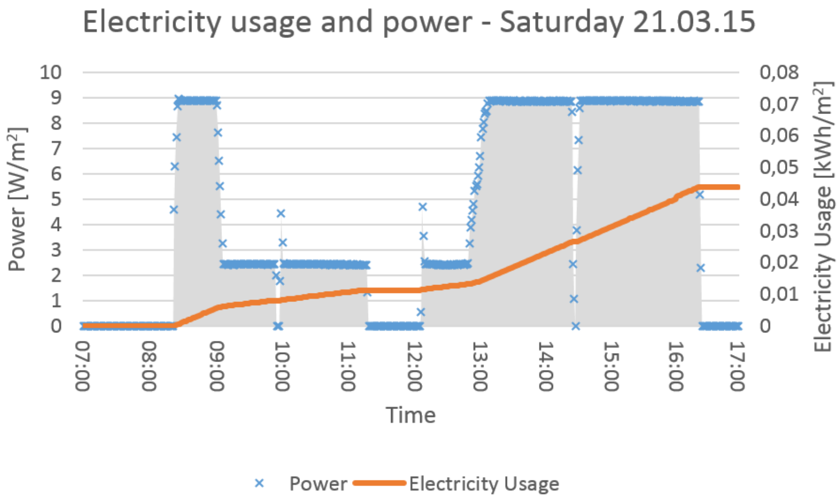

Figure I.33. The effect and electricity usage of the armature during Saturday 21.03.15

Effect and electricity usage for Saturday 21.03.15:

- Total time the armature was on: 7 hours and 13 minutes.
- Total electricity used by the armature: 0.0439 $[\frac{\text{KWh}}{\text{m}^2}]$.
- Average effect: 5.703 $[W/m^2]$.
- Maximum effect: 8.944$[W/m^2]$.
- Electricity usage per hour: 0.00609 $\frac{\text{KWh}}{\text{hm}^2}$

Sunday 22.03.15

White thick clouds covering the entire sky dome throughout the day as seen in figure I.34.

Figure I.34. The sky during Sunday 22.03.15

During Sunday the sky was covered with white thick clouds, this is shown in graph I.35. Towards the afternoon the diffuse component of solar irradiance increases a little which may be due to a thinner cloud layer.

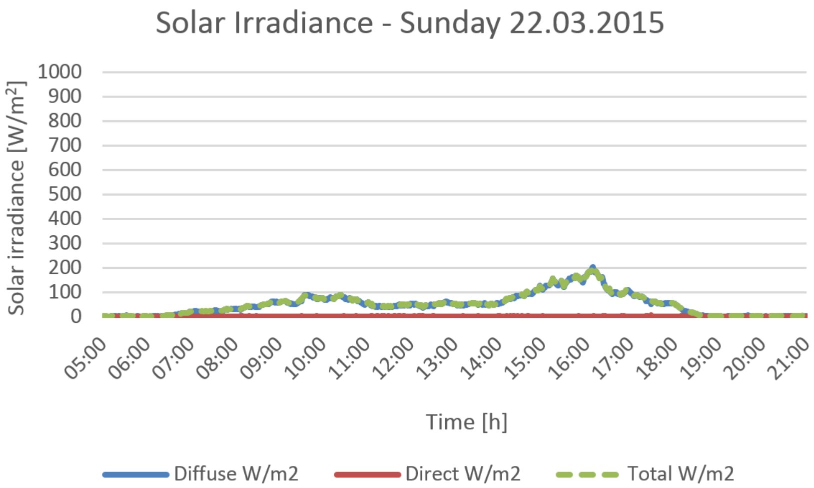

Figure I.35. The diffuse, direct and total irradiation for Sunday 22.03.2015

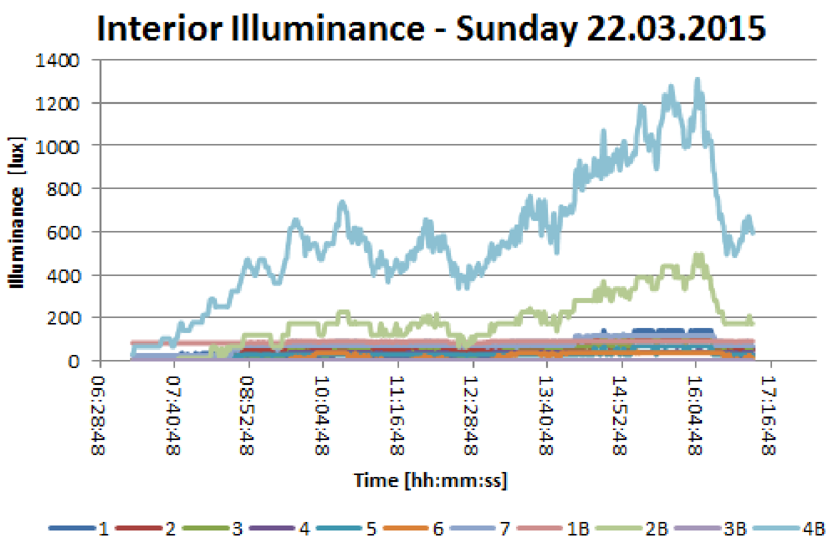

Figure I.36. Results from the interior illuminance measurements, Sunday 22.03.15

The sky was covered by a thick layer of white clouds on this day, see I.35. This, and the fact that the occupant was not present in the office, resulted in very low illuminance levels. The maximum peak value reached approximately 1300 lux at 16 : 00.

The occupant was not using his office during this Sunday, therefore the results for both effect and electricity usage were 0 all day.

Monday 23.03.15

The sky conditions during Monday the 23^rd of March 2015 was very shifting. In the morning between 07:00-10:30 there were light grey clouds covering the whole sky dome as seen in figure I.37

.

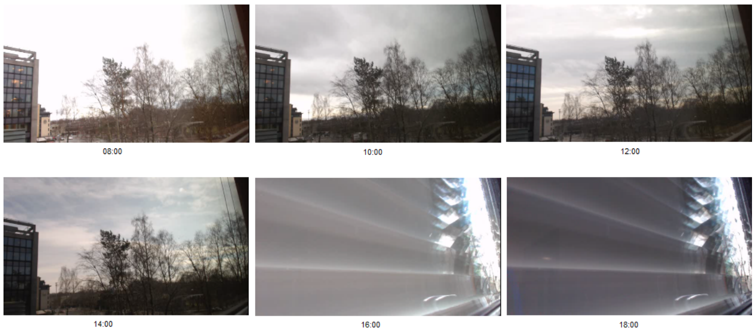

Figure I.37. The sky during Monday 23.03.15.

Between 10:30-12:30 the sky cleared and some small patches of blue sky were visible as seen in figure I.37. From 12:30 and until the evening it was a blue sky with altostratus clouds. The position of the sun was clearly visible.

During Monday the 23^{rd} the conditions was shifting. It was many clouds in the morning, and it cleared in the afternoon. This shifting and unstable conditions are clearly shown in the graph.

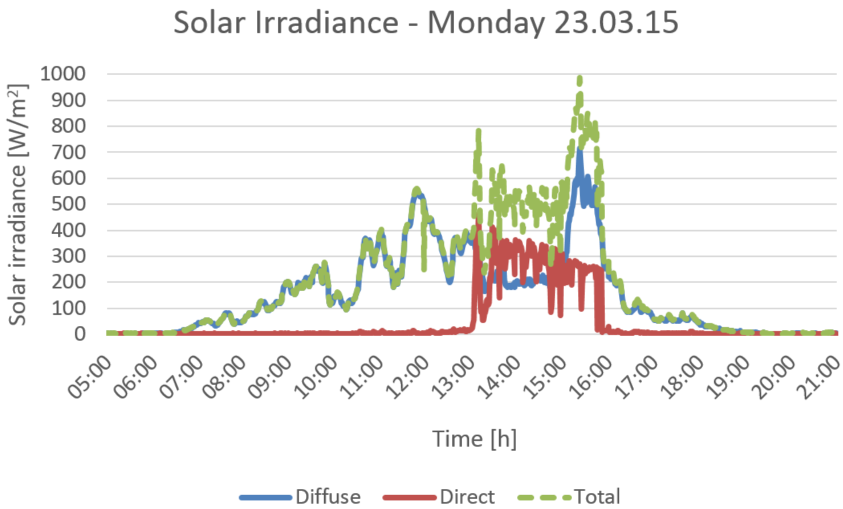

Figure I.38. The diffuse, direct and total irradiation for Monday 23.03.2015

During Monday the 23^{rd} the total solar irradiation maximum reached 986 W/m^2.

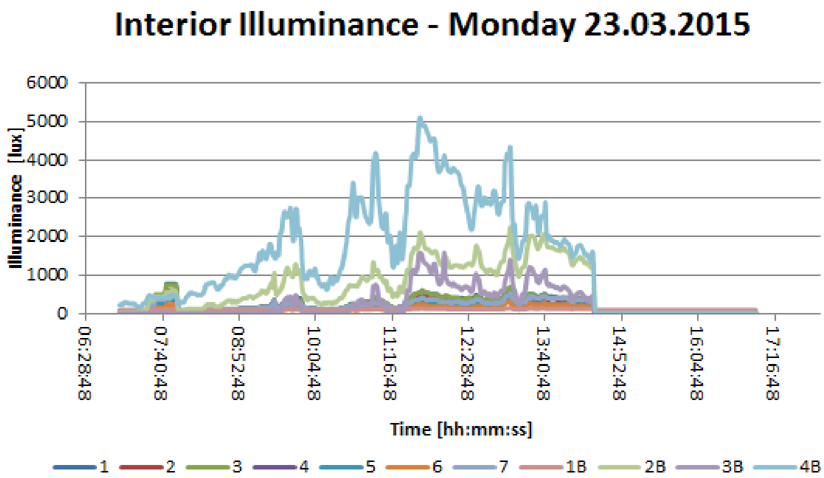

Figure I.39. Results from the interior illuminance measurements, Monday 23.03.15

The occupant was not present in the office on this day, which means that the illuminance is from daylight only. At around 14 : 30 the solar shading was activated with the panels completely shut, which caused the sudden drop in illuminance, see L.3 on page 292. The maximum peak value reached approximately 5100 lux at 11 : 45.

The occupant was not using his office during Monday the 23^{rd}, therefore the results for both power and electricity usage were 0 all day.

The solar shading is activated and is fully down and fully closed from 14:29.

Tuesday 24.03.15

Mostly blue sky as seen in figure I.40, with some scattered white clouds in the distance.

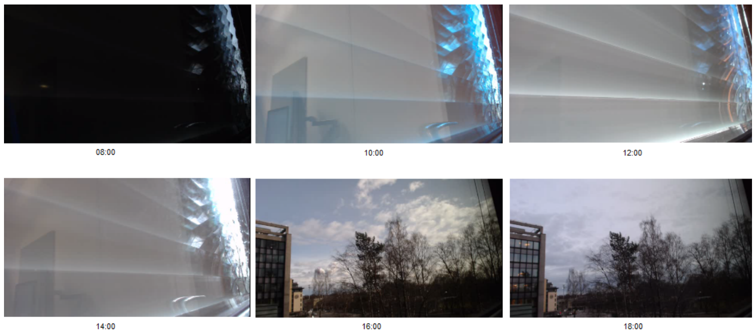

Figure I.40. The sky during Tuesday 24.03.15.

During Tuesday it was mostly blue sky with some very transparent and diffuse clouds, this can be seen in graph I.41 where the direct component is larger than the diffuse component, but around 12:30 the conditions shifted and the results were varying and the diffuse component became larger than the direct component. This may be due to shifting conditions in the weather where the scattered clouds which were in the distance in the morning then covered the sun in the afternoon.

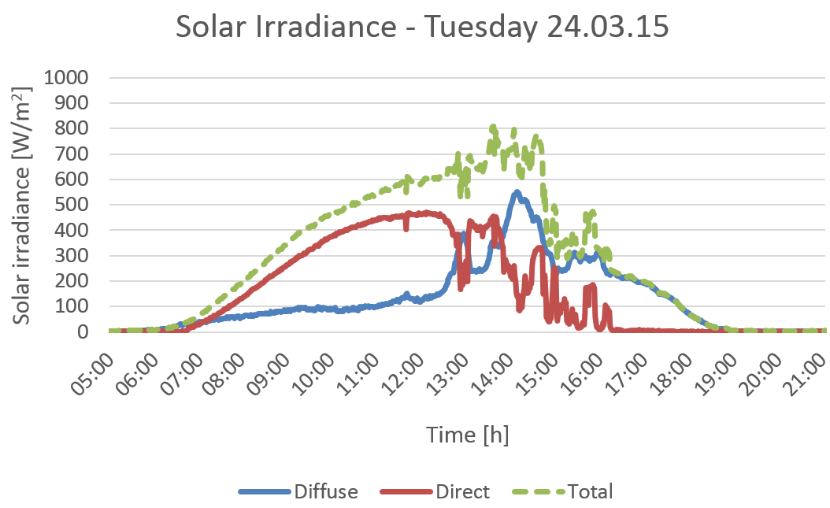

Figure I.41. The diffuse, direct and total irradiation for Tuesday 24.03.2015

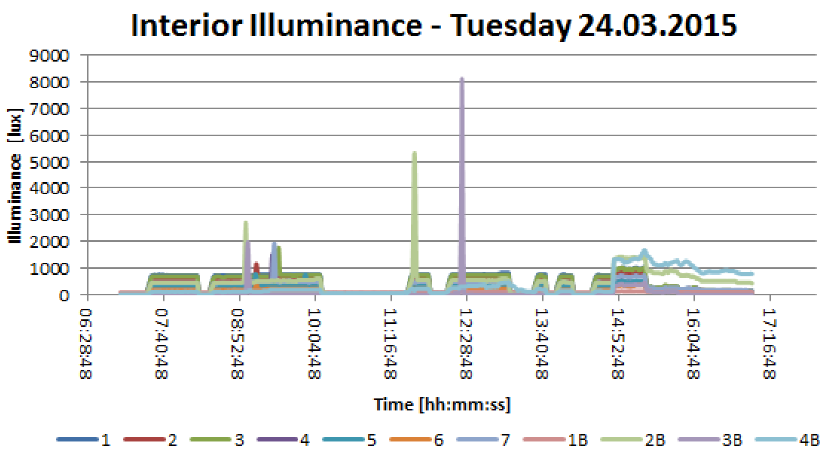

Figure I.42. Results from the interior illuminance measurements, Tuesday 24.03.15

As seen in I.41 the sky was more or less clear until 12 : 30 where it shifted and became more varying. The solar shading was activated until 14 : 30 which is the reason for the low illuminance levels, see L.3 on page 292.

The user arrived in his office at 08:23 and left at 15:16 as seen in graph I.43. The armature was either turned fully off or using maximum effect during this day, except when the armature was starting or turning off when it had some steps of different effect.

The solar shading is active from the morning until 14:48. The blinds are fully down and fully closed.

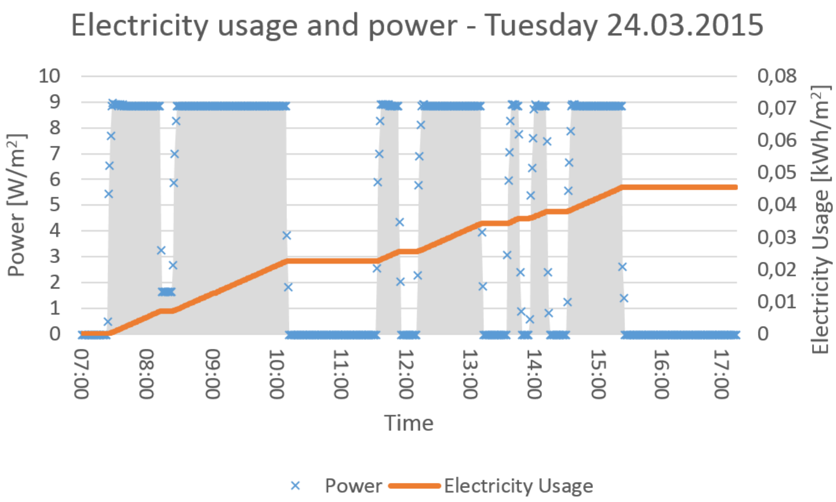

Figure I.43. The effect and electricity usage of the armature during Tuesday 24.03.15

Effect and electricity usage for Tuesday 24.03.15:

- Total time the armature was on: 4 hours and 38 minutes.
- Total electricity used by the armature: 0.0384 $[\frac{\mathrm{KWh}}{\mathrm{m}^2}]$.
- Average effect: 7.933 $[W/m^2]$.
- Maximum effect: 8.944 $[W/m^2]$.
- Electricity usage per hour: 0.00828 $\frac{\mathrm{KWh}}{\mathrm{hm}^2}$

Wednesday 25.03.15

White clouds throughout the whole day as seen in figure I.44, the sun was not visible but you had to squint a little when looking at the sky.

Figure I.44. The sky during Wednesday 25.03.15, mostly blue sky.

During this Wednesday the sky was covered with white clouds which can be seen in the graph as the direct component is close to zero, and the diffuse component is oscillating due to a varying sky cover.

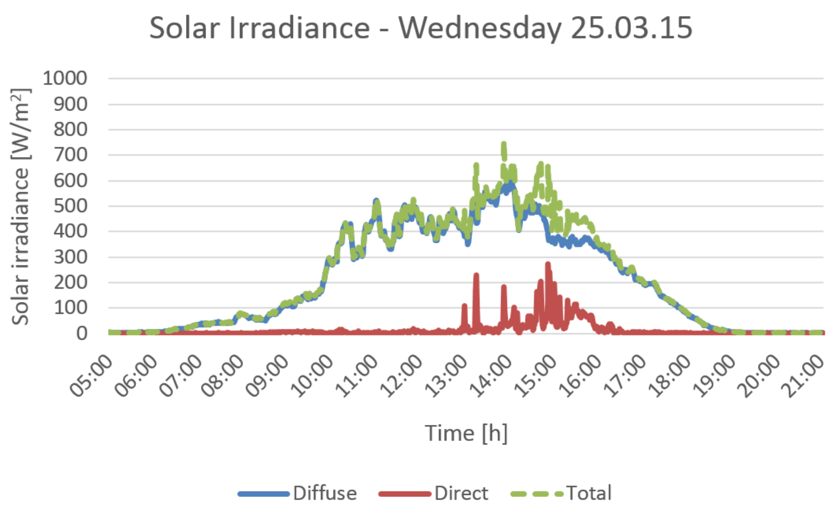

Figure I.45. The diffuse, direct and total irradiation for Wednesday 25.03.2015

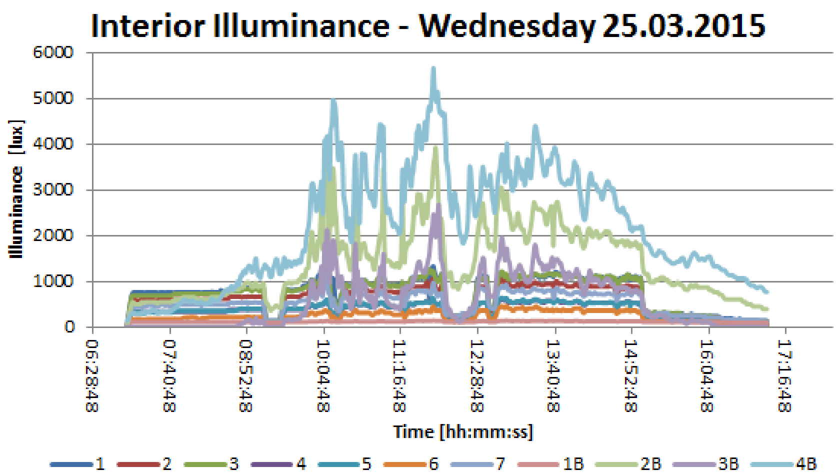

Figure I.46. Results from the interior illuminance measurements, Wednesday 25.03.15

The sky was cloudy as seen in I.45. The illuminance level in the back of the room were fairly stable throughout the day when the occupant was present in the room. The sensors close to the window naturally had higher values. The maximum peak value reached 5665 lux at 11 : 45.

At 06:59 the user arrived, and he left at 15:02. From 11:42 to 11:55 was the armature using between approximately 5.809-7.866 W/m^2. And at 13:21 until 13:30 the armature was using 8.435 W/m^2. The reasons for this is unclear, but it may be due to some sunlight reaching the cell office through some scattering in the cloud layer.

The office was in use from 06:59 until 15:02 that day which means the office was in use for 8 hours and 3 minutes that day. The lunch was from 11:55 until 12:23, it lasted for 28 minutes.

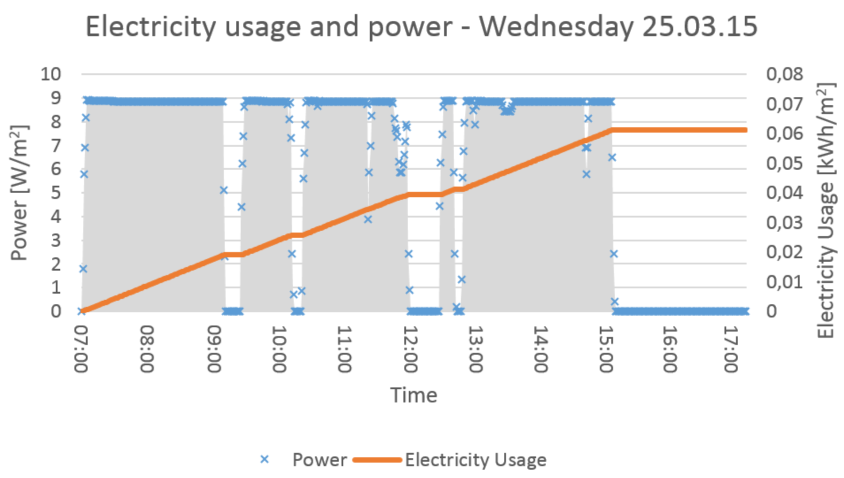

Figure I.47. The effect and electricity usage of the armature during Wednesday 25.03.15

Effect and electricity usage for Wednesday 25.03.15:

- Total time the armature was on: 7 hours and 03 minutes.
- Total electricity used by the armature: 0.0612 $[\frac{\text{KWh}}{\text{m}^2}]$.
- Average effect: 8.208 $[W/m^2]$.
- Maximum effect: 8.944 $[W/m^2]$.
- Electricity usage per hour: 0.00886 $\frac{\text{KWh}}{\text{hm}^2}$

Thursday 26.03.15

During Thursday the $26^t h$ of March 2015 is was a snowstorm. Thick dark clouds was covering the whole sky dome, and heavy snow was falling thorough the whole day as seen in figure I.48.

Figure I.48. The sky during Thursday 26.03.15, snowstorm.

The pyranometer was covered in snow from around 05:00 because of to the snowstorm. The results was increasing which is incorrect as the pyranometer was fully covered in snow, therefore the pyranometer was re-set at 08:30. After this all results was zero as seen in graph I.49, which is as expected as the pyranometer was fully covered.

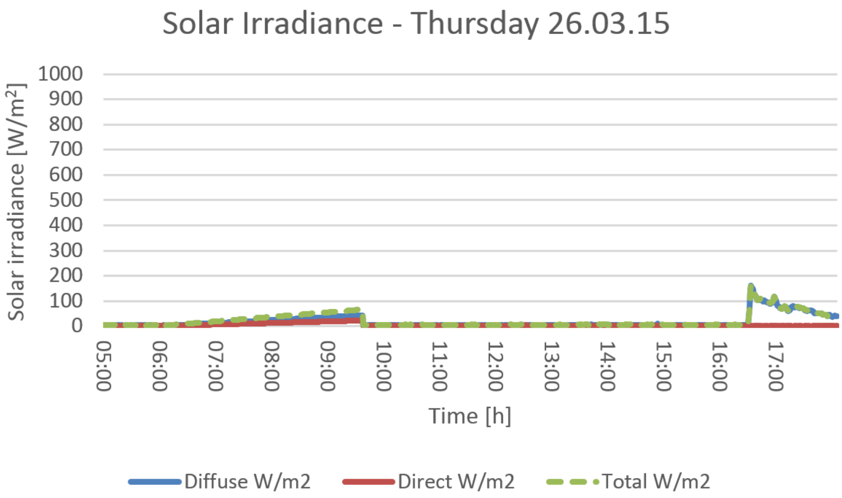

Figure I.49. The diffuse, direct and total irradiation for Thursday 26.03.2015

In the measurement data for the previous day Wednesday the 25^{th} there was a slight increase in total solar irradiance at 05:24 and the sun rise was at 06:05. The increase in the solar irradiation even though the pyranometer was covered in snow might be due to the pyranometer measuring the solar irradiance even though there is a snow layer covering it. The increase in solar irradiance should be zero as the pyranometer is covered in snow, so the increase in solar irradiation may be due to inaccuracies and errors with the instrument as mention in section D.2.4.

It was not possible to clear the pyranometer from snow as it was a snowstorm with a lot of wind and the pyranometer was placed on the roof and not easily accessed.

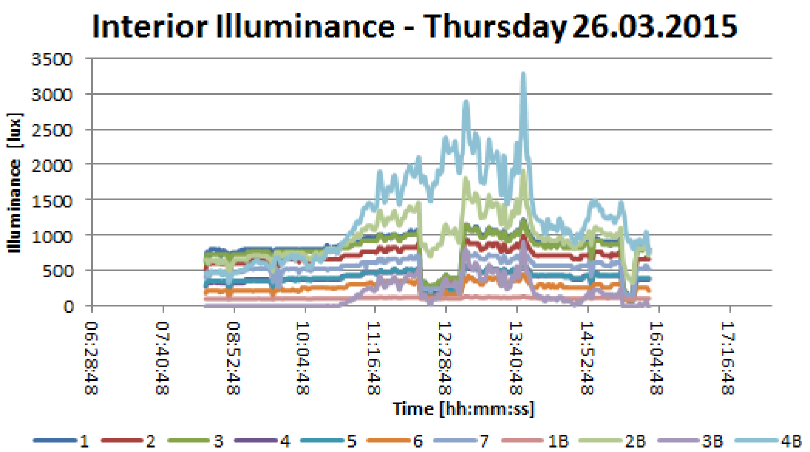

Figure I.50. Results from the interior illuminance measurements, Thursday 26.03.15

Due to complications with the equipment, the measurements were only logged from 08 : 24 to 15 : 55. Due to the blizzard, see I.49 the illuminance levels were fairly low and stable. The maximum peak value reached 3280 lux at 13 : 47.

The graphs show that it is a great variation in illuminance levels in the room from a day with sunny clear sky to a day with overcast sky conditions.

The user arrived at his office at 08:00 and left at 15:24.

There is a drop from 08:44 to 08:47, from 09:28 to 09:31, and from 14:53 to 14:56 to 5.494, 5.410 and 5.373 W/m^2 respectively. This is probably due to the occupant sitting so still the sensor does not recognize his movement.

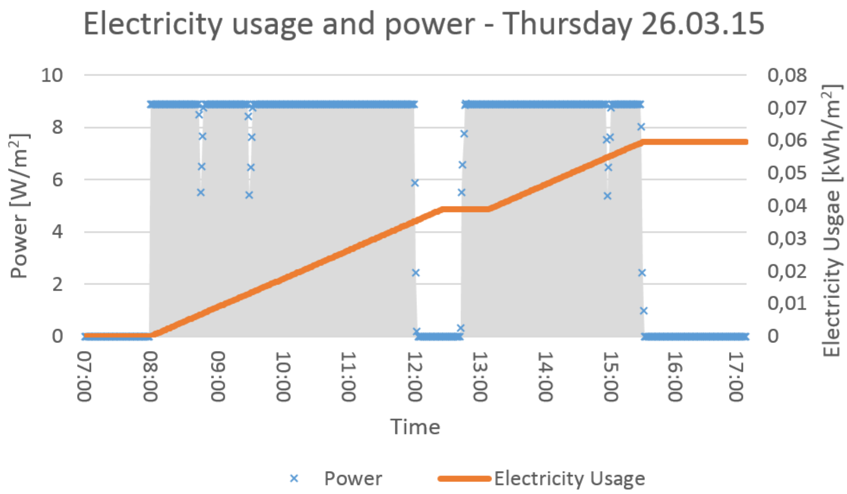

Figure I.51. The effect and electricity usage of the armature during Thursday 26.03.15

Effect and electricity usage for Thursday 26.03.15:

- Total time the armature was on: 4 hours and 43 minutes.
- Total electricity used by the armature: 0.0595 $[\frac{\text{KWh}}{\text{m}^2}]$.
- Average effect: 8.688 $[W/m^2]$.
- Maximum effect: 8.919 $[W/m^2]$.
- Electricity usage per hour: 0.00886 $\frac{\text{KWh}}{\text{hm}^2}$

Approximately 40 cm of snow fell within a few hours that morning, picture I.52 shows how well the pyranometer was covered of snow before it was dug up.

Figure I.52. The pyranometer after the snow storm.

I.1 Measurements Summary

Irradiance Summary

The most overcast days during the measurement period was Monday the 16^{th} when the total solar irradiation maximum reach 278 W/m^2, and Sunday the 22^{nd} when the total solar irradiation maximum reached 203 W/m^2. During Sunday the 22^{nd} there was no one in the office and there was therefore no artificial lighting, during Monday the 16^{th} the occupant was present.

The days during the measurement period with the most clear sky was Saturday the 14^{th} and Saturday the 21^{st}. During Saturday the 14^{th} there was no one in the office, while for Saturday the 21^{st} the occupant was present and there was artificial lifting companying the available daylight. During Saturday the 14^{th} the maximum direct solar irradiation reached 433 W/m^2, while for Saturday the 21^{st} the direct solar irradiation maximum reached 487 W/m^2.

Reflectance J

The reflectance of the different surfaces in the room was measured with a hand-held illuminance meter, as seen in F.1 on page 239. Point measurements were conducted on the four walls of the room, the ceiling,the floor as well as on all the furniture in the room.

J.1 Purpose of Reflectance Measurements

Knowing the reflectance of the different surfaces in the room is useful for understanding how the light will spread in the room. It is also important for simulation purposes.

J.2 Conduction of Reflectance Measurements

First, the illuminance received by the surface in interest was measured by holding the photocell on the surface out towards the room as seen in J.1. It was assured that there was no shadow on the measuring point as this could have created inaccurate results. Then the luminance from the surface was measured, at the same measuring point, by holding the photocell 10 cm towards the surface as seen in J.2.

Figure J.1. Measuring the illuminance received by the surface

Figure J.2. Measuring luminance from the surface

The reflectance of the surface can be found from the relationship between these two measurements by the use of the following equation:

$$r = E_r/E_f \tag{J.1}$$

Where:

E_r	The measured luminance of the surface in interest (photocell towards the surface) [lux]
E_f	The measured illuminance received by the surface (photocell towards the room) [lux]

J.2.1 Measuring Period

The point measurements were conducted 16.03.2015 at 15:00 o'clock, when there was no direct sunlight in the room.

Cleanliness K

Even though it is stated that the cleanliness of the glazing will not affect the daylight factor (Statens Byggeforskningsinstitut, 2008), the effect of the cleanliness on the light transmittance of the glazing is measured.

K.1 Purpose of Transmittance Measurements

The windows are only cleaned twice a year by a professional cleaning company. These measurements were conducted to see how much the cleanliness of the windows affects the amount of light entering the room.

K.2 Conduction of Transmittance Measurements

Because of the external venetian blinds, it is not possible to open the windows on the third floor. Therefore the measurements of the transmittance were carried out on the seventh floor and ground floor. It was performed twice on the seventh floor on one windows, and three times on the ground floor on three different windows. The window and glazing type were the same for all measurements. The indoor and outdoor illuminance was measured on the same place on the glazing for all windows. The transmittance was measured by a lux meter.

These measurements were done in two rounds, first when the windows were not cleaned, and afterwards when the window was cleaned. The lux meter was placed 1 cm from the glazing on the inside of the room, and the lighting level was measured. As the windows cannot be opened on the seventh floor either, the exterior lux was measured right outside the window. The conduction of the measurements can be seen in figure K.1.

Figure K.1. Conduction of cleanliness measurements

The transmittance of the window is the relationship between these two measurements and can be calculated by the following equation:

$$LT = E_i/E_e \tag{K.1}$$

Where:

E_i	The measured indoor lighting level [lux]
E_e	The measured exterior lighting level [lux]

The results from the two measurements were then compared to see if the cleanliness had a significant effect on the light level in the room.

K.2.1 Equipment

The handhold illuminance meter is described in section F.2 on page 239, and the inaccuracies for this instrument is described in F.6 on page 243.

K.2.2 Measuring Period and Frequency

For these experiments point measurements were conducted. The first cleanliness measurement was conducted on the seventh floor, while the rest of the point measurements were conducted on the ground floor on different glazings. The glazing type was the same for all measurements. Some test measurements were conducted prior to the real experiment in order to check if the results were reasonable.

K.2.3 Measurements Results

The results of the measurements are displayed in graph K.2. The light transmittance is seen in 3.3.1 on page 18.

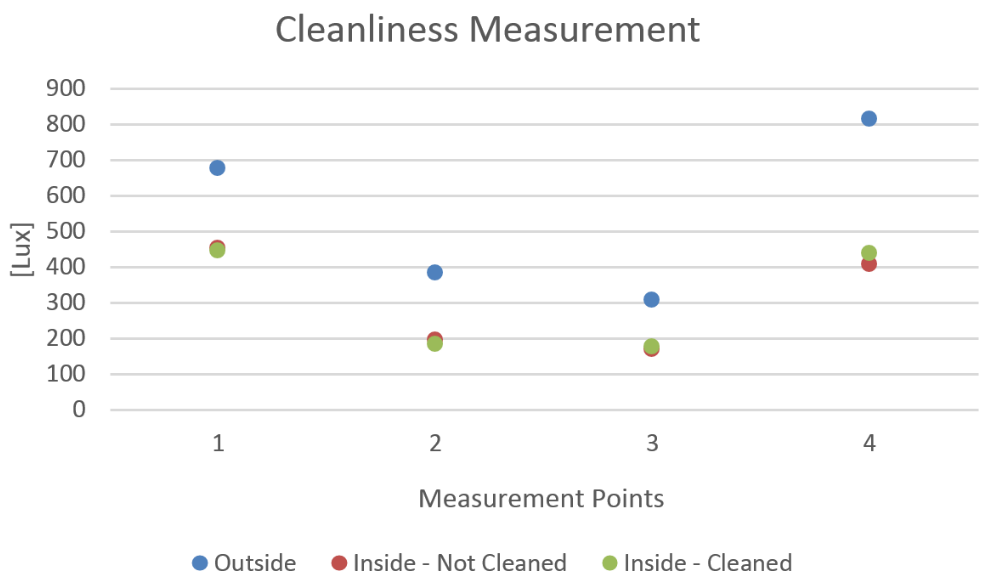

Figure K.2. Results from the cleanliness measurements

As seen in graph K.2 the inside illuminance before and after the glazing was cleaned are fairly similar.

K.2.4 Errors and Inaccuracies

The first point measurement was conducted on the seventh floor. The roof causes shade on the glazing, but as the distance from where the outside illuminance is measured to where the inside illuminance is measured is very small, the space between the two glazing is only 10 mm. Therefore the difference in the shading level from outside the glazing to inside due to the roof will be very small.

The exterior light level might have changed between the measurements as they are not conducted at the exact same time and the sky condition may vary.

There was a construction site next to the case building, therefore the glazings were quite filthy. The filthiness may vary from one glazing to another and this may cause varying results for the light transmittance before and after cleaning.

Solar Shading L

The shading system is initially programmed to be activated when the sensor receives 20 klux, and the position of the panels is angled according to the seasons. The panels will therefore have a different angle for each month of the year. The timing and position of the blinds are not logged and therefore needs to be observed throughout the measuring period. The reflectance of the blinds also needs to be measured on the under- and upper side of the panels. This is to determine the light distribution into the room. The reflectance of the venetian blinds is likely to affect the interior lux-level.

Figure L.1. Venetian blinds seen from the outside

Figure L.2. Venetian blinds seen from the inside

L.1 Purpose of Measurements

The daylight distribution in the room will be affected by the solar shading. The reflectance of the panels might also have an impact on the distribution of daylight in the room. The effect of the solar shading on the interior illuminance levels and the power of the armature should be evaluated to get a clear picture of the daylight availability in the room.

L.2 Conduction of Measurements

Since the timing and position of the solar shading is not logged, they should be observed throughout the measuring period. A Logitech web camera was attached to the window frame to constantly videotape the activation of the solar shading.

L.3 Measurement Results

At the time of the measurements, the control for the solar shading did not work properly. The shading was only activated when the occupants expressed the need for it. The blinds was then completely closed at the entire façade until there was no longer a need for shading.

Figure L.3. The solar shading completely closed

The shading was activated at 14 : 30 on the 23^{rd} of March, and kept closed until 14 : 30 the following day. This was the only time during the measurement period that the shading was activated. The change of light level in the room when the shading was activated can clearly be seen in graph L.4 on the next page.

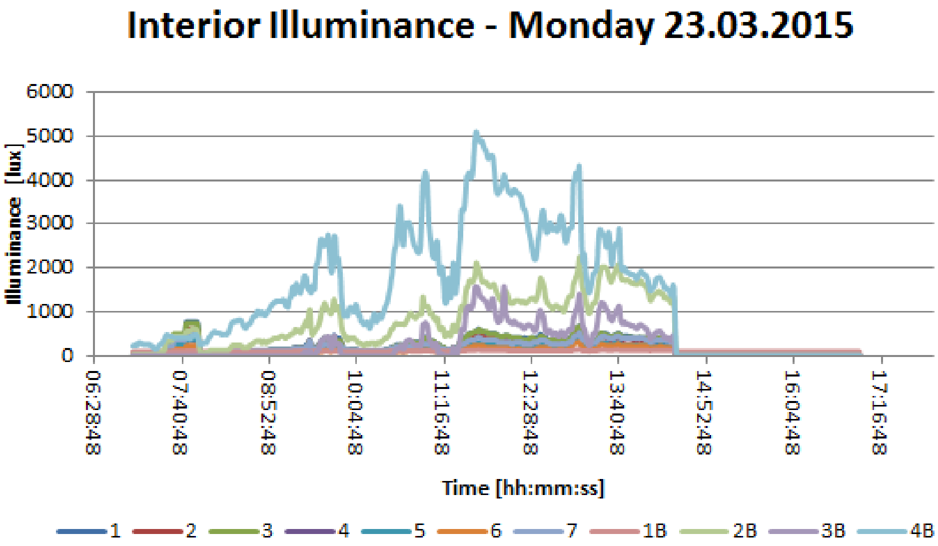

Figure L.4. Interior illuminance when the shading was activated from $14:30$

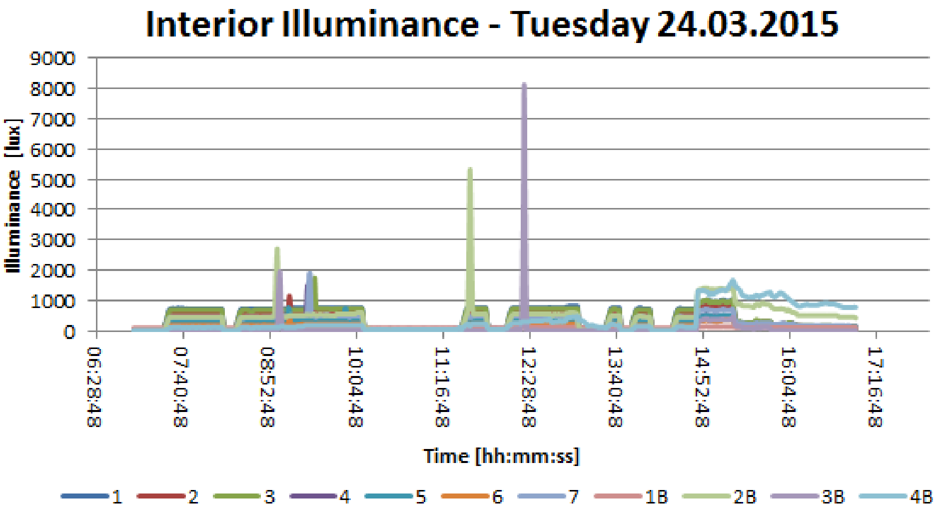

Figure L.5. Interior illuminance when the shading was activated until $14:30$

Graph L.5 shows the interior illuminance in the room on the 24^{th} of March when the solar shading was activated until $14:30$. Since the blinds are completely shut, the values are very low throughout the day. However, it can also be seen that some of the sensors have high peak values in the middle of the day. It is clear that some direct sunlight will come in through the small gap between the shading and the window frame, and hit the side wall behind the desk.

L.4 Accuracy

The shading system is initially programmed to be activated when the sensor receives 20 klux, and the position of the panels is angled according to month. However, this my be changed by the building owner to accommodate the wishes of the occupants. These changes are not documented, which leads to an uncertainty on the position of the panels. Due to the fact that the windows cannot be opened this angle cannot be measured manually either. The reflectance of the blinds cannot be measured due to this. At the time of the measurements the control for the solar shading did not work properly, and the shading would only be activated when the occupants expressed the need for this. The blinds would then be completely closed at the entire façade until there was no longer a need for shading, usually at the end of the working day. This does not give a clear picture of the daylight distribution in the room when the solar shading is activated.

Occupancy Profiles M

M.0.1 Hours per Day

The following graph M.1 shows the frequency and distribution curve for the number of hours per day for all of the open landscape cell offices, including the ones with only two people.

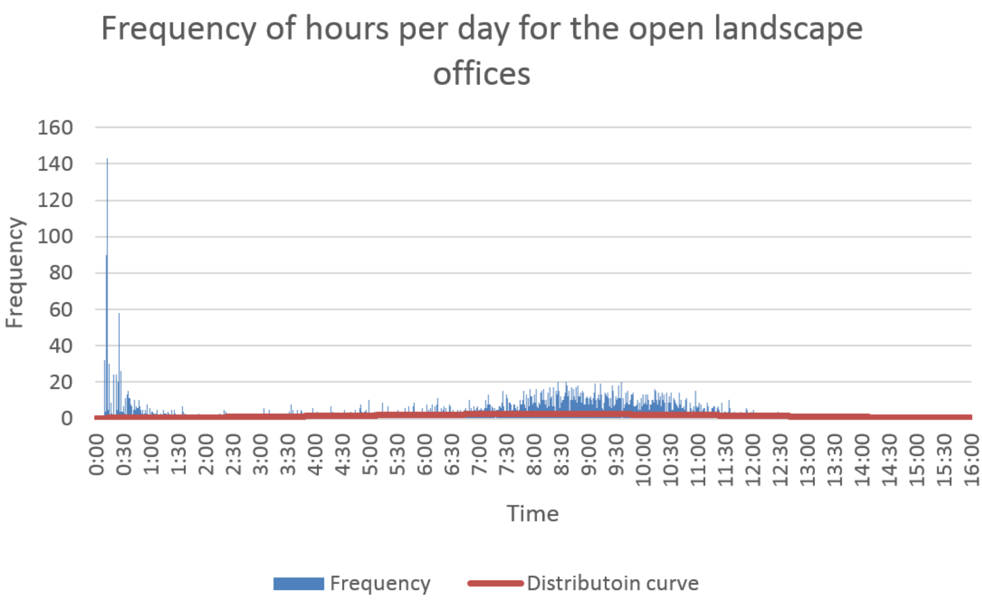

Figure M.1. Frequency and distribution curve of hours per day for open landscape offices

- The mean is 7 hours and 8 minutes
- The median is 8 hours and 15 minutes
- The mode is 0:13 and occurs for 143 of the days
- The standard deviation is 3 hours and 53 minutes

There is a very high frequency between 10 and 25. As this is not representative for a regular working day, it is chosen to exclude the days of only 0 to 30 minutes. The result can be seen in the following graph M.2.

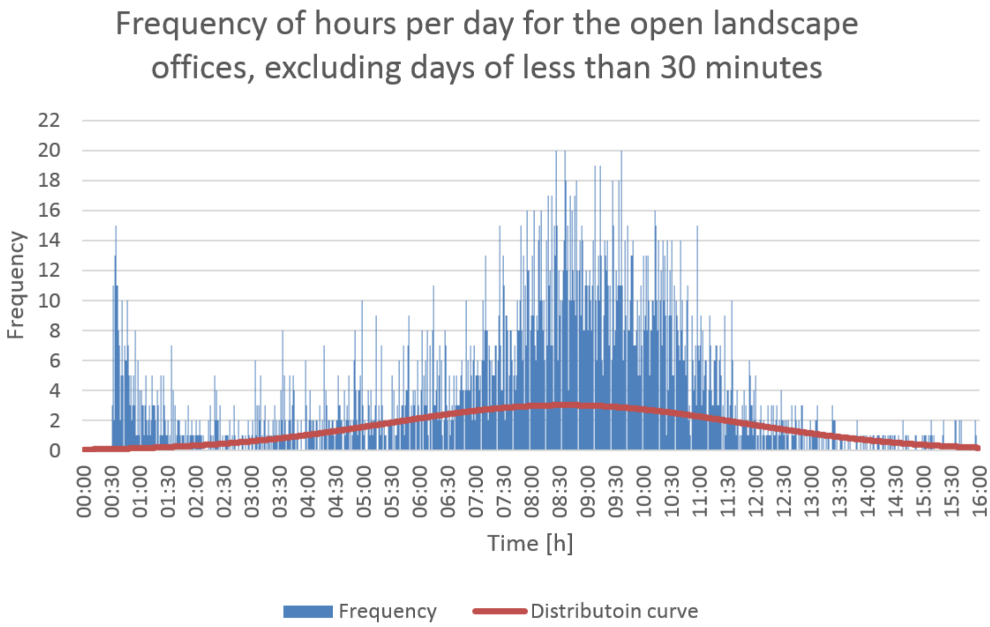

Figure M.2. Frequency and distribution curve of hours per day for open landscape offices except days shorter than 30 minutes

- The mean is 8 hours and 3 minutes
- The median is 8 hours and 36 minutes
- There are three modes at 8:27, 8:36 and 9:37, each occur for 20 of the days
- The standard deviation is 3 hours and 9 minute

M.0.2 Distribution of Hours Per Day

To determine at which hours the office is occupied, the time of arriving and leaving the different offices is investigated. The graphs M.3 and M.4 shows the average time of arriving and leaving the cell offices for 2013 and 2014.

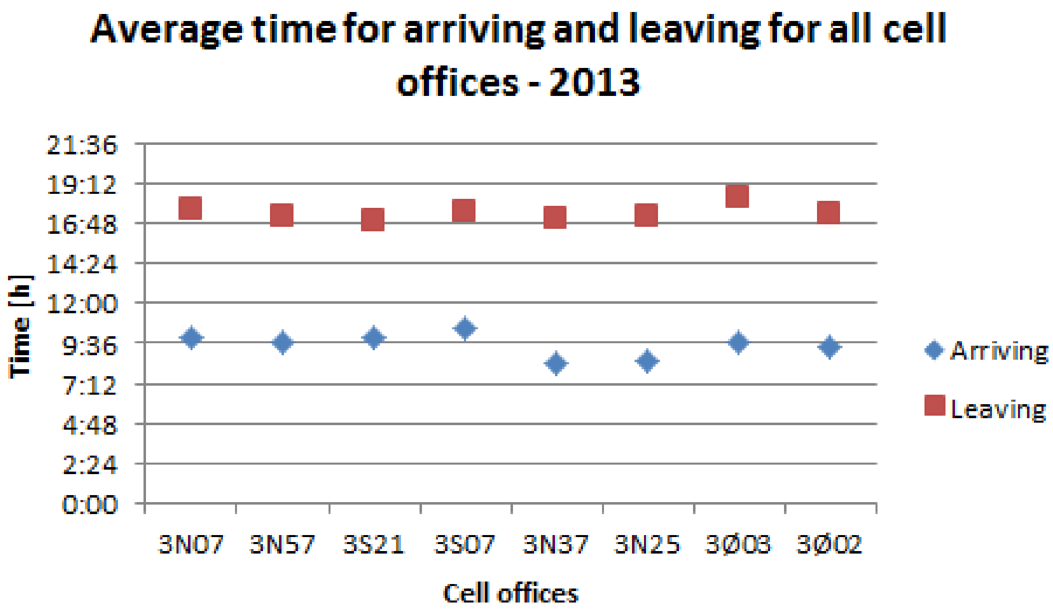

Figure M.3. Average time of arriving and leaving the different cell offices in 2013

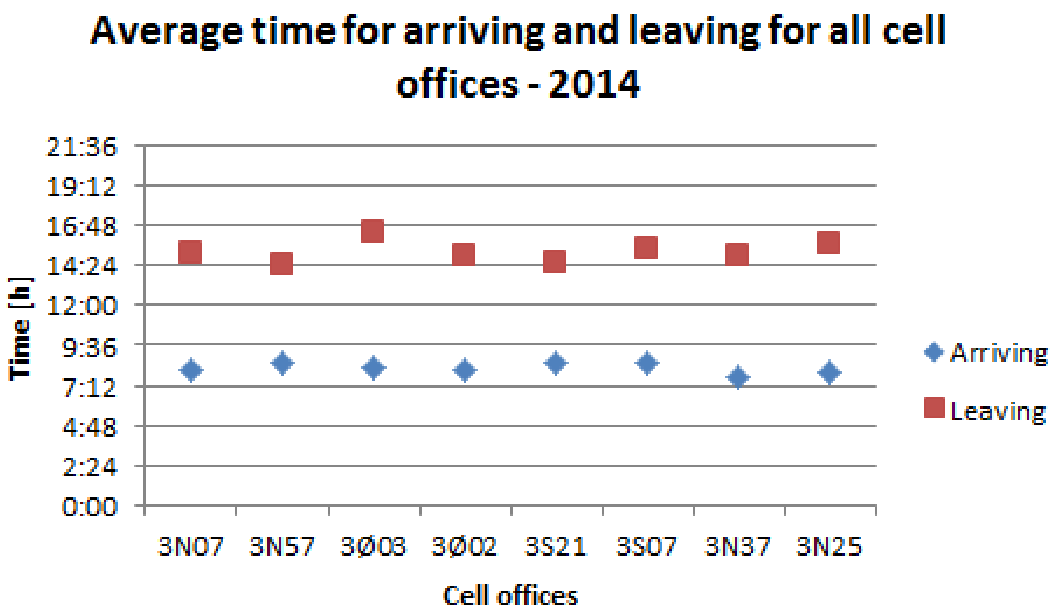

Figure M.4. Average time of arriving and leaving the different cell offices in 2014

Comparing the two graphs, it can be seen that the average time for arriving and leaving is later in 2013 compared to 2014. It shows that the offices were occupied for about one hour longer in 2013 and at different hours.

To have a closer look at how the hours are distributed between arriving and leaving the office, the frequency of presence in the room at certain hours of the day is investigated. The following graph M.5 shows the frequency of presence in cell office 3N07 during working hours in 2014.

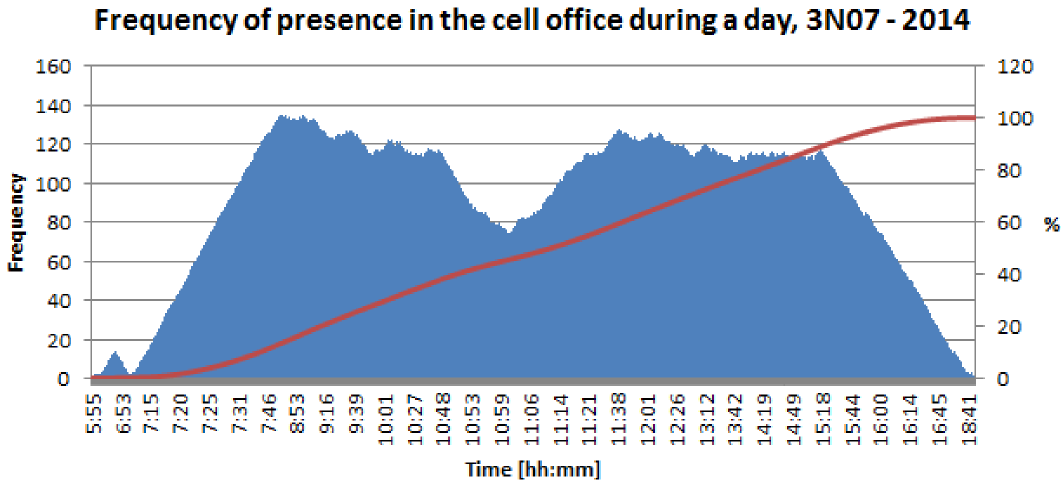

Figure M.5. Frequency of presence in cell office 3N07 during working hours in 2014

The graph can be viewed as an occupancy profile for cell office 3N07 for 2014. Looking at the most frequent values in the beginning and the end of the day shows that the occupant most typically is arriving to the office at 08:00 and leaving at 15:15. It can also be seen that there is a typical reduction of occupancy from 10:45 to 11:16 which most likely is when the occupant is out for lunch.

The mean value is larger than the median which means that the data is skewed to the right. This shows that the mass of the data is concentrated on the left of the graph, meaning that the hours in the first part of the day is more frequent than in the last part of the day.

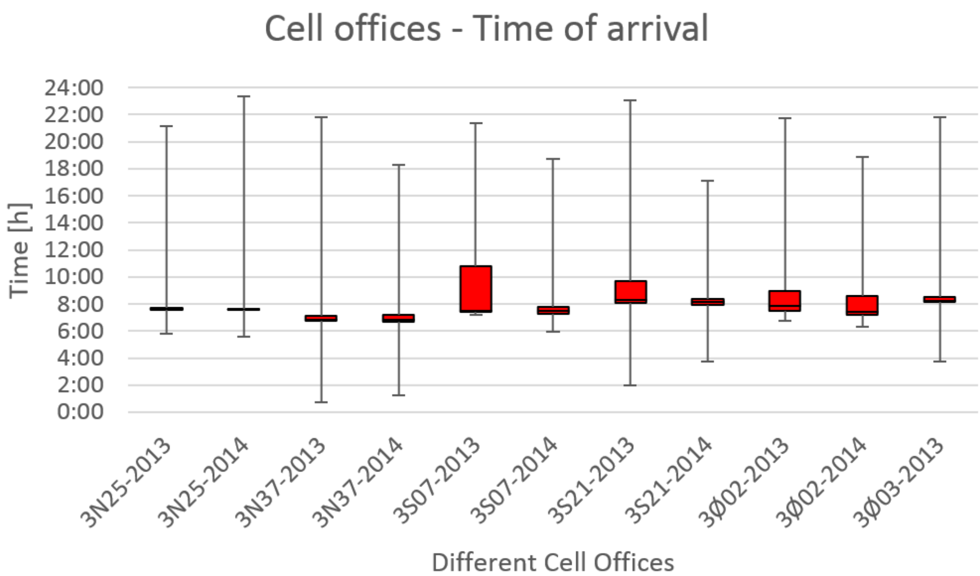

Figure M.6. Box plot diagram of the arrival time for the cell offices

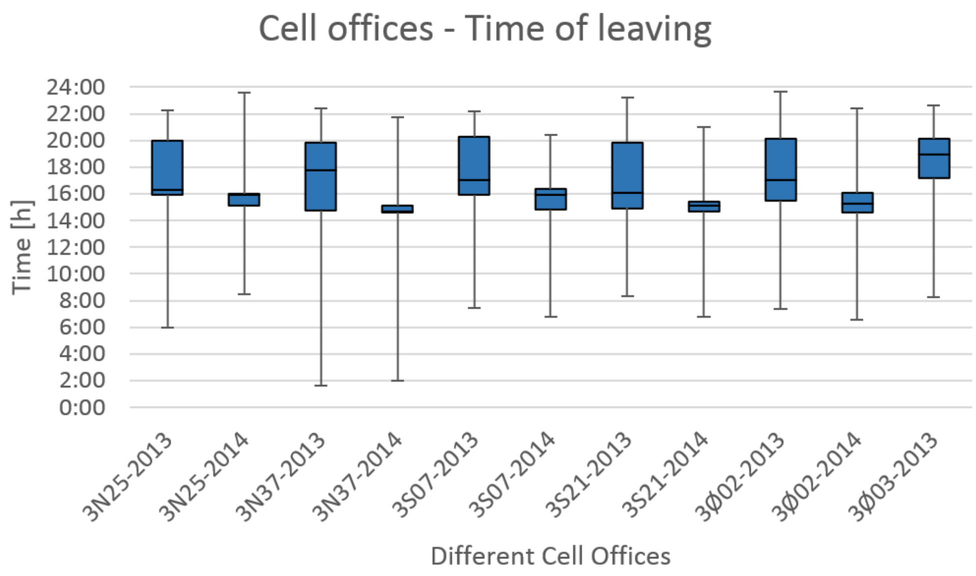

Figure M.7. Box plot diagram of the leaving time for the cell offices

M.0.3 Days per Week

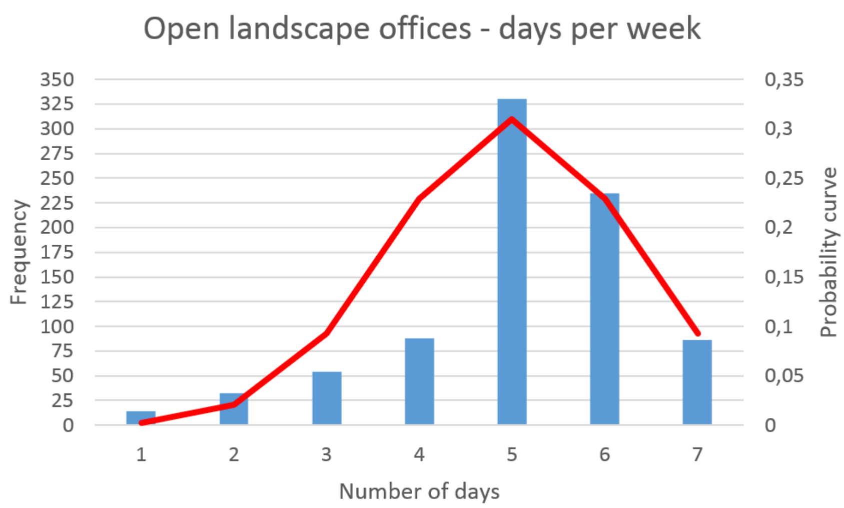

Figure M.8. Frequency histogram and distribution curve for days per week for all the open landscape offices

- The mean is 5.07 days
- The median is 5 days
- The mode is 5 and occurs 330 times
- The standard deviation is 1.29 days

M.0.4 Weeks per Year

Holiday schedule for Oslo schools:

2013:

- Christmas break: Including Tuesday of week 1
- Winter break: Week 8
- Easter break: Week 13 + Monday and Tuesday 2 in week 14
- Summer vacation: Week 26-33
- Joint Norwegian summer holiday: Week 28-30
- Fall break: Week 40
- Christmas break: Tuesday-Friday in week 52

2014:

- Christmas break: Including Wednesday of week 1
- Winter break: Week 8
- Easter break 16 + Monday in week 17
- Summer vacation: Week 26-33
- Joint Norwegian summer holiday: Week 28-30
- Fall break: Week 40
- Christmas break: Wednesday-Friday in week 52

M.0.5 Days per Year

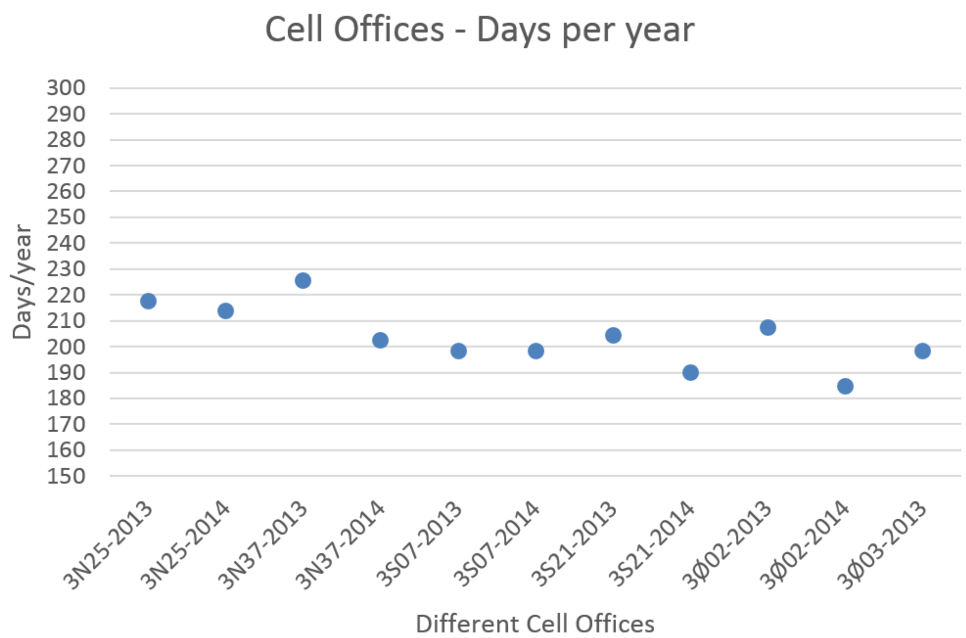

Figure M.9. Days of use per year for the cell offices

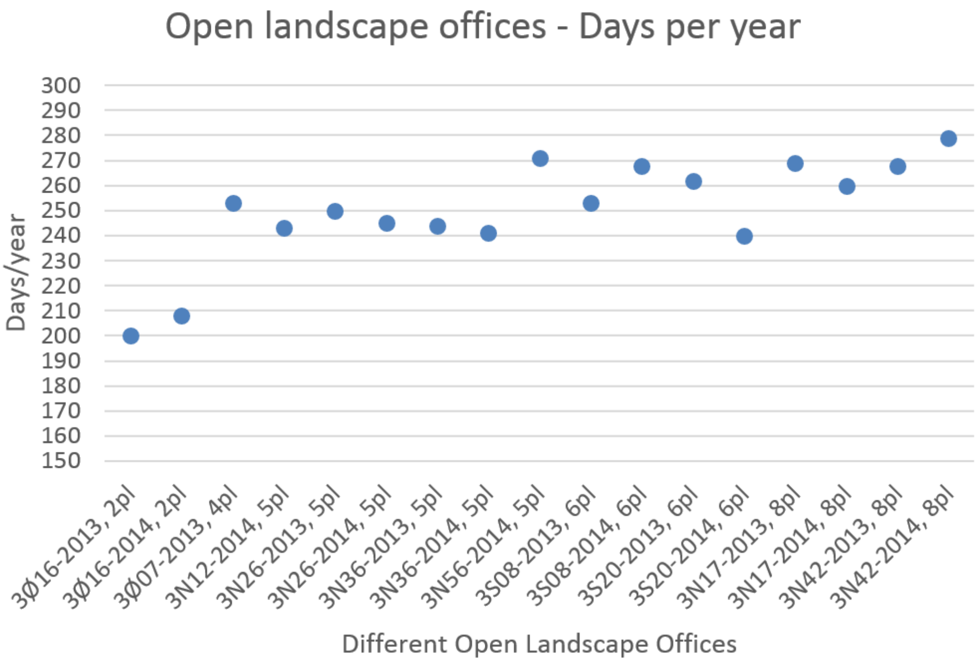

Figure M.10. Days of use per year for the open landscape offices

M.0.6 Hours per Year

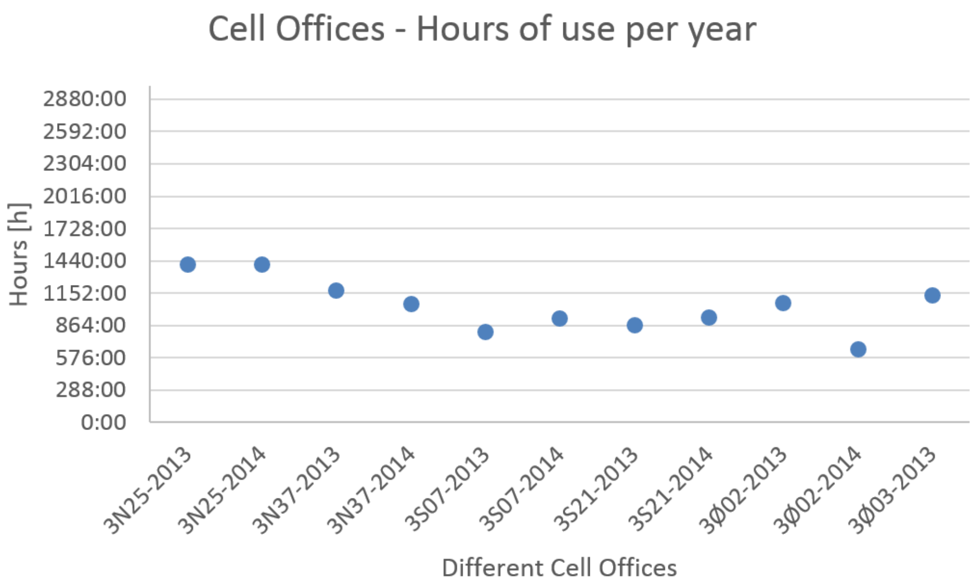

Figure M.11. Hours of use per year on average over a year for the cell offices

As seen in graph M.11, the maximum average hours of use over a year for the cell offices is 1414 hours and 6 minutes for cell office *3N25-2014*, while the average hours of use over a year for the open landscape offices is 2511 hours and 17 minutes for open landscape office *3N17-2013, 8pl* as seen in graph M.12.

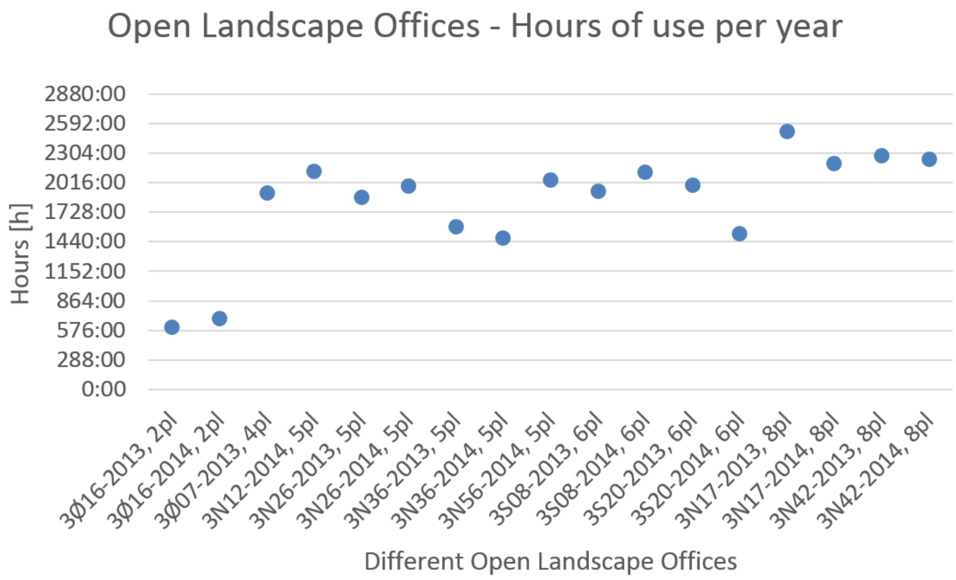

Figure M.12. Hours of use per year on average over a year for the open landscape offices

Hours per year for the offices are obtained by multiplying the established hours per day with days per week and with weeks per year from sections 8, 9 and 10. The result is:

- Cell offices: 1320
- Open landscape offices: 2500

M.0.7 Occupancy Dependent on Number of People

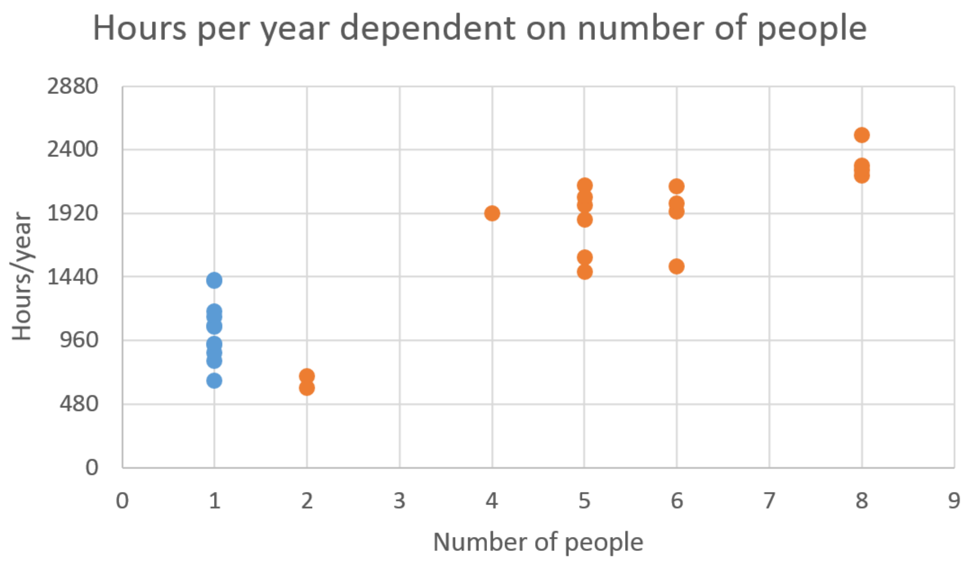

Figure M.13. Weeks per year dependent on number of people in the office

The median of days per week for the offices was applied in section 11.1 on page 111, graph M.14 show the result of the dependency of of number of people in the office due to the average, for comparison with the median in graph 11.2 on page 112.

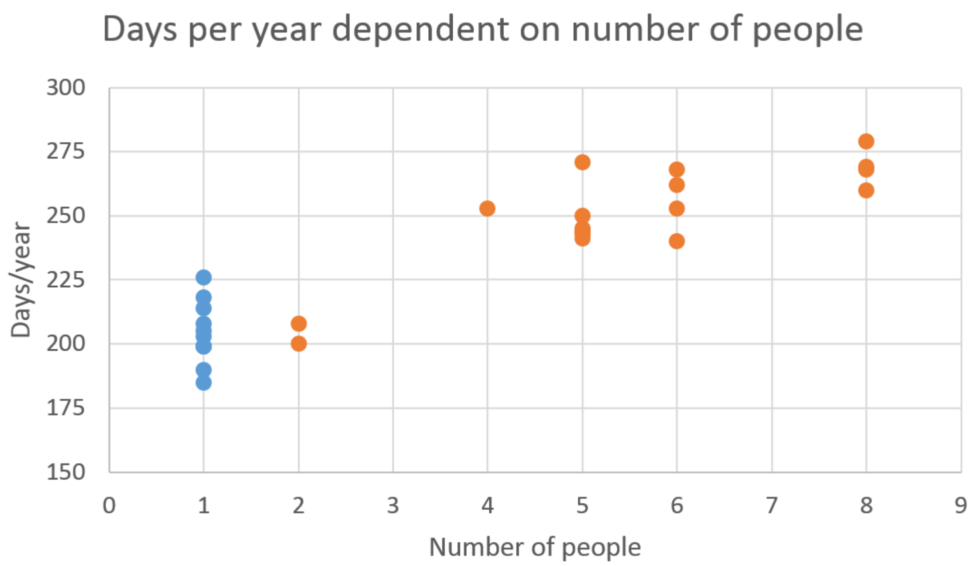

Figure M.14. Days per year dependent on number of people in the office

SINTEF Byggforsk and Energy Numeric Indicator N

N.1 SINTEF Byggforsk

Byggforskserien Byggdetaljer 421.625 Dagslysinnfall og sparepotensial for belysningsenergi explains how the daylight can be calculated for a building and how to estimate the saved electricity usage due to available daylight.

N.1.1 Calculation of Available Daylight

In order to estimate the saved electricity usage due to daylight it is necessary to initially estimate the available daylight.

Calculation of the Daylight Factor

Byggforskserien Byggdetaljer 421.626 Beregning av gjennomsnittlig dagslysfaktor og glassareal explains four different calculation methods for the daylight factor:

- Estimation of average daylight factor by applying graphs developed by SINTEF Byggforsk, the graphs can be found in **??** on page ??.
- Estimation of daylight factor by applying simulation software, some simulation software programs are explained in B on page 201.
- Estimation of the size of the glazed area according to *Svensk Standard SS 91 42 01 Byggnadsutformning â€“ dagsljus â€“ förenklad metod för kontroll av erforderlig fönsterglasaria* and check if it is at least 10 % of the usable floor area.
- Apply the 10 %- rule (Direktoratet for byggkvalitet (DiBK), 2011) and check if the daylight surface which is not shaded is at least 10 % of the usable floor area according to *NS 3940 Areal - og volumberegninger av bygninger.*

The amount of reflected light off the surfaces can help increase the daylight factor (SINTEF Byggforsk, 2004). If the reflection factor of the surfaces is unknown, then the following values can be applied:

- 20-30 % for floors
- 50 % for walls
- 70 % for ceilings

The transmission of the glazing is an important factor when estimating the daylight factor (SINTEF Byggforsk, 2004). The transmission factor specified in the data sheet for the product should be applied in calculation. If this is unknown then a transmission factor of 80 % should be applied for double glazed windows and 70 % for triple glazed windows, these values are for overcast sky.

The daylight factor is not a measure of the amount of daylight entering the building (SINTEF Byggforsk, 2004). The daylight factor does not consider the cardinal orientation nor the difference between different solar conditions. Therefore it is important to apply the daylight factor in conjunction with solar duration curve (SINTEF Byggforsk, 2004).

Solar Duration Curve

The solar duration curve provides information about how much available daylight the building will receive due to the cardinal orientation, geographical placement and time of year (SINTEF Byggforsk, 2004). The solar duration curve is based on the position of the sun and statistical weather data. Figure N.1 is a duration curve for Oslo.

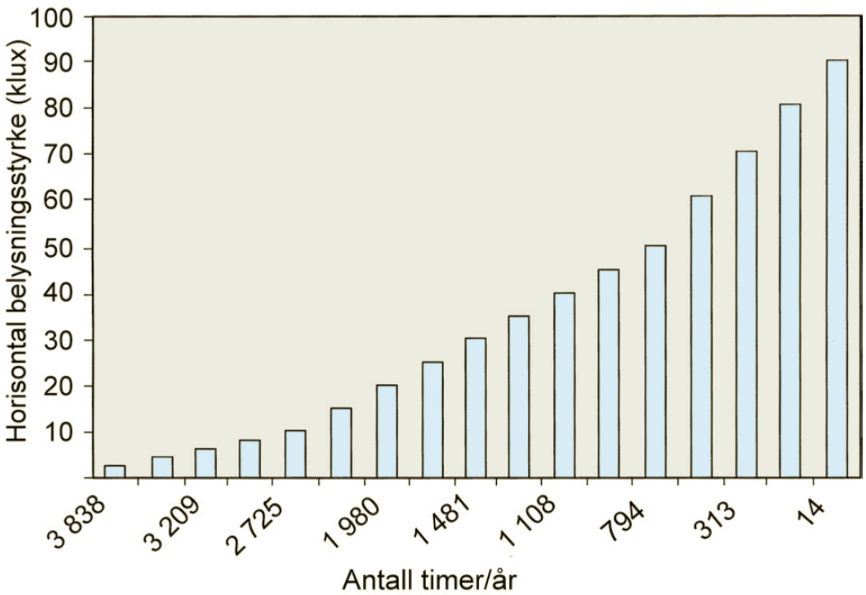

Figure N.1. Solar duration curve for diffuse horizontal illuminance for Oslo thought the whole day (SINTEF Byggforsk, 2004).

Estimation of Available Daylight Indoor

When the amount of available daylight on a horizontal plane at the location of the building is known as well as the daylight factor, it is possible to estimate the available daylight indoor. It is necessary to know the available daylight inside when estimate the saved electricity usage for artificial lighting (SINTEF Byggforsk, 2004).

If the daylight factor is 2 %, then between 08:00-16:00 it is expected to have 606 hours of daylight level above 500 lux where the daylight factor is calculated, for Oslo as seen in figure N.2 (SINTEF Byggforsk, 2004). When the daylight level is above 500 lux it is not necessary with artificial lighting.

E_{hor} i klux[1)]	Antall timer	Belysningsstyrke i lux innendørs når DF = 2 %	Tilskudd fra elektrisk belysning i lux	Effektforbruk i kW etter neddimming
= 0	2 920	= 0	500	0,12
> 0	2 775	> 0	500	0,12
> 2	2 538	> 40	460	0,11
> 4	2 358	> 80	420	0,10
> 6	2 130	> 120	380	0,091
> 8	1 959	> 160	340	0,082
> 10	1 799	> 200	300	0,072
> 15	1 416	> 300	200	0,048
> 20	969	> 400	100	0,024
> 25	606	> 500	0	0
> 30	379	> 600	0	0
> 35	231	> 700	0	0
> 40	123	> 800	0	0
> 45	46	> 900	0	0
> 50	4	> 1 000	0	0

Figure N.2. Solar duration curve for Oslo between 08:00-16:00 (SINTEF Byggforsk, 2004).

The latitude and longitude mattes for the amount of available daylight at the geographical location (SINTEF Byggforsk, 2004). The latitude matters for the solar elevation and thereby how much solar light is lost throughout the atmosphere. The hour of sunrise, sunset and when the sun is in zenith is dependent on the longitude. Latitude and longitude for Norway can be seen in figure N.3.

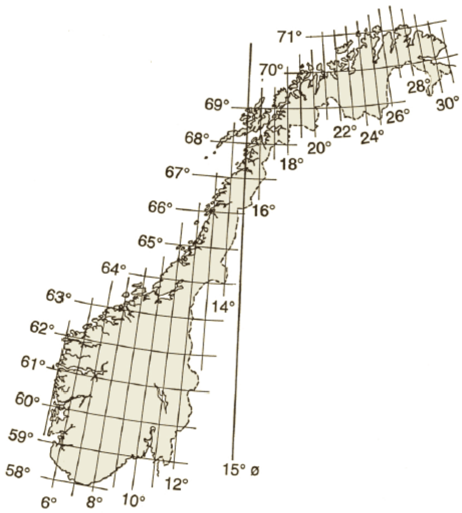

Figure N.3. Latitude and longitude for Norway (SINTEF Byggforsk, 2004).

It is developed empirical equations which will calculate the mean light level as a function of the elevation of the sun, the equations for different sky conditions can be seen in figure N.4.

Himmeltype	Horisontal belysningsstyrke, E_{hor} (lux)[1]	
Klar himmel	$1\,100 + 15\,500 \cdot \sqrt{\sin(h)}$	
Midlere skydekke	$1\,200 \cdot h - 2\,800$	$(8^\circ < h < 50^\circ)$
Overskyet	$500 \cdot h$	

[1] h = solhøyden i grader

Figure N.4. Empirical equations for calculation of horizontal light level when the sun is in zenith (SINTEF Byggforsk, 2004).

The solar elevation for different months and latitudes can be found in figure N.5.

Breddegrad	Maksimale solhøyder i grader											
	Jan.	Febr.	Mars	April	Mai	Juni	Juli	Aug.	Sept.	Okt.	Nov.	Des.
58	12,0	21,2	32,0	43,6	52,0	55,4	52,4	44,4	32,9	21,5	12,2	8,6
59	11,0	20,2	31,0	42,6	51,0	53,4	51,4	43,4	31,9	20,5	11,2	7,6
60	10,0	19,2	30,0	41,6	50,0	52,4	50,4	42,4	30,9	19,5	10,2	6,6
61	9,0	18,2	29,0	40,6	49,0	52,4	49,4	41,4	29,9	18,5	9,2	5,6
62	8,0	17,2	28,0	39,6	48,0	51,4	48,4	40,4	28,9	17,5	8,2	4,6
63	7,0	16,2	27,0	38,6	47,0	50,4	47,4	39,4	27,9	16,5	7,2	3,6
64	6,0	15,2	26,0	37,6	46,0	49,4	46,4	38,4	26,9	15,5	6,2	2,6
65	5,0	14,2	25,0	36,6	45,0	48,4	45,4	37,4	25,9	14,5	5,2	1,6
66	4,0	13,2	24,0	35,6	44,0	47,4	44,4	36,4	24,9	13,5	4,2	0,6
67	3,0	12,2	23,0	34,6	43,0	46,4	43,4	35,4	23,9	12,5	3,2	0
68	2,0	11,2	22,0	33,6	42,0	45,4	42,4	34,4	22,9	11,5	2,2	0
69	1,0	10,2	21,0	32,6	41,0	44,4	41,4	33,4	21,9	10,5	1,2	0
70	0	9,2	20,0	31,6	40,0	43,4	40,4	32,4	20,9	9,5	0	0
71	0	8,2	19,0	30,6	39,0	42,4	39,4	31,4	19,9	8,5	0	0

Figure N.5. Maximal solar elevation as a function of the 21^st in every month (SINTEF Byggforsk, 2004).

N.1.2 Estimation of Saved Electricity Usage For Artificial Lighting

The saving potential is dependent on the type of control strategy. In order to save electricity the armature must be controlled due the amount of available daylight (SINTEF Byggforsk, 2004). This control strategy can either be manual or automatic.

Manual Control System

The manual control strategy is dependent on the user, the user has to turn on and off as well as dim the artificial light. It is also important that a manual control strategy is not shared between different users in order for it to be effective (SINTEF Byggforsk, 2004). The potential problem with a manual control system is that some users may not turn off the artificial light when needed and the saving potential is therefore very dependent on the user.

Automatic Control System

There exists to main types of automatic system. The one type has a sensor which measure when the available daylight level is above 500 lux and switches the artificial lighting off. The other is an automatic dimming system where the artificial lighting compensates for insufficient available daylight level.

N.2 Energy Numeric Indicator - LENI

Lighting Energy Numeric Indicator (LENI) is a numeric indicator of the total annual lighting energy required in a building which can be applied to compare the energy required for lighting in different buildings that have the same function but different size and design (Technical Committee CEN/TC 169, 2006). The LENI-number for the building is calculated according to equation N.1.

$$LENI = \frac{W}{A} \cdot \left[\frac{kWh}{m^2 \cdot year}\right] \tag{N.1}$$

Where:

W	The total annual energy use for lighting $[\frac{\mathrm{kWh}}{\mathrm{year}}]$
E_{dir}	The total useful floor area of the building $[\mathrm{m}^2]$

LENI is defined in NS-EN 15193:2007, in the standard an effective and flexible approach to determine energy use for lighting (Voltimum, 2015). The LENI method is more accurate in determining how the space will be used and lit compared to previous methods. When determining the LENI number two calculations have to be made, first for the building considered, then for a notational building which has the same size, shape and activities as the real building (Voltimum, 2015). The building considered must have lower electricity usage for artificial lighting compared to the notational building. The calculated LENI number obtained reflects the energy usage for the whole building. The LENI number enables comparison between different buildings of the same function, but of different size and design.

There are two methods to calculate the LENI-method, a rapid and an extensive method (Karlsen, 2014). The raid method gives an conservative value of the yearly energy usage for artificial lighting, while the extensive method applies the actual value of every single room. The extensive method can be applied for all building types and geographical locations, while the rapid method applied standard values for different types of buildings (Karlsen, 2014).

SBi-anvisning 219 Dagslys i Rum og Bygninger O

This chapter contains excerpts from the instruction on daylight in rooms and buildings, by the Danish Building Research Institute (SBi). The instruction describes methods for calculating and controlling that the building regulation criteria for sufficient daylight in a commercial building are met. Daylight factor is often used as an indicator on the daylight availability in a room, and this instruction presents standard values and calculation methods for a standard office room, as well as correction factors for evaluation of daylight availability under different conditions.

O.1 Rules and Regulations

The electricity usage for artificial lighting accounts for approximately 30% of the energy usage in buildings today. For the energy frame calculation, the electricity usage should be multiplied with a primary energy factor of 2.5 when compared to the heating demand. Daylight utilization combined with a energy efficient control system for the artificial lighting is important for the energy frame to be adhered.

The following regulations concerns daylight and windows and are collected from the Danish building regulations 2010.

Daylight conditions

Offices should have a satisfying amount of daylight available. The daylight availability in an office can be considered sufficient when the glazing area corresponds to minimum 10% of the floor area, provided that the glazing has a light transmittance of minimum 0.75. The daylight availability can also be determined by the daylight factor which should be 2% in the working area.

Windows should be placed and shaded in such a way that the room will not suffer from overheating, draft or glare. Glare caused by reflection should also be taken into account. Windows facing east, south and west should be shaded, especially if the glazing area constitutes a substantial part of the wall area.

Energy Consumption

The building's supplied energy demand for heating, ventilation, cooling, water heating and artificial lighting should not, per m^2 exceed $71.3\,\mathrm{kWh/m^2}$ per year, attributed with 1650 kWh per year divided by the heated floor area, A. The energy consumption per $kWh/m^2 * year$ can be expressed by O.1.

$$71.3 + 1650/A \tag{O.1}$$

O.2 Daylight Factor

The daylight availability in a room is usually expressed by the daylight factor on a horizontal plane with a height of 0.85. This plane is defined as the work plane, which is the height where the daylight is most important. The daylight factor is defined as the relation between the illuminance at a point on the work plane and the exterior illuminance on a horizontal plane. A method on how to determine the daylight and solar radiation on the building surfaces can be found in the appendix O.6 on page 323.

Standard Daylight Factor

For ordinary rectangular rooms the daylight factor can be determined from standard graphs. The following values are used in the standard calculations:

- CIE overcast sky
- Free horizon, no surrounding buildings or vegetation that can create shade
- The window has a light transmittance of 0.8 (corresponding to a typical energy glazing)
- Windows are placed 0.85 above the floor
- Mean reflectance from surfaces in the room of 0.5
- The room has a width of 4 m and a height of 2.8 m
- Furniture is not considered
- The wall has a thickness of 10 cm and there is no shading from the construction around the window
- No solar shading installed

The standard daylight factors for a 4 m deep room with different window areas can be seen in O.1, O.2 on the facing page and O.3 on the next page.

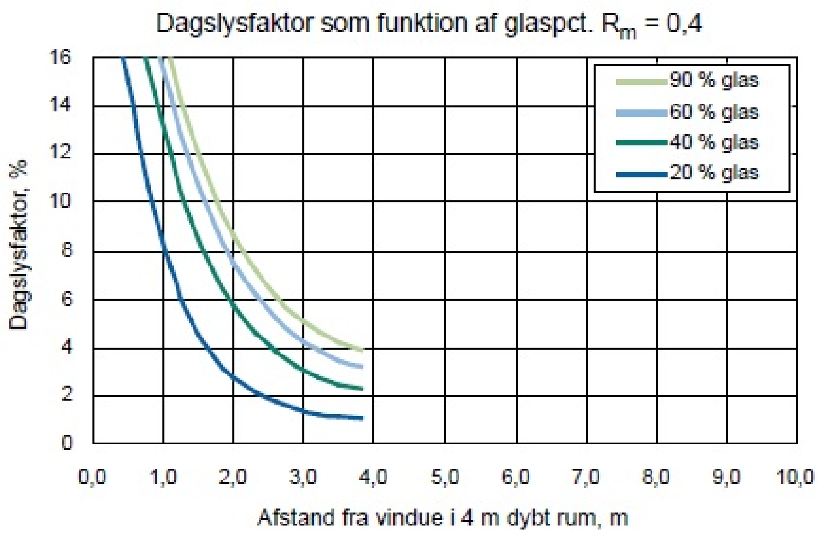

Figure O.1. Daylight factors for a 4 m deep room with different window areas

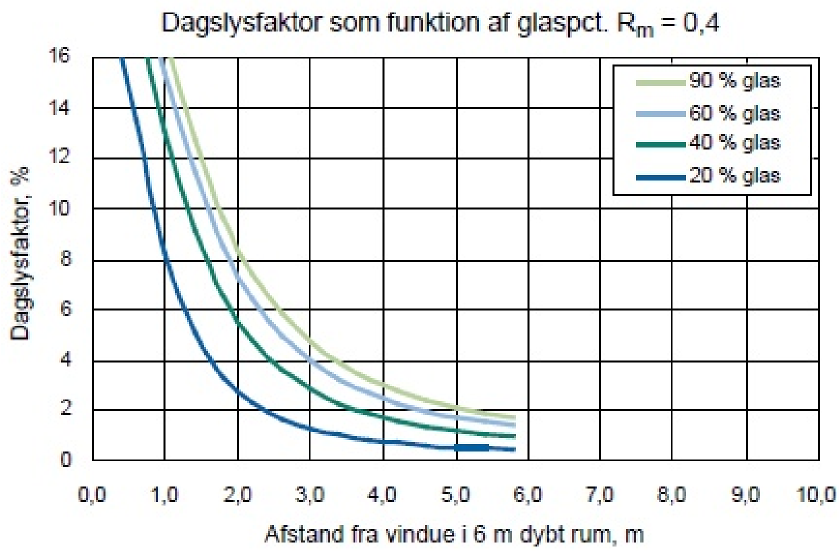

Figure O.2. Daylight factors for a 6 m deep room with different window areas

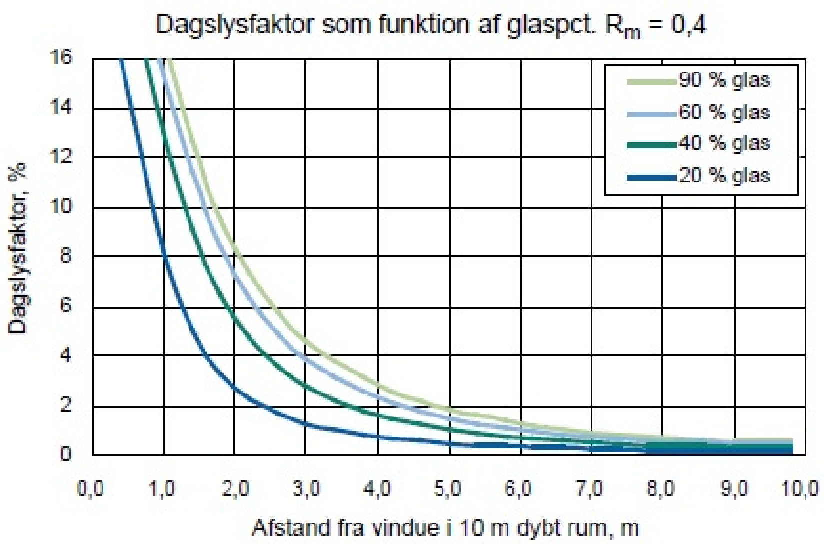

Figure O.3. Daylight factors for a 10 m deep room with different window areas

O.3 Correction of Daylight Factor

The standard daylight factor can be a good approximation, but it should be corrected to fit the actual conditions of the building. In this section the most important correction factors for the daylight factor is presented.

Correction for Windows

The standard daylight factors are calculated with the glazing percentage, which means how much of the total facade area is glazed. This does not take the window frame into account. For rooms with other glazing percentages, an interpolation between the graphs can be performed.

For rooms with windows in more than one façade, the daylight factor should be calculated only considering the windows in one facade at a time. The resulting daylight factors from the different calculations should then be added together.

Correction for Light Transmittance

For ordinary windows it can be assumed that the daylight factor at any point in the room is directly proportional to the light transmittance of the window. The standard daylight factors should be corrected for the light transmittance by multiplying it with the correction factor expressed by O.2.

$$\text{Correction factor for light transmittance} = \frac{LT_{actual}}{LT_{reference}} \tag{O.2}$$

The following table shows examples of typical values for different window types. The last column shows the correction factor that should be multiplied with the standard daylight factor.

Antal glas	Rudetype	Beskrivelseskode *)	U	LT	g	Ra	LT_{dif}	LR_{ud}	Faktor
2	Almindelig/traditionel termorude	4-12-4	2,9	81	0,76	97	68	15	1,01
3	3-lags termorude	4–12-4-12-4	1,9	74	0,68	96	59	20	0,93
	Energiruder								
2	Rude med ét energiglas, hård belægning på indv. glas	4-20-eh4	1,7	74	0,72	98	63	17	0,93
2	Rude med ét energiglas, belægning på indv. glas	4-12ar-e4	1,4	79	0,63	97	66	12	0,99
2	Rude med ét energiglas, belægning på indv. glas	4-15ar-e4	1,2	79	0,63	97	66	12	0,99
2	Rude med ét energiglas	4e-15ar-4	1,2	79	0,57	97	65	12	0,99
2	Rude med ét energiglas	4se-12ar-4	1,3	80	0,59	97	66	12	1,00
2	Rude med ét energiglas	6se-15ar-4	1,1	79	0,57	97	66	14	0,99
3	Rude med to energiglas	4se-12kr-4-12kr-se4	0,6	71	0,50	95	49	14	0,89
2	Rude med ét energiglas og ét jernfattigt glas	4w-15ar-se4	1,1	81	0,65	97	67	13	1,01
2	Rude med ét energiglas og to jernfattige glas	4w-15ar-se4w	1,1	82	0,67	98	68	13	1,03
	Solafskærmende belagt glas m. energibelægning								
2	Rude med ét solafskærmende glas	6se-coollite-15ar-4	1,1	67	0,41	94	54	9	0,84
2	Rude med ét solafskærmende glas	6se-neutral-15ar-4	1,2	70	0,42	95	57	7	0,88
2	Rude med ét solafskærmende glas	6se-brillant-15ar-4	1,1	65	0,36	93	53	15	0,81
2	Rude med ét solafskærmende glas	6se-brillant-15ar-4	1,1	50	0,27	90	42	18	0,63
2	Rude med ét solafskærmende glas	6se-brillant-15ar-4	1,1	29	0,20	88	24	11	0,36
2	Rude med ét solafskærmende glas	6se-silver-15ar-4	1,2	58	0,47	95	50	33	0,73
2	Rude med ét solafskærmende glas og ét jernfat-tigt glas	6se-neutral-15ar-4w	1,1	72	0,43	96	58	10	0,90
	Solafskærmende gennemfarvet glas + energiglas								
2	Rude med ét gennemfarvet glas og ét energiglas	6grå-15ar-se4	1,2	39	0,37	95	29	6	0,49

Figure O.4. Typical parameters for different window types

Correction for Wall Thickness

The wall thickness will have an effect on the window's ability to transmit daylight into the room as it causes some shade. This will reduce the daylight factor. The reduction factor can be read from graph O.5 where the y-axis shows the reduction factor, and the x-axis shows the relationship between the wall thickness and the window dimensions. The relationship is found by the following formula:

$$\frac{2 * \text{wall thickness [m]}}{\text{height of the window} + \text{width of the window}} \tag{O.3}$$

The reduction factor is found by following the curve for the reflectance of the wall.

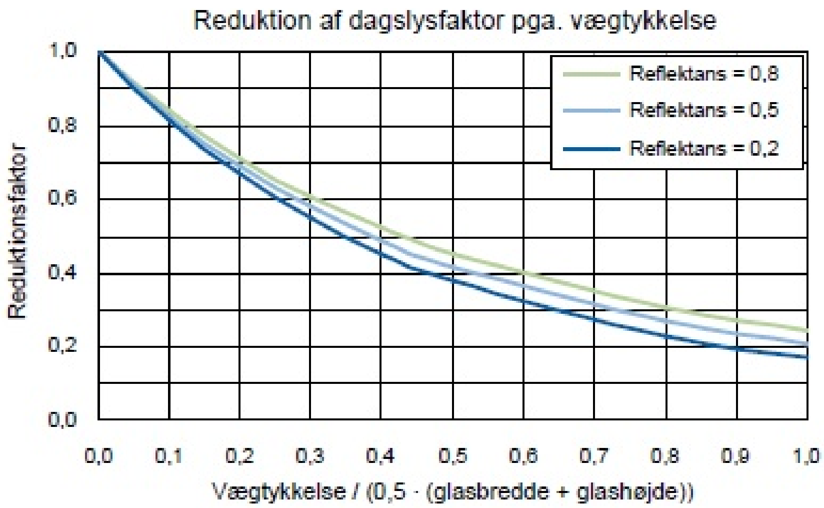

Figure O.5. Reduction factor for wall thickness

Correction for Surroundings

The standard daylight factors are calculated assuming that there is no surrounding obstacles to create shadow on the building. Large surrounding buildings can cause a significant reduction of daylight hitting a façade. From graph O.6 on the following page the reduction factor for a room with a window facing towards another building with a mean reflectance of $R_m = 0.10$ can be determined. The graphs for an opposing building with a mean reflectance of $R_m = 0.25$ and $R_m = 0.40$ can be found in the appendix O.3. The graphs are calculated using CIE overcast sky O.9.1 on page 326. The daylight factor is corrected by multiplying it to the reduction factor.

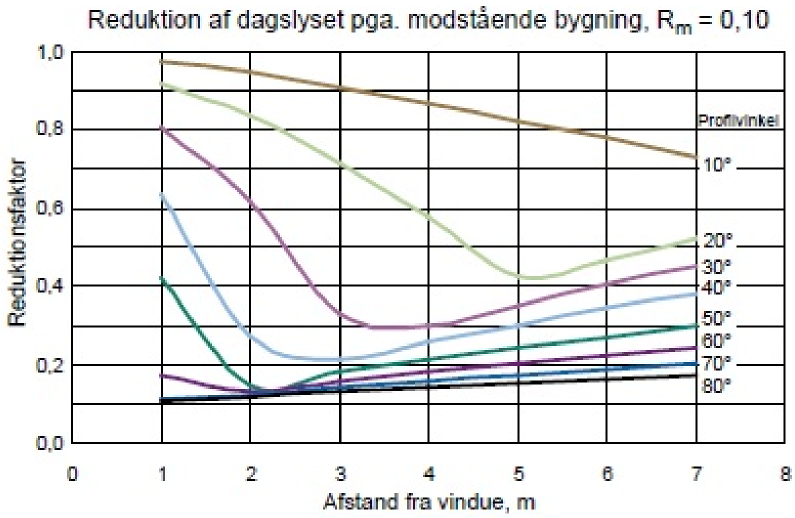

Figure O.6. Reduction factor for a facing building

The reduction is expressed as the distance inside the room away from the window, for different profile angles and reflectance values from the opposing building. The distance from the office to the opposite building is measured horizontally from the work plane. The height of the opposite building is measured measured from the work plane to a point on the top of the building. The profile angle is defined as the angle between these two measures. The profile angle is illustrated in the following picture O.7.

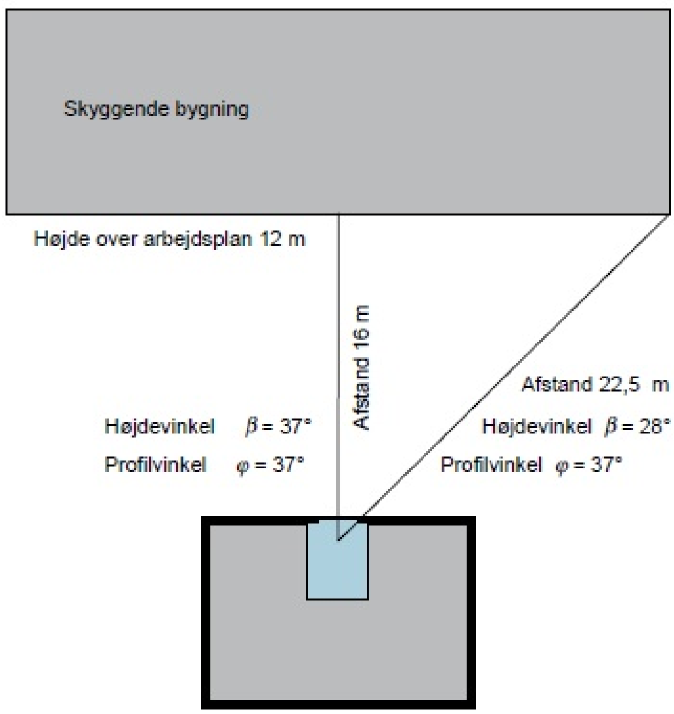

Figure O.7. Example on how to determine the profile angle

In the following graphs O.8 on the facing page and O.9 on the next page the reduction factor for an opposing building with an average reflection of $R_m = 0.25$ and $R_m = 0.40$ respectively can be determined.

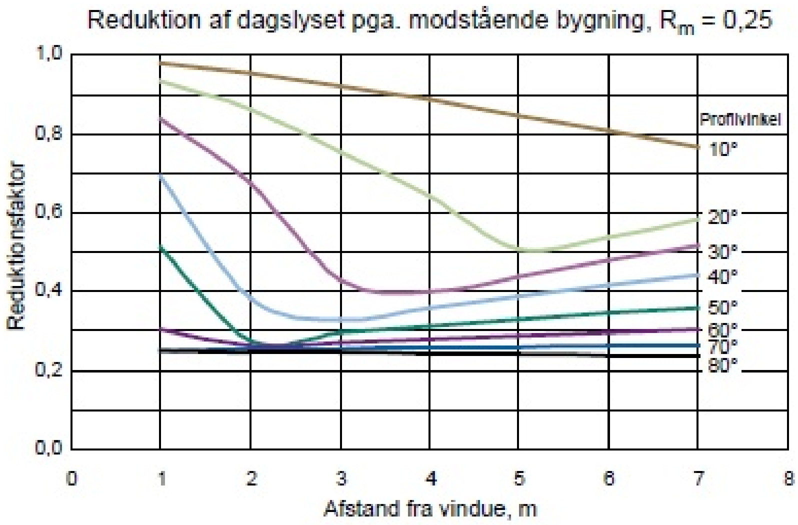

Figure O.8. Reduction factor for an oposing building with an average reflectance of $R_m = 0.25$

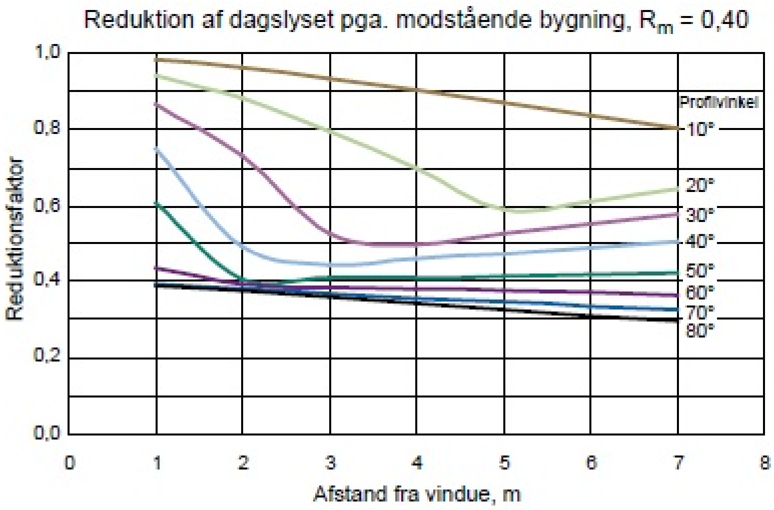

Figure O.9. Reduction factor for an oposing building with an average reflectance of $R_m = 0.40$

Correction for Overhang

The size of the overhang is defined by the angle from the middle of the window to the edge of the overhang. The graph O.10 on the following page shows the reduction of daylight on the work plane as a function of distance from the window. The graph displays the reduction factor for different sized overhangs.

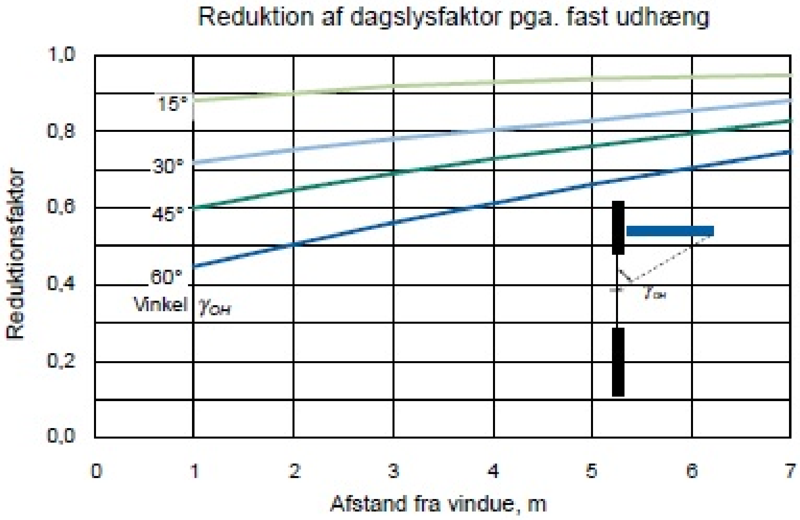

Figure O.10. Reduction factor for different sized overhangs

Correction for The Mean Reflectance

In side lit rooms the daylight will first hit the floor and other vertical and horizontal surfaces close to the window. Taking advantage of the reflectance of the different surfaces that receive direct daylight will ensure that the daylight is better distributed to the whole room. About half of the illuminance in the back of the room is reflected light, if the reflectance of the surfaces is 50%. Usually the ceiling has the highest reflectance, while the floor has the lowest. Under these circumstances the rooms mean reflectance R_m can be used to determine the daylight factor from tables or diagrams.

The mean reflectance for the rooms surfaces, including the window area can be calculated by the following equation:

$$R_m = \frac{A_{w,1} * R_{w,1} + ... + A_{w,n} * R_{w,n} + A_c * R_c + A_f * R_f + A_g * R_g}{A_{total}} \tag{O.4}$$

Where:

A_{total}	The total area of the surfaces in the room including the window area
$A_{w,n}$ and $R_{w,n}$	The area and reflectance of the wall surfaces
A_c and R_c	The area and reflectance of the ceiling
A_f and R_f	The area and reflectance of the floor
A_g and R_g	The area and reflectance of the glazing

The following graph O.11 on the next page shows how the daylight factor on the work plane varies as a function of the mean reflectance in a 6 m deep room.

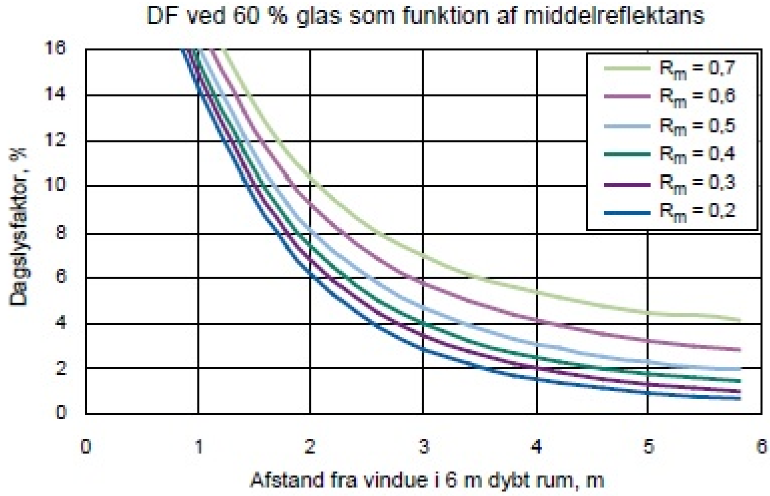

Figure O.11. The variation in the daylight factor as a function of the mean reflectance

The mean reflectance will usually be between 0.4 and 0.6 in an ordinary office room.

Table O.12 on the following page shows some typical reflectance values for different materials and colours. The values should be seen as an approximation. The actual reflectance of the surfaces in the room should be measured for more accurate values.

Overflade	Reflektans
Bygningsmaterialer	
Ren hvid gips	0,85
Hvid cementpuds	0,75
Kalkpuds, lys, tør	0,40-0,45
Puds, ny, hvidtet	0,70-0,80
Puds, gammel, hvidtet	0,50
Gennemsnit for almindelige lofter	0,60
Cementpuds, beton, ren, tør	0,25-0,45
Cement, beton, meget snavset	0,05
Hvide fliser	0,80-0,85
Hvid marmor	0,60-0,65
Gule mursten, nye	0,25-0,35
Røde mursten, nye	0,25
Mursten, snavsede	0,05
Almindeligt glas, 1 lag (udefra/indefra)	0,08/0,08
Almindeligt glas, 2 lag (udefra/indefra)	0,15/0,15
Almindeligt glas, 3 lag (udefra/indefra)	0,20/0,20
Almindeligt glas (energiglas) (udefra/indefra)	0,12-0,15 / 0,12-0,15
Solafskærmende rude (belagt + energibelægning), 2 lag (udefra/indefra)	0,10-0,40 / 0,15-0,20
Solafskærmende rude (gennemfarvet), 2 lag (udefra/indefra)	0,06-0,10 / 0,10-0,15
Linoleum, lysegrå	0,15
Linoleum, mørkebrun	0,05
Malede overflader, farver, tapet	
Oliefarve, ny, hvid	0,80-0,90
Oliefarve, gammel, hvid	0,70-0,80
Limfarve, ny, hvid	0,70-0,80
Limfarve, snavset, hvid	0,40
Sort	0,05
Mørkegrå	0,10-0,35
Lysegrå	0,40-0,65
Mørkebrun	0,05-0,15
Beige	0,40–0,50
Lysebrun	0,30-0,45
Violet, mørk	0,05-0,25
Violet, lys	0,35-0,60
Blå, mørk	0,10-0,30
Blå, lys	0,40-0,70
Grøn, mørk	0,10-0,25
Grøn, lys	0,35-0,70
Gul	0,40-0,70
Rød, mørk	0,10-0,20
Rød, lys	0,35-0,50
Rosa	0,35-0,60

Figure O.12. Typical reflectance values for different materials and colours

Correction for Inventory

Furniture that will be considered as the permanent inventory in the room should be considered in the daylight factor calculation. This is especially important in open landscape offices where the inventory can serve as partitions between the office spaces. The reflectance of the inventory have a big impact on the daylight distribution in the room and can contribute to the illuminance in the back of the room. The reflectance of the permanent inventory should be included in the mean reflectance calculation. The following graph O.13 shows the correction factor for a room with shelves in different heights. The shelves are placed between the windows and reach at least 2 m into the room.

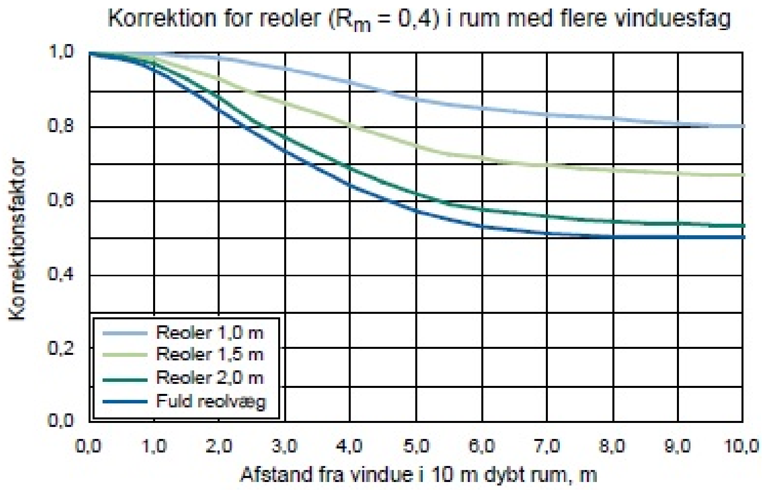

Figure O.13. Correction factor for a room with shelves in different heights

Correction for Solar Shading

A proper shading system should be installed in such a way that it allows maximum daylight incidence into the room, and at the same time reduces the occurrence of unwanted glare and overheating. The graphs O.14 on the following page and O.15 on the next page show the correction factor for white- and dark blinds respectively. The graphs shows values for blinds positioned in different angles, and the first graph also includes values for a white curtain.

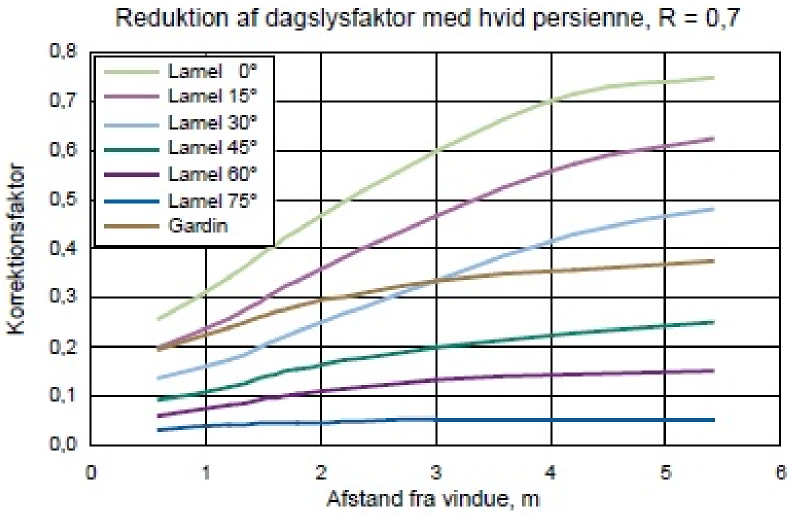

Figure O.14. Correction factor for a white curtain and white blinds positioned in different angles

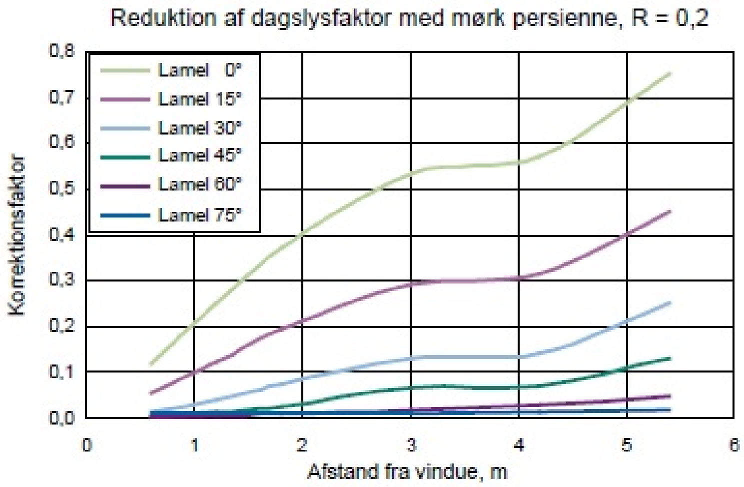

Figure O.15. Correction factor for a dark blinds positioned in different angles

Correction for Cleanliness of Windows

For ordinary windows, the cleanliness does usually not have a significant impact on the light transmittance.

O.4 Daylight Autonomy

Daylight autonomy is an expression for how how much of the required light level in the room can be covered by daylight alone during occupancy hours. This can be used to determine the energy consumption for artificial lighting.

O.5 Solar Light Factor

The daylight factor is merely used to determine the minimum daylight condition in a room. It is calculated from a theoretical overcast sky (CIE) where the luminance is evenly distributed in every cardinal orientation. In reality, there are great variations in the luminance on the sky. To evaluate the daylight conditions in a room over a longer time span, the solar light factor of the window should be used. The solar light factor takes the orientation and weather conditions into consideration. It is defined as the relationship between the illuminance in a point on the plane and the simultaneous exterior illuminance on the window without surrounding obstacles. The solar light factor can be expressed by the following equation:

$$SF = \frac{E_{RP}}{E_{window}} = \frac{SF1 * E_D + SF2 * E_{dif} + SF3 * E_{ref}}{E_D + E_{dif} + E_{ref}} \tag{O.5}$$

Where:

E_{RP}	The illuminance on the reference point, RP
E_{window}	The illuminance on the window plane
E_D	The illuminance from direct radiation on the window plane
E_{dif}	The illuminance from diffuse radiation on the window plane
E_{ref}	The illuminance from reflected radiation on the window plane
$SF1$	The solar light factor for direct sunlight
$SF2$	The solar light factor for diffuse daylight
$SF3$	The solar light factor for reflected light

The solar light factor is utilized in various simulation software such as SimLight (Bsim).

O.6 Daylight and Solar Radiation on a Building Surface

The radiation that hits a exterior surface consists of three parts: direct radiation, diffuse radiation and reflected radiation from the surroundings. The illuminance on the surface depends on the spectral spreading of the solar radiation. The spectral spreading depends on the sky condition which is why the luminous efficacy for the solar radiation from different sky conditions should be determined. The luminous efficacy (lumen per watt, lm/w) is an expression for the relationship between the illuminance on a surface (lux), and the equivalent radiation (w/ m^2)that hits the surface.

The following values express the luminous efficacy from direct sunlight, overcast sky and clear sky (without sunlight). These are the values that is normally used in Denmark.

Direct sunlight: $K_D = 103lm/W$
Overcast sky: $K_oc = 121lm/W$
Clear sky $K_cl = 146lm/W$

From these values, the illuminance can be calculated from current solar radiation data where the diffuse and direct radiation is measured separately. From each of these radiation components, the illuminance can be calculated using O.6.

$$\text{Illuminance (lux)} = \text{luminous efficacy(lm/w)} * \text{radiation(w/ m}^2\text{)} \tag{O.6}$$

For the reflected radiation component it can be assumed that the luminous efficacy does not change by the reflectance. The ground reflectance is usually set to 0.1, but this value has to be set higher in cases with snow on the ground.

Direct sunlight

Luminance (candela per m^2) is defined as the amount of light emitted from a surface that meets the eye. Direct sunlight can cause high luminance from surfaces and create glare. This should be prevented by installing solar shading. Since direct sunlight has a much higher intensity than diffuse daylight, it may reach deeper into the room by being reflected on the surfaces. The direct sunlight has a high intensity perpendicular on the beams direction but will rapidly decrease with an increasing angle of incidence. The variation of the angle of incidence is dependent on the area and orientation of the window. The south façade the largest angle of incidence will occur during spring and autumn, while for the east and west façade it will be largest during summer. This is illustrated in O.16

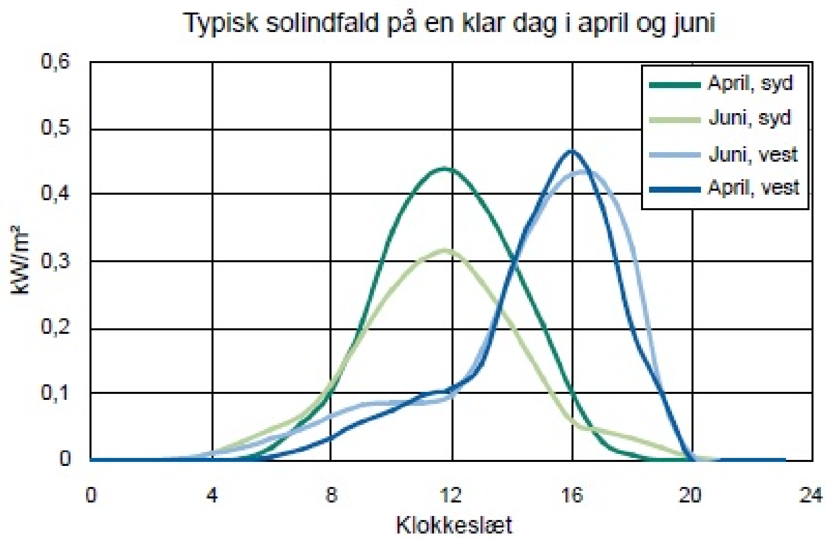

Figure O.16. Agle of incident on the south, west and east facade

Diffuse light

Diffuse light from the sky and reflected light from surrounding surfaces hits the façade from all directions. For a clear sky the horizontal illuminance is larger than the illuminance in zenith. For an overcast sky, the opposite is the case and the illuminance is largest in zenith and decreases towards the horizon.

O.7 Daylight Variations Throughout the Day and the Year

The intensity of the daylight can vary significantly from second to second. When analysing the daylight throughout a day it it therefore important to use the right time interval. O.17 and O.18 show the different in values by comparing hourly average daylight with average per minute. The graphs show that when using hourly average data, the maximum and minimum values will not be taken into account. This gives a less accurate picture of the daylight during the day.

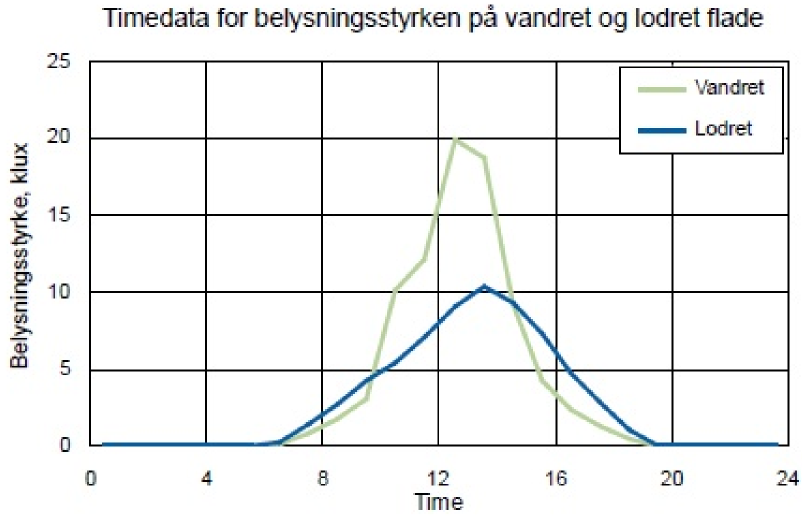

Figure O.17. Hourly average illuminance on a vertical and horizontal surface for a day in april

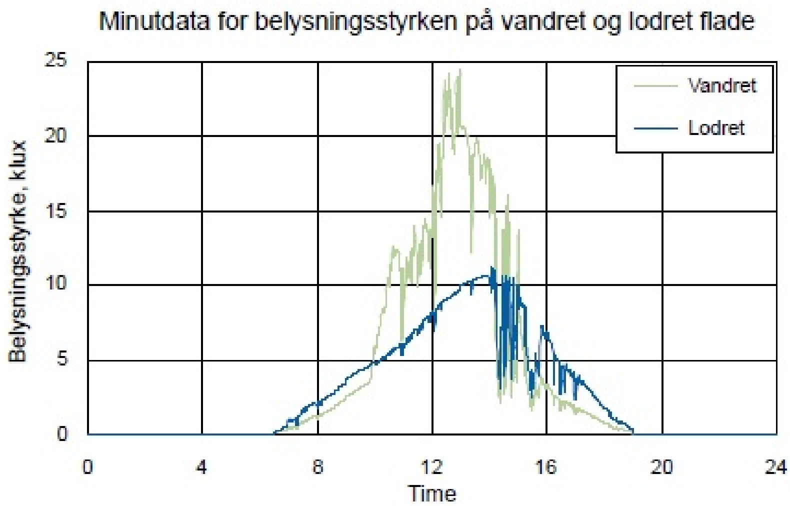

Figure O.18. Minute average illuminance on a vertical and horizontal surface for a day in april

The graphs clearly show that the hourly average will make the maximum and minimum values from the data can disappear. In comparison with the illuminance per minute, the hourly average does not have values higher than 20 klux.

When evaluating the daylight on building surfaces with different orientations throughout a year, the reference year weather data can be used.

O.8 Orientation

The illuminance in a point on a horizontal surface, calculated from the direct sunlight, cannot immediately be used for evaluating the duration of the illuminance in that point. For a room with a certain orientation, the illuminance in that point should be calculated with consideration to the window orientation. Graph O.19 shows the duration of the illuminance on a horizontal plane and vertical planes in each cardinal orientation throughout a year.

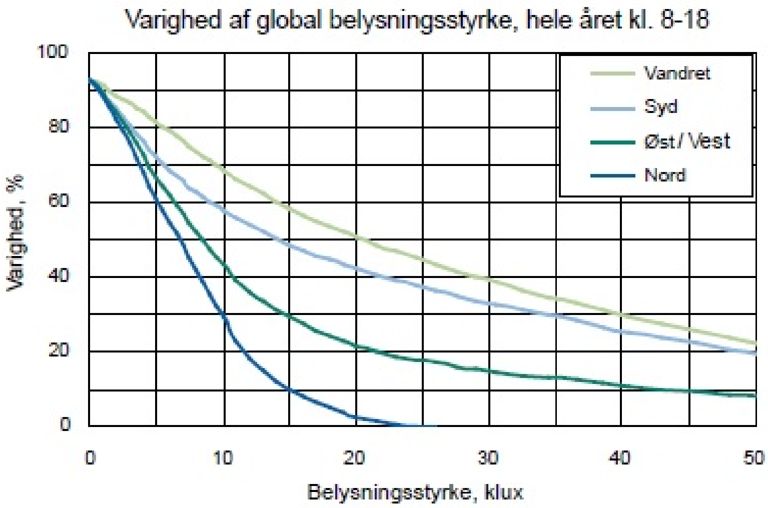

Figure O.19. The duration of the illuminance on a horizontal and four vertical planes

O.9 Standard Sky Models for Daylight Factor Calculation

The interior illuminance will vary simultaneously with the exterior illuminance. The daylight factor is a good indicator on how much daylight the room gets. The daylight factor is calculated during overcast sky conditions to determine the worst case scenario.

Two different standardised sky models are used for calculating the daylight factor. An evenly overcast sky and a CIE overcast sky. The evenly overcast sky model is a combination of overcast, intermediate and clear sky (without sun). This model is used for the most simple calculations. The CIE sky model corresponds to entirely overcast sky conditions. This is the most realistic and widely used model.

O.9.1 CIE Overcast Sky

The CIE overcast sky can be expressed by O.7. The relative luminance distribution is dependent on the elevation angle from the plane, but is independent on the suns position and the orientation of the room. The luminance in zenith will be 3 times larger than at the horizon.

$$L_\theta = L_z * 1 + 2sin\theta/3 \tag{O.7}$$

Where:

L_θ	The sky luminance at elevation angle θ $[cd/m^2]$
L_z	The sky luminance in zenith $[cd/m^2]$

From the illuminance in zenith, the illuminance on the vertical and horizontal plane cal be calculated using the following formulas O.8 and O.9.

Horizontal:

$$E_H = 7\pi/3 * L_z \tag{O.8}$$

$$E_V = (\pi/6 + 4/9) * L_z \tag{O.9}$$

Where:

E_H	Illuminance on the horizontal plane [lux]
E_V	Illuminance on the vertical plane
L_z	The sky luminance in zenith $[cd/m^2]$

The relationship between the illuminance on the vertical plane E_V and the illuminance on the horizontal plane E_H for the overcast CIE sky model is equal to 0.396.

O.9.2 CIE Clear Sky

CIE have also defined the luminance distribution for a clear sky. The luminance directly from the sun itself is not taken into account in this definition. For a clear sky the luminance is complex and unevenly distributed. It is characterized by the fact that the luminance in the horizon it larger than the luminance in zenith.

The illuminance on a horizontal plane under a clear sky can be expressed by the empirical formula O.10

$$E_H = 1100 + 15500 * \sqrt{sin\theta} \tag{O.10}$$

Where:

θ	The solar elevation angle $[\circ]$

This formula can only be used for clear sky without direct sunlight. For clear sky with sunlight O.11 can be used.

$$E_H = 1710 * \theta \tag{O.11}$$

O.9.3 Intermediate Sky

The illuminance on a horizontal plane under a intermediate sky can be expressed by the emperical formula O.12.

$$E_H = 1200 * \theta - 2800 \tag{O.12}$$

Where:

θ	The solar elevation angle ($8\circ < \theta < 50\circ$ [$\circ$]

O.20 illustrates the luminance for an overcast, intermediate and clear sky.

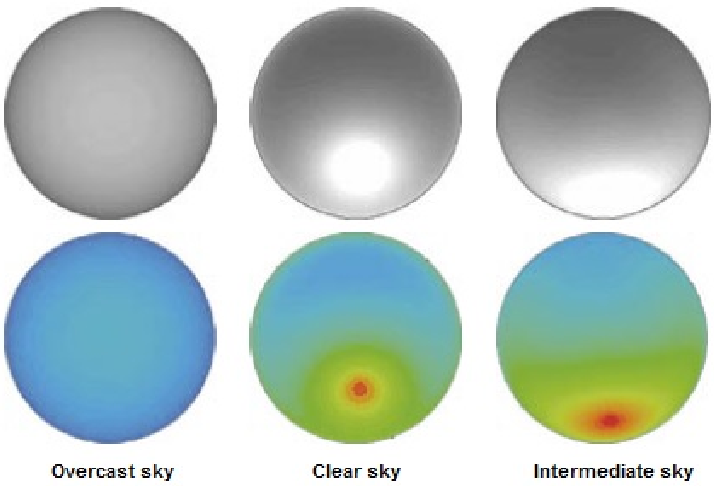

Figure O.20. Luminance distribution for overcast, intermediate and clear sky

Electronic Appendix P

The report and appendix are attached as a pdf file on the DVD.

P.1 The Excel Spreadsheets for the *CIE Sky Method* and the *Hourly Average Method*

Attached as .xls files

P.2 All Supporting Files

All supporting documents and files for this report are attached on the DVD.

Plan Drawings of Every Floor

Attached as .dwg file

Files from Simulation Software

The BSim models are attached as .dbk files

The SimLight models are attached .dbk files

The Relux models are attached as .rdf files

The VELUX Daylight Visualizer models are attached as .ViZ files

Weather Data

The Norwegian reference year is attached as a .xls file

Measurement Results

The measurement results for solar irradiance and interior illuminance are attached as .xmls files.

The measurement results for the electricity usage of the armature is attached as .xls files